DOI: 10.31577/ahs-2022-0023.01.0001

ACTA HYDROLOGICA SLOVACA

Volume 23, No. 1, 2022, 3 – 9

Global changes and hydrosphere

Viliam NOVÁK*

Increasing population led to the increasing demand to food, raw materials, water and energy. Anthropogenic demands provoke land use structure changes, intensification of its exploitation, deforestation, fossil fuel combustion and related carbon dioxide production. Those phenomena are changing water and energy fluxes of biosphere, and conditions for life. Actual climate change is a result of other global changes both natural and anthropogenic. It is mostly felt as a change of ecosystem temperature, increase of precipitation intensities and totals, as well as their irregular distribution in time and space. Flood periods are followed by long periods without precipitations. Water consumption is increasing; it is renewable resource, but water resources are unevenly distributed and often polluted, therefore unsuitable for use as fresh water. Increasing population as well as increasing consumption of resources lead to the imbalance between our planet production and consumption. To preserve good conditions for population of the Earth, it is necessary to decrease consumption of energy, raw materials and food to reach equilibrium between Earth´s ecosystem production and consumption of the ecosystem products.

KEY WORDS: ecosystem, biosphere, hydrosphere, global changes, climate change

Introduction

The Planet Earth surface area is 520×10^6 km^2, land comprises less than one third of our planet surface (149×10^6 km^2). Area of arable land comprises 12% of dry land only, (19.8×10^6 km^2), thus creating ecosystem of crops, which is the basic source of food for mankind. Animals, fish and plants are important part of food supply too. It could be a surprise, that the deserts area is approximately the same as the area of arable land. Forests cover a major part of land (60×10^6 km^2), which represents 38% of the land`s surface. Land glaciers are covering the area 15.7×10^6 km^2, which is a little bit less than is the area of arable land. The rest of dry land is covered by steppes, savannas, non-vegetated surfaces in Antarctic zone, residential zones, industrial areas, water surfaces, non-permeable surfaces like roads and buildings. Earth is populated approximately by 1.5 million of animal species, and about one million of them are insects, therefore our planet is often called as "planet of insects". Existence of individual animal species is dependent on other animal or plant species. It means that elimination one of species can lead to extinction of another. Any animal and plant species are important element in food chain link of animals and human beings. During a period of time 1600–1975 about 136 species of birds and 68 species of mammals went extinct, but in 20th century 85 mammals' species disappeared from the planet of Earth for good.

According to the Food and Agricultural Organization (FAO), up to 60% of worlds ecosystems are degraded and used in unsustainable way. In European Union, only 17% of biotopes preserved by European legislative are in favourable state. Therefore this geological era is proposed to be indicated as anthropocene (Crutzen, 2002).

In Slovakia, there are only 14.68% of natural ecosystems in natural state, which is exceptionally low value. The rest of ecosystems are highly modified (Izakovičová and Špulerová, 2018), and 75.1% of mammals were living in unfavourable conditions in 2017, (MŽP SR, 2018). Therefore, protection and preservation of all the assortment of existing animal and plant species is so important for mankind.

The only anomaly among living species of the Earth is human beings. It is the only living species, which can adapt to changing conditions, and to change environment in such a way, that it not only preserves, but even increases its population in an uncontrolled way. As it was mentioned before, man is changing the biosphere of the planet and thus endangers mankind as well as the rest of living organisms (Kutílek et al., 2013). Some philosophers assume existence of human beings on the Earth as anomaly, and danger for functional planet (Münz, 2019). Human's activity significantly influences our ecosystem. Selected indicators are showing the increasing rate of human activity since the beginning of industrial revolution in an exponential way (population, global HDP, water consumption, cars

number, paper production, etc.) Those processes are influencing the state of ecosystem, characterized by indicators like land use changes, carbon dioxide concentration, rain forests clearing, soil degradation, biodiversity, air temperature, floods, droughts and many others (Nemešová, 2007).

Area of living species is biosphere, which is subsystem of hydrosphere. Hydrosphere is an area of water presence on the Earth (subsurface water, surface and atmospheric, as well as sea water). Hydrosphere is an area about 10 km below Earth surface and about 40 kilometres above the Earth surface (Rejmers, 1985). Biosphere is a part of hydrosphere; it comprises area where organisms are living, as well as living organisms itself. It is thin, very vulnerable area, characterized mostly by influx of photosynthetic active radiation, suitable biosphere temperature, specific properties of an atmosphere and other properties needed for photosynthesis.

Plants (their seeds) and a man (if there is enough sources of energy) can survive in all the temperature interval present on the Earth (-88°C to +58°C). Biomass, which is the first element in nutrition chain of animals is product of photosynthesis, which can perform in the air temperature interval 0°C to +40°C, but optimum air temperature is about 30°C, depending on plant species. Therefore, the existence of human being on the Earth is limited by environment (ecosystem) properties, suitable to produce biomass, which is the source of energy of all living organisms of the Earth.

The share of arable land is approximately 12% of the land surface of the Earth (with possible increasing of it up to 14%). It is clear, that Earth`s biomass production is limited and can supply only limited number of population. The same is valid for supply by water, energy and especially for non- renewable resources like oil, raw materials, gas, etc.

The aim of this contribution is to demonstrate the effect of global changes on the Earth's ecosystem and on the hydrosphere particularly, with special attention to the water regimen of Slovakia.

Global changes and climate change

Global changes refer to planetary scale changes in the Earth system. Global changes comprise change in an environment, human society and economy. In principle, any activity in the ecosphere is influencing the Earth globally, but it is assumed that „global change" is such a change which can be clearly identified at global scale. All those changes can contribute to well known effect called „climate change" which is only one of many particular global changes, and could contribute to creation of new conditions for life (Nemešová, 2007).

Risks for the ecosystems on the Earth

Natural (non-anthropogenic) risks

Significant decrease of solar radiation is not expected in the next million of years. The time interval during which solar energy income of the Earth will cover the necessary rate of energy needed to preserve actual state of our planet life is limited. Calculations show, that the Sun's fuel could last the next 4 billion years. Today's average rate of solar radiation income to the upper boundary of the Earth`s atmosphere can be expressed by the so called Solar constant: 1,360 Wm^{-2}. It is expected, that Sun radiation rate will be decreasing, depending on the quantity of remaining fuel. Conditions for preserving existing state of life can cease long before total burn out of the Sun.

Collision of the Earth with space object is not excluded, it can have a fatal consequence for the life on the Earth.

Volcanic activity can significantly change energy balance of the Earth, by clouds of aerosols following volcanic eruption, they can last in an atmosphere from two to three years. Absorption and reflexion of radiation by solid particles can lead to summer cooling and winter warming (Kirchner et al., 1999). Currently, there are 26 active volcanoes, but there are about 1500 potentially active volcanoes worldwide.

Anthropogenic risks

Increasing population

It was estimated, about 180 million people inhabitating the Earth two thousand years ago. In 1820, there were about one billion people, and about 110 years later (in 1930) there were approximately 2 billion of people. In 2019 lived on the Earth 7.75 billion of people. During the last 90 years there was a gain of 5 billion. It is assumed, that in 2050 the number of inhabitants will increase to about 10 billion, then, their number is assumed to be slowly decreased. Approximately 6 billion of them live now in Asia and Africa. Even now, Africa is generating a population gain higher than 3% every year, i. e. gain higher than 50 million per year. It is expected, that in sub-Saharan Africa and Asia there will live more than three quarters of Earth`s population by 2050. Sub-Saharan Africa and some Asian countries are economically known as developing countries with a low GDP. This trend in population generates pressure on increase of food production, as well as on production of raw materials, fresh water and energy. In those countries there is shortage of arable land, fresh water, fertilizers and energy. Deficit of resources to intensify agriculture in countries with the highest population increase is main reason of increasing emigration, mostly to Europe. Some researchers assume even the decrease of inhabitants number at the end of this century, as it is observed in Europe even now. Precondition of such trend is relatively high standard of living, but this can hardly be expected in near future in Africa and Southern Asia.

Climate change

The climate is a generalized characteristic of weather, typical for a particular area; it can be characterized by averaged meteorological characteristics, such as an air temperature, wind velocity, and precipitation. There are no doubts, that climate of the Earth has been changing. During the last century the average temperature of the Earth increased about 1°C. Climate change is not homogeneous across the globe; it is more intensive in southernmost and northernmost parts of the Earth.

The reasons of climate change

Natural reasons of climate change

Natural reasons of climate change are due to changes of interrelations between the Earth and the Sun, resulting in the rate of solar energy delivery change. Among those reasons are irregularities of Earth`s orbiting, the changes of the angle of Earth axis in relation to the ecliptic, wobbling of the Earth`s axis during its orbiting. Even the Sun is periodically changing its radiation rate (Kutílek and Nielsen, 2010). Those phenomena dominated in climate change in pre-industrial age (up to 19th century). The ice age ended at about 10 thousand years ago, a medieval warm period (9–13 century) and little ice age (14–19 century) were mostly results of natural (non-anthropogenic) change of climate.

Anthropogenic reasons of climate change

are anthropogenic activities, mostly during the last two centuries and they are becoming more intensive (Kutílek, 2008). The most important reason of anthropogenic climate change is related to land use changes. The production of carbon dioxide by fossils burning and permafrost thawing are contributing to climate change, too.

Land use changes

Probably the most important contribution of human activities to the climate change is continuous change of land use by increasing population. The most important activities are deforestation of rain forests (Brazil, Africa, South Asia), elimination of wetlands, increasing area of arable land, overgrazing, monoculture agriculture, increasing urban and industrial areas as well as transportation facilities (highways), (Kutílek, 2008). Those activities are characterized by elimination or modification of natural surfaces, followed by the change of their water and energy balance structure. Obvious result is decrease of evapotranspiration totals and increase of local runoff. Solar energy not used to water phase change is heating biosphere and thus contributing to global warming. Tropical rain forests are characteristic by high precipitation totals (more than 3,000 mm of water layer per year), and by high income of solar energy (average income is 350 Wm^{-2}; for comparison, on the territory of Slovakia this income is 125 Wm^{-2}). High income of water and energy is resulting in extremely high annual evapotranspiration totals more than 2500 mm of water layer per year (in Slovakia, there is evaporated approximately 500 mm water layer per year) (Shuttleworth, 1988, Novák, 2012). What does it mean for water and energy balance of the Earth?

Intensive deforestation of rain forest and its change to agricultural land, buildings, transport infrastructure is changing properties of evaporating surface, especially their albedo. If it will go in this way, to the end of this century all the tropical forests will be cleared and replaced by another surfaces. The most important is, that evapotranspiration rate will decrease significantly, approximately to one half of the previous state. Therefore, about half of the solar energy reaching soil surface at constant rate will be not used as latent heat of evapotranspiration, but will be heating biosphere and thus increasing its temperature. This is the primary reason of warming with adjective „global“, because it is contributing to temperature increase locally and around the globe.

The most important „glasshouse“ gas is water vapour, because it disperses long wave radiation of the Earth in all the spectrum range more effective than carbon dioxide, with its relatively narrow range of its dispersion. Concentration of water vapour is proportional to air temperature. Increasing temperature of atmosphere increases water vapour concentration and thus increase the „greenhouse“ effect of the atmosphere. Currently, atmosphere (water vapour and carbon dioxide as its component) is increasing biosphere temperature to about 33°C. Without this function of atmosphere there will be average air temperature -18°C, instead of current 15°C. The problem, we are dealing with is actual increasing of this effect, so we should try to eliminate anthropogenic effects on air temperature. Until now (2020) this additional increase of greenhouse effect on average air temperature is about 1°C. The biosphere is very sensitive area and increase of greenhouse effect can dramatically change conditions of life on the Earth.

It was estimated, that about 60 percent of dry land of the Earth is anthropogenically modified. Usually, natural (green) surfaces are replaced by artificial ones, like fields, residential areas, transportation infrastructure. Common feature of such changes is evapotranspiration decrease and runoff increase. The sensitivity of climate change on land use modification is proportional to water and energy fluxes changes in particular areas. This is the case of rain forests (RF). About 90 percent of incoming radiation is consumed as latent heat of evapotranspiration (Shuttleworth, 1988). Areas, replacing rain forests evaporate much less and the difference between consumption of solar energy by RF and by cleared areas is heating environment.

According to FAO, about 100,000 km^2 of RF is eliminated over the globe annually (majority of it, about 60,000 km^2 of RF is cleared in Amazonia). Then, energy saved by decreasing of evapotranspiration is 82 MW km^{-2} (or 82 W m^{-2}). This enormous quantity of energy can heat boundary layer of the atmosphere and thus contributing to the increase of air temperature. Recalculating this amount of energy saved by evapotranspiration decreasing to the Globe area, it gains 0.016 Wm^{-2}, which is comparable to the contribution of the carbon dioxide concentration increasing.

Energy contribution by the above mentioned evapotranspiration decreasing cannot be dispersed homogeneously around the Globe. Therefore the majority (it is not known how much) of this saved energy will be heating in particular dry land area and thus increasing local air temperature and changing climate. As a result, climate of „newly modified“ territory will be changed too, with less precipitation, because local evapotranspiration will decrease and this contribution to formation of precipitation will be decreased, too.

On the territory of Slovakia, such land use change cannot influence the air temperature (or climate) as strongly as it

can be in area of RF. To replace forests by fields and impermeable surfaces (roads, buildings), additional 20 MW km^{-2} (or 20 W m^{-2}) of energy can be spent on heating of boundary layer of the atmosphere. Fact is, that on territory of Slovakia the share of green surfaces (especially forests) is increasing, which is positive feature. But arable land is changing to transportation infrastructure or another impermeable surfaces like factories and stores, thus changing the best arable lands to impermeable surfaces with low evaporation rates and intensive local runoff.

One more hypothetical (but realistic) example of the influence of land use change on energy fluxes in the atmosphere. About 5 percent of Slovak territory is covered by impermeable layers (buildings, transportation infrastructure) contributing to the climate change. So called „heat islands" are created by towns with an air temperature higher about few degrees of Celsius than their surroundings. Assuming, 1 percent of the Earth dryland is covered by impermeable layers, and evaporation from them will be half of those from neighbouring natural areas, it can increase the heat flux recalculated to the dryland by 0.18 W m^{-2}, which is about the same quantity as is result of carbon dioxide contribution per decade. This illustration would like to demonstrate, the importance of state of the land surface in formation of climate.

Fossil fuels burning

Fossil fuels (oil, gas, coal), as well as renewable sources (biomass) burning is producing greenhouse gas carbon dioxide (CO_2). This gas, as a part of the atmosphere, disperses energy of long - wave radiation of the Earth to all directions and thus increasing temperature of the biosphere. Production of CO_2 in Europe has significantly decreased, but world production of it is still continuously increasing.

Carbon dioxide concentration is changing. From 318 ppm in 1960 (ppm means parts of CO_2 molecules, per million of all air particles), to 420 ppm at 2020. But, also greenhouse gas water vapour concentration increases, because it also depends on air temperature and ranges from 6,000 ppm (at 0°C) to 20,000 at 20°C. Nevertheless, absorption spectrum of water vapour is much broader than this spectrum for carbon dioxide.

The role of carbon dioxide as a greenhouse gas was early understood, but problem was to evaluate quantitatively the role of increasing carbon dioxide concentration in an atmosphere on infrared energy fluxes emitting by CO_2 back to the Earth's surface. A few years ago there were published results of measurements how much infrared light radiated by the Earth is returned back by the carbon dioxide in an atmosphere and thus increasing the greenhouse effect (Feldmann et al., 2015). From results of thousands measurements performed in Oklahoma and Alaska during the decade 2000–2010 was found, that back radiation due to increased carbon dioxide concentration is 0.2 Wm^{-2} per decade (0.02 Wm^{-2} per year). Since the start of industrial revolution it is about 1.82 W m^{-2}. Is it significant quantity to change climate? The average income of solar energy on the Earth is 350 W m^{-2}. It is necessary to compare this result with possible influence of land use change on energy balance of the Earth.

Permafrost thawing

Permafrost is permanently frozen subsoil, thawing at the surface in summer; it is characteristic of Arctic tundra, covering about 24% of Northern hemisphere. Thickness of permafrost layer is up to 80 m. As a result of temperature increasing, permafrost containing significant part of frozen organic matter is thawing, and releasing methane (CH_4), which is also product of animals, and carbon dioxide (CO_2) as a result of organic matter decomposition. Especially methane (0.00018% of the atmosphere) is responsible for 1/6 of global warming in the last decades (Knoblauch et al., 2018).

The influence of global change on hydrosphere

Increasing population of the Earth and their demand on consumption of food, raw material, energy and water is the main reason of accelerated non-reversible changes of the environment. Related anthropogenic activities are important reason of soil degradation, desertification, deforestation, soil erosion and overgrazing which are amplifying climate change. On the contrary, climate change is contributing to the enhancing of land use change.

All the water on Earth can cover its surface by the layer of 2,800 metres thick; as a part of it, the thickness of fresh water layer would be about 70 metres. Technically, all the water on the Earth can be treated by known technologies to fresh water; but it needs complicated and expensive technology.

Sea level changes are mostly results of climate change. Increased temperature of the atmosphere is responsible for two important effects: glaciers and icebergs melting, and water expansion with increasing water temperature.

The sea level since the beginning of 20th century has risen about 20 cm, during the last 20 years it was 5 cm (Vinas and Rasmussen, 2015). According to NASA in the time interval 1992–2019 sea level risen in average about 7.4 cm (Holgate, 2007). The rise of sea level is not smooth, but its rise is sensitive to short term fluctuations of weather. There are even short time intervals of sea level decrease, but in general, there is the tendency of sea level increase. Potential rise of sea level due to Greenland glacier melting (1.7×10^6 km^2) is 6 metres, melting of Antarctic continental glacier (14×10^6 km^2) could cause sea level rise up to 58 metres. Complete melting of those glaciers is not expected in near future. Real values of sea level rise are about 5 mm per year, during this century it is expected sea level rise about 50 cm.

Coefficient of thermal expansion of water is around 1×10^{-4} m K^{-1} (its value depends on temperature too). It means the sea level will rise 0.0001 of water layer thickness when temperature of water will rise about 1°C. The average sea depth is approximately 2800 meters, then the increase of water temperature about 1°C can rise sea level due to thermal expansion of water about 28 cm. This is not expected in near future. Usually, the sea level rise is associated with increasing of inundated land area, followed by evaporation increase. Additional

consumption of energy as latent heat of evaporation can contribute to air temperature decrease, which works as autoregulation mechanism of Earth temperature.
Water cycle is basic process to preserve life on the Earth. Approximately 90% of incoming energy from the Sun is used to change liquid or solid state of water to water vapour by evaporation from seas or rain forests. Evapotranspiration of the dry land is usually less intensive, because low soil water content is frequently limiting evapotranspiration rate. In general, more than 50% of solar energy reaching the Earth`s surface is consumed by the process of evapotranspiration, but seas and RF are consuming about 90% of solar radiation reaching the Earth´s surface as latent heat, and therefore is so important to keep RF areas in good state.
Without consumption of solar energy by evapo-transpiration, temperature of biosphere would increase to the level not compatible with life on Earth. As it will be shown later, anthropogenic changes of land surfaces can significantly contribute to modification of water and energy balance equation structure and strongly influence climate of the Earth. Consumption of energy by evapotranspiration from surface of the globe (latent heat of evaporation) is equivalent to 2×10^4 of all energy, transformed by the Earth´s plant stations. Therefore, evapotranspiration is the main consumer of energy on Earth and is creating favourable conditions for life (Novák, 2012).
Other basic feature of the water cycle of the Earth is permanent cleaning (distillation) of water by evaporation. Natural water cycle works as gigantic distillation system powered by solar energy. First phase of it is evapotranspiration. Result of its function is clean, distilled water, permanently returning to the Earth surface by precipitation. To do so, it is necessary to keep atmosphere clean, because precipitation during the fall to the surface is dissolving the stuff in the atmosphere. The most dangerous kind of precipitation were so called „acid rains", the water is dissolving sulphur in the air as a product of coal burning, so the result is a low concentration sulphur acid. Such rain was devastating plants and small animals. So, one of the main precondition of good water quality preservation is clean atmosphere. Water infiltrating the soil, groundwater and rivers is dissolving minerals containing in the surface soil layers. Water with concentration of minerals less than 500 mg per litter which meets additional 82 criteria according to Slovak standards, can be used as fresh water (Nariadenie vlády SR číslo 354/2006 Z.z.).

Is there enough fresh water for all of us?

Assuming „business as usual", i.e. discharge of rivers will not change, and one billion (1×10^9) people by 2050, then the discharge of water in rivers can cover approximately 10,000 litres of fresh water for one person and one day. WHO recommends a minimum consumption of 70 litres of water per person per day. The average actual discharge of the Amazon River only can deliver 1,300 litres/person/day, which represents about 16 times of minimum consumption quantity per person and day. Why we are dealing with rivers only? The rest of precipitation (about two thirds of total precipitation from the dry land) evaporates, mostly as a transpiration participating in biomass production. Therefore, rivers discharge recharging groundwater in surrounding collectors represents real resources of mankind consumption, assuming good quality of river water.
In conclusion, there is enough fresh water for everybody even in the future. But, fresh water resources are not distributed evenly over the globe and are not available everywhere. Correction of uneven geographic distribution of water, e.g. by desalinisation of salt water, can be realised by the richest countries only. On the other hand, a lack of fresh water can lead to existential problems (lack of water for irrigation), to health problems and generate pressure on emigration.

Water and Slovakia

Average river discharge from the Slovak territory is approximately 400 m^3s^{-1}, or 6,400 litres per capita and day. The average discharge of the Danube River at Bratislava profile is 2,000 m^3s^{-1}, which represents five times the amount of all the Slovak rivers discharge. Of course, Danube as an international river body cannot be exploited without limits according to international agreements. Water from Danube is infiltrating and thus recharging groundwater, mainly in the upper part of Žitný ostrov. Therefore, the upper part of Žitný ostrov was declared a protected water resource area (Chránená vodohospodárska oblasť); it is one of ten protected water resource areas in Slovakia. According to Slovak Hydrometeorological Institute (SHMÚ) and Slovak Agency of Environment Protection (SAŽP), (Kollár, 2001), the estimated potential capacity of fresh water resources of Slovakia is 146.7 m^3s^{-1}, and as a part of it, the estimated capacity of groundwater resources is 79 m^3s^{-1}. Žitný ostrov resources of groundwater itself are estimated by 25 m^3s^{-1}. Estimated capacity of readily existing resources of water in Slovakia (surface and groundwater resources) is 32,800 l s^{-1}, which covers about three times the contemporary fresh water consumption – 12,800 l s^{-1}. Actual public fresh water consumption in Slovakia is approximately 80 litres per capita and day, just above the minimum consumption limit recommended by WHO. This is result of economic stimulation of fresh water consumption, because the price of fresh water is relatively high. Groundwater resources cover 80% of fresh water consumed in Slovakia. The quality of fresh water depends on its protection against pollution. The main risks of Žitný ostrov groundwater pollution are over fertilizing, intensive application of herbicides and pesticides as well as illegal waste dumping.

What can be expected in water and energy resources in Slovakia?
Forests in Slovakia belong to temperate climatic zone forests, their area is increasing and covers about 42% of Slovak territory. But, reduction of arable land area (14,400 km^2, i.e. 29% of Slovak territory) is significant. Enlarged are impermeable surfaces (buildings,

communications, industrial objects), in the last decades, which can lead to local runoff increase and decrease of evaporation, followed by the temperature increase.

As a result of a climate change, there was measured air temperature increase during the last century about 1°C. This gain increases potential evapotranspiration, i.e. maximum possible under given meteorological conditions. Global increase of evaporation, particularly from oceans and seas is resulting in increased precipitation totals around the world. Evapotranspiration in Slovakia during the past 30 years increased about 10%; but potential evapotranspiration increased even more, reflecting higher temperature of the atmosphere (Pekárová et al., 2017). As a result, the runoff – especially in southern parts of Slovakia – is decreasing and recharge of groundwater by infiltration from rivers is decreasing too. Therefore, there is an urgent need to retain as much water as possible in catchments. The effective method of water retention increase are relatively big water reservoirs (with volume of several million cubic meter) and managed aquifer recharge (ISO/TR 13793:2014).

Arrangement of small water reservoirs is not a good solution. In reservoirs with a small retention volume, water quickly increases its temperature, followed by eutrophisation and overgrowing. Water in such reservoirs cannot be used even for irrigation and communal consumption. Suitable method to increase retention of water is artificial infiltration of water from channels or rivers to recharge groundwater. Utilisation of infiltration basins with permeable bottom to recharge groundwater are often used in some countries.

Other frequent myth is the idea of increasing retention of water in the landscape by forestation. Forestation of land is good idea, because green woody surfaces with relatively high rate of transpiration are consuming solar energy, thus decreasing ambient temperature, as well as incorporating carbon dioxide in the process of photosynthesis, they are decreasing outflow, and they are important anti – erosion element, but they are not accumulating water. On the contrary, water retention by forests is small, because forests are intensifying water circulation. About one third of precipitation in coniferous forests is intercepted and evaporated (in leafy forests it is about one fifth of precipitation), this part of precipitation even do not reach soil surface. This phenomenon is not felt negatively, because forests are usually located in mountains with high precipitation totals. But, the runoff is decreased by this phenomenon significantly.

Climate change is accompanied by increasing risk of local floods. Forests interception capacity with its maximum up to 6 mm water layer cannot prevent floods, because rain intensity is often higher than 10 mm per hour and such precipitation total is often higher than 100 mm. If the soil is fully saturated with water from previous precipitation events, practically all the precipitation can outflow and result is „flash flood“ (Pekárová et al., 2011). The floods in last years were observed even in the small, forested catchments.

Idea about „green landscape“ is good solution. Green canopies are consuming energy to transpirate, absorbing carbon dioxide in photosynthesis, they are important anti – erosion element, suitable environment for animals and what is for people most important - produce biomass as the basic element of food chain of all living organisms.

Ecosystem stability and climate change

There is no doubt: current global changes (climate change, land use change, fossil fuels burning, interactions of the Earth and outer space) are strongly influencing biosphere (ecosystem) and its components: plants and living organisms. Climate is the most important phenomenon responsible for distribution of vegetation and living organisms across the Globe. Flow of water and energy is determined by the input of energy from the Sun. Global warming increases temperature of the ecosystems in the range 1°C to 4°C and changes their properties. In principle, those phenomena are initiating shift of plant and animal species to the poles direction. Plant species (including crops) were changing their territories, even in the past, but the rate of global changes (and climate as their part) are accelerating and suggests that such changes can be realised relatively fast, up to ten times faster, than it was previously, following warming after the last glacial maximum. It is not clear if plant communities (and animals as well) would be able to follow relatively rapid shift of climate zones. It is expected, that some plant species will not be able to follow climate change speed and will die out, because they will not be able to adapt to such climate change. This so called „filtration“ effect will be proportional to the rate of such changes. It is expected, that areas with natural conditions suitable to alpine and arctic plant and animal species will be smaller, fragmented and isolated, so it is expected that some of them die out (Malcolm and Pitelka, 2000). Displacement of so called invasive plants observed in the last decades even in Slovakia is probably the effect of climate zones shift to northern direction.

Conclusions

Global changes refer to planet scale changes in the environment, human society and economy. Climate change is only one of many particular global changes. Reasons of such changes are natural and anthropogenic. Natural reasons of climate change depend mainly on interactions among the Earth and outer space.

Since the nineteenth century, increasing population caused pressure to increase consumption of food, raw material and energy, therefore started the so called industrial revolution, induced great scale land use change, emission of greenhouse gases, replacing natural surfaces by artificial ones. This activity changed the structure of mass and energy fluxes in the ecosystem. It was estimated, about 60 percent of the Earth`s surfaces are anthropogenically modified. Those anthropogenic changes of land surface led to the decreasing evapotranspiration and a part of solar energy previously spent as latent heat of evaporation is increasing the Earth`s temperature. By combustion of fossil fuel, carbon dioxide is produced and its concentration in the atmosphere is increasing. Part of planet`s long – wave radiation catched by the CO_2 molecules is dissipated back

to the Earth surface and thus increasing ecosystem temperature. According to the measurement, the average annual increase of back long-wave radiation is 0.02 W m^{-2}. Clearing of forests – especially rain forests – decreased evapotranspiration, carbon dioxide sequestration and thus secondary contributes to global temperature increase; the annual increase of energy rate flux per year is 0.016 W m^{-2}. Assuming, that 1% of land is anthropogenically changed, then the „saved" energy flux is 0.0022 W m^{-2}. Sum of those three anthropogenically induced fluxes is 0.038 W m^{-2}; which can contribute to the increasing of the Globe atmosphere temperature. For comparison, the average solar energy flux to the Earth surface is 350 W m^{-2}.

Increasing demand on food, raw materials and energy creates pressure on their production. Arable land areas, needed to produce biomass as a basic source of food are limited as well as areas suitable for cattle breeding. Deposits of raw materials are limited and it is expected to be exhausted in the next century. Results of analysis have shown, that renewable resources of energy can cover about ten per cent of expected demand at the end of this century (Makarieva, et al., 2008).

There is enough fresh water even for growing population of the Earth, but fresh water resources are not distributed evenly over the Globe and are not available everywhere, therefore it can be expected tensions related to the water resources. In Slovakia, there are used about one third of readily existing water resources only, therefore even in conditions of climate changes there is enough fresh water for all. The weak point is in regional and local availability of fresh water. There is need for completing and enhancing the water supply infrastructure.

To preserve environment of the planet sustainably suitable for life, it is necessary to achieve equilibrium between production of the ecosystem and its consumption by living organisms. Until now, civilisation is consuming much more, than sustainable productivity of Earth`s ecosystem can bear.

Acknowledgement

This contribution was supported by the Scientific Grant Agency VEGA Project No. 2/0150/20.

References

Crutzen, P. J. (2002): Geology of Mankind. Nature, v. 415, 23.

Feldman, D. R., Collins, W. D., Gero, P. J., Torn, M. S., Mlawer, E. J., Shippert, T. J. (2015): Observational determination of surfavce radiative forcing by CO_2 from 2000–2010. Nature, 519, 339–343.

Holgate, S. J. (2007): On the decadal rate of sea level change during the twentieth century. Geophysical Research Letters, 34. 10.1029/2006GL028492.

ISO/TR 13973:2014(E). Artificial recharge to groundwater. Technical Report, 32p.

Izakovičová, Z., Špulerová, J. (2018): Dopad globálnych megatrendov na krajinu a jej ekosystémy. Ústav krajinnej ekológie SAV, Bratislava.

Kirchner, I. G., Stenchikov, H. F., Graf, A. A, Robock, J. A. (1999): Climate model simulation of winter warming and summer cooling following the 1991 Mount Pinatubo volcanic erruption. J. Geophys. Res.,104, 19,039–19,055.

Knoblauch, C., Beer, C., Liebner, S., Grogoriev, M. N, Pfeifer, M. N. (2018): Methan production as a key to the greenhouse budget of thawing permafrost. Nature Clim. Change, 8, 31–312.

Kollár, A. (2001): Water resources, their exploitation and protection. Život. Prostr., 35, 160–162. (In Slovak.)

Kutílek, M. (2008): Global warming rationally. Dokořán, Praha, 185 p. (In Czech.)

Kutílek, M., Nielsen, D. R. (2010): Facts about global warming. Catena Verl. GMBH, Reiskirchen, Germany, 227 p.

Kutílek, M., Landgráfová, R., Navrátilová, H. (2013): Homo adaptabilis (Lidé jsou přizpůsobiví). Dokořán, Praha, 158 p. (In Czech.)

Makarieva, A. M., Gorskhov, V.G., Li Bai-Lian. (2008): Energy budget of the biosphere and civilisation: Rethinking environmental security of global renewable and non-renewable resources. Bilogical Complexity, v.5, 281–288.

Malcolm, J. R, Pitelka, L. F. (2000): Ecosystem and global climate changes. Pew Center on Global Climate Changes, Arlington, Va.

Műnz, T. (2019): Are we leaving? Petrus, Bratislava, p. 228. (In Slovak.)

MŽP SR (2018): The state of an environment in Slovak republic in 2017. Annual Report, Ministry of Environment, Slovak republic, (MŽP SR), Bratislava, SAZP SR.

Nemešová, I., (2007): Climate change as a part of global change. Meteorol. Zprávy, 60, 1–6. (In Czech.)

Novák, V. (2012): Evapotranspiration in the Soil – Plant – Atmosphere System. Springer Science + Business Media, Dordrecht, 253 p.

Pekárová, P., Miklánek, P., Pekár, J. (2017): Hydrological balance structure changes of Slovakia. In: 24th Int. Poster Day Transport of water, chemicals and energy in the SPAC, Inst. Hydrol. SAV, Bratislava, 204–210.

Pekárová, P., Svoboda, A., Novák, V., Miklánek, P. (2011): Historic hydrology and integrated management of catchment and landscape. Vodohospodársky Spravodajca, 54, 4–7. (In Slovak.)

Rejmers, N. F. (1985): Alphabet of nature: Biosphere. Horizont, Praha, 176 p. (In Czech.)

Shuttleworth, W. J. (1988): Evaporation from the Amazonian rainforest. Proc. Roy. Soc., London, B233, 321–346.

Vinas, M. J., Rasmussen, C. (2015): Warming seas and melting ice sheets. News, August, 25.

Ing. Viliam Novák, DrSc. (*corresponding author, e-mail: viliamnovak42@gmail.com)
Institute of Hydrology SAS
Dúbravská cesta 9
84104 Bratislava
Slovak Republic

DOI: 10.31577/ahs-2022-0023.01.0002

ACTA HYDROLOGICA SLOVACA

Volume 23, No. 1, 2022, 10 – 20

The drought characteristics and their changes in selected water-gauging stations in Slovakia in the period 2001–2020 compared to the reference period 1961–2000

Lotta BLAŠKOVIČOVÁ*, Katarína MELOVÁ, Soňa LIOVÁ, Jana PODOLINSKÁ, Beáta SÍČOVÁ, Martin GROHOĽ

Reassessing the hydrological characteristics with regard to drought is very important in the context of a changing climate. In this paper, we evaluate the drought in terms of changes in hydrological characteristics for the 20-year period 2001–2020. The evaluation of changes is based on a comparison of data for this period with the currently valid reference period 1961–2000 in 13 selected water-gauging stations. In the analysis of the occurrence of subnormal mean annual discharges (Q_r <90% $Q_{a,1961-2000}$), in most of the evaluated stations, the percentage incidence of such years is higher in the period 2001–2020 than in the reference period. The distribution of runoff throughout the year in the period 2001–2020 in comparison with the reference period in most stations confirms the changes identified in the previous evaluation of the period 2001–2015, i.e. the transfer of part of the usual increased spring runoff to previous, winter months. An exception was water-gauging stations on streams in the mountainous areas of northern Slovakia, where changes are reflected to a lesser extent.

KEY WORDS: hydrological drought, mean monthly discharge, runoff distribution change

Introduction

Currently, much attention is paid to the issue of climate change and drought. Drought and its increasing occurrence are considered to be the one of the most serious impacts of climate change. The Slovak Hydrometeorological Institute (SHMI) has been dealing for a long time with the assessment of drought from various aspects, also in accordance with the recommendations of the publication Tallaksen and Van Lanen (2004) and the WMO manual (WMO, 2008). The partial results were published also in monographs Fendeková et al. (2010; 2017). SHMÚ also regularly assesses the validity of long-term and design hydrological characteristics as well as the representativeness of the reference period in accordance with national Decree 418/2010 (Decree of the Ministry of Agriculture, Environment and Regional Development of the Slovak Republic on the implementation of certain provisions of the Water Act) §8 point (3). The long-term hydrological characteristics were determined for the currently valid reference period in Slovakia 1961–2000, which we can consider as stable in terms of trends. In next periods, changes in the long-term characteristics were continuously reassessed in view of the possible need to change the reference period. After 15 years, the hydrological characteristics associated with drought, their development and changes in terms of the hydrological regime of surface streams in Slovakia were evaluated in detail. In three partial reports Evaluation of hydrological drought (Poórová et al., 2018; Blaškovičová et al., 2020; Blaškovičová et al., 2021), selected flow and non-flow characteristics of drought in the period 2001–2015 were compared in water-gauging stations with long-term observation against the reference period 1961–2000. In this paper, given that we have data for the next 5 years, we evaluate the drought for selected water-gauging stations in terms of changes in hydrological characteristics for the 20-year period 2001–2020 compared to the reference period. The analyzes serve not only as a basis for evaluating the character of the last 20 years in terms of changes in hydrological characteristics and their regime in time and space, but also the suitability of a representative period is assessed in accordance with Slovakia's Water Plan at least every six years. That is the first step to further re-evaluation of the representative period and possible need for its change.

Data and methods

The evaluation of changes is based on a comparison of data from the period of hydrological years 2001–2020 with the reference period 1961–2000 in 13 selected water-gauging stations (WS) with the representation of different areas of Slovakia (Table 1, Fig. 1). We also

evaluated the Danube River itself in the Bratislava profile, although its regime has a different character due to its size (several times higher than other rivers in Slovakia) and, as its runoff is created mainly outside our territory, it does not even reflect the climatic and runoff conditions of Slovakia. However, it is an important source of water flowing into our territory, also ensuring the replenishment of groundwater in the most important source of drinking water in Slovakia, Žitný ostrov.

In selected WSs we have evaluated:

- mean annual discharges (Q_r) – their evolution in the compared periods,
- long-term mean discharges (Q_a) – changes in the period 2001–2020 compared to the reference period 1961–2000, evaluation of 20-years moving averages in the period 1961–2020,
- changes in long-term mean monthly discharges (Q_{ma}) and changes in the runoff distribution during the year in the compared periods,
- frequencies of occurrence of extremely small monthly flows (Q_m) and their changes in the compared periods,
- changes in the flow duration curves (FDC) – in particular low-flow quantiles (M-day discharges, Q_{Md}),
- non-flow characteristics: the number of days of low-flow periods analyzed, i.e. days with mean daily discharges (Q_d) lower than the selected limits; the values of M-day discharges Q_{364d}, Q_{355d}, Q_{330d} and Q_{270d} for reference period 1961–2000 used as limits.

Table 1. List of selected water-gauging stations

Station number	Stream	Station	Catchment area [km^2]	Altitude [m a.s.l.]
5140	Danube	Bratislava	131 331.10	128.43
5100	Močiarka	Láb	47.10	144.33
5160	Blatina	Pezinok	19.09	238.59
6540	Nitra	Nedožery	181.57	287.00
5400	Belá	Podbanské	93.49	922.62
6300	Rajčianka	Poluvsie	243.60	393.03
6450	Vlára	Horné Srnie	341.79	238.00
7015	Hron	Brezno	582.08	490.93
7065	Štiavnička	Mýto p. Ďumbierom	47.10	616.75
7730	Štítnik	Štítnik	129.63	284.95
8870	Torysa	Košické Olšany	1 298.30	185.88
8530	Hnilec	Stratená	68.23	789.24
7930	Javorinka	Ždiar-Podspády	34.89	907.80

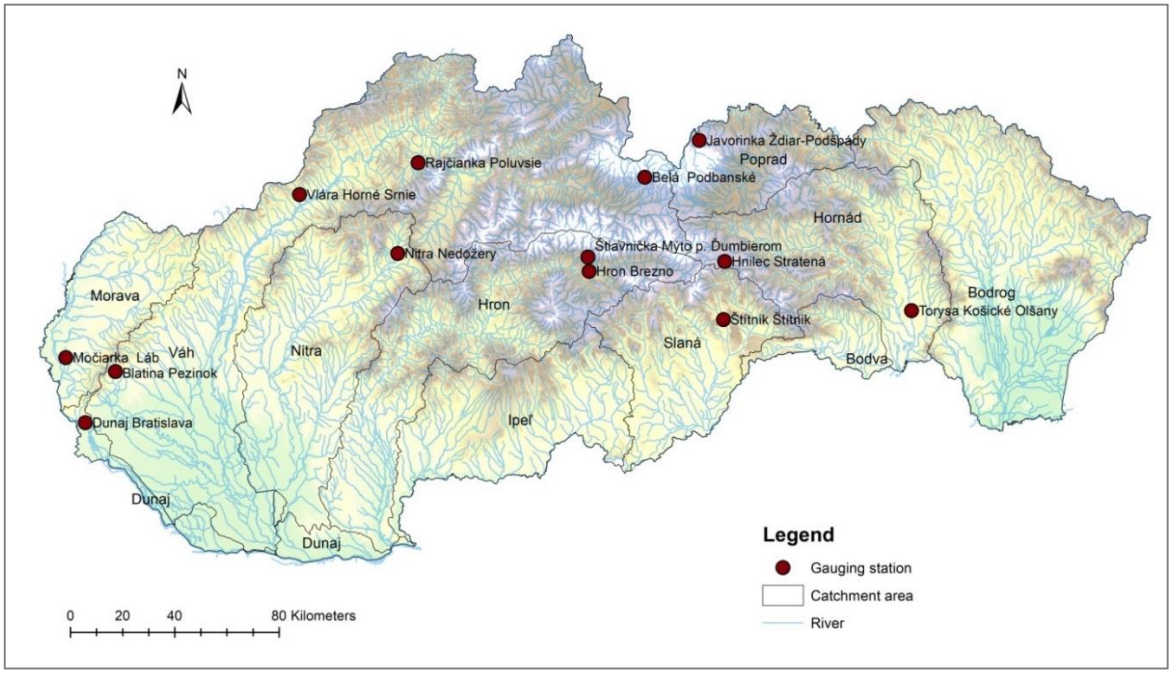

Fig. 1. Situation of selected water-gauging stations.

Results and discussion

Mean annual discharges (Q_r) and mean long-term discharges (Q_a): The evaluation of the Q_r series for the period 1961–2020 shows a different evolution in selected stations. In most of the evaluated WSs, the simple linear trend manifests itself as declining. In several profiles, this is mainly due to several significantly above-average Q_r values at the beginning of the evaluated period (in its first 10 years). The exceptions are WSs in the northern part of Slovakia – Podbanské – Belá and Ždiar-Podspády – Javorinka, where the linear trend is growing.

This is also in line with the comparison of Q_a values in the period 2001–2020 against the reference period 1961–2000 (Fig. 2). In most evaluated WSs, the value of $Q_{a,2001-2020}$ is lower compared to the reference period. The more significant decrease (below -10%) was reflected in the WS in the west and south-west of Slovakia: Láb –Močiarka (-32%), Pezinok – Blatina and Nedožery – Nitra (-15%), Poluvsie – Rajčianka (-13%). We recorded a decrease of -7% in WS Mýto p. Ďumbierom – Štiavnička and a slight decrease to -5% in 3 WSs: Štítnik – Štítnik, Košické Oľšany – Torysa and Bratislava – Danube. We record a slight increase in $Q_{a,2001-2020}$ compared to the reference period (up to 5%) in only 3 of the evaluated WSs; these are mountain streams in the north and center part of Slovakia – Belá, Javorinka and Hnilec.

For a better assessment of the position of the evaluated 20-year period 2001–2020 in the whole period 1961–2020, we processed the moving averages of Q_a of individual 20-years with a step of 1 year. It is interesting, that the mean long-term discharge in the 20-years 2001–2020 with the value of 1988 $m^3 s^{-1}$ on the Danube River in Bratislava is the lowest in the whole evaluated period (Fig. 3).

Similar results are also in WS Láb – Močiarka, where $Q_{a,2001-2020}$ is also the lowest value among the moving averages of the whole period. The mean values in assessed period 2001–2020 in WSs Nedožery – Nitra, Poluvsie – Rajčianka and Horné Sŕnie – Vlára (Fig. 4) have been the 2. lowest among the moving averages, while the lowest values Q_a have come for previous 20-year period 2000–2019.

The position of $Q_{a,2001-2020}$ values in the rest of WSs range between 14th to 22nd lowest of all 41 moving averages. An exception present the three mountain profiles – WSs on the rivers Belá, Javorinka (Fig. 5) and Hnilec, where the values of $Q_{a,2001-2020}$ were among the 7th to 11th highest values of the whole period.

Identifying the 10 driest years in the series of mean annual discharges of the period 1961–2020, in most evaluated WSs, 4 to 6 years are from the period 2001–2020. Taking into account the lengths of compared periods, this represents a higher frequency of occurrence of driest years from period 2001–2020 than from the reference period. The exceptions present the profiles in the northern part of Slovakia (Javorinka, Poprad with Dunajec basins) and also the Danube River, where of the 10 driest years only 2 have come from the period 2001–2020. Among the 10 driest years in the individual evaluated WSs years identified as the most numerous in the period 2001-2020 in addition to the years 2012, 2003, 2007, 2004, 2008 (evaluated as the driest in the period 2001–2015 in the partial report (Poórová et al, 2018)), the years from the other 5-years have been added: 2017, 2018 and 2019.

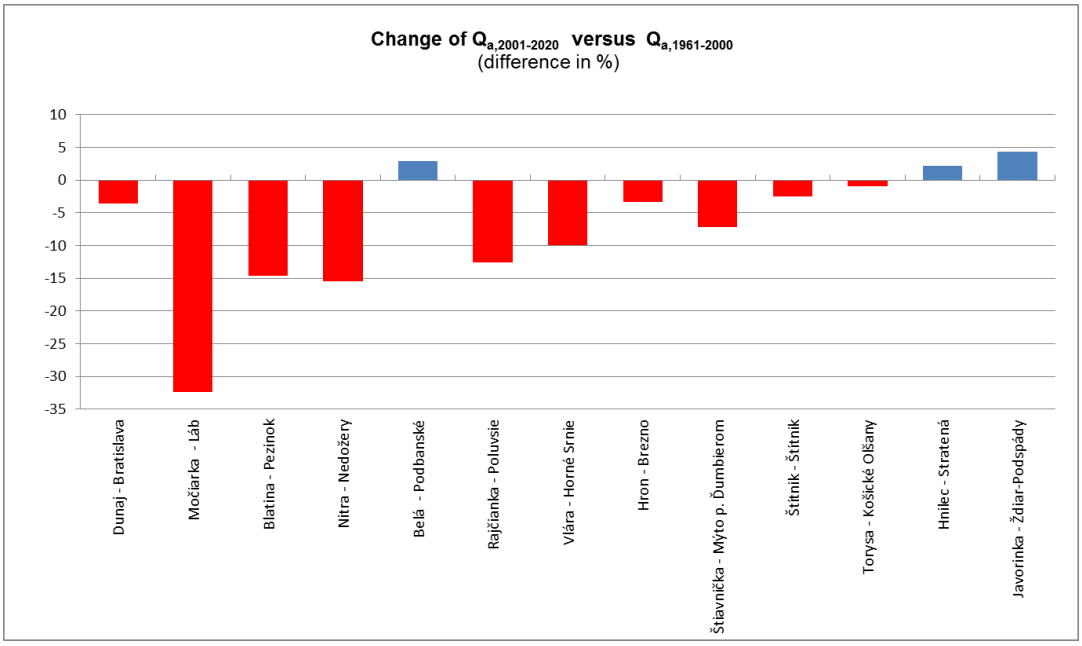

Fig. 2. The change of mean long-term discharges in the period 2001–2020 compared to reference period 1961–2000.

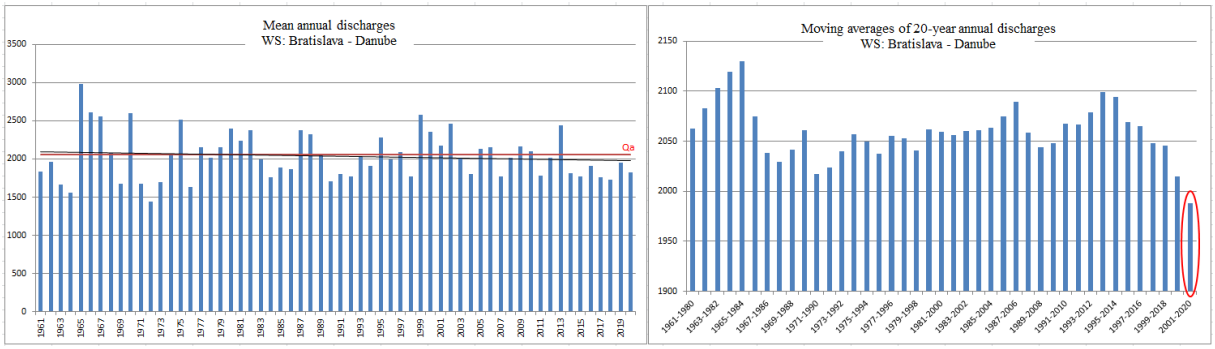

Fig. 3. Q_r series and moving averages of 20-years Q_a in the period 1961–2020, step 1 year; WS: Danube in Bratislava.

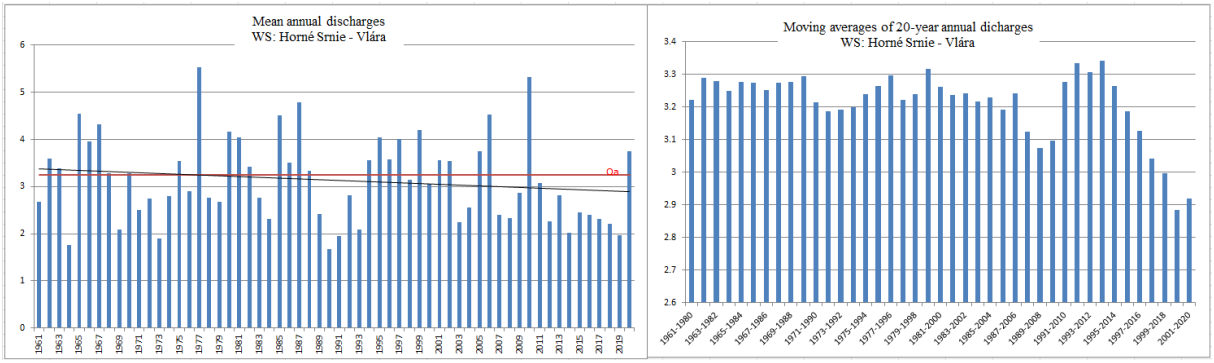

Fig. 4. Q_r series and moving averages of 20-years Q_a in the period 1961–2020, step 1 year; WS: Horné Srnie – Vlára.

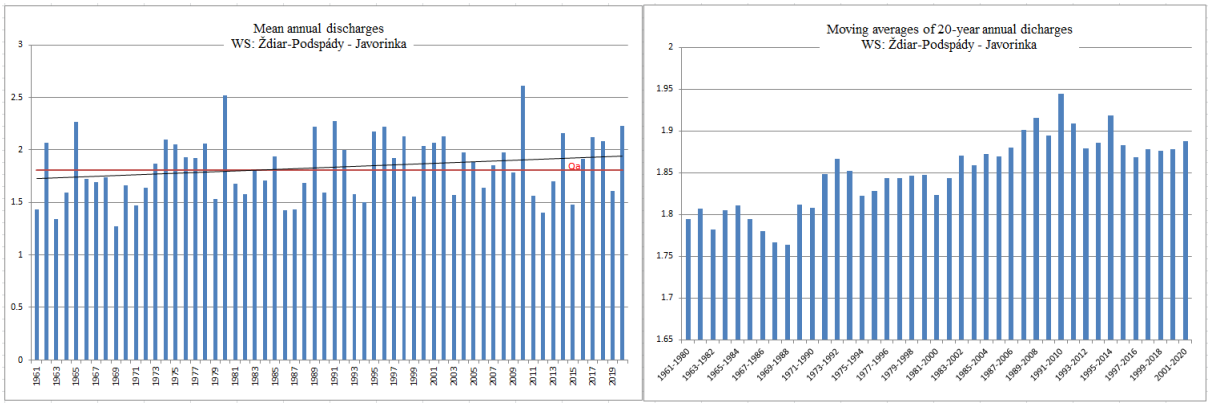

Fig. 5. Q_r series and moving averages of 20-years Q_a in the period 1961–2020, step 1 year; WS: Ždiar-Podspády – Javorinka.

When analyzing the occurrence of sub-normal mean annual discharges (Q_r <90% $Q_{a,1961-2000}$), in a larger part of the evaluated WSs the higher percentage occurrence of such years can be seen in the period 2001–2020 than in the reference period. The percentage of occurrence of such years in the period 1961–2000 among the 13 evaluated stations was about 37% on average, while in the period 2001–2020 it was almost 50%. We recorded approximately the same percentage of occurrence in both periods in 4 stations (streams Belá, Štiavnička, Torysa, Javorinka), of which only in Javorinka the share of below-average years was lower in the period 2001–2020 compared to the reference period.

Mean monthly discharges (Q_m) and long-term mean monthly discharges (Q_{ma}): When assessing monthly flows, a large part of the evaluated profiles shows an increase in long-term mean monthly discharges in the winter months (especially in January and February) in the period 2001–2020 compared to the reference period. That is considered to be a consequence of earlier snow melting, as one of the impacts of the climate change. On the contrary, the decline is visible especially in the months of April, May and also October, as we can see e.g. in the graph for WS Štítnik – Štítnik (Fig. 6).

The decrease of $Q_{ma,2001-2020}$ in WSs, where also the significant decrease of $Q_{a,2001-2020}$ has been identificated, is manifestated in most months of the year, e.g. WS Poluvsie – Rajčianka (Fig. 7). Similarly, in WSs

with increase of $Q_{a,2001-2020}$ there is prevailing number of months with increase of long-term mean monthly discharge values in this period.

Since the changes in Q_{ma} are also related to the overall change of $Q_{a,2001-2020}$ compared to the reference period, we also analyzed the changes in the runoff distribution throughout the year. The changes identified in the evaluation of the period 2001–2020 in comparison with the reference period 1961–2000 have confirmed in most of the evaluated stations the results of analyzes of period 2001–2015 (Blaškovičová et al., 2019), i.e. transfer of part of the spring runoff (typical maxima in the regimes of Slovak streams in March and April) to the previous (winter) months (Fig. 8), but in some cases also to the summer months. The increase in the share of runoff in the months of January to March and the subsequent decrease in the spring months compared to the reference period, passing in the part of the evaluated WSs to the summer months, is noticeable.

Again the difference is in the WSs on the streams in the mountain areas of northern Slovakia (Podbanské – Belá, Ždiar-Podspády – Javorinka), where no significant change in the distribution of runoff was recorded in the evaluated period compared to the period 1961–2000.

Average monthly discharges classified according to water category (Table 2) in the evaluated and reference period also allow the assessment of changes in the frequency of occurrence of significantly below-average values (<60%) in the evaluated period compared to the reference period.

The occurrence of extremely dry average monthly discharges (less than 20% Q_{ma}) in some of the WSs has been not recorded at all in any of the evaluated periods (6 WSs, mostly mountain streams – Hron in Brezno, Štiavnička, Hnilec, Javorinka, and larger streams – Danube, Nitra). In other 4 WSs, a rare occurrence of such values was recorded in the reference period (1 to 4 occurrences in the period), but in the period 2001–2020 they were not recorded at all. Of the remaining three evaluated WSs, in two of them there was an increase in the incidence of extremely dry months in the period 2001–2020 compared to the reference period in terms of the length of the period (Blatina by 21%, Vlára by up to 271%), in WS Štítnik – Štítnik there was a decrease of 67% (in the reference period there were a total of 6 occurrences, in the period 2001–2020 only 1).

Dry months (Q_m < 40% Q_{ma}) were not recorded only on the Danube in the evaluated periods. The steadiness of this significantly larger river in comparison with other rivers in Slovakia can be seen in Fig. 9, with color differentiation of the monthly discharge relative values (Q_m / $Q_{ma,1961-2000}$); in the right part of the table the values are sorted from the smallest monthly values to the largest for individual months in both periods. It is obvious that in addition to the absence of Q_m / Q_{ma} < 40%, resp. 20% of long-term values there is also the rare occurrence of opposite extremes – relative monthly discharges greater than 200% Q_{ma}.

In other evaluated WSs, the increase in the frequency of occurrence of Q_m < 40% $Q_{ma,1961-2000}$ prevailed – in 6 WSs (the largest increase in WS Nedožery-Nitra (by 270%) and WS Poluvsie – Rajčianka (by 200%)). The largest increases in the frequency of dry months in individual calendar months prevailed in April, alternatively also in the summer months. There were 5 WSs without change, or only with minor changes in the frequency of occurrence (changes up to 10%, mostly an increase in the frequency of occurrence). Only in one WS (Ždiar-Podspády – Javorinka) a decrease in the frequency of Q_m < 40% Q_{ma} (by -56%) was recorded.

In the frequency of subnormal months (Q_m < 60% $Q_{ma,1961-2000}$), we recorded a predominant increase (in 8 WS), on average by 46%. In 3 WSs there were changes up to 10% (2x decrease, 1x increase) and in 2 WSs there was a decrease (by 13% and 39%). In general, the increase in the frequency of occurrence in April prevailed. We recorded a decrease in the frequency of occurrence of monthly flows less than 60% of Q_{ma} on the Torysa and Javorinka streams; the mountain streams Belá, Štiavnička and Hnilec were almost unchanged.

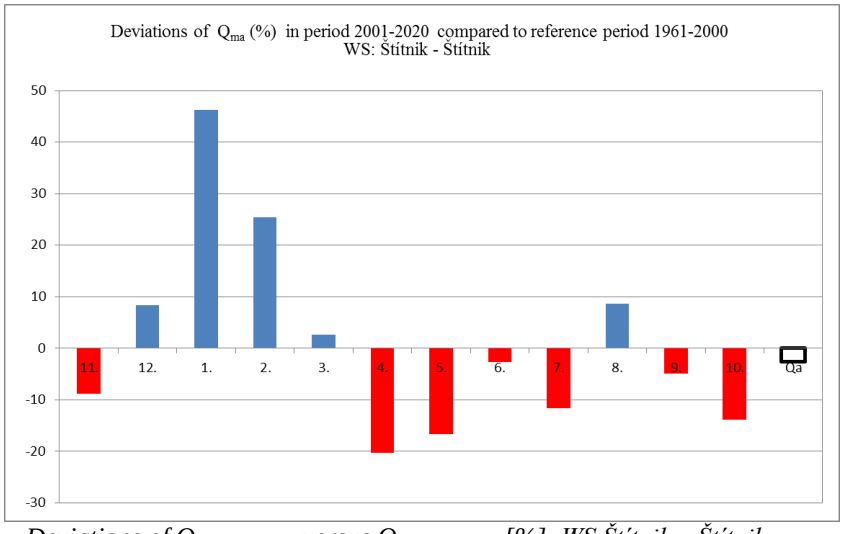

Fig. 6. Deviations of $Q_{ma,2001-2020}$ versus $Q_{ma,1961-2000}$ [%], WS Štítnik – Štítnik.

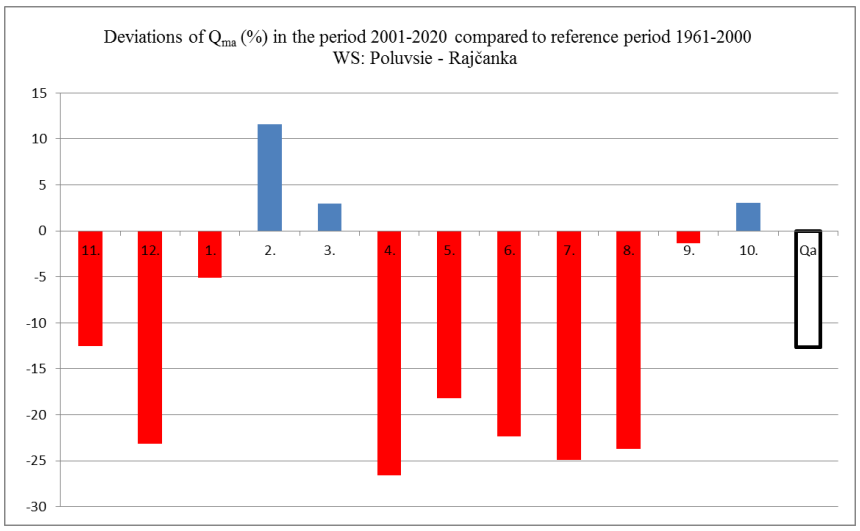

Fig. 7. Deviations of $Q_{ma,2001-2020}$ versus $Q_{ma,1961-2000}$ [%], WS Poluvsie –Rajčianka.

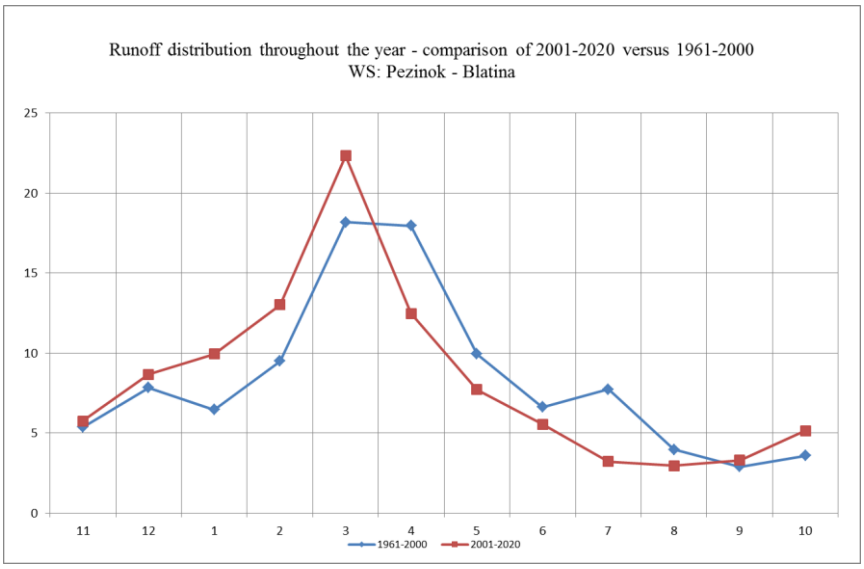

Fig. 8. The change of runoff distribution throughout the year [%] in the period 2001–2000 compared to the reference period; WS Pezinok – Blatina.

Table 2. Categories of mean monthly discharges (% of corresponding long-term $Q_{ma,1961-2000}$)

Category % Q_{ma}	Description
0–20	Extremely dry month
21–40	Dry month
41–60	Significantly subnormal month
61–80	Subnormal month
81–120	Normal month
121–160	Above normal month
161–200	Significantly wet month
> 200	Extremely wet month

Mesiac:	11.	12.	1.	2.	3.	4.	5.	6.	7.	8.	9.	10.
1961	98.7	76.9	66.0	119.9	86.1	82.1	104.1	109.6	79.3	95.8	71.1	63.2
1962	65.9	107.8	95.9	105.7	78.7	107.9	127.2	116.8	91.1	81.8	68.1	59.9
1963	66.3	59.4	58.4	47.0	98.0	101.4	88.3	87.4	75.4	78.0	100.7	90.1
1964	85.4	56.9	48.5	54.5	66.9	86.6	96.7	69.3	64.8	73.7	79.5	124.0
1965	159.1	95.3	93.7	74.0	123.4	150.0	192.1	259.5	152.2	117.9	124.8	89.7
1966	73.3	117.7	95.9	146.7	95.7	107.0	112.2	109.6	175.8	202.3	153.6	104.0
1967	108.6	148.7	149.2	142.3	139.1	125.8	126.3	140.9	112.7	90.8	107.5	88.1
1968	77.2	84.2	126.7	101.8	90.7	103.9	77.5	80.4	93.5	127.3	110.4	167.4
1969	86.7	63.4	71.8	78.7	87.7	84.5	81.0	82.2	81.1	91.0	91.8	66.2
1970	64.5	54.9	62.2	148.4	118.8	142.7	141.3	142.4	122.9	180.5	136.8	149.1
1971	137.4	104.9	76.5	73.5	77.3	83.1	68.1	89.6	71.4	64.8	72.8	72.8
1972	65.1	73.8	58.3	52.7	44.6	69.3	67.6	76.2	92.8	94.3	63.9	65.6
1973	119.2	74.2	55.8	62.4	70.4	87.7	113.7	90.9	75.4	66.5	68.3	88.4
1974	113.8	103.8	132.1	107.0	86.4	65.2	75.4	104.8	130.9	96.2	86.3	119.5
1975	115.9	217.6	167.7	109.6	70.4	89.3	108.2	100.3	186.5	114.7	111.5	84.2
1976	77.9	67.7	153.3	80.8	59.8	62.1	69.1	85.2	57.3	81.1	100.3	86.2
1977	85.7	85.6	76.8	181.7	133.9	106.3	107.3	79.6	76.8	141.6	104.6	78.7
1978	94.0	88.2	84.1	68.4	120.9	86.1	98.5	89.9	108.1	93.1	107.0	136.1
1979	85.0	73.8	78.2	104.1	126.3	117.6	107.5	127.8	107.5	102.9	100.6	90.8
1980	143.5	144.4	87.7	138.4	72.8	116.7	112.5	113.0	142.5	107.5	101.5	123.4
1981	97.9	99.7	110.9	108.4	155.2	106.6	78.2	74.5	118.3	104.3	102.0	177.1
1982	173.8	156.5	175.9	143.4	97.7	95.4	102.6	112.6	94.9	100.0	86.0	93.3
1983	78.5	89.5	157.8	113.9	102.6	112.5	96.4	93.4	77.9	85.6	81.7	79.0
1984	63.3	76.4	89.2	85.8	62.8	80.5	82.4	81.2	81.1	90.1	130.2	115.4
1985	72.7	63.0	60.6	117.4	79.3	77.3	94.5	94.5	81.7	158.6	113.6	73.6
1986	71.8	96.0	145.3	78.5	83.6	101.2	102.8	101.3	70.9	78.9	76.4	75.2
1987	74.9	66.4	119.2	108.6	129.9	128.3	122.0	134.9	129.4	128.9	103.0	91.3
1988	93.7	136.3	102.0	92.6	165.4	167.2	109.9	95.5	81.3	90.5	122.6	86.6
1989	89.3	187.2	125.1	96.9	88.5	83.7	77.9	77.5	99.4	99.3	109.2	112.3
1990	98.6	85.2	70.1	106.4	102.1	69.1	69.0	80.6	97.2	61.6	83.2	85.8
1991	114.2	77.5	111.5	55.7	67.2	48.1	79.0	98.4	105.1	152.0	66.2	69.1
1992	75.7	100.7	88.7	88.1	112.6	103.4	102.9	82.1	67.4	58.8	68.7	78.7
1993	163.2	137.6	101.1	73.7	96.2	87.5	70.1	69.5	108.5	96.2	114.2	110.4
1994	83.4	120.7	132.2	89.5	110.5	126.4	96.0	84.6	64.0	62.1	79.5	68.3
1995	90.3	85.3	115.1	128.5	99.9	127.4	102.4	139.1	97.0	84.8	156.6	93.0
1996	113.9	101.2	88.6	59.4	67.9	92.7	108.3	76.7	90.7	82.7	142.3	167.1
1997	139.8	94.7	71.1	86.7	114.4	89.0	96.5	77.6	164.0	97.9	74.9	103.3
1998	75.2	106.5	87.5	64.2	88.3	77.5	64.2	72.6	83.2	72.3	128.5	144.6
1999	220.6	120.9	107.6	140.8	162.1	113.4	158.4	113.5	106.5	85.3	92.3	96.2
2000	86.0	99.5	101.7	164.0	166.0	137.8	111.8	84.4	83.4	108.3	107.7	132.4
2001	97.4	80.0	95.7	103.2	147.3	114.4	95.2	106.0	86.7	79.5	163.8	100.6
2002	97.5	122.8	123.0	140.7	163.3	91.2	87.2	80.9	71.9	193.0	131.4	183.6
2003	248.8	154.9	184.0	102.9	96.6	69.8	76.5	64.9	50.9	50.9	68.1	113.8
2004	68.0	57.2	113.9	108.9	93.1	90.2	78.4	100.7	85.1	72.9	88.6	96.1
2005	95.3	65.4	90.7	103.6	122.8	118.6	107.2	73.1	109.3	135.3	106.6	101.3
2006	67.6	67.3	67.1	74.9	128.2	186.9	123.1	115.5	72.1	118.2	96.2	77.8
2007	100.5	62.9	99.3	94.3	97.6	58.2	64.0	64.3	75.5	71.4	186.7	105.3
2008	145.6	127.4	106.5	79.4	109.6	96.1	92.5	83.4	91.5	97.7	79.8	82.0
2009	79.1	87.8	66.4	65.1	140.9	135.2	101.3	119.4	129.0	95.9	94.6	97.0
2010	96.9	88.3	87.2	76.0	101.0	72.4	90.2	142.5	91.5	132.7	132.3	98.9
2011	95.7	111.6	172.9	95.0	71.4	59.6	52.0	65.6	79.5	92.2	84.1	120.5
2012	66.7	79.6	164.1	88.3	115.3	87.0	86.4	112.0	86.4	76.7	113.3	111.6
2013	105.7	117.7	170.8	147.7	100.6	101.9	102.8	191.7	84.8	73.1	120.8	114.8
2014	128.1	80.3	78.2	70.5	55.7	55.4	94.2	63.2	73.4	115.9	144.5	137.0
2015	112.7	78.4	144.9	79.9	77.3	92.1	109.2	86.6	58.5	58.4	65.4	79.5
2016	66.9	69.7	75.0	135.6	78.9	71.6	82.0	118.8	106.4	107.1	94.5	92.0
2017	100.0	66.1	60.7	87.7	106.6	72.1	88.5	58.5	70.9	95.8	127.5	112.0
2018	127.9	103.0	187.1	102.1	73.3	86.9	72.8	68.1	56.1	49.0	69.1	68.4
2019	62.3	97.0	123.2	98.8	130.2	85.3	108.2	112.4	67.7	77.1	80.0	89.2
2020	92.9	75.0	72.7	136.7	92.1	56.5	58.8	81.8	84.2	102.7	110.5	136.4

11.	12.	1.	2.	3.	4.	5.	6.	7.	8.	9.	10.
63.3	54.9	48.5	47.0	44.6	48.1	64.2	69.3	57.3	58.8	63.9	59.9
64.5	56.9	55.8	52.7	59.8	62.1	67.6	69.5	64.0	61.6	66.2	63.2
65.1	59.4	58.3	54.5	62.8	65.2	68.1	72.6	64.8	62.1	68.1	65.6
65.9	63.0	58.4	55.7	66.9	69.1	69.0	74.5	67.4	64.8	68.3	66.2
66.3	63.4	60.6	59.4	67.2	69.3	69.1	76.2	70.9	66.5	68.7	68.3
71.8	66.4	62.2	62.4	67.9	77.3	70.1	76.7	71.4	72.3	71.1	69.1
72.7	67.7	66.0	64.2	70.4	77.5	75.4	77.5	75.4	73.7	72.8	72.8
73.3	73.8	70.1	68.4	70.4	80.5	77.5	77.6	75.4	78.0	74.9	73.6
74.9	73.8	71.1	73.5	72.8	82.1	77.9	79.6	76.8	78.9	76.4	75.2
75.2	74.2	71.8	73.7	77.3	83.1	78.2	80.4	77.9	81.1	79.5	78.7
75.7	76.4	76.5	74.0	78.7	83.7	79.0	80.6	79.3	81.8	79.5	78.7
77.2	76.9	76.8	78.5	79.3	84.5	81.0	81.2	81.1	82.7	81.7	79.0
77.9	77.5	78.2	78.7	83.6	86.1	82.4	82.1	81.1	84.8	83.2	84.2
78.5	84.2	84.1	80.8	86.1	86.6	88.3	82.2	81.3	85.3	86.0	85.8
83.4	85.2	87.5	85.8	86.4	87.5	94.5	84.4	81.7	85.6	86.3	86.2
85.0	85.3	87.7	86.7	87.7	87.7	96.0	84.6	83.2	90.1	91.8	86.6
85.4	85.6	88.6	88.1	88.3	89.0	96.4	85.2	83.4	90.5	92.3	88.1
85.7	88.2	88.7	89.5	88.5	89.3	96.5	87.4	90.7	90.8	100.3	88.4
86.0	89.5	89.2	92.6	90.7	92.7	96.7	89.6	91.1	91.0	100.6	89.7
86.7	94.7	93.7	96.9	95.7	95.4	98.5	89.9	92.8	93.1	100.7	90.1
89.3	95.3	95.9	101.8	96.2	101.2	102.4	90.9	93.5	94.3	101.5	90.8
90.3	96.0	95.9	104.1	97.7	101.4	102.6	93.4	94.9	95.8	102.0	91.3
93.7	99.5	101.1	105.7	98.0	103.4	102.8	94.5	97.0	96.2	103.0	93.0
94.0	99.7	101.7	106.4	99.9	103.9	102.9	95.5	97.2	96.2	104.6	93.3
97.9	100.7	102.0	107.0	102.1	106.3	104.1	98.4	99.4	97.9	107.0	96.2
98.6	101.2	107.6	108.4	102.6	106.6	107.3	100.3	105.1	99.3	107.5	103.3
98.7	103.8	110.9	108.6	110.5	107.0	107.5	101.3	106.5	100.0	107.7	104.0
108.6	104.9	111.5	109.6	112.6	107.9	108.2	104.8	107.5	102.9	109.2	110.4
113.8	106.5	115.1	113.9	114.4	112.5	108.3	109.6	108.1	104.3	110.4	112.3
113.9	107.8	119.2	117.4	118.8	113.4	109.9	109.6	108.5	107.5	111.5	115.4
114.2	117.7	125.1	119.9	120.9	116.7	111.8	112.6	112.7	108.3	113.6	119.5
115.9	120.7	126.7	128.5	123.4	117.6	112.2	113.0	118.3	114.7	114.2	123.4
119.2	120.9	132.1	138.4	126.3	125.8	112.5	113.5	122.9	117.9	122.6	124.0
137.4	136.3	132.2	140.8	129.9	126.4	113.7	116.8	129.4	127.3	124.8	132.4
139.8	137.6	145.3	142.3	133.9	127.4	122.0	127.8	130.9	128.9	128.5	136.1
143.5	144.4	149.2	143.4	139.1	128.3	126.3	134.9	142.5	141.6	130.2	144.6
159.1	148.7	153.3	146.7	155.2	137.8	127.2	139.1	152.2	152.0	136.8	149.1
163.2	156.5	157.8	148.4	162.1	142.7	141.3	140.9	164.0	158.6	142.3	167.1
173.8	187.2	167.7	164.0	165.4	150.0	158.4	142.4	175.8	180.5	153.6	167.4
220.6	217.6	175.9	181.7	166.0	167.2	192.1	259.5	186.5	202.3	156.6	177.1
62.3	57.2	60.7	65.1	55.7	55.4	52.0	58.5	50.9	49.0	65.4	68.4
66.7	62.9	66.4	70.5	71.4	56.5	58.8	63.2	56.1	50.9	68.1	77.8
66.9	65.4	67.1	74.9	73.3	58.2	64.0	64.3	58.5	58.4	69.1	79.5
67.6	66.1	72.7	76.0	77.3	59.6	72.8	64.9	67.7	71.4	79.8	82.0
68.0	67.3	75.0	79.4	78.9	69.8	76.5	65.6	70.9	72.9	80.0	89.2
79.1	69.7	78.2	79.9	92.1	71.6	78.4	68.1	71.9	73.1	84.1	92.0
92.9	75.0	87.2	87.7	93.1	72.1	82.0	73.1	72.1	76.7	88.6	96.1
95.3	78.4	90.7	88.3	96.6	72.4	86.4	80.9	73.4	77.1	94.5	97.0
95.7	79.6	95.7	94.3	97.6	85.3	87.2	81.8	75.5	79.5	94.6	98.9
96.9	80.0	99.3	95.0	100.6	86.9	88.5	83.4	79.5	92.2	96.2	100.6
97.4	80.3	106.5	98.8	101.0	87.0	90.2	86.6	84.2	95.8	106.6	101.3
97.5	87.8	113.9	102.1	106.6	90.2	92.5	100.7	84.8	95.9	110.5	105.3
100.0	88.3	123.0	102.9	109.6	91.2	94.2	106.0	85.1	97.7	113.3	111.6
100.5	97.0	123.2	103.2	115.3	92.1	95.2	112.0	86.4	102.7	120.8	112.0
105.7	103.0	144.9	103.6	122.8	96.1	101.3	112.4	86.7	107.1	127.5	113.8
112.7	111.6	164.1	108.9	128.2	101.9	102.8	115.5	91.5	115.9	131.4	114.8
127.9	117.7	170.8	135.6	130.2	114.4	107.2	118.8	91.5	118.2	132.3	120.5
128.1	122.8	172.9	136.7	140.9	118.6	108.2	119.4	106.4	132.7	144.5	136.4
145.6	127.4	184.0	140.7	147.3	135.2	109.2	142.5	109.3	135.3	163.8	137.0
248.8	154.9	187.1	147.7	163.3	186.9	123.1	191.7	129.0	193.0	186.7	183.6

Fig. 9. Relative values of mean monthly discharges $Q_m/Q_{ma,1961\text{-}2000}$ and their sorting by categories (on the right) in both assessed periods (WS Bratislava – Danube).

Mesiac:	11.	12.	1.	2.	3.	4.	5.	6.	7.	8.	9.	10.
1961	81.8	85.6	76.9	102.1	77.3	110.4	60.4	121.6	83.7	43.5	27.5	38.2
1962	102.9	99.4	110.7	49.9	133.3	181.2	222.5	101.0	51.5	38.8	40.7	31.5
1963	164.9	75.8	110.8	50.8	155.4	92.0	130.8	103.5	43.8	53.2	81.5	157.1
1964	112.8	34.0	44.4	33.8	72.4	48.4	33.3	39.8	86.8	29.4	19.4	117.6
1965	83.3	73.8	93.2	89.0	115.1	112.0	263.6	438.7	169.8	175.9	79.8	39.5
1966	56.4	166.5	86.7	206.2	63.6	61.8	82.2	105.3	289.0	278.2	142.9	61.0
1967	93.8	194.8	110.5	237.6	234.4	119.7	56.7	53.3	20.8	21.0	41.1	25.1
1968	28.2	89.5	93.0	205.2	101.8	48.7	44.3	99.6	37.4	140.0	222.0	158.5
1969	76.9	46.9	86.3	141.7	79.7	51.1	29.8	28.3	25.8	49.2	28.5	13.8
1970	46.4	18.3	62.7	28.6	161.4	210.9	64.6	82.6	227.0	94.6	49.7	76.8
1971	173.3	76.2	116.0	55.7	70.7	81.2	95.5	72.7	49.9	27.3	35.8	25.0
1972	31.7	63.2	38.4	27.8	22.3	59.8	105.8	72.8	401.8	325.5	125.8	66.1
1973	72.6	44.6	27.3	93.0	73.9	101.9	49.6	27.5	23.8	27.9	29.7	28.7
1974	33.3	83.3	162.1	77.9	18.6	20.8	26.9	86.8	84.7	84.9	91.5	632.1
1975	150.6	326.5	126.5	40.6	50.6	93.7	60.7	102.5	173.6	94.8	51.6	85.3
1976	47.6	67.0	261.4	61.0	59.9	85.5	120.8	82.9	48.9	56.8	70.7	71.3
1977	130.9	282.3	133.1	321.5	78.6	188.9	150.5	70.8	43.6	475.7	133.6	56.0
1978	287.4	48.7	62.6	76.8	55.4	129.8	116.4	45.9	43.7	45.7	54.9	100.3
1979	29.4	76.8	108.6	121.9	79.8	72.5	96.4	113.5	46.8	63.8	74.0	30.7
1980	159.8	187.0	56.9	124.4	69.8	147.5	138.8	52.6	202.7	164.4	215.0	220.2
1981	134.9	167.0	119.5	85.6	224.8	55.4	66.8	58.2	81.1	71.4	137.1	242.3
1982	173.2	134.7	226.9	44.1	101.8	58.0	72.1	64.0	169.7	118.5	69.5	48.9
1983	29.1	66.1	163.2	88.1	119.4	119.5	87.5	37.9	34.2	23.9	26.9	28.8
1984	20.9	25.1	26.1	65.4	67.7	93.1	125.2	46.1	42.3	57.4	274.9	161.4
1985	255.1	54.2	85.7	77.2	157.3	60.7	202.5	186.4	68.7	653.4	89.0	45.5
1986	134.8	164.6	159.5	87.3	115.3	71.7	45.7	231.5	34.7	71.3	68.2	48.2
1987	30.2	45.3	112.1	322.1	96.5	158.4	254.1	319.4	66.0	79.8	53.4	45.6
1988	100.5	170.9	94.9	81.1	159.5	130.3	77.3	52.6	27.8	33.4	100.9	28.1
1989	24.0	183.2	75.4	123.6	59.9	49.4	76.8	38.8	30.8	49.8	50.7	34.0
1990	28.4	73.0	23.7	35.3	47.5	77.2	78.5	49.1	51.0	21.0	102.2	40.3
1991	142.4	80.5	80.0	24.4	55.3	40.2	107.0	61.4	33.0	50.0	24.8	17.9
1992	118.1	26.1	123.8	134.6	157.2	90.3	52.8	30.8	19.4	9.3	17.6	29.2
1993	25.5	57.0	107.7	23.2	134.4	79.1	26.0	30.4	22.9	25.5	36.0	69.7
1994	31.7	116.5	214.7	78.8	62.1	196.9	174.1	136.1	34.6	45.3	36.5	61.5
1995	71.0	118.2	135.7	147.6	101.5	155.3	188.1	186.8	55.4	40.3	165.4	49.8
1996	105.0	76.3	85.8	14.5	63.5	156.8	180.6	124.4	144.6	96.1	399.3	205.3
1997	158.4	61.1	32.4	114.2	48.9	92.9	103.5	93.0	747.5	114.3	116.1	74.2
1998	150.7	114.1	51.8	37.5	31.4	73.8	34.1	38.5	35.8	24.4	555.0	678.6
1999	263.5	95.2	83.1	69.7	226.2	107.8	56.8	279.0	91.0	73.0	38.3	40.7
2000	38.4	30.7	29.8	200.0	195.8	115.2	40.7	33.8	54.5	51.6	22.7	15.3
2001	138.5	49.0	95.1	54.8	128.7	134.0	50.8	26.7	306.8	97.6	333.3	75.4
2002	82.4	24.1	193.7	226.6	58.0	48.1	42.7	39.1	79.4	160.2	91.2	462.8
2003	209.0	94.3	193.0	38.1	48.3	55.7	29.7	42.6	35.4	12.9	10.4	22.7
2004	20.7	37.7	80.9	132.5	123.9	48.3	55.0	128.0	53.9	40.5	31.8	49.4
2005	123.2	63.6	155.9	42.8	167.3	180.9	166.3	46.0	74.0	140.1	62.0	30.6
2006	27.4	76.7	99.3	89.0	256.8	275.7	182.6	90.3	47.7	82.1	62.2	40.6
2007	90.2	34.1	102.6	104.3	121.2	41.9	33.8	58.6	33.1	37.3	127.5	48.2
2008	145.0	90.9	123.0	48.7	71.1	57.8	51.6	30.7	47.5	131.4	39.4	35.6
2009	26.7	59.1	76.0	42.3	268.5	71.5	25.1	31.2	44.5	22.8	21.7	87.1
2010	117.1	128.8	137.5	159.3	83.9	65.1	356.9	426.3	83.8	127.9	459.3	108.5
2011	146.0	236.1	139.3	64.5	37.6	42.5	55.6	46.0	219.3	159.6	41.3	34.6
2012	15.9	18.3	112.4	100.5	149.1	38.6	23.7	47.5	28.9	19.4	22.9	96.7
2013	59.4	42.5	55.6	145.2	107.5	134.5	72.0	97.6	16.2	25.0	139.0	40.4
2014	54.0	51.5	46.4	58.1	24.1	29.0	43.3	19.1	32.1	123.5	418.3	237.3
2015	113.7	84.9	151.9	110.0	61.3	100.5	42.2	22.8	15.1	43.9	31.7	21.6
2016	53.1	54.9	55.2	184.0	44.1	45.2	54.1	26.8	41.2	250.7	47.7	70.5
2017	76.7	53.1	33.7	130.3	53.4	114.6	113.0	22.9	18.8	16.4	58.4	111.8
2018	167.9	139.5	198.2	58.3	52.7	27.1	28.2	15.0	12.4	9.0	29.7	16.5
2019	11.7	18.8	34.8	140.8	63.9	20.4	177.8	44.4	19.4	21.2	38.9	40.0
2020	60.0	58.5	31.9	147.9	63.7	22.9	24.6	233.9	65.8	49.4	172.0	1026.3

11.	12.	1.	2.	3.	4.	5.	6.	7.	8.	9.	10.
20.9	18.3	23.7	14.5	18.6	20.8	26.0	27.5	19.4	9.3	17.6	13.8
24.0	25.1	26.1	23.2	22.3	40.2	26.9	28.3	20.8	21.0	19.4	15.3
25.5	26.1	27.3	24.4	31.4	48.4	29.8	30.4	22.9	21.0	22.7	17.9
28.2	30.7	29.8	27.8	47.5	48.7	33.3	30.8	23.8	23.9	24.8	25.0
28.4	34.0	32.4	28.6	48.9	49.4	34.1	33.8	25.8	24.4	26.9	25.1
29.1	44.6	38.4	33.8	50.6	51.1	40.7	37.9	27.8	25.5	27.5	28.1
29.4	45.3	44.4	35.3	55.3	55.4	44.3	38.5	30.8	27.3	28.5	28.7
30.2	46.9	51.8	37.5	55.4	58.0	45.7	38.8	33.0	27.9	29.7	28.8
31.7	48.7	56.9	40.6	59.9	59.8	49.6	39.8	34.2	29.4	35.8	29.2
31.7	54.2	62.6	44.1	59.9	60.7	52.8	45.9	34.6	33.4	36.0	30.7
33.3	57.0	62.7	49.9	62.1	61.8	56.7	46.1	34.7	38.8	36.5	31.5
38.4	61.1	75.4	50.8	63.5	71.7	56.8	49.1	35.8	40.3	38.3	34.0
46.4	63.2	76.9	55.7	63.6	72.5	60.4	52.6	37.4	43.5	40.7	38.2
47.6	66.1	80.0	61.0	67.7	73.8	60.7	52.6	42.3	45.3	41.1	39.5
56.4	67.0	83.1	65.4	69.8	77.2	64.6	53.3	43.6	45.7	49.7	40.3
71.0	73.0	85.7	69.7	70.7	79.1	66.8	58.2	43.7	49.2	50.7	40.7
72.6	73.8	85.8	76.8	72.4	81.2	72.1	61.4	43.8	49.8	51.6	45.5
76.9	75.8	86.3	77.2	73.9	85.5	76.8	64.0	46.8	50.0	53.4	45.6
81.8	76.2	86.7	77.9	77.3	90.3	77.3	70.8	48.9	51.6	54.9	48.2
83.3	76.3	93.0	78.8	78.6	92.0	78.5	72.7	49.9	53.2	68.2	48.9
93.8	76.8	93.2	81.1	79.7	92.9	82.2	72.8	51.0	56.8	69.5	49.8
100.5	80.5	94.9	85.6	79.8	93.1	87.5	82.6	51.5	57.4	70.7	56.0
102.9	83.3	107.7	87.3	96.5	93.7	95.5	82.9	54.5	63.8	74.0	61.0
105.0	85.6	108.6	88.1	101.5	101.9	96.4	86.8	55.4	71.3	79.8	61.5
112.8	89.5	110.5	89.0	101.8	107.8	103.5	93.0	66.0	71.4	81.5	66.1
118.1	95.2	110.7	93.0	101.8	110.4	105.8	99.6	68.7	73.0	89.0	69.7
130.9	99.4	110.8	102.1	115.1	112.0	107.0	101.0	81.1	79.8	91.5	71.3
134.8	114.1	112.1	114.2	115.3	115.2	116.4	102.5	83.7	84.9	100.9	74.2
134.9	116.5	116.0	121.9	119.4	119.5	120.8	103.5	84.7	94.6	102.2	76.8
142.4	118.2	119.5	123.6	133.3	119.7	125.2	105.3	86.8	94.8	116.1	85.3
150.6	134.7	123.8	124.4	134.4	129.8	130.8	113.5	91.0	96.1	125.8	100.3
150.7	164.6	126.5	134.6	155.4	130.3	138.8	121.6	144.6	114.3	133.6	117.6
158.4	166.5	133.1	141.7	157.2	147.5	150.5	124.4	169.7	118.5	137.1	157.1
159.8	167.0	135.7	147.6	157.3	155.3	174.1	136.1	169.8	140.0	142.9	158.5
164.9	170.9	159.5	200.0	159.5	156.8	180.6	186.4	173.6	164.4	165.4	161.4
173.2	183.2	162.1	205.2	161.4	158.4	188.1	186.8	202.7	175.9	215.0	205.3
173.3	187.0	163.2	206.2	195.8	181.2	202.5	231.5	227.0	278.2	222.0	220.2
255.1	194.8	214.7	237.6	224.8	188.9	222.5	279.0	289.0	325.5	274.9	242.3
263.5	282.3	226.9	321.5	226.2	196.9	254.1	319.4	401.8	475.7	399.3	632.1
287.4	326.5	261.4	322.1	234.4	210.9	263.6	438.7	747.5	653.4	555.0	678.6
11.7	18.3	31.9	38.1	24.1	20.4	23.7	15.0	12.4	9.0	10.4	16.5
15.9	18.8	33.7	42.3	37.6	22.9	24.6	19.1	15.1	12.9	21.7	21.6
20.7	24.1	34.8	42.8	44.1	27.1	25.1	22.8	16.2	16.4	22.9	22.7
26.7	34.1	46.4	48.7	48.3	29.0	28.2	22.9	18.8	19.4	29.7	30.6
27.4	37.7	55.2	54.8	52.7	38.6	29.7	26.7	19.4	21.2	31.7	34.6
53.1	42.5	55.6	58.1	53.4	41.9	33.8	26.8	28.9	22.8	31.8	35.6
54.0	49.0	76.0	58.3	58.0	42.5	42.2	30.7	32.1	25.0	38.9	40.0
59.4	51.5	80.9	64.5	61.3	45.2	42.7	31.2	33.1	37.3	39.4	40.4
60.0	53.1	95.1	89.0	63.7	48.1	43.3	39.1	35.4	40.5	41.3	40.6
76.7	54.9	99.3	100.5	63.9	48.3	50.8	42.6	41.2	43.9	47.7	48.2
82.4	58.5	102.6	104.3	71.1	55.7	51.6	44.4	44.5	49.4	58.4	49.4
90.2	59.1	112.4	110.0	83.9	57.8	54.1	46.0	47.5	82.1	62.0	70.5
113.7	63.6	123.0	130.3	107.5	65.1	55.0	46.0	47.7	97.6	62.2	75.4
117.1	76.7	137.5	132.5	121.2	71.5	55.6	47.5	53.9	123.5	91.2	87.1
123.2	84.9	139.3	140.8	123.9	100.5	72.0	58.6	65.8	127.9	127.5	96.7
138.5	90.9	151.9	145.2	128.7	114.6	113.0	90.3	74.0	131.4	139.0	108.5
145.0	94.3	155.9	147.9	149.1	134.0	166.3	97.6	79.4	140.1	172.0	111.8
146.0	128.8	193.0	159.3	167.3	134.5	177.8	128.0	83.8	159.6	333.3	237.3
167.9	139.5	193.7	184.0	256.8	180.9	182.6	233.9	219.3	160.2	418.3	462.8
209.0	236.1	198.2	226.6	268.5	275.7	356.9	426.3	306.8	250.7	459.3	1026.3

Fig. 10. Relative values of mean monthly discharges $Q_m/Q_{ma,1961\text{-}2000}$ and their sorting by categories (on the right) in both assessed periods (WS Horné Sŕnie – Vlára).

In comparison with the above picture of monthly flows on the Danube, an example of WS with less balanced monthly discharges is e.g. WS Horné Sŕnie – Vlára (Fig. 10), where we can see both the occurrence (and increase in frequency) of dry and extremely dry monthly discharges (< 40% Q_{ma}, < 20% Q_{ma}) as well as the occurrence of extremely wet months (> 200% Q_{ma}).

Flow Duration Curve (M-day discharges (Q_{Md})): Comparing the values of M-day discharges in the period 2001–2020 compared to the reference period (tab. 3) in the area of lowest discharges we have identified the increase of values of Q_{364d} in 8 WSs, from these in 1 *WS* the change is less than 5% (Danube). The decrease has been found in 5 WSs, two of them less than 5%. Similar it has been in evaluation of changes in Q_{355d}: increase in 8 WSs (in 2 WSs less than 5%), decrease in 5 WSs (in 1 WS less than 5%). For Q_{330d} the increase has been found in 7 WSs and the decrease in 6 WSs; for Q_{270d} there has been found the increase in 8 WSs and the decrease in 5 WSs.

The decrease in the smallest quantiles Q_{355d} and Q_{364d} is the largest in percentage terms in WSs Nedožery-Nitra (- 30%; -31%), Horné Sŕnie – Vlára (-25%; -43%) and Poluvsie – Rajčianka (-28%, - 15%) (Fig. 11a). These are WSs, where a decrease in Q_a in the evaluated period by more than 10% has been also recorded. The streams Močiarka and Blatina (SW Slovakia) also show a relatively significant decrease in Q_a (-32%, -15%), however, there has been identified an increase in values of the quantiles Q_{355d} and Q_{364d} (Fig. 11b).

Non-flow characteristics: The results of the evaluation of the number of days with Q_d less than or equal to the selected flow limits (calculated with respect to the different lengths of the compared periods) partially correspond to the changes in the values of M-day flows (Table 4).

For the limit $Q_{364d,1961\text{-}2000}$, the frequencies of occurrence of sublimit daily discharges in the period 2001–2020 in the already mentioned WSs on the streams Nitra, Rajčianka and Vlára (with a significant decrease in Q_a and Q_{364d} in the evaluated period) were 4.6 to 7.0 times higher than in the reference period. In other evaluated stations we recorded a significantly lower frequency of days with $Q_d \leq Q_{364d,1961\text{-}2000}$. In WS Mýto p. Ďumbierom – Štiavnička, Brezno – Hron, Pezinok - Blatina and Štítnik – Štítnik the frequency of occurrence has decreased by 40.5 to 68.6%. In 4 WSs the period 2001–2020 was even without any recorded occurrence of sublimit days and in 1 WS there was a decrease of almost 100%. These were the mountain streams Belá, Hnilec and Javorinka, and WSs Láb – Močiarka and Košické Olšany – Torysa. On the Danube in Bratislava, the frequency of occurrence of $Qd \leq Q_{364d,1961\text{-}2000}$ in the evaluated period was up to 81% lower compared to the reference period, while in the reference period of 40 years, such below-limit discharges occurred only in 5 years (1962, 1963, 1964, 1972 and 1991; months I, II and XII).

At the Q_{355d} limit, we recorded a decrease in the frequency of below-limit Q_d in 7 WSs, including the Danube River (Močiarka, Blatina, Hron, Torysa, Hnilec, Javorinka and Danube).

The increase has been significantly manifested on Rajčianka (+478%), Nitra (+341%), and Vlára (+97%); on Belá, Štiavnička and Štítnik there was an increase of 5 to 44%.

Sublimit flows for limit Q_{330d} show an increase in 7 WSs (largest on Belá (+186%) and Nitra (+150%), in other WSs there was a decrease in the frequency of occurrence ranging from -6% (Hron – Brezno) to -53% (Javorinka – Ždiar-Podspády).

At the Q_{270d} limit, the decrease in the frequency of occurrence of sublimit Q_d in the evaluated period in comparison with the reference one prevails in WSs (decrease in 9 WSs, increase in 4 WSs). The largest increase has been identified in Belá in Podbanské (+254%).

Table 3. Changes in M-day discharge kvantiles (in %) in the period 2001–2020 compared to the reference period 1961–2000 (decrease marked in light red)

Stream	WS	Q_{30d}	Q_{90d}	Q_{180d}	Q_{270d}	Q_{330d}	Q_{355d}	Q_{364d}
Dunaj	Bratislava	-5.7	-6.7	-4.5	0.3	4.4	3.5	4.5
Močiarka	Láb	-32.9	-33.9	-29.3	-27.0	-11.3	13.9	87.0
Blatina	Pezinok	-17.7	-10.2	-3.7	-4.0	-6.7	7.7	33.3
Nitra	Nedožery	-14.6	-12.9	-13.3	-26.0	-28.8	-30.0	-31.2
Belá	Podbanské	0.1	1.1	7.9	15.7	11.0	11.1	-2.9
Vlára	Horné Sŕnie	-7.8	-21.7	-19.4	-16.8	-28.3	-25.4	-43.1
Rajčianka	Poluvsie	-7.1	-12.6	-17.6	-21.7	-29.1	-27.8	-15.1
Hron	Brezno	-9.9	-3.1	9.0	5.2	0.7	4.8	8.5
Štiavnička	Mýto p. Ď.	-15.7	-2.7	4.4	8.2	2.1	-2.0	5.8
Štítnik	Štítnik	0.3	-2.4	2.4	-6.6	-2.9	-8.8	-2.1
Torysa	Košické Olšany	-12.9	-0.6	5.7	11.5	12.0	12.0	3.2
Hnilec	Stratená	-12.0	-2.0	12.2	25.1	16.7	23.0	25.0
Javorinka	Podspády	-0.3	1.1	6.9	17.6	17.4	20.8	33.2

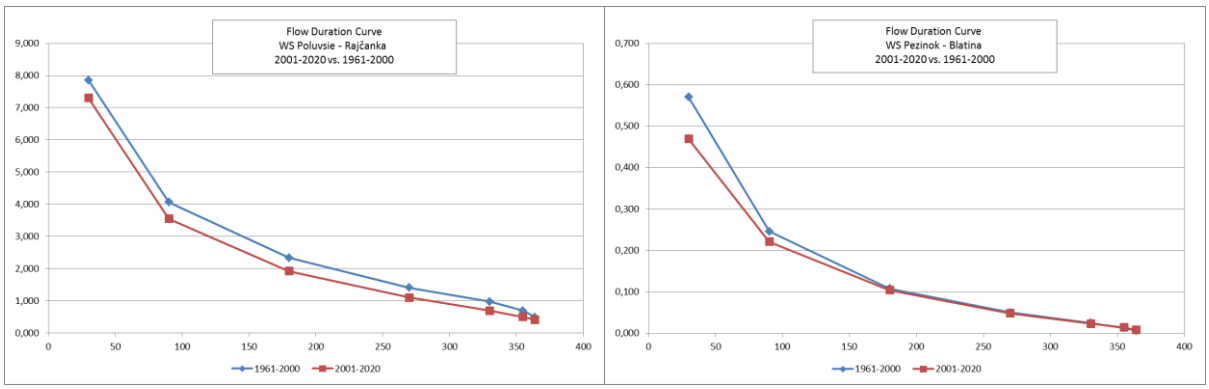

a *b*

Fig. 11. Different types of changes of Q_{Md} values in two WSs with decrease in Q_a: a) Poluvsie – Rajčianka, b) Pezinok – Blatina.

Table 4. Changes in the frequency of occurrence $Qd \leq$ limit for Q_{270d}, Q_{330d}, Q_{355d}, Q_{364d} in the period 2001–2020 compared to the reference period 1961–2000 (difference in %, converted to the same length of the period)

Stream	Water-gauging station	$Q_d \leq$ limit			
		Q_{270d}	Q_{330d}	Q_{355d}	Q_{364d}
Dunaj	Bratislava	-1.2	-21.1	-29.1	-81.1
Močiarka	Láb	74.6	72.2	-51.4	*
Blatina	Pezinok	-1.4	20.6	-7.6	-57.4
Nitra	Nedožery	39.4	149.8	341.3	547.1
Belá	Podbanské	254.2	185.6	5.2	*
Vlára	Horné Sŕnie	-4.7	36.5	97.2	361.5
Rajčianka	Poluvsie	-2.5	47.2	478.0	602.0
Hron	Brezno	-8.6	-6.2	-35.8	-65.3
Štiavnička	Mýto p. Ď.	-16.5	-15.5	18.1	-68.6
Štítnik	Štítnik	11.1	9.7	44.2	-40.5
Torysa	Košické Olšany	-15.7	-41.4	-65.4	*
Hnilec	Stratená	-35.9	-36.5	-46.6	*
Javorinka	Podspády	-23.3	-52.8	-86.8	-96.1

** without occurence of Qd ≤ limit in period 2001–2020*

Conclusion

The results of analyzes in 13 selected water-gauging stations in Slovakia, in which we compared the hydrological characteristics with respect to drought assessment, showed in the period 2001–2020 compared to the reference period 1961–2000 differences in long-term characteristics as well as changes in the occurrence of some discharge characteristics, which we classify as low-flow characteristics. Changes in comparison with the evaluation for the period 2001–2015 (in partial reports Drought assessment, SHMI), confirm the deviations of the characteristics from the reference period, in some profiles also their deepening. For example, the decrease in Q_a in the period 2001–2020 compared to the reference period 1961–2000 recorded in the evaluated WSs with the exception of mountain streams is even more pronounced in comparison with the period 2001–2015 in most stations, e.g. in WS Pezinok – Blatina the decrease in Q_a in comparison with the reference period decreased from the difference -7.6% for the period 2001–2015 to -14.7% for the period 2001–2020. Negative changes in the runoff regime have been also recorded for other characteristics, e.g. at an increased frequency of extreme flow values, as can be seen e.g. in the left part of fig. 10, where an increase in the incidence of $Q_m < 20\%\ Q_{ma,1961\text{-}2000}$ is evident in the last years of the evaluated 20-year period. Changes in the distribution of runoff are also evident in the comparison of average values from 12 stations (excluding WS Danube – Bratislava) for both periods (Fig. 12).

The changes as well as their regional differences evaluated so far only in 13 water-gauging stations point to the need for their further comprehensive evaluation in larger number of WSs on the surface flows of Slovakia

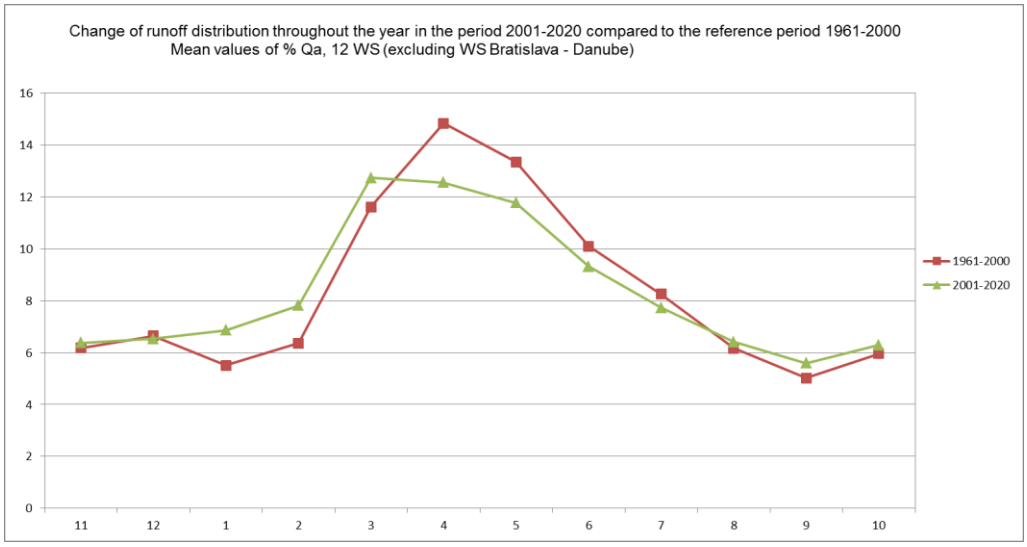

Fig. 12. Change of the runoff distribution throughout the year in the period 2001–2020 compared to the reference period 1961-2000 based on averages from values of 12 WSs.

and according to the size of the analyzed deviations and trends after 2000 and confirmation of their country-wide, resp. regional changes considering the need of changing the reference period.

References

Blaškovičová, L., Jeneiová, K., Šimor, V., Poórová, J., Melová, K., Podolinská, J., Liová, S., Síčová, B., Groholʼ, M., Gápelová, V., Ľupták, Ľ., Lovásová, Ľ., Magerčák, V., Paľušová, Z. (2019): Hodnotenie hydrologického sucha, časť 2: Hodnotenie zmien a trendov mesačných a ročných prietokov, partial report, SHMÚ, Bratislava, 64 p. ISBN 978-80-99929-14-3

Blaškovičová, L., Melová, K., Jeneiová, K., Podolinská, J., Liová, S., Síčová, B., Poórová, J., Šimor, V., Groholʼ, M., Slivková, K., Gápelová, V., Ľupták, Ľ., Lovásová, Ľ., Magerčák, V., Paľušová, Z. (2020): Hodnotenie hydrologického sucha, časť 3: Hodnotenie M-denných prietokov a neprietokových charakteristík, partial report, SHMÚ, Bratislava, 92 p. ISBN 978-80-99929-26-6

Blaškovičová, L., Melová, K., Danáčová, Z., Lovásová, Ľ., Šimor, V., Poórová, J. (2015): Minimum balance discharge in relation to ecological flows, Acta Hydrologica Slovaca, vol. 16, 23–30.

Fendeková, M., Poórová, J., Slivová, V. (Eds.) et al. (2017): Hydrologické sucho na Slovensku a prognóza jeho vývoja, monograph, UK Bratislava.

Fendeková, M., Ženišová, Z. (Eds) et al. (2010): Hydrogeologické sucho, monograph, Bratislava, 2010., ISBN 978-80-969342-7-0.

Poórová, J., Blaškovičová, L., Melová, K., Paľušová, Z., Jeneiová, K., Lovásová, Ľ., Podolinská, J., Šimor, V., Groholʼ, M., Gápelová, V., Ľupták, Ľ., Liová, S., Magerčák, V., Síčová, B. (2018): Hodnotenie hydrologického sucha, časť 1: Hodnotenie vodnosti roka a zmien rozdelenia odtoku v roku, partial report, SHMÚ, 110 p. ISBN 978-80-99929-09-9

Tallaksen, L., Van Lanen, H. (2004): Hydrological drought, Processes and estimationmethods for streamflow and groundwater, Elsevier, The Netherlands. ISBN-13: 978-0-444-51767-8

WMO (2008): Manual on Low Flow Estimation and Prediction, Operational Hydrology Report No. 50, World Meteorological Organization.

Ing. Lotta Blaškovičová, PhD. (corresponding author, e-mail: lotta.blaskovicova@shmu.sk)
Mgr. Katarína Melová, PhD.
Slovak Hydrometeorological Institute
Jeséniova 17
833 15 Bratislava
Slovak Republic

Ing. Soňa Liová
Slovak Hydrometeorological Institute
Regional Office Žilina
Bôrická cesta 103
011 13 Žilina
Slovak Republic

RNDr. Jana Podolinská
Slovak Hydrometeorological Institute
Regional Office Banská Bystrica
Zelená 5
974 04 Banská Bystrica
Slovak Republic

Ing. Beáta Síčová
Ing. Martin Groholʼ
Slovak Hydrometeorological Institute
Regional Office Košice
Ďumbierska 26
041 17 Košice
Slovak Republic

DOI: 10.31577/ahs-2022-0023.01.0003

ACTA HYDROLOGICA SLOVACA

Volume 23, No. 1, 2022, 21 – 31

The assessment of changes in the long-term water balance in the Krupinica River basin for the period 1931–2020

Dana HALMOVÁ*, Pavla PEKÁROVÁ, Jana PODOLINSKÁ, Katarína JENEIOVÁ

The study is focused on the evaluation of changes in the hydrological balance of the Krupinica River basin to the Plášťovce station for the entire 90-year period as well as for the three 30-year subperiods 1931–1960, 1961–1990 and 1991–2020. In the first part of the study, the hydrological balance is processed in an annual step on the basis of measured series of average monthly flows from the Krupinica: Plášťovce; monthly precipitation totals on the Krupinica catchment area and average monthly temperatures in the catchment area. The hydrological balance in the monthly step was processed in the second part. Changes in water resources in the river basin over the three mentioned time subperiods were analyzed. The long-term annual precipitation total in the Krupinica River basin for the whole period was 660 mm, the annual runoff depth was 182 mm and the balance evaporation was 478 mm. A comparison of 30-year periods shows a significant decrease in the runoff of Krupinica – from 231 mm to 144 mm. This was even more pronounced in the runoff coefficient – it fell from 0.32 over 0.27 to 0.21 in the last period 1991–2020. In the third part, a simple regression relationship between runoff, precipitation and air temperature was derived to estimate the future development of the annual runoff from the basin. The relationship shows that a 100 mm decrease in precipitation in the Krupinica River basin will cause an average decrease of 52 mm in runoff. And an increase in the average annual temperature by 1°C in the Krupinica River basin results in a decrease in runoff of about 33.5 mm.

KEY WORDS: water (hydrological) balance, Krupinica River, long-term trends

Introduction

Water is essential for life. In addition to minerals, forests, fertile soils, it is another component of the country's natural wealth. Therefore, it must be managed wisely and it is necessary to monitor it, get to know it and try to understand its cycle in the country.

The time series of a hydrological components is the basic basis for assessing the regime of a hydrological process. It is possible to statistically analyse hydrological data in various steps (hourly, daily, monthly, annual, irregular). At present, the attention of hydrologists is in the first place: 1. analysis of changes in long-term runoff trends, and 2. changes in the hydrological balance in river basins. In trend analysis the parametric and non-parametric tests can be used. Generally, the zero hypothesis H0 – there is no trend has to be tested against the alternative hypothesis H1 – there is a trend. Distribution-free tests have the advantage that their power and significance are not affected by the actual distribution of the data. This is in contrast to parametric trend tests, such as the regression coefficient test, which assume that the data follow the Normal distribution, and whose power can be greatly reduced in the case of skewed data. The Mann–Kendall trend test (Mann, 1945; Kendall, 1975) based on the statistic S has therefore been widely used for testing trends in many natural time series that deviate significantly from the Normal distribution, such as temperature, rainfall, river flow, and water quality time series. Another widely used non-parametric trend test is Spearman's Rho test.

Trends of average, maximum and minimum annual discharges for the period 1877–2013 on the Danube in Bratislava were analyzed by the MK test with Blaškovičová et al. (2013). They found, that average annual flows have a balanced trend, annual low flows are on a declining trend and maxima are rising slightly. According to Pekárová et al. (2008), trends of the Danube River have a maximum of 30 days and 330 days. The difference in the maxima compared to the results of Blaškovičová was caused by the fact that in the case of Blaškovičová the water years 2010 and 2013 were already included in the analysis. Poórová et al. (2013) examined the trends of minimum annual and monthly discharges for the period 1961–2012 in Slovak river basins. According to their results, annual lows are declining in the Morava, Dolný Váh, Nitra, Hron, Ipľa, Slaná and Bodva river basins. Flows in the upper Váh, Poprad, Hornád and Bodrog river basins have an increasing trend of annual minima. Jeneiová et al.

(2015) focused on detecting changes in long-term data series of the annual peak discharges from nine stations in southern Slovakia. Trend was detected by modified MK test and Theil-Sen slope for moving time windows. It is clear from their results that the significance and magnitude of the detected trend changes with the length of the observation. Detection of changes therefore should not focus only on the statistical analysis of the time series but also in the identification of drivers behind the detected changes. Blahušiaková and Matoušková (2015; 2016) used different methods for identifying trends in data series: simple mass curve analysis, linear regression, frequency analysis of flood events, use of the Indicators of Hydrological Alteration software, and the MK test. Analyses are performed for data from two periods (1931–2010 and 1961–2010). The Mann-Kendall test shows a significant decrease in runoff in the winter period. The main causes of runoff decline are: the considerable increase in air temperature, the decrease in snow cover depth and changes in seasonal distribution of precipitation amounts. Ďurigová et al. (2019) analyzed average monthly and seasonal flows on selected Slovak streams using basic descriptive statistics, trend analysis, periodic component analysis, ARARCH model and multidimensional analysis. They found that the biggest changes in the trend and periodic component are on the Hron stream. Of the smaller river basins, in particular the Kysuca, Bystrica and Čierny Váh rivers, show statistically significant declining trends. Ďurigová and Hlavčová (2020) detected the changes in the upper Váh River basin according to decadal analysis. Their results of the air temperature analysis indicate an apparent upward trend in all the stations. Between the warmest and the coldest decades, the average difference in each river basin is 1.5°C. The precipitation regime in the earlier decades had a variable or decreasing character. Since the 1980s, there has been a slight increase. The increase in air temperature appears to affect the decreasing flow rate due to increasing evapotranspiration. The increase in precipitation in recent decades has been reflected in some stations by an increase in discharges. Šimor and Ľupták (2021) evaluated the trends for the period 1961–2000 in terms of significance and magnitude at selected water gauging stations and their possible change after the addition of 15 years (1961–2015). Trends were evaluated in a selection of 65 Slovak gauging stations with long-term observations, which was considered as unaffected. In both periods, non-significant trends prevail over significant trends in both minimum and average annual discharges, despite the occurrence of two extreme years.

To assess and better understand the evolution of water bearing is in addition to hydrological characteristic necessary assessment climatological characteristics, in particular air temperature and evaporation. Trend analysis of Zeleňáková et al. (2018) applied to precipitation and temperature monthly data for the period from 1962 to 2014 is presented for the hydrological year (from November to October) in sixteen climatic stations in Eastern Slovakia. The topography of this part of the country is very diverse and it affects the climate. The MK test coupled with Sen's slope was applied to identify the significant long-term climatic trends, as well as the magnitude of those trends. Another example of using the MK test is study of Ptak et al. (2022) where authors have determined the trends of water temperature over the study period, their magnitude, identified the break points in the data series and examined the relationships among the air temperature, river discharge and water temperature. The determination of tendencies of changes in the water temperature of the Vistula River involved the analysis of trends of changes by means of the MK test. The analysis of Holko et al. (1998; 2020) identifies the data series of Jalovecký creek that appear to exhibit trends or changes in behaviour, either in magnitude or in variability. Trends and change points detection are calculated for these time series using the MK test and the Wild Binary Segmentation method.

The MK test is based on the assumption of a linear trend in the whole observed series. However, it is also necessary to monitor long-term fluctuations – the alternation of multi-year dry and wet periods. Halmová et al. (2021) analyzed changes in N-year minimum daily discharges at selected gauging stations and long-term trends of 1- to 90-day minimum discharges at five gauging stations along the length of the Danube River and at its 5 selected significant tributaries. Average daily flows with the longest possible series of observations (since 1901 or since 1921) were used as input data. The analyzes show that there is a more or less regular alternation of water and dry periods along the entire length of the Danube. Multi-year dry seasons along the length of the Danube occur in the same periods. In contrast, on the Danube tributaries, the dry seasons are time-shifted.

After analyzing the flow trends, it is necessary to examine the effect of air temperature increase and the effect of precipitation increase / decrease on runoff. The hydrological balance is an expression of the basic relationships between the elements of the hydrological cycle. Reliable determination of the basic components of the water balance of the area (precipitation, runoff, balance evaporation) depends primarily on the accuracy of direct measurement of the first two components, from which the calculation is determined (Majerčáková et al., 1998). Considerable attention is paid to the methods of hydrological balance of forest river basins and they are described in professional hydrological and forest-hydrological literature. The hydrological balance of the six river basins of the Western and High Tatras (Roháčska, Jalovecká, Žiarska, Račkova, Tichá and Kôprová dolina) for the hydrological years 1989–1998 was prepared by Holko et al. (2001). Their results showed that even with all existing data and modern calculation methods, the existing metering network does not provide a satisfactory answer to the doubts that arise in determining the basic components of the hydrological balance in individual mountain basins. The hydrological balance of mountain river basins remains an insufficiently clarified problem. Garaj (2020) dealt with the hydrological balance of 10 Slovak river basins in his dissertation. Földes et al. (2020) detected trends and seasonal changes in the future horizons using the outputs of the Community Land Model (CLM)

scenario, which is a moderately pessimistic scenario that compares well to current processes in the atmosphere, in mountainous regions of Northern Slovakia (four selected climatological station namely: Bardejov, Červený Kláštor, Javorina and Tatranská Lomnica). This region of Slovakia belongs to a slightly warm climatic area, with a mountain climate and low temperature inversions.

Krajewski et al. (2019) investigated trends in temperature, precipitation and river-flow characteristics in a small watershed, typical for Central Poland, with 53 years of observations (1963–2015) using the Mann-Kendall test. Authors founded that this short period already allows for detecting some changes in hydro-meteorological variables. These changes could be characterized by a significant increase in the mean annual air temperature on a daily basis, and a significant decrease in the mean annual discharge on a daily basis and in the minimum annual discharge on a daily basis.

Most of the mentioned studies deal with the analysis of changes in individual components of the hydrological balance since 1961 or only since 1981. The motivation for our work was to analyze changes in individual components of the hydrological balance in a uniform way for the longest possible time period not affected by human activity.

The study is focused on the evaluation of changes in long-term trends and the hydrological balance of the Krupinica river basin to the Plášťovce station for the whole 90-year period 1931–2020, as well as for the three 30-year subperiods 1931–1960, 1961–1990 and 1991–2020. One of the partial goals was to derive a simple regression relationship between runoff, precipitation and air temperature according to which it is possible to estimate the future development of the annual runoff from the Krupinica river basin at the Plášťovce gauging station.

Material and methods

River basin description and data

The Krupinica River springs in the Javorie Mountains below the peak of Veľký Lisec. It is a right-hand tributary of the river Ipeľ. The river cuts into the Pliešovská basin, Štiavnické vrchy, Krupinská planina and Ipeľská pahorkatina. The Krupinica catchment area to Plášťovce gauging station is 302.79 km^2. The long-term average flow at the Plášťovce station in the period 1931–1960 was 2.2 m^3 s^{-1}. For the period 1931–1960, the long-term average annual air temperature in the river basin was 8.38°C. On average, 695 mm of rainfall fell in the catchment area during the hydrological year (Charakteristické hydrologické údaje slovenských tokov, 1963). From this value 229 mm drained through the river network and 466 mm evaporated. The streams in the river basin form a mostly parallel river system. Due to the not very rugged terrain, the average altitude reaches 450 m above sea level.

The average monthly values of precipitation and air temperature from the stations Banská Štiavnica (latitude 48 26 58, longitude 18 55 18; 575 m above sea level) and Bzovík (latitude 48 19 9, longitude 19 5 38; 355 m above sea level), and average monthly discharges from the gauging station Krupinica: Plášťovce for the years 1931–2020 were used to evaluate the hydrological balance.

Methods

Two non-parametric tests were used to analyze long-term trends in hydrological and meteorological data: the Mann-Kendall test (MK test coupled with Sen's slope to identify the significant long-term climatic trends, as well as the magnitude of those trends) based on the statistic S, and the Spearman's ρ (rho) test. The Mann-Kendall test estimates the gradients between each datum and all the subsequent data in a sequence and tests the null hypothesis based on the standardized sum of the number of positive gradients minus the sum of the number of negative gradients. A description of these tests can be found in a variety of papers.

The hydrological balance was carried out in two time steps: 1. in the annual step, i.e. for the calendar year; 2. for 3 30-year periods in a monthly step for the hydrological year (from November to October).

The hydrological balance quantifies the water circulation in a closed river basin system with one concentrated runoff in the final profile on the watercourse. The only entry into the river basin is atmospheric precipitation in the river basin. The difference in soil water reserves at the beginning and end of the balance period can be neglected for a sufficiently long period (year). In this case, we can identify the annual total evapotranspiration with the difference between precipitation and runoff. With the monthly balance, if we determine the monthly total evapotranspiration in an independent way, we can determine from the equation of the hydrological balance the change of water supply in the river basin in the respective month.

We used a balance equation in the form:

$$P = R + ET + \Delta S \qquad (1)$$

where

P – average annual precipitation total [mm],
R – average annual runoff [mm],
ET – balance evaporation [mm],
ΔS – average total losses Δt.

As already mentioned, the term ΔS has a higher significance in shorter time intervals Δt. In the case of a long-term balance (30 years), this term can be neglected and replaced by $\Delta S = 0$.

Calculation of monthly potential evapotranspiration

For the calculation of the long-term monthly hydrological balance for the periods of the hydrological years 1930/31–1959/60, 1960/61–1989/90, and 1990/91–2019/20, it is necessary to know the annual course of the current evapotranspiration in the studied river basin.

Evapotranspiration or evaporation data availability is low. The average monthly and annual values of potential evapotranspiration for the Banská Štiavnica station for

the period 1951–1980 can be found in tabular form in Tomlain's work (1991). In locations outside such a station, but at significantly different altitudes, the applicability of such data is limited.

We used the Thornthwaite method to calculate the average monthly values of potential evapotranspiration for the 48th parallel.

To calculate (PET) using Thornthwaite method, first the Monthly Thornthwaite Heat Index (i_m) calculation is required, using the following formula:

$$i_m = (T_m/5)^{1.514} \quad (2)$$

where

T_m – the mean monthly temperature.

The Annual Heat Index (I) is calculated, as the sum of the Monthly Heat Indices (i_m):

$$I = \sum_{m=1}^{12} i_m \, . \quad (3)$$

A Potential Evapotranspiration (PET) estimation is obtained for each month, considering a month is 30 days long and there are 12 theoretical sunshine hours per day, applying the following equation:

$$PET_{uadjusted} = 16(10t/I)^{\alpha} \quad (4)$$

where

α is:

$$\alpha = 6.75 \times 10^{-9} I^3 - 7.71 \times 10^{-7} I^2 + 1.792 \times 10^{-5} + 0.49239. \quad (5)$$

Obtained values are corrected according to the real length of the month and the theoretical sunshine hours for the latitude of interest. For latitude 50°, the values of correction coefficients are in Table 1.

Results and discussion

Development of the trend of selected characteristics of hydrological data in the Krupinica river basin

The monthly and annual precipitation total for the Krupinica River basin after Plášťovce was determined from precipitation measurements from the Banská Štiavnica and Bzovík meteorological stations for calendar years. We have data from the Bzovík station only since 1961. Therefore, for the calculation of average monthly precipitation totals in the Krupinica River basin, only data from the Banská Štiavnica station (575 m n.m.) were used, which were converted to average river basin altitude (450 m n.m.) based on the determined precipitation gradient (data were multiplied by constant 0.8465). The values of the average monthly air temperature from the Banská Štiavnica station were similarly adjusted by a gradient to the average altitude of the Krupinica River basin (data were increased by 0.6°C) (Fig. 1).

From the daily measurements of water levels at the station Krupinica: Plášťovce, the annual runoff heights R in mm from the basin were calculated. Fig. 1 shows the course of annual runoff values for the period of the calendar years 1931–2020. Subsequently, polynomial functions were used to analyze the long-term trend. During the observed period 1931–2020, the Krupinica: Plášťovce flows decreased. Despite the increase in precipitation after 1990, flows continued to decline. In this river basin, the runoff coefficient k, decreased significantly, from 0.35 to 0.2. In Fig. 1 also shows the average annual air temperatures T in the river basin and the balance evaporation ET for calendar years. The air temperature has risen sharply over the last thirty years, from 8°C to 9.5°C. The balance evaporation has a very similar course (Table 2). While the decrease in runoff until ca 1990 was due to a decrease in precipitation, after 1990 the decrease in runoff is mainly due to a sharp rise in air temperature.

The analysis of the trends of selected components in the Krupinica River basin showed different results for three shorter subperiods and for the whole 90-year period.

The trend analysis of the average annual air temperature T for three thirty-year periods showed an increasing trend at the level of significance $\alpha = 0.1$ in the years 1931–1960 and a growing trend at the level of significance $\alpha = 0.001$ in the years 1991–2020. The trend analysis of the average annual air temperature T for three thirty-year periods showed an increasing trend at the level of significance $\alpha = 0.1$ in the years 1931–1960 and a growing trend at the level of significance $\alpha = 0.001$ in the years 1991–2020. For the entire observed period, the trend at the level of significance $\alpha = 0.001$ was increasing.

In the time period 1991–2020, a growing trend of annual evapotranspiration ET was demonstrated at the level of significance $\alpha = 0.05$, and at the level of significance $\alpha = 0.1$ in the period 1931–2020.

Regarding the trend analysis of precipitation and runoff from the river basin, for the period 1991–2020 an increasing trend of precipitation P at the level of significance $\alpha = 0.05$ and a decreasing trend of runoff from the basin R for the whole period 1931–2020 at the level of significance $\alpha = 0.001$ was demonstrated.

Annual hydrological balance of the Krupinica River basin

The values of the basic components of the water balance of the Krupinica River basin calculated for the calendar years 1931–2020 and the three 30-year subperiods are given in Table 3. The long-term annual precipitation total in the Krupinica River basin for the whole period was 660 mm, and balance evaporation 478 mm.

Table 1. Monthly values of correction coefficients for monthly PET values for latitude 50°

I	II	III	IV	V	VI	VII	VIII	IX	X	XI	XII
0.74	0.78	1.02	1.15	1.33	1.36	1.37	1.25	1.06	1.01	0.78	0.74

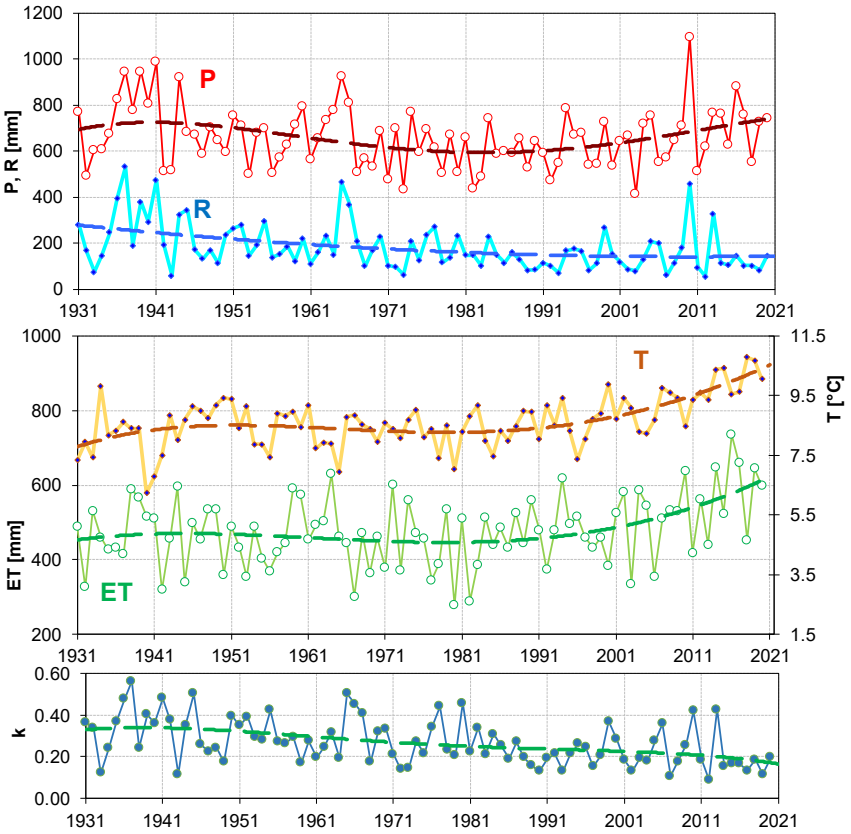

Fig. 1 Annual precipitation totals P and annual basin runoff R, over the Krupinica River basin up to Plášťovce, (upper), course of the annual evaporation ET and mean annual basin air temperature T; Runoff coefficient k (lower); time period 1931–2020. Polynomial trends.

Table 2. Results of MK test for trends of selected characteristics at Krupinica: Plášťovce (*P* – annual precipitation totals, *R* – annual basin runoff over the Krupinica basin up to Plášťovce, *ET* – annual evaporation, *T* – mean annual basin air temperature)

	Mann-Kendall trend				Sen's slope estimate	
Time series	First year	Last Year	Test Z	Signific.	A	B
T [°C]	1931	1960	1.855	+	0.033	7.452
T [°C]	1961	1990	0.642	n.s.	0.009	7.386
T [°C]	1991	2020	3.925	***	0.066	3.661
T [°C]	1931	2020	3.491	***	0.012	7.496
ET [mm]	1931	1960	0.000	n.s.	-0.261	460.7
ET [mm]	1961	1990	0.000	n.s.	-0.002	459.2
ET [mm]	1991	2020	2.319	*	5.162	141.8
ET [mm]	1931	2020	1.693	+	0.727	443.4
P [mm]	1931	1960	-0.624	n.s.	-2.000	959.5
P [mm]	1961	1990	-0.999	n.s.	-3.685	1119.6
P [mm]	1991	2020	1.998	*	5.960	-8.540
P [mm]	1931	2020	-0.812	n.s.	-0.572	834.2
R [mm]	1931	1960	-1.213	n.s.	-2.794	422.4
R [mm]	1961	1990	-1.570	n,s,	-2.333	398.3
R [mm]	1991	2020	-0.178	n.s.	-0.362	164.6
R [mm]	1931	2020	-4.224	***	-1.305	291.7

Z, Mann-Kendall test statistic; f(year) = A*(year-firstDataYear) + B
n.s, – Non-significant, +, Significant at 5%; *, Significant at 1%; **, Significant at 0.1%; ***, Significant at 0.01%

The highest runoff in the Krupinica River during the measurement period was in 1937 – 532 mm. The lowest annual runoff of 55.7 mm was in 2012. The runoff coefficient in the Krupinica River basin fluctuates from 9% to 56% with an average of 27%. A comparison of 30-year periods shows a significant decrease in the Krupinica outflow – from 231 mm to 144 mm, which was even more pronounced in the outflow coefficient. It fell from 0.32 through 0.27 to 0.21 in the last period 1991–2020.

The changes in percentiles (10-, 50-, and 90-) for annual precipitation series, air temperatures, and runoff for individual subperiods are visually compared in Fig. 2.

Table 3. **Krupinica River basin annual water balance for 4 periods 1931–1960, 1961–1990, 1991–2020, and 1931–2020. *P* – precipitation amount on basin, *R* – runoff depth, *ET* – yearly balance evaporation (*ET* = *P* - *R*), *Qa* – mean annual discharge, *q* – specific (unit) discharge, *k* – runoff coefficient, c_s – coefficient of asymmetry (decadal), c_v – variation coefficient (decadal), average annual air temperature in the Krupinica River basin**

Time period	*P* [mm]	*R* [mm]	*ET* [mm]	Q_a [$m^3 s^{-1}$]	*q* [$l s^{-1} km^{-2}$]	*k*	c_s	c_v	*T* [°C]
1931–1960	695	231	464	2.22	7.31	0.32	0.48	0.42	8.38
1961–1991	623	172	452	1.65	5.43	0.27	0.84	0.43	8.29
1991–2020	662	144	517	1.39	4.57	0.21	1.25	0.52	9.20
1931–2020	660	182	478	1.75	5.77	0.27	0.87	0.46	8.63

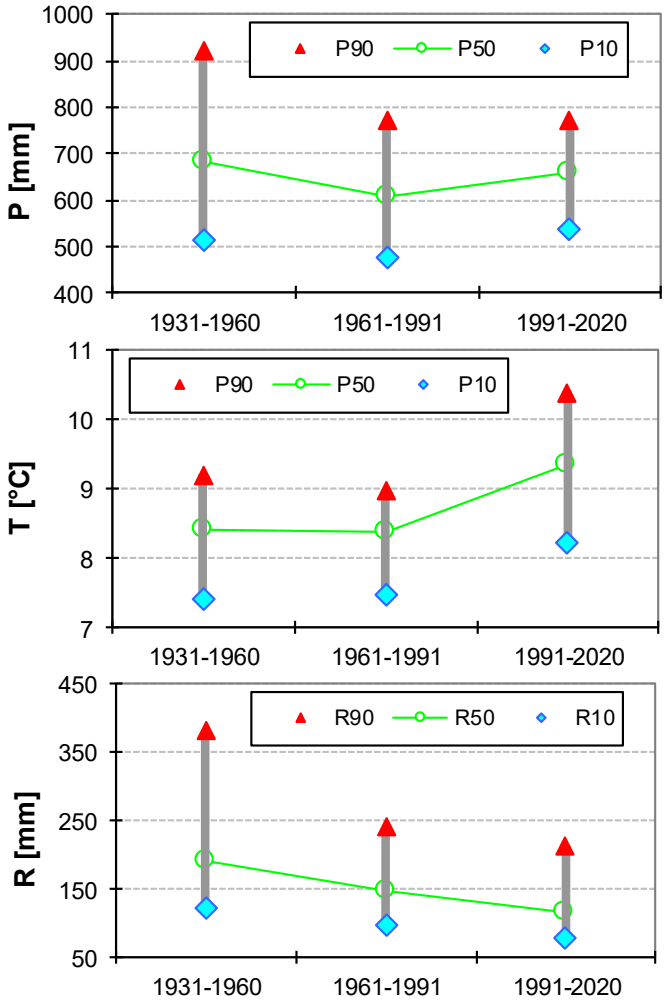

Fig. 2. The course of percentiles (10-, 50-, and 90-) for the series of annual precipitation P, air temperature T and outflow Krupinica R.

Long-term hydrological balance of monthly values in the Krupinica River basin

The Thornthwaite method was used to calculate the intra-annual distribution of potential evapotranspiration. The monthly PET, m values for the three subperiods examined are given in Table 4.

Maximum precipitation also occurs in the months with maximum evaporation and the availability of water should not be a factor modifying the annual distribution of the current evapotranspiration compared to the potential one. This fact makes it possible to assume that the annual course of potential and current evapotranspiration will be very similar in the studied river basin and the relations (2–5) can also be used for the intra-annual distribution of current evapo-transpiration or balance evaporation.

Tables 5 a–c show the values of the monthly elements of the water balance equation, determined from the long-term monthly averages of measured precipitation and runoff for the periods 1930/31–1959/60, 1960/61–1989/90, and 1990/91–2019/20. Based on the percentage distribution of evaporation in the year according to PET in the Krupinica River basin, the monthly values of ET evaporation were calculated from the annual balance evaporation.

Table 4. Average monthly potential evapotranspiration PET, m in mm for the Krupinica River basin according to relations (2-5) for 3 periods 1930/31–1959/60, 1960/61–1989/90, and 1990/91–2019/20

PET,m mm	XI	XII	I	II	III	IV	V	VI	VII	VIII	IX	X
1930/31–1959/60	11.5	1.6	0.3	0.8	13.3	45.7	87.7	113.0	128.8	112.5	74.2	41.7
1960/61–1989/90	11.7	1.2	0.4	2.2	15.8	47.1	87.5	110.8	124.0	109.1	72.2	43.5
1990/91–2019/20	13.3	1.2	0.7	3.3	16.9	49.8	89.9	116.7	131.7	116.6	70.5	40.8

Table 5. Long – term water (hydrological) balance terms time course, Krupinica, period *a*) 1930/31–1959/60; *b*) 1960/61–1989/90; *c*) 1990/91–2019/20

a	XI	XII	I	II	III	IV	V	VI	VII	VIII	IX	X	Year
P [mm]	70.3	53.4	37.2	45.2	51.7	47.7	73.1	77.6	68.6	60.9	45.7	63.2	695
R [mm]	21.6	21.9	18.7	28.8	55.2	30.5	19.7	12.0	8.4	4.7	4.1	4.9	231
ET [mm]	8.5	1.2	0.2	0.6	9.8	33.6	64.5	83.1	94.7	82.8	54.6	30.7	464
S=P-R-ET	40.2	30.2	18.3	15.8	-13.3	-16.4	-11.1	-17.4	-34.6	-26.5	-12.9	27.6	0
sum S	40	70	89	105	91	75	64	46	12	-15	-28	0	
ET [%]	1.8	0.3	0.0	0.1	2.1	7.2	13.9	17.9	20.4	17.8	11.8	6.6	100
ET+R	30.1	23.1	19.0	29.3	65.0	64.1	84.2	95.1	103.2	87.5	58.7	35.6	695
b	XI	XII	I	II	III	IV	V	VI	VII	VIII	IX	X	Year
P [mm]	60.5	53.4	41.9	43.1	39.1	44.9	63.5	76.2	54.1	54.5	47.9	41.0	620
R [mm]	10.8	14.6	11.7	20.8	37.7	25.7	14.9	11.7	5.2	4.4	4.8	9.3	172
ET [mm]	8.4	0.9	0.3	1.6	11.3	33.7	62.7	79.5	88.9	78.3	51.8	31.2	449
S=P-R-ET	41.3	37.9	29.9	20.7	-9.9	-14.5	-14.1	-15.0	-40.0	-28.2	-8.7	0.6	0
sum S	41.3	79.2	109.1	129.7	119.8	105.3	91.2	76.3	36.3	8.1	-0.6	0.0	
ET [%]	1.9	0.2	0.1	0.4	2.5	7.5	14.0	17.7	19.8	17.4	11.5	6.9	100
ET+R	19.2	15.5	12.1	22.4	49.0	59.4	77.6	91.1	94.1	82.7	56.6	40.5	620
c	XI	XII	I	II	III	IV	V	VI	VII	VIII	IX	X	Year
P [mm]	59.1	51.8	43.6	41.4	44.2	45.5	68.0	65.2	70.7	57.3	57.3	57.5	662
R [mm]	9.0	12.4	11.7	16.0	32.1	20.9	11.3	10.4	5.9	3.7	4.3	6.5	144
ET [mm]	10.6	0.9	0.6	2.6	13.4	39.6	71.4	92.7	104.6	92.6	56.0	32.4	517
S=P-R-ET	39.6	38.4	31.3	22.8	-1.3	-15.0	-14.7	-38.0	-39.8	-39.0	-2.9	18.6	0
sum S	39.6	78.0	109.2	132.1	130.8	115.8	101.1	63.1	23.3	-15.7	-18.6	0.0	
ET [%]	2.0	0.2	0.1	0.5	2.6	7.7	13.8	17.9	20.2	17.9	10.8	6.3	100
ET+R	19.5	13.4	12.3	18.6	45.5	60.5	82.7	103.1	110.5	96.4	60.3	38.9	662

The courses of the elements of the hydrological balance determined from the long-term monthly averages in the river basin are shown in Fig. 3.

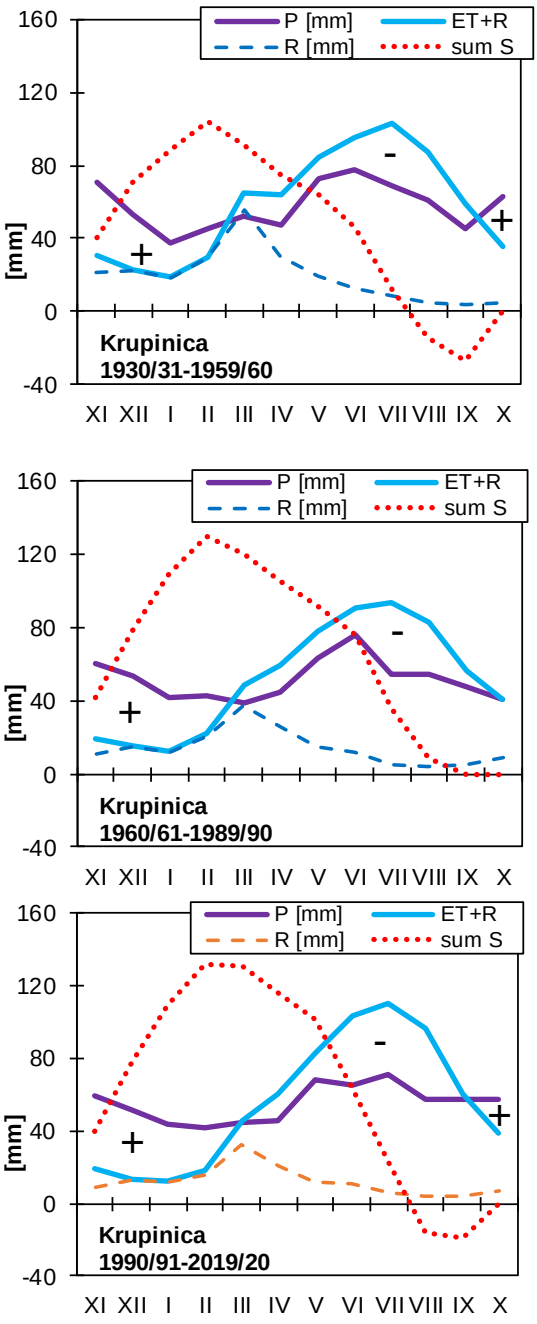

Fig. 3. Water (hydrological) balance components time course, determined from the long term monthly means in the river Krupinica basin up to Plášťovce, periods 1930/31–1959/60, 1960/61–1989/90, and 1990/91–2019/20.

Water resources (S) in the Krupinica River basin increased in the first and third periods from September to March, from April to August the accumulated water resources in the river basin were exhausted. In the second period 1960/61–1989/90, water resources increased from November to March, in the remaining period water supplies were exhausted. The largest fluctuation of changes in water resources (S) in the river basin was in the long term in the last period – 1990/91–2019/20, with a 30-year average of 150.7 mm. The hydrological balance compiled in this way makes it possible to set aside the average monthly changes in water resources in the river basin, and in a narrower sense in the soil and groundwater.

In terms of monthly precipitation totals, their long-term average (for the periods 1930/31–1959/60, 1960/61–1989/90, and 1990/91–2019/20) in the river basin is relatively balanced. The maximum precipitation fell in May-July, the minimum in January-March (Fig. 4a). The highest average monthly runoff in all three periods occurred in March – the period of melting snow (Fig. 4b) and highest long-term monthly balance evapotranspiration ET in July (Fig. 4c). During these months, almost 38% of the total annual outflow flows. The largest runoff is the month of March c_v = 0.59, the largest fluctuations in the runoff are recorded in August c_v = 1.72.

Dependence of annual runoff on precipitation and air temperature

A simple regression relationship between runoff, precipitation and air temperature can be used to estimate the future development of the annual runoff from the river basin (Fig. 5). Such relations were derived by Oto Dub in 1966 or Friga (Šipikalová et al., 2006), who determined several regional relations for different river basins.

For the Krupinica River basin, the following relationship was derived from the data of the time period 1931–2020:

$$R = 0.519*P - 33.475*T + 131 \qquad (6)$$

where:

R – average annual runoff [mm],
P – average annual precipitation total [mm],
T – average annual air temperature [°C].

From relation (6) it follows that a decrease of precipitation in the Krupinica River basin by 100 mm will cause a decrease of runoff by 52 mm. An increase in the average annual temperature of 1°C results in a decrease of the runoff of 33.5 mm. By analogy, an increase in the average annual air temperature by 1°C results in an increase in evapotranspiration of 33.5 mm.

More accurate results for individual months and for other runoff components can only be obtained by mathematical modelling – using the precipitation-runoff balance model in a monthly (daily) step. Modelling procedures are gradually becoming a standard part of the solution and design optimization of water management systems in the world, mostly based on the observed hydrological series of flows, precipitation, temperatures, etc. Based on the information from these series, it is possible to determine the parameters of the system, such as e.g. water tank volume, dimensions of safety overflows, the height of the dam, required irrigation needs and others.

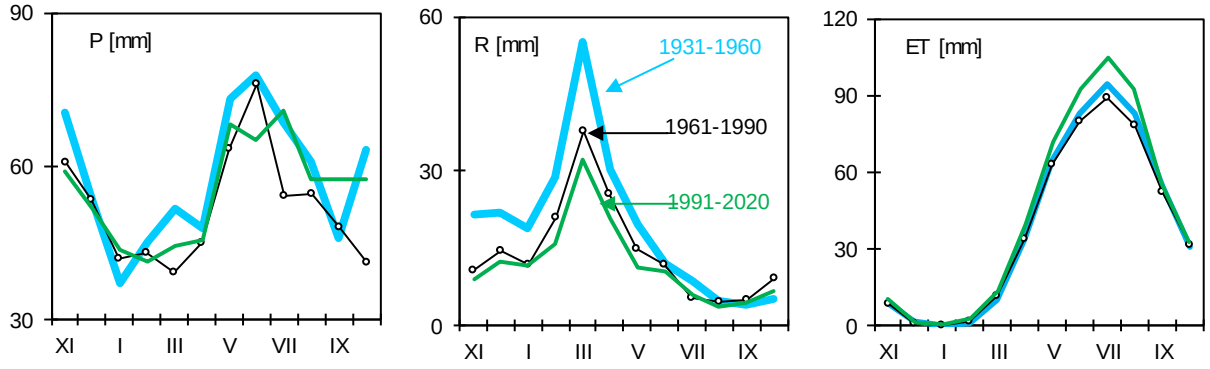

Fig. 4. Water (hydrological) balance elements comparison, determined from the long–term monthly means of the river Krupinica basin up to Plášťovce, for three 30- years periods: 1930/31–1959/60, 1960/61–1989/90, and 1990/91–2019/20. a) Long-term monthly precipitation P, b) Long-term monthly runoff R, c) Long-term monthly balance evapotranspiration ET.

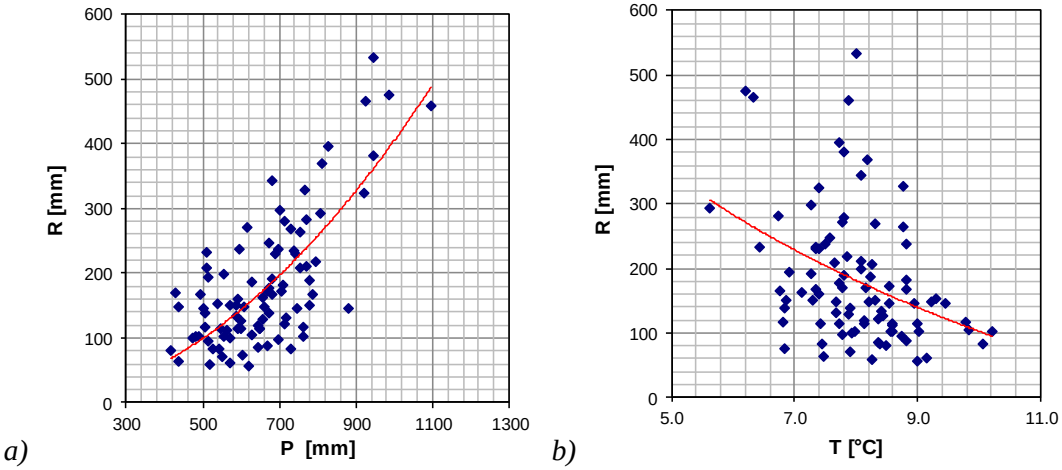

Fig. 5. Dependence of a) annual runoff on the annual total precipitation in the Krupinica River basin; b) annual runoff at the average annual air temperature in the Krupinica River basin for the period 1931–2020.

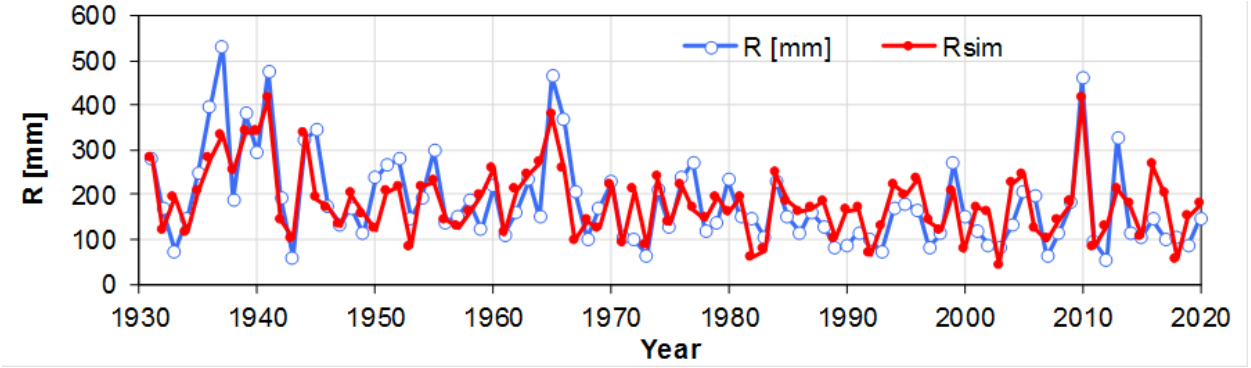

Fig. 6. The course of measured annual outflows R and simulated (Rsim) according to relation (6).

Conclusion

The analysis of the hydrological regime of the Krupinica River basin detected significant changes in the last 30 years (1991–2020). Even if this time period is relatively short, there is a need to closely observe and evaluate these changes. The changes in water balance need to be assessed in all significant catchments in Slovakia, while taking into the account also the level of anthropogenic influences. Due to climate changes, it is recommended to also assess the expected changes in rainfall and air temperature (Szolgay et al., 2007; Horvát et al., 2009; Földes et al., 2020; Sabová et al. 2021; Šipikalová et al., 2015). This task is needed and requires close cooperation between climatologists, hydrologist and water managers from different fields (governmental agencies, universities, research institutes). There is also a need for wider practical use of water balance models (Kožín et al., 2015; Fendeková et al., 2017) and special statistical methods for evaluation of changes in the runoff (Bačová Mitková and Halmová, 2021; Keszeliová et al., 2021)
The results of this study point to changes in the hydrological regime of Slovak rivers. This is also one of the reasons why are the hydrological characteristic of currently valid reference period in Slovakia (1961–2000) carefully revised and evaluated. One of the possible new reference periods is 1991–2020, which is recommended by the World Meteorological Organisation. During evaluation it also needs to be taken into the account, that the reference period should be selected and calculated based on type of application.

Acknowledgement

This work was supported by the project APVV No. 20-0374 "Regional detection, attribution and projection of impacts of climate variability and climate change on runoff regimes in Slovakia, and the project "VEGA No. 2/0004/19 "Analysis of changes in surface water balance and harmonization of design discharge calculations for estimation of flood and drought risks in the Carpathian region".

References

Bačová Mitková, V., Halmová, D. (2021): Statistical analysis and trend detection of the hydrological extremes in the Váh river at Liptovský Mikuláš. Acta Horticulturae et Regiotecturae – Special Issue Nitra, Slovaca Universitas Agriculturae Nitriae, 80–89.

Blahušiaková, A., Matoušková, M. (2015): Rainfall and runoff regime trends in mountain catchments (Case study area: the upper Hron River basin, Slovakia). J. Hydrol. Hydromech., 63, 3, 183–192. DOI: 10.1515/johh-2015-0030.

Blahušiaková, A., Matoušková, M. (2016): Evaluation of the hydroclimatic extremes in the upper Hron River basin, Slovakia. AUC Geographica, 51, 2, 189–204.

Blaškovičová, L., Danáčová, Z., Lovasová, L., Simor, V., Škoda, P. (2013): Evolution of selected hydrological characteristics of the Danube at Bratislava. Hydrological Final Report. Slovak Hydrometeorological Institute, Bratislava, pp. 1–15. (In Slovak)

Ďurigová, M., Ballová, D., Hlavčová, K. (2019): Analyses of Monthly Discharges in Slovakia Using Hydrological Exploratory Methods and Statistical Methods. Slovak J. Civ. Eng. 2019, 27, 36–43.

Ďurigová, M., Hlavčová, K. (2020): The detection of changes in the upper Váh river basin according to decadal analysis. Acta Hydrologica Slovaca, 21, 1, 39–47.

Fendeková, M., Danáčová, Z., Gauster, T., Labudová, L., Fendek, M., Horváth, O. (2017): Analysis of hydrological drought parameters in selected catchments of the southern and eastern Slovakia in the years 2003, 2012 and 2015. Acta Hydrologica Slovaca, 18, 2, 135–144.

Földes, G., Labat, M. M., Kohnová, S. (2020): CLM climate scenario and its impact on seasonality changes in short-term rainfall intensities in mountainous regions of Slovakia. Acta Hydrologica Slovaca, 21, 1, 3–8, doi: 10.31577/ahs-2020-0021.01.0001.

Garaj, M. (2020): Identification of changes in the hydrological balance in partial river basins of the Danube region. Dissertation. (Identifikácia zmien hydrologickej bilancie v čiastkových povodiach Dunajského regiónu. Dizertačná práca), STU v Bratislave, Stavebná fakulta. Evidenčné číslo: SvF-104305-88014. (in Slovak)

Halmová, D., Pekárová, P., Pekár, J., Miklánek, P., Bačová Mitková, V. (2021): Identification of the historical drought occurrence on the Danube River and its tributaries. Acta Hydrologica Slovaca, 22, 2, 237–247. DOI: 10.31577/ahs-2021-0022.02.0027

HMÚ (1963): Characteristic hydrological data of Slovak flows. (Charakteristické hydrologické údaje slovenských tokov). HMÚ, Bratislava, 37 pp. (in Slovak)

Holko, L. (1998): The accuracy of flow measurement in a mountain basin and its impact on the water balance. (Presnosť merania prietoku v horskom povodí a jej vplyv na vodnú bilanciu). Acta Hydrol. Slovaca, 1, 41–49. (in Slovak)

Holko, L., Parajka, J., Majerčáková, O., Faško, P. (2001): Hydrological balance of selected catchments in the Tatra Mountains region in hydrological years 1989–1998. J. Hydrol. Hydromech., 49, 3–4, 200–222.

Holko, L., Danko, M., Sleziak, P. (2020): Analysis of changes in hydrological cycle of a pristine mountain catchment.2. Isotopic data, trend and attribution analyses. J. Hydrol. Hydromech., 68, 2, 192–199. ISSN 1338-4333.

Horvát O., Hlavčová K., Kohnová S., Danko M. (2009): Application of the FRIER distributed model for estimating the impact of land use changes on the water balance in selected basins in Slovakia. J. Hydrol. Hydromech., 57, 4, 213–225. DOI: 10.2478/v10098-009-0020-2.

Jeneiová, K., Kohnová, S., Parajka, J., Szolgay, J. (2015): Detection of changes in the annual maximum discharge series in southern Slovakia. Acta Hydrologica Slovaca, Vol. 16, Thematic issue, 53–58. (in Slovak, with English abstract). (in Slovak)

Kendall, M. G. (1975): Rank Correlation Methods. Griffin, London.

Keszeliová, A., Hlavčová, K., Danáčová, M., Danáčová, Z., Szolgay, J. (2021): Detection of changes in the hydrological balance in seven river basins along the Western Carpathians in Slovakia. Slovak Journal of Civil Engineering, 29, 4, 49–60. DOI: 10.2478/sjce-2021-0027

Kožín, R., Hanel, M., Kašpárek, L., Peláková, M., Vizina, A., Treml, P. (2015): Possibilities of mitigating the effects of climate change by using areas protected for the accumulation of surface water. (Možnosti zmírnění dopadů změny klimatu využitím území chráněných pro akumulaci povrchových vod). Vodohospodářské

technicko - ekonomické informace VTEI/ 2015/ 4–5. 11-17. (in Czech)

Krajewski, A., Sikorska-Senoner, A., Ranzi, R., Banasik, K. (2019): Long-term changes of hydrological variables in a small lowland watershed in central Poland. Water 11(3). doi:10.3390/w11030564.

Majerčáková, O., Škoda, P., Šťastný, P., Faško, P. (2004): The development of water balance components for the periods 1931–1980 and 1961–2000. Journal Hydrol. Hydromech. 52, 4, 355–364. (In Slovak)

Mann, H. B. (1945): Nonparametric tests against trend. Econometrica, 13, 245–259.

Pekárová, P., Halmová, D., Miklánek, P., Onderka, M., Pekár, J., Škoda, P. (2008): Is the Water Temperature of the Danube River at Bratislava, Slovakia, Rising? Journal of Hydrometeorology, Vol. 9, 1115–1122.

Poórová, J., Blaškovičová, L., Škoda, P., Šimor, V. (2013): Trends in minimum annual and monthly discharges on Slovak streams. (Trendy minimálnych ročných a mesačných prietokov na slovenských tokoch.) In: Proc. Seminar Sucho a jak mu čelit. Prague, 20– 23. (in Slovak)

Ptak, M., Sojka, M., Graf, R., Choiński, A., Zhu, S., Nowak, B. (2022): Warming Vistula River – the effects of climate and local conditions on water temperature in one of the largest rivers in Europe. J. Hydrol. Hydromech., 70, 2022, 1, 1–11. https://doi.org/10.2478/johh-2021-0032.

Sabová, Z., Kohnová, S., Hlavčová, K. (2021): Analysis of changes in monthly and m-daily maximum discharges using the MPI and KNMI climate scenarios in the Myjava and Hron river basins in Slovakia. Acta Hydrologica Slovaca, 22, 2, 167–176. DOI: 10.31577/ahs-2021-0022.02.0020

Szolgay, J., Hlavčová, K., Lapin, M., Parajka, J., Kohnová, S. (2007): Impact of climate change on the runoff regime in Slovakia. (Vplyv zmeny klímy na odtokový režim na Slovensku.) Key Publishing, Ostrava. ISBN 978-80-87071-50-2. (in Slovak)

Šimor,V., Ľupták, Ľ. (2021): Trend changes analysis of the minimum and average annual discharges in selected Slovak rivers during the two periods 1961–2000 and 1961–2015. Acta Hydrologica Slovaca, 22, 2, 207–219.

Šipikalová, H., Škoda,P., Demeterová,B., Majercáková, O. (2006): New hydrological data of surface waters. (Nové hydrologické údaje povrchových vôd.) Vodohospodársky spravodajca 5-6, 2006, roč. XLIX, 26–29. (in Slovak)

Šipikalová, H., Škoda, P., Podolinská, J., Liová, S. (2015): The assessment of the reference period 1961–2000 in the setting of hydrological characteristics (Posúdenie referenčného obdobia 1961–2000 pri stanovovaní hydrologických charakteristík). In: Proc: Manažment povodí a povodňových rizík 2015 a Hydrologické dni 2015. (in Slovak)

Tomlain, J. (1991): Evaporation from the surface of soil and plants. (Výpar z povrchu pôdy a rastlín). Zborník prác SHMÚ, zväzok 33/I, Klimatické pomery na Slovensku, vybrané charakteristiky. 163–172. (in Slovak)

Zeleňáková, M., Purcz, P., Blišťan, P., Vranayová, Z., Hlavatá, H., Diaconu, D.C., Portela, M. M. (2018): Trends in Precipitation and Temperatures in Eastern Slovakia (1962–2014). Water, 10, 727; doi: 10.3390/w10060727.

Ing. Dana Halmová, PhD (*corresponding author, e-mail: halmova@uh.savba.sk)
RNDr. Pavla Pekárová, DrSc.
Institute of Hydrology SAS
Dúbravská cesta č. 9
841 04 Bratislava
Slovak Republic

RNDr. Jana Podolinská
Slovak Hydrometeorological Institute
Zelená 5
974 04 Banská Bystrica
Slovak Republic

Ing. Katarína Jeneiová, PhD.
Slovak Hydrometeorological Institute
Jeséniova 17
833 15 Bratislava
Slovak Republic

DOI: 10.31577/ahs-2022-0023.01.0004

ACTA HYDROLOGICA SLOVACA

Volume 23, No. 1, 2022, 32 – 41

Study of trends in the time series of maximum water discharges in the Tisza basin rivers within Ukraine

Valeriya OVCHARUK*, Maryna GOPTSIY

Nowadays, due to global and local climate changes, according to leading experts, the likelihood of extreme natural phenomena increases. One of the dangerous natural phenomena with impacts on humans and the economy are floods. The Tisza River, which originates in Ukraine and flows further through Romania, Hungary, Slovakia, and Serbia, has repeatedly become a source of disasters for the population due to the devastating consequences of floods, which have been increasing in recent years. The purpose of this study is to analyze the long-term series of observations of the maximum water discharge on the rivers of the Tisza basin, within Ukraine. Using the methods of statistical analysis, tendencies in the time series of annual maximum water discharges were investigated, its temporal homogeneity was estimated also, as well as the significance of the trends. Using the method of residual mass curves, high-water and low-water periods were distinguished. We also obtained preliminary dependences of the maximum runoff modules on the catchment areas and their heights, which in the future can serve as a basis for the development of a regional calculation method for determining the maximum runoff of ungauged rivers in the region.

KEY WORDS: maximum water discharges, flood, trends

Introduction

The rivers of the Tisza basin are characterized by a flood regime and flow through the territory of Western Ukraine. Within this area, the mountain system of the Eastern Carpathians is located, which is subdivided into the Outer Eastern Carpathians (the Carpathian Rivers within the Dniester and Prut basin) and the Inner Eastern Carpathians (the Transcarpathian rivers – the Danube basin, namely the Tisza with tributaries). At the study territory, catastrophic floods are periodically observed, which lead to significant economic losses, and sometimes to human casualties. The floods of 1911, 1913, 1957, 1969, 1998, 2001, 2008, and 2020 can be classified as exceptionally high on the territory of the Ukrainian Carpathians (Margaryan et al., 2020). The issues of studying, statistical analysis, and calculations and forecasts of floods in the Tisza basin are relevant both for Ukraine and for neighboring countries through which the Tisza flows. The issue of assessment and management of flood risks in the Upper Tisza Basin in Hungary was considered in Szlávik (2000) and Linnerooth-Bayer et al. (2003) Janál and Kozel (2019) provides test results for the Fuzzy Flash Flood model. The model is implemented in the Czech Hydrometeorological Institute (CHMI) as an alternative tool for flash flood forecasting. In the publications of Blöschl et al. (2017, 2019) the Tisza basin was included in the analysis of flood trends in rivers in Europe. According to (Blöschl et al., 2017), there is a tendency for an increase in the influence of the Atlantic on the maximum runoff in winter, but the dates of annual maximums are still noted in the warm season. Thus, further study and systematization of data on the maximum runoff in the Tisza basin, taking into account the measurement data of recent years, is of scientific and practical interest.

Material and methods

The water gauge stations (WGS) on Transcarpathian Rivers have observation periods from 56 to 103 years, up to 2015 inclusive. According to the existing time series of observation of the maximum runoff in the territory of the Ukrainian Carpathians, the absolute values of the maximum water discharge at the rivers of Transcarpathia vary from 62.7 $m^3 s^{-1}$ (Studeny-Nizhniy Studeny, A= 25.4 km^2) to 1680 $m^3 s^{-1}$ (Uzh – Uzhgorod, A = 1970 km^2). Almost all considered Mountain Rivers of Transcarpathia belong to the category of small rivers; however, the length of the studied rivers in 90% of cases is more than 10 km. The catchments are characterized by slopes (from 8.1‰ to 41.1‰) and an average elevation from 300 to 1100 m. The Ukrainian Carpathians are densely covered with forests, therefore, the forest cover of catchments on the rivers of Transcarpathia from 18 to 77%, but there are almost no swamps and lakes in the studied catchments (table.1).

Table 1. Initial information about catchments and observing period at the river of Tisza basin (within Ukraine)

№	River - water gauge stations	Observation period	n, years	Length L [km]		The slope of the river I [‰]		Catchment area, A [km^2]	The average elevation H_{av} [m]	Wetlands f_w [%]	Forest f_{fr} [%]	Plowing [%]	Lakes, f_l [%]
				from the source	from the farthest point of the river network	average	weighted average						
1	Tisa-Rakhiv	1947–2015	69	4	53	15.3	9.1	1070	1100	0	68	5	1
2	Teresva-Ust-Chorna	1947–1976 1978–2015	68	2	34	20	17.2	572	1100	0	77	<5	0
3	Rika-Mizhhirya	1946–2015	70	28	28	24.3	12.5	550	800	0	41	<5	0
4	Golyatynka-Maidan	1956–1994 1999–2015	56	18	18	23.4	23	86	790	0	40	<5	0
5	Pylypets-Pylypets	1956–2015	60	6.2	6.2	41.1	30	44.2	820	0	29	<5	0
6	Studeny-Nizhniy Studeny	1954–1994 1999–2015	58	7.5	7.5	31.6	22.7	25.4	800	0	18	<5	0
7	Borzhava-Dovge	1946–2015	70	37	37	35.9	12.6	408	620	0	71	10	0
8	Latorytsia-Pidpolozzia	1946–2015	70	24	24	17.7	12.3	324	720	0	50	5	0
9	Latorytsia-Svalyava	1961–2015	54	53	53	11.4	7.4	680	700	0	61	5	0
10	Latorytsia-Mukacheve	1946–2015	70	85	85	8.1	4.5	1360	570	0	63	5	0
11	Latorytsia-Chop	1956–2015	60	135	135	5.2	1.9	2870	310	<1	41	10	< 1
12	Vicha-Nelipine	1957–2015	59	36	36	20	14.5	241	760	0	72	<5	0
13	Stara-Znyatseve	1952–2015	64	28	28	19.6	6	224	300	0	42	10	0
14	Uzh-Zhornava	1952–2015	64	28	28	19.6	12.3	286	670	0	45	<5	0
15	Uzh-Zaricheve	1946–2015	70	68	68	10.6	6.3	1280	560	0	54	5	0
16	Uzh-Uzhhorod	1946–2015	70	95	95	8.1	4.1	1970	530	0	57	15	0

To analyze the initial information, the method of mathematical and statistical analysis, spatial generalization, extrapolation, and correlation was used. To assess the statistical homogeneity of the initial information three criteria were used: F-test (Fisher criterion), Student's t-test, and Wilcoxon criterion (Manual, 1984). The assessment of cyclical fluctuations of maximal runoff is performed using the time series trends and residual mass curve (Manual, 1984; Guide, 1994). The current ordinates of residual mass curves from the time when a curve was plotted and by the end of the year may be found using the following equation:

$$\sum_{i=1}^{n}(Ki - 1) = f(t), \quad (1)$$

Where Ki = Qi/Qave are modular coefficients of the year; Qi and Qave are the discharge of the year and the average discharge for the n period.

For statistical processing was used the method of moments and maximum likelihood, practical application of these methods may be seen in Lukianets et al. (2019) and Gorbachova (2015).

Results and discussion

The database on the maximum annual water discharges in the Tisza River basin has been formed for the period from the beginning of regular observations until 2015 including (for 8 out of 16-time series – this is from 1946–1947; for 2 – from 1952; and for 6 – from 1956–1957). The data analysis confirms that the studied region is characterized by a floodwater regime, so the maximum values of runoff can be observed in any month of the year. However, floods are local and do not cover the entire territory at once. The absolute maximum water discharges in the long-term period were observed in 1957, 1966, 1968, 1980, 1998, and 2001, which can be

classified as historical maximums (Fig. 1); the floods in 2008 and 2020 were also quite large, in terms of consequences and losses, however, the maximum water discharges in the considered catchments did not exceed the historical maximums.

For further research, the database of the dates of the observed maximum water discharges for each year of the existing series of observations for 16 watersheds was created, which are evenly distributed in the study area. As noted above, the maximum annual discharges at the rivers of the Tisza basin can be observed in any month of the year. For each time series, the observed dates were sorted by months, and the number of years of observation for each catchment was taken as 100%, and the percentage of maximal discharges cases was determined for the months (table 2). This percentage ranges in a fairly wide range from 0% to 26% of cases over a long period of observations. Then for each catchment 1–2 months were defined, in which the annual maximum water discharges were most often observed. For WGS Tisa-Rakhiv it is April and July, for WGS Pylypets-Pylypets it is July and November, for WGS Stara-Znyatseve it is January and March and for WGS Uzh-Zaricheve it is March and December, and for other catchments, it was only one leading month for each.

Thus, for the long-term observation period (from 54 to 70 years), the largest number of cases of annual maximum water discharges is observed in December – 44% (for 7 of 16 catchments), in March – 37.5% (for 6 of 16 catchments) and in July – 25% (for 4 of 16 catchments) (table.2). Since in some cases the maximum discharges were observed in two different months, the amount is not 100%.

This distribution can be explained by different types of

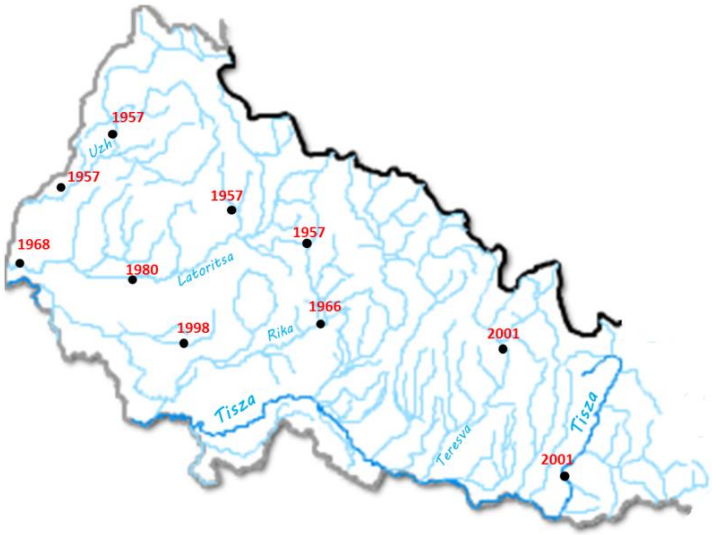

Fig. 1. The dates passed of absolute maximum water discharges (Q, m^3s^{-1}) at the river of Tisza basin (within Ukraine).

Table 2. Distribution of the observed maximum water discharges (*Q*, $m^3 s^{-1}$) by months over a multi-year period (as a percentage)

№	River- water gauge stations	I	II	III	IV	V	VI	VII	VIII	IX	X	XI	XII
1	Tisa-Rakhiv	6	7	**12**	16	6	4	16	1	7	6	7	**12**
2	Teresva-Ust-Chorna	4	1	**13**	15	10	7	**7**	1	6	6	9	**19**
3	Rika-Mizhhirya	7	4	**14**	6	7	7	**9**	3	3	7	16	**17**
4	Golyatynka-Maidan	5	5	**9**	5	5	11	16	9	2	7	11	**14**
5	Pylypets-Pylypets	7	5	**10**	0	2	5	17	7	3	15	**17**	**13**
6	Studeny-Nizhniy Studeny	3	3	**10**	5	12	19	19	12	2	5	3	**5**
7	Borzhava-Dovge	11	11	**17**	4	6	9	**1**	1	0	6	11	**21**
8	Latorytsia-Pidpolozzia	9	11	**19**	4	3	1	**9**	4	3	4	11	**21**
9	Latorytsia-Svalyava	7	6	**26**	4	6	2	**9**	2	4	9	9	**17**
10	Latorytsia-Mukacheve	10	11	**16**	9	4	1	**7**	1	3	7	13	**17**
11	Latorytsia-Chop	15	14	**24**	17	3	0	**1**	0	1	1	7	**15**
12	Vicha-Nelipine	8	5	**19**	5	3	8	**15**	3	0	7	10	**15**
13	Stara-Znyatseve	22	19	**22**	5	3	2	**3**	0	0	0	5	**20**
14	Uzh-Zhornava	8	6	**19**	6	5	5	**10**	5	5	6	11	**14**
15	Uzh-Zaricheve	10	14	**20**	9	4	1	**4**	1	3	4	7	**20**
16	Uzh-Uzhhorod	10	13	**20**	9	4	1	**4**	1	1	4	9	**23**

precipitation, which are observed in the cold and warm periods of the year over the territory of Transcarpathia. The Ukrainian Carpathians, of which Transcarpathia is a part, belong to the zone of sufficient moisture, where the amount of precipitation reaches the highest values in the territory of Ukraine. However, within this zone, we can distinguish mesoclimatic subregions, where the formation and frequency of precipitation significantly depend on local factors. Most precipitation (over 1400 mm) falls in the highest part of the Carpathian Mountains – in the east and northeast of the region. The amount of precipitation decreases in the south-western direction (up to 500–600 mm) – in the area of Chop and Berehove. Precipitation falls mainly in summer (over 60%), especially in June, and in the mountains – in July. In summer, there are showers and thunderstorms. Snow cover in the mountainous part of the region is established in mid-November, rises in early April, and its duration is up to 110 days (Nizhniy Studeny). The plain snow cover lasts from late December – to early January to early March near Berehove (51 days). In the plains, there are often winters without stable snow cover. During the year, Transcarpathia is dominated by air masses of temperate latitudes. On the plains, the south-western winds blow most often, in the foothills and mountains – mountain-valley, and above 1000 m the western air transfer prevails. In winter, northern winds penetrate the Carpathians along the depressions of river valleys. At the same time, cold air often descends from the mountains to the plain in the form of northern and northeastern winds.

Thus, the significant heterogeneity of the precipitation field, which is due to the heterogeneous conditions of precipitation, causes the formation of floods almost throughout the year. On the other hand, the factors of the underlying surface, in particular the catchment area, are also a factor in the formation of floods. Thus, local precipitation forms floods, mostly on small rivers. Long-lasting rainfall precipitation can already form floods on medium-sized rivers.

For example, in fig. 2, are represented 6 characteristic distributions of the dates of the observed maximum water discharge by months. For the catchment area of the Tisza River - WGS Rakhiv, which is located in the highlands and has an area of more than 1000 km^2, the predominance of floods in the warmer season is characteristic. On the other hand, if we consider the catchment area with approximately the same area, but already with an average elevation of 560 m (Uzh river – WGS Zaricheve), the distribution changes and the maximum discharge is observed in the winter-spring period.

As the average catchment height decreases (Stara river – WGS Znyatseve, A=224 km^2, H = 300 m), the percentage occurrences of maximum in the winter-spring period is already more than 80%, so this is a river with a clear maximum during the spring flood. If we consider small catchments located in the high mountains, for example, Pylypets river – WGS Pylypets (A=44.2 km^2, H= 820 m), then here more than 60% of the maximum discharge occurs in the summer–autumn period. After analyzing all the constructed distributions of the observed maximum water discharges by months during the year, it should be noted that for each catchment there are 2–4 months, in which extremely high runoff values are most often observed. Generally, the studied region in different combinations are months such as November, December, January, February, March, and July.

The next stage of the study was the assessment of the statistical homogeneity of time series. Two parametric tests (Fisher's and Student's) and the nonparametric Wilcoxon test were used for the assessment. The results are listed in Table 3. The standard significance level for these criteria is 5% (Methodological recommendations, 2010). However, given that the observed maximum annual discharges are often close to a 1% probability of being exceeded, a 1% significance level was also used. As can be seen from Table 3, at the 5% significance level, – 50% (8 out of 16) time series turned out to be heterogeneous. At the 1% significance level, the results change significantly – only one of the 16 series (6%) turned out to be heterogeneous. The reasons for statistical heterogeneity can be different; however, the most common for hydrological time series is their insufficient length and the presence of trends caused by climate change and anthropogenic activity. In our case, the duration of observations at the WGS does not differ significantly and ranges from 54 to 70 years, while the heterogeneous Golyatynka-Maidan series has one of the shortest observation durations - 56 years. On the other hand, the Golyatynka-Maidan catchment also has one of the smallest catchment areas (A = 86 km^2). It is possible that the combination of these two factors led to the temporal heterogeneity of the series, but for the final conclusion, it is necessary to investigate possible trends for all catchments.

To study temporal trends in chronological series of maximum runoff, chronological graphs of annual maximum water discharge on the 16 WGS of the Tisza basin within Ukraine were constructed. The results of the estimation of linear trend signification are listed in Table 4. The estimation was based on the significance of the Pearson coefficient. . In case the value of R was more than double the root mean square error of the linear trend correlation coefficient ($2\sigma_R$), the trend was considered significant (Methodological recommendations, 2010). For the case when R was equal to 0.01, the trend was considered invariability. The trend analysis shows both an increase (3 cases or 19%) and decreases in runoff (12 cases or 75%), and in some cases – invariability (1 case or 6%) in fluctuations in the maximum annual water discharge. Thus, there is no definite regularity in the distribution of trends in maximal runoff in the Transcarpathian region. For 4 catchments, there is a statistically significant trend towards a decrease in runoff and, no one case statistically significant trend toward an increase. To illustrate various cases of trends, Fig. 3 shows examples for 6 river catchments of the study area.

The method of residual mass curves was used for further analysis. As shown in Fig. 4, on almost all rivers of the Tisza River basin, perennial fluctuations in maximum water flow are synchronous. Since 2001, there has been

a long low-water phase, also at all the catchments considered; there are full water content cycles. As the low-water phase has been observed in recent decades, the onset of the next high-water phase on the rivers of the Tisza River Basin can be expected to exceed the maximum water discharges rather than now. That was confirmed in 2020, then Transcarpathia, once again, suffered from a flood, but currently, we have no officially published data to analyze that flood.

In Ukraine, as in other countries of the former Soviet Union, methods for determining the maximum flow of untrained rivers are developed separately for spring floods and rainfall floods. As the above analysis has shown, in modern conditions on the territory of Transcarpathia, the maximum water discharge is observed almost all year round. Therefore, it is of interest to obtain the calculated dependences for the annual maximums.

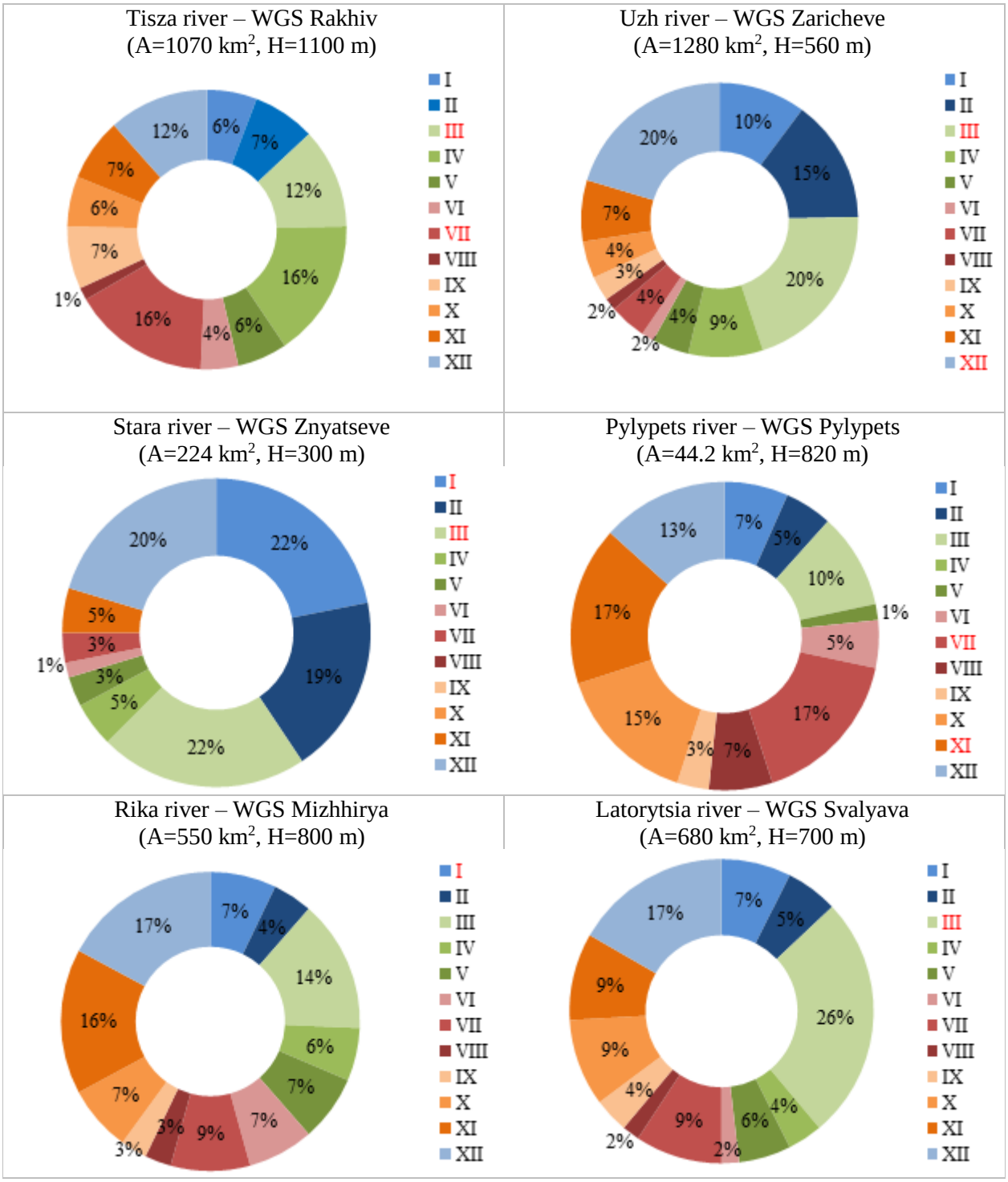

Fig. 2. Distribution of the observed maximum water discharges (Q, $m^3 s^{-1}$) by months at the river of Tisza basin within Ukraine.

Table 3. Estimates of statistical homogeneity of the initial information by three criteria: F-test (Fisher's test), Student's t-test, and Wilcoxon's test

№	River – water gauge stations	Significance level 1%				Significance level 5%			
		Fisher criterion	Student's criterion	Wilcoxon criterion	Conclusion	Fisher criterion	Student's criterion	Wilcoxon criterion	Conclusion
1	Tisa-Rakhiv	Yes	Yes	Yes	homogeneous	Yes	Yes	Yes	homogeneous
2	Teresva-Ust-Chorna	No	Yes	Yes	homogeneous	Yes	Yes	No	***not homogeneous***
3	Rika-Mizhhirya	No	Yes	Yes	homogeneous	Yes	No	No	***not homogeneous***
4	Golyatynka-Maidan	Yes	No	No	***not homogeneous***	Yes	No	No	***not homogeneous***
5	Pylypets-Pylypets	Yes	Yes	No	homogeneous	Yes	No	No	***not homogeneous***
6	Studeny-Nizhniy Studeny	Yes	Yes	No	homogeneous	Yes	No	No	***not homogeneous***
7	Borzhava-Dovge	Yes	Yes	No	homogeneous	Yes	No	No	***not homogeneous***
8	Latorytsia-Pidpolozzia	Yes	Yes	Yes	homogeneous	Yes	Yes	Yes	homogeneous
9	Latorytsia-Svalyava	Yes	Yes	No	homogeneous	Yes	No	No	***not homogeneous***
10	Latorytsia-Mukacheve	Yes	Yes	Yes	homogeneous	Yes	Yes	Yes	homogeneous
11	Latorytsia-Chop	Yes	Yes	Yes	homogeneous	Yes	Yes	Yes	homogeneous
12	Vicha-Nelipine	No	Yes	Yes	homogeneous	No	Yes	Yes	homogeneous
13	Stara-Znyatseve	Yes	Yes	Yes	homogeneous	Yes	Yes	Yes	homogeneous
14	Uzh-Zhornava	Yes	Yes	Yes	homogeneous	Yes	No	No	***not homogeneous***
15	Uzh-Zaricheve	Yes	Yes	Yes	homogeneous	Yes	Yes	Yes	homogeneous
16	Uzh-Uzhhorod	Yes	Yes	Yes	homogeneous	No	No	No	***not homogeneous***

Table 4. Assessment of the significance of linear trends at the rivers of Transcarpathia

№	River – water gauge stations	n, years	Equation	R^2	R	σ_R	$2\sigma_R$	Conclusion	trend direction
1	Tisa-Rakhiv	69	y = 0.1127x + 88.785	0.0001	0.01	0.12	0.24	No	invariability
2	Teresva-Ust-Chorna	68	y = -0.0007x + 1.6981	0.0059	0.08	0.12	0.24	No	decrease
3	Rika-Mizhhirya	70	y = -1.5031x + 3251.7	0.0541	0.23	0.11	0.23	**Yes**	**decrease**
4	Golyatynka-Maidan	56	y = -0.6321x + 1302.3	0.1903	0.44	0.11	0.22	**Yes**	**decrease**
5	Pylypets-Pylypets	60	y = -0.214x + 457.87	0.0392	0.20	0.13	0.25	No	decrease
6	Studeny-Nizhniy Studeny	58	y = -0.2092x + 431.99	0.0956	0.31	0.12	0.24	**Yes**	**decrease**
7	Borzhava-Dovge	70	y = -0.909x + 1976.9	0.0448	0.21	0.11	0.23	No	decrease
8	Latorytsia-Pidpolozzia	70	y = -0.2914x + 757.71	0.0051	0.07	0.12	0.24	No	decrease
9	Latorytsia-Svalyava	54	y = -2.7846x + 5754.4	0.1089	0.33	0.12	0.24	**Yes**	**decrease**
10	Latorytsia-Mukacheve	70	y = 0.0004x + 1.1713	0.0014	0.04	0.12	0.24	No	increase
11	Latorytsia-Chop	60	y = 0.5347x - 805.95	0.0100	0.10	0.13	0.26	No	increase
12	Vicha-Nelipine	59	y = 0.1129x + 310.94	0.0013	0.04	0.13	0.26	No	increase
13	Stara-Znyatseve	64	y = -0.0617x + 151.38	0.0111	0.11	0.12	0.25	No	decrease
14	Uzh-Zhornava	64	y = -0.8209x + 1748	0.0982	0.31	0.11	0.23	**Yes**	**decrease**
15	Uzh-Zaricheve	70	y = -1.3613x + 3202.5	0.0128	0.11	0.12	0.24	No	decrease
16	Uzh-Uzhhorod	70	y = -5.4038x + 11334	0.0964	0.31	0.11	0.22	No	decrease

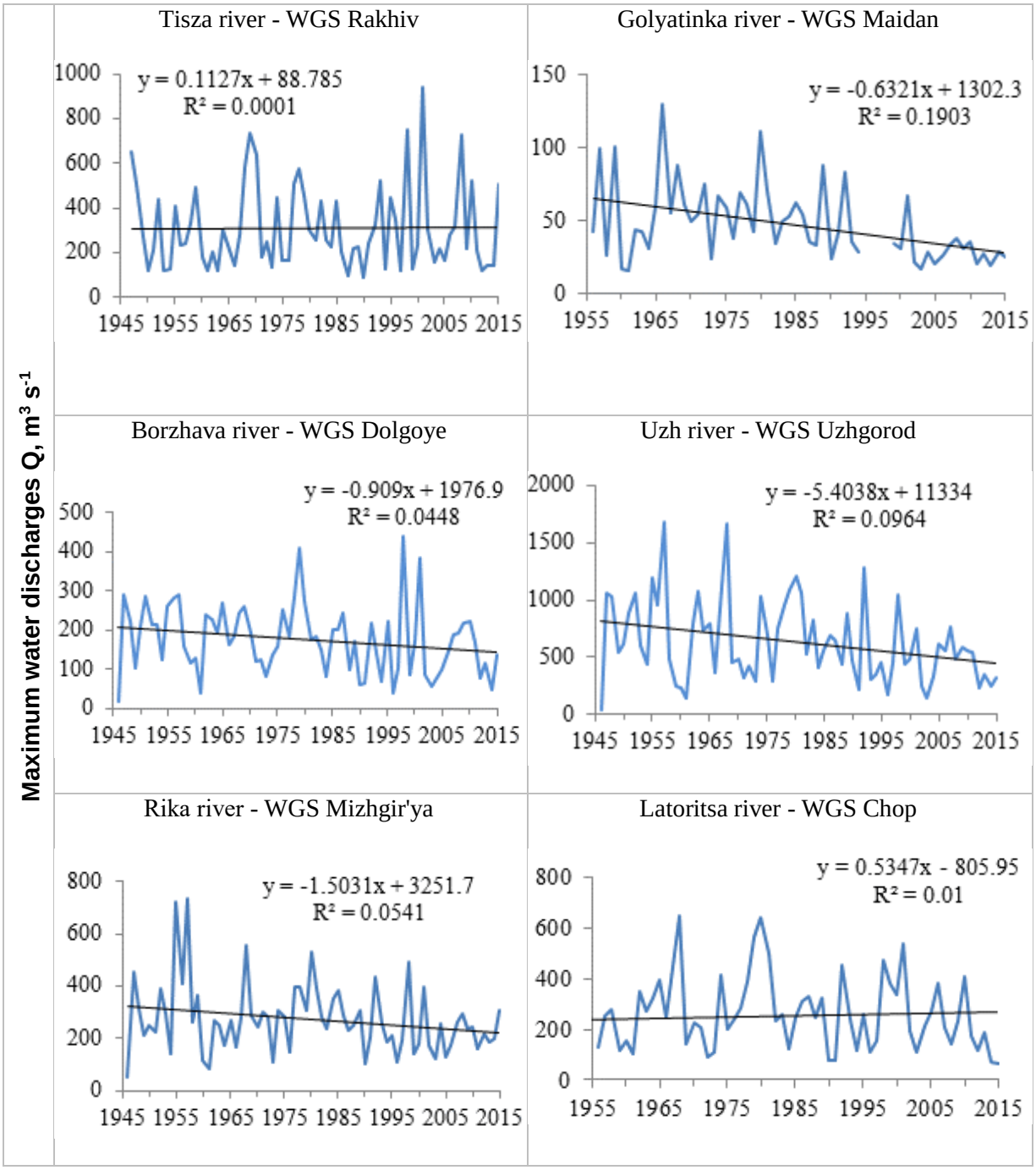

Fig. 3. The time series of maximum water discharges at the river of Tisza basin within Ukraine (Q, $m^3 s^{-1}$).

The final stage of the work was the study of the patterns of change in the maximum annual discharge from the factors of the underlying surface – the areas of catchments and their average elevations (Fig. 5). For the comparability of the discharges from watersheds of different sizes, when constructing the calculated dependencies, runoff modules were used, which are specific and allow comparing runoff values of different scales. Analyzing the obtained results, we can note that for the rivers under consideration there is a regular decrease in the absolute maximum runoff modules with an increase in the catchment areas. The reduction process can be described as an exponential function, which allows one to take into account the reduction deceleration in the area of large and small catchments (Fig. 5). On the other hand, taking into account that a mountainous region is being considered, the dependence of the investigated value on the average elevations of catchments was built – here there is a regular increase in the maximum runoff modules with an increase in the terrain elevation. In both cases, the dependencies are statistically significant, however, in the case of

the average elevations; there is a significant deviation for the catchments with an average height above 1000 m.

Figure 6 shows that if we exclude catchments with an average elevation of more than 1000 m, the coefficient of the accuracy of the approximation increases significantly and will be 0.94. In this case, the obtained dependence can be used to calculate the annual maximum runoff modules for ungauged watersheds with an average elevation of less than 1000 m.

With regard to high-mountain catchments (with a height of more than 1000 m), there is not enough data to substantiate the calculated dependence and it is necessary to use data on neighboring basins. This task is for further research.

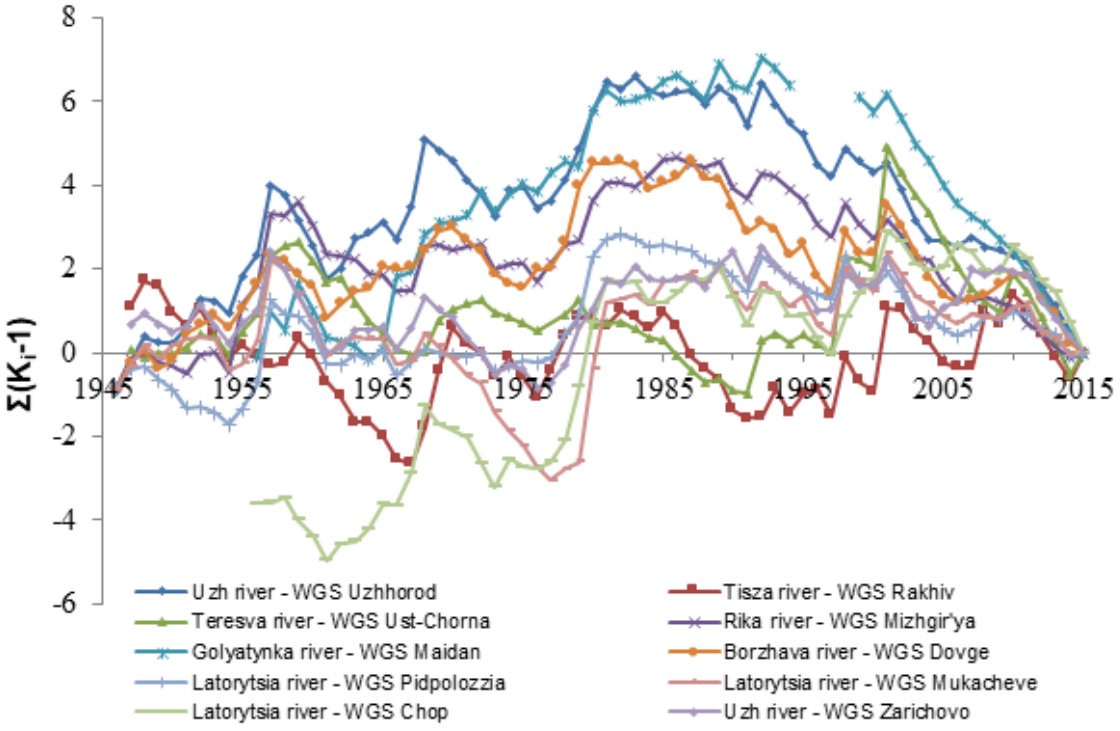

Fig. 4. The residual mass curves of maximum water discharge (Q, $m^3 s^{-1}$) at the river of Tisza basin within Ukraine.

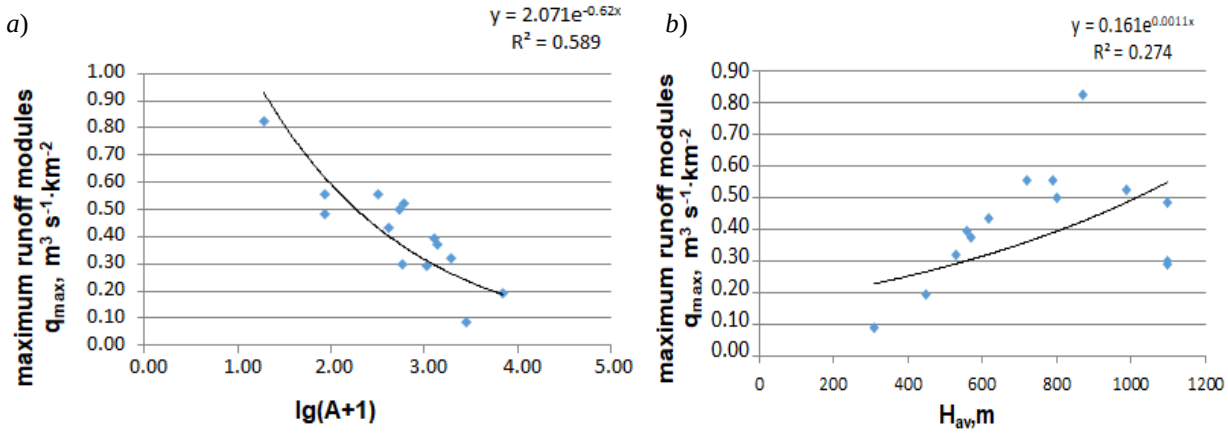

Fig. 5. Relationships of the value of maximum runoff modules (q_{max} $m^3 s^{-1} \cdot km^{-2}$) a) on the area and b) an average elevation of catchments at the river of Tisza basin within Ukraine.

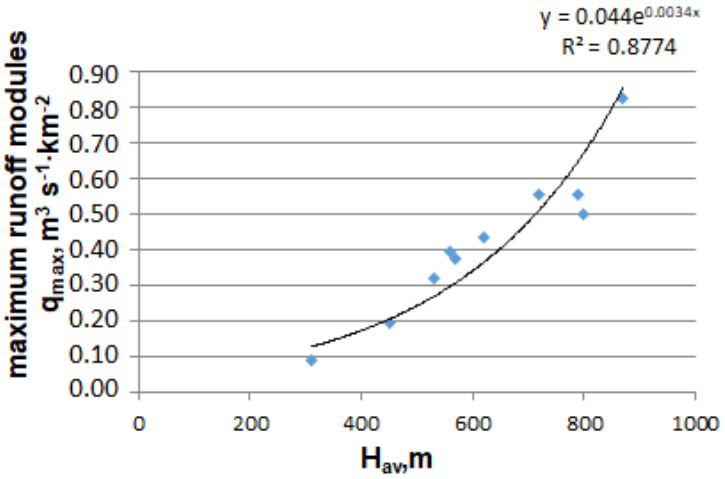

Fig. 6. Relationships of the value of maximum runoff modules (q_{max} $m^3s^{-1}km^{-2}$) on an average elevation of catchments less than 1000 m at the river of Tisza basin within Ukraine.

Conclusion

- Analysis of data on annual flow maximums showed that for the Tisza basin within Ukraine, now under climate change, floods were observed throughout the entire calendar year;
- For the long-term observation period (from 54 to 70 years), the largest number of cases of annual maximum water discharges is observed in December – 44%; in March – 37.5% and in July – 25%. Water resources engineers can use the results obtained, both for individual rivers and for the region as a whole, in planning water intakes from rivers, as well as in justifying the throughput of hydraulic structures.
- The study of the statistical homogeneity of time series shows that at the 1% significance level only one of the 16 series (6%) turned out to be heterogeneous. Time trends in the multiyear maximum water discharges also are not unambiguous. On the territory of Transcarpathia, for 4 catchments, there is a statistically significant trend towards a decrease in the runoff, and no one statistically significant trend cases to an increase.
- The novelty of the study consists in obtaining the calculated dependences of the maximum annual runoff modules on the underlying surface factors. This approach is new, in comparison with the existing similar ones separately for spring floods and rain floods.
- The study of the regularities of the distribution of the maximum annual runoff modules showed that there are statistically significant depen-dences on the catchment area and their average height. Such dependencies can be described by an exponential function. When plotting the dependence on the height no more than 1000 m, the coefficient of the accuracy of the approximation significantly increases, and the dependence can be recommended for practical use for determining the maximum discharge of ungauged rivers in Transcarpathia.

References

Blöschl, G. et al. (2017): Changing climate shifts timing of European floods. Science, Vol. 357, Issue 6351, 588–590. https://doi.org/10.1126/science.aan2506

Blöschl, G. et al. (2019): Changing climate both increases and decreases European river floods. Nature 573(7772), 108–111 https://doi.org/10.1038/s41586-019-1495-6

Gorbachova, L. (2015): The intra-annual streamflow distribution of Ukrainian rivers in different phases of long-term cyclical fluctuations. Energetika. 2015. Vol. 61. No. 2. P. 71–80.

Guide to Hydrological Practices (1994): Data Acquisition and Processing, Analysis, Forecasting and Other Applications. 5th edition. WMO. No. 168. 735 p.

Janál, P., Kozel, T. (2019): Fuzzy logic based flash flood forecast. Proceedings of the XXVIII Conference of the Danubian Countries on Hydrological Forecasting and Hydrological Bases of Water Management (Kyiv, Ukraine, November 6–8, 2019) https://doi.org/10.15407/uhmi.conference.01.10

Linnerooth-Bayer, J., Vári, A., Ferencz, Z. (2003): Flood Risk Management in the Upper Tisza Basin in Hungary. In: Beer T., Ismail-Zadeh A. (eds) Risk Science and Sustainability. NATO Science (Series II: Mathematics, Physics and Chemistry), vol 112. Springer, Dordrecht. https://doi.org/10.1007/978-94-010-0167-0_17

Lukianets, O., Malytska, L., Moskalenko, S. (2019): Maximum riverine runoff in the basin of Tysa and Prut within Ukraine. Proceedings of the XXVIII Conference of

the Danubian Countries on Hydrological Forecasting and Hydrological Bases of Water Management (Kyiv, Ukraine, November 6–8, 2019) https://doi.org/10.15407/uhmi.conference.01.18

Manual to Determining the Calculated Hydrological Characteristics (1984): edited by A. Rozhdestvensky and A. Lobanova. Leningrad: Gidrometeoizdat. 447 (in Russian)

Margaryan, V. G, Ovcharuk, V. A., Goptsiy, M. V., Borovskaia, G. A., (2020): Comparative analysis and estimate of the long-term fluctuations of the river maximum runoff of the mountain territories of Armenia and Ukraine under of global climate change, Sustainable Development of Mountain Territories, 12(1), 61–75 DOI: 10.21177/1998-4502-2020- 12-1-61-75

Methodological recommendations for assessing the homogeneity of hydrological characteristics and determining their calculated values from heterogeneous data (2010) / edited by A. Rozhdestvensky and A. Lobanova. State Hydrological Institute, St. Petersburg: Publishing house Nestor-History, 162 p. (in Russian).

Szlávik, L. (2000): Emergency Flood Reservoirs in the Tisza Basin. In: Marsalek, J., Watt, W. E., Zeman, E., Sieker, F. (eds) Flood Issues in Contemporary Water Management. NATO Science Series (Series 2. Environment Security), vol 71. Springer, Dordrecht. https://doi.org/10.1007/978-94-011-4140-6_38

Valeriya Ovcharuk, Doctor of Geographical Sciences, Associate Professor (*corresponding author, e-mail: valeriya.ovcharuk@gmail.com)
Hydrometeorological Institute of Odessa State Environmental University
15 Lvovskaya Str.
Odessa, 65016
Ukraine

Maryna Goptsiy, Ph.D. in Geography
Department of Land Hydrology of Odessa State Environmental University
15 Lvovskaya Str.
Odessa, 65016
Ukraine

DOI: 10.31577/ahs-2022-0023.01.0005

ACTA HYDROLOGICA SLOVACA

Volume 23, No. 1, 2022, 42 – 51

Estimation, trend detection and temporal changes in maximum annual flow volume series of the Hron River in Slovakia

Veronika BAČOVÁ MITKOVÁ*

The floods characterized by the volume exceedance probabilities and return periods with specific T-year flows may assist in enhancing the accuracy of local flood frequency estimates, and support the detection and interpretation of any changes in flood occurrence and their magnitudes. Therefore, the present paper deals with the trend detection and with temporal changes in the maximum flows volume series of the Hron River at Banská Bystrica and at Brehy gauging stations in Slovakia during the 90 years. The period 1931–2020 mean daily flows of the waves belong to the maximum annual flows and the series of maximum annual flows of the Hron River at Banská Bystrica and at Brehy gauging stations were used as input data. Subsequently the annual maximum runoff volumes with t-day duration were calculated. The Log-Pearson distribution type III were used to determine the T-year values of the maximum runoff volumes with t-day duration. The results indicated that there are decreasing linear trends in maximum annual runoff volumes with some duration of the flow.

KEY WORDS: the Hron River, trend detection, Log-Pearson III distribution, annual maximum runoff volumes, wave duration

Introduction

One of the basic tasks of hydrology is to correctly estimate the patterns occurrence, circulation, temporal and spatial distribution of water on Earth. With the surface water, it is mainly determining of the hydrological characteristics such as discharge, water stages or wave volume. The basic need for the dimensioning of flood protection structures are designed values of hydrological characteristics which can had disaster effect. In assessment of the climate change impacts on the river discharge regime (extremes, flood hydrographs and drought periods), it is expected that an increase in air temperature may cause (or already has caused) an increase in extreme discharges and flood volumes (Blöschl et al., 2017; 2019). It is necessary to regularly to check the validity of the assumptions in order to have correct statistical results (IACWD, 1982). Significant changes to the river basins may have an influence on the hydrological extremes and can affect the frequency analysis. It is well known that in some small streams there have been floods with an atypical ratio of extreme flood wave volume to its culmination, which are among the phenomena no one expected. Therefore, for engineering praxis it is necessary to study the flood wave volume in time. Flood peak and volume have been shown to be interdependent (Szolgay et al., 2015), and this dependence should be taken into account when estimating design floods (Mediero et al., 2010). The design methods of the flood estimation must consider both flood volume and peak discharge. Determination of design values for extreme floods with a very low probability of exceedance, meaning with a long return period (once every 100-, 500- or 1000-years), is a very difficult and complex process, coupled with great uncertainty. There exist many studies for estimating the designed extreme hydrological characteristics; most of them are focused on the study of such extremes as discharges, water stages, discharge volume from basin area or joint probability distributions of the hydrological characteristics (e. g. Bačová Mitková and Halmová 2014; Papaioannou et al., 2016; Balistrocchi et al., 2017 or Huang and Fan 2021). In applied hydrology, the problem is the assignment values of the of flood wave volume with a certain probability of exceedance to the corresponding T-year discharges. Guo and Adams (1998) derived analytical expressions for the probability density function (PDF) of runoff event volume and the expected average annual runoff volume. The probability method SCHADEX for extreme flood estimation presented Paquet et al. (2013). Gądek and Bodziony (2015) presented the hypothetical flood wave volume in non-gauged basins for the area of the Upper Vistula River. Mediero et al. (2010) have also addressed the modelling of flood flows and flood wave volumes using special statistical methods. Based on our own experience in the field of frequency analysis of hydrological extremes (Mitková et al. 2004; Bačová

Mitková at al. 2016; Pekárová and Miklánek eds. 2019) and the knowledge of other already mentioned studies, we decided to use a very flexible Log-Pearson type III distribution as a statistical method. The floods characterized by the volume exceedance probabilities and by the return periods with specific *T*-year discharges may assist in enhancing the accuracy of local and regional flood frequency estimates and support the detection and interpretation of any changes in flood occurrence and magnitudes.

The present paper deals with the estimation, trend detection and temporal changes in annual maximum volumes of the flow waves belong to annual maximum flows at the Hron River. A 90-year series of the mean daily flows and annual maximum flows for Banská Bystrica and Brehy gauging stations were available. Therefore, it is possible to compile a 90-year volume series of the highest (annual) 2-, 5-, 10-, and 15-consecutive days wave volumes. Then their probability distribution functions and trends may be analysed.

The aim of the present paper is:

- assess the maximum annual runoff volumes V_{tmax} lasting 2-, 5-, 10-, and 15-days of the waves belong to annual maximum discharges of the Hron River at Banská Bystrica and at Brehy gauging stations (1931–2020);
- determine their the theoretical exceedance probability curves;
- estimate the *T*-year annual maximum runoff volumes with *t*-day duration of the waves belong to annual maximum discharges;
- analyse changes in the maximum annual runoff volumes V_{tmax} of the Hron River at Banská Bystrica and at Brehy gauging stations during the period of 1931–2020;
- analyse the changes in the maximum annual runoff volumes V_{tmax} in wet and dry periods within the period 1931–2020.

Material and methods

The series of 90-years (1931–2020) mean daily flows and annual maximum flows of the Hron River at Banská Bystrica and Brehy gauging stations were used as input data. The location of the selected river in Slovak territory illustrates Figure 1. The Hron River is the second longest river in Slovakia. It is 298 km long and flows only through the territory of Slovakia and feeds into the Danube near Štúrovo. The Hron springs in the Horehronie valley, connected to the Low Tatras and the Spiš-Gemer Karst and can be characterized as a nivo-pluvial river. Scenarios of changes to selected components of the hydrosphere and biosphere in the Hron River basin are described, for example, in the monograph of Pekárová and Szolgay (2005).

The Hron River at Banská Bystrica

The Hron River at Banská Bystrica drains into a basin of 1 766.48 km². The long-term average daily flow reached 25.73 $m^3 s^{-1}$ at Banská Bystrica for the period 1931–2020. The course of mean daily flows is illustrated in Figure 2. The course of annual maximum flows, long-term linear trend and 5-year moving trend are illustrated in the Figure 3a. The annual maximum flows of the Hron at Banská Bystrica show a decreasing long-term trend in period of 1930–2020 and we can reject the hypothesis *H0* at significance level α=0.1 (Mann-Kendall nonparametric test). The maximum annual flow during the period 1931–2020 at the station Banská Bystrica station was 560 $m^3 s^{-1}$ (in 1974) (Fig. 3a). The negative deviations of annual flows from the long-term annual flow have been shown more frequently since 1981, what indicate a predominance of dry years (Fig. 3b).

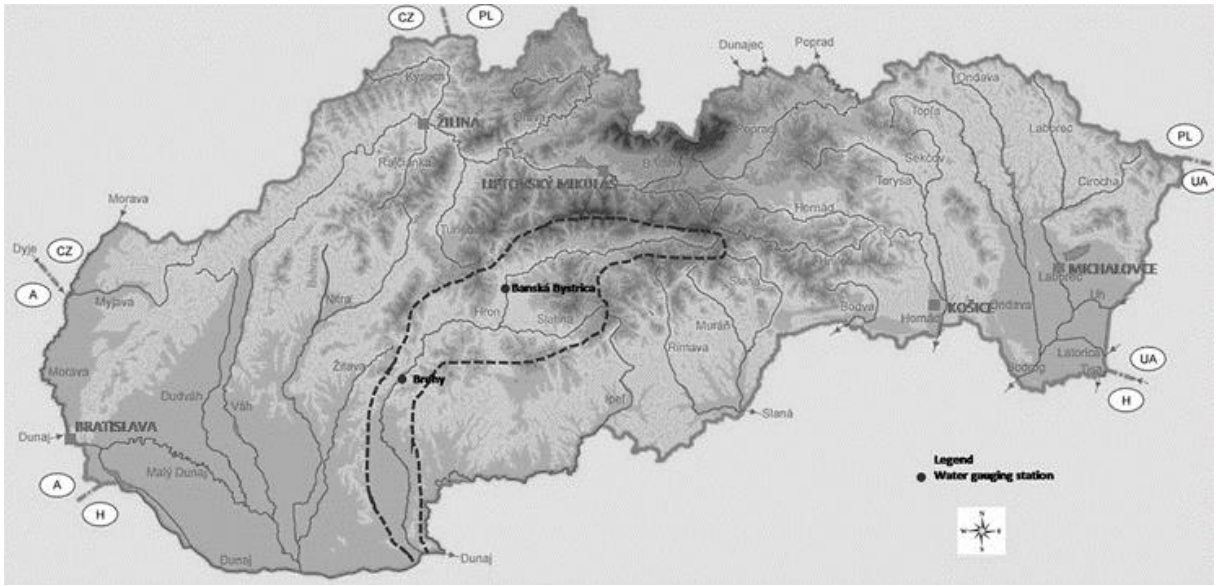

Fig. 1. The Hron River basin location in Slovak territory and gauging stations' locations on the Hron River.

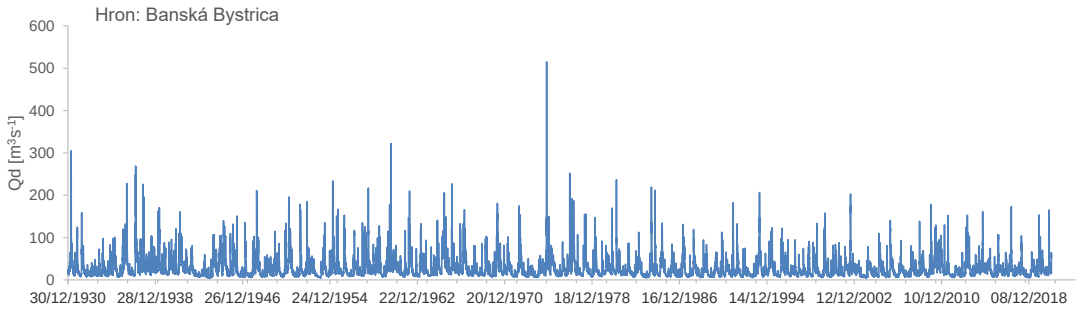

Fig. 2. The mean daily flows of the Hron River at Banská Bystrica.

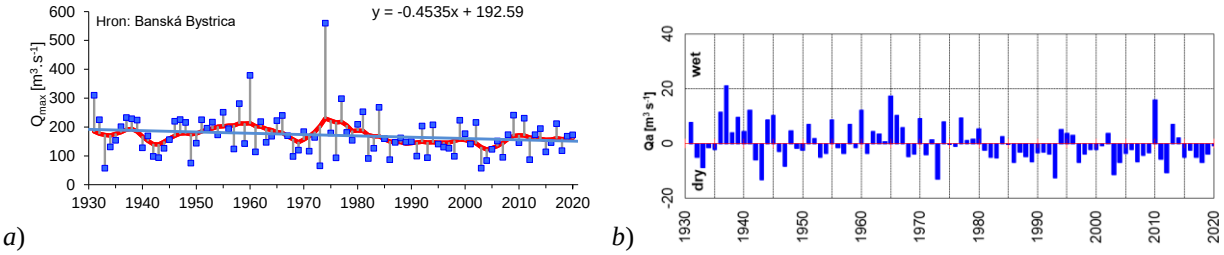

a) *b)*

Fig. 3. a) the maximum annual flows of the Hron River at Banská Bystrica (1931–2020), their linear trend and 5-year moving trend and b) the deviation of the annual flows from long-term annual flow during the period of 1931–2020.

The Hron River at Brehy

The Hron River at Brehy drains into a basin of 3821.35 km². The long-term average daily flow reached 46.57 $m^3 s^{-1}$ at Brehy for the period 1931–2020. The course of mean daily flows is illustrated in Figure 4. The course of annual maximum flows, long-term linear trend and 5-year moving trend are illustrated in Figure 5a. The annual maximum flows of the Hron at Brehy show a decreasing long-term trend in the period of 1930–2020 and we can reject the hypothesis *H0* at significance level α=0.1 (Mann-Kendall nonparametric test). The maximum annual flow during the period 1931–2020 at the Brehy station was 1050 $m^3 s^{-1}$ (in 1974) and the second highest maximum occurred in 1960 at value of 1000 $m^3 s^{-1}$ (Fig. 5a). The negative deviations of annual flows from the long-term annual flow have been shown more frequently since 1981, what indicate a predominance of dry years (Fig. 5b). However, the highest positive deviation was in 2010, which ranks this year among the wettest.

Figure 6a illustrates the distribution of the annual maximum flows occurrence in individual months during the period of 1931–2020 and in dry and wet years (Hron: Banská Bystrica). The maximum number of events with annual maximum flow occurs in April. It can be caused by snowmelts in higher parts of the basin and rainfall occur in the lower parts of the basin (Fig. 6a). The dry and wet years have annual maximum flows occurrence also in April.

Figure 6b illustrates the distribution of the annual maximum flows occurrence in individual months during the period of 1931–2020 and in dry and wet years (Hron: Brehy). The maximum number of events with annual maximum flow occurs in March. The maximum number of events with annual maximum flow in wet years occurs in April.

Determination of the maximum runoff volumes with t-day duration

In Czechoslovakia, Bratránek (1937) was the first who investigated the issue of runoff volumes. He used direct and indirect methods of peak vs. flood volume assessment. The direct method was based on compiling runoff volumes higher than a chosen flow threshold with assistance of the probability of exceedance (related to the *T*-year return period). The *T*-year flows were then determined by extrapolating probability curves to the domain of low exceedance probability. The calculation of the maximum runoff volumes with *t*- day duration of the Hron River was done according to Zatkalík (1970). When calculating the maximum volumes of flood waves, he chose as a basis a procedure taking into account the duration of the flood wave in days – *t*. The introduction of this parameter allows a clear assessment of the probability of exceeding the volume of a given flood wave and creation of a basis for solving the problem of design flood, which would consist in allocating such a flood wave volume that would be maximum for a given *T*-year peak flow. To determine the volume of the wave belonging to annual maximum flow, it is necessary to identify the beginning and end of the wave. It is quite difficult to identify the beginning and end of the flow wave, in some cases. In our analysis, the beginning and end of the wave were determined

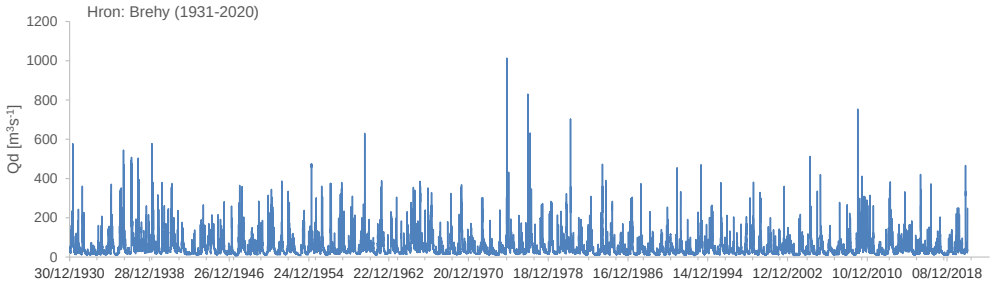

Fig. 4. The mean daily flows of the Hron River at Brehy.

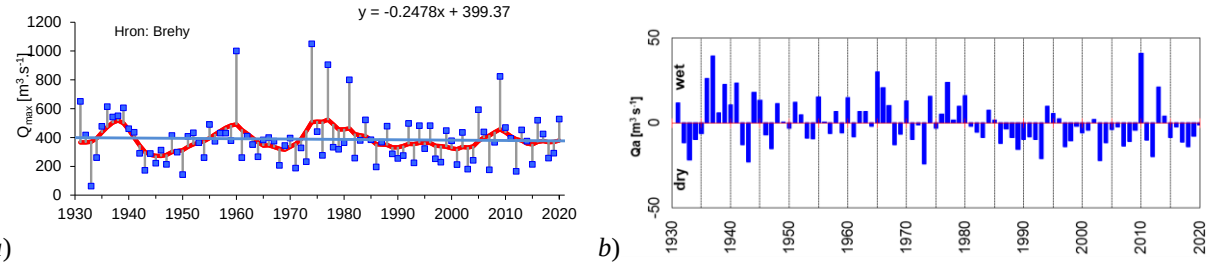

a) *b)*

Fig. 5. a) the maximum annual flows of the Hron River at Brehy (1931–2020), their linear trend and 5-year moving trend and b) the deviation of the annual flows from long-term annual flow during the period of 1931–2020.

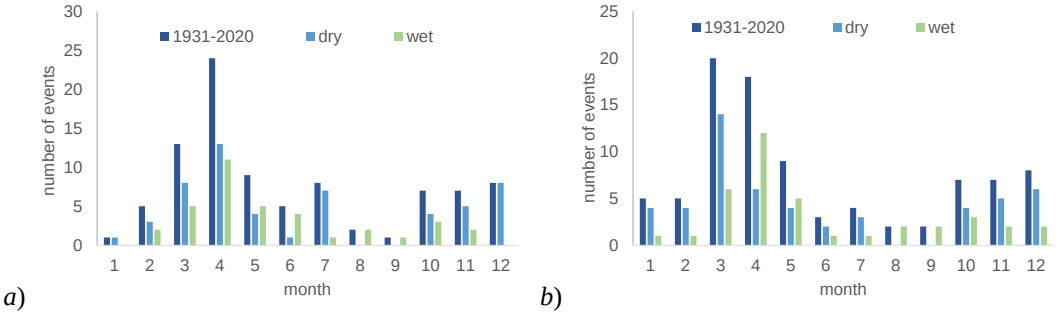

a) *b)*

Fig. 6. Monthly distribution of the annual maximum flows for whole period 1931–2020 and for dry and wet years of the Hron River a) at Banská Bystrica and b) at Brehy gauging stations.

approximately at the level of the long-term average daily flow. To define the volumes of individual waves, we introduced the parameter *t* - flow duration in days. In this way, we determined the maximum runoff volumes with t-day duration of 2-, 5-, 10- and 15- days based on mean daily flows. If the wave duration was less than 15 days, the steady flows were included into the analysis. In the case of an example *t*=5 days, the fifth 5-daily move averages were calculated around the culmination maximum flow. Consequently, only one maximum value was included into the statistical data set for analysis. A more detailed description of the methodology can be found in previous works e.g. Halmova et. al., (2008), Bačová and Halmová (2021) or Pekarová et al., (2018).

Log-Pearson III distribution

For the estimation of the maximum annual runoff volume V_{tmax} series distribution function, we used Log-Pearson type III distribution. The Log-Pearson distribution type III. is used to estimate extremes in many natural processes and it is one of the most commonly used probability distribution in hydrology (Bobee, 1975; Pilon and Adamowski, 1993; Griffis and Stedinger, 2007; Pawar and Hire, 2018). In some previous works (Pekárová et al., 2018; Pekárová and Miklánek, 2019) we compared LPIII distribution with theoretical probability distributions, which were and still are also among the most used in Slovak hydrological practice. The Log-Pearson Type III distribution is a three-parameter gamma distribution with a logarithmic transformation of the variable. The cumulative distribution function and probability distribution function according to Hosking and Wallis (1997) are defined as:

If $\gamma \neq 0$ let $\alpha=4/\gamma 2$ and $\xi=\mu-2\sigma/\gamma$

If γ >0 then:

$$F(x) = G(\alpha, \frac{x-\xi}{\beta})/\Gamma(\alpha) \quad (1)$$

$$f(x) = \frac{(x-\xi)^{\alpha-1} e^{-(x-\xi)/\beta}}{\beta^{\alpha}\Gamma(\alpha)} \quad (2)$$

where:
ξ – location parameter;
α – shape parameter;
β – scale parameter;
Γ – Gamma function.

If γ <0 then

$$F(x) = 1 - \frac{G\left(\alpha, \frac{x-\xi}{\beta}\right)}{\Gamma(\alpha)} \quad (3)$$

$$f(x) = \frac{(\xi-x)^{\alpha-1} e^{-(\xi-x)/\beta}}{\beta^{\alpha}\Gamma(\alpha)} \quad (4)$$

The Kolmogorov-Smirnov test was performed to test the assumption that the flow magnitudes follow the theoretical distributions. The *p*-value ($p \geq 0.05$) was used as a criterion for rejection of the proposed distribution hypothesis.

Mann-Kendal nonparametric test

The Mann-Kendall nonparametric test (M-K test) was used for determining the significant trends detection in time series. The nonparametric tests are more suitable for the detection of trends in hydrological time series, which are usually irregular, with many extremes (Hamed, 2008; Gilbert, 1987). By M-K test, we want to test the null hypothesis *H0* of no trend, i.e. the observations x_i is randomly ordered in time, against the alternative hypothesis *H1*, where there is an increasing or decreasing monotonic trend. For *n* (number of tested values) ≥ 10, the statistic *S* is approximately normally distributed with the mean and variance as follows:

$$E(S) = 0 \quad (5)$$

$$VAR(S) = \frac{1}{18}\left[n(n-1)(n-2) - \sum_{p=1}^{q} t_p (t_p - 1)(2t_p + 5) \right] \quad (6)$$

Where:
q – is the number of tied groups,
t_p – the number of data values in the *p* group.

The standard test statistic Z is computed as follows:

$$Z = \begin{cases} \frac{S-1}{\sqrt{VAR(S)}} & if \quad S > 0 \\ 0 & if \quad S = 0 \\ \frac{S+1}{\sqrt{VAR(S)}} & if \quad S < 0 \end{cases} \quad (7)$$

.

The presence of a statistically significant trend is evaluated using the *Z* value. A positive (negative) value of *Z* indicates an upward (downward) trend. The statistic Z has a normal distribution. To test for either an upward or downward monotone trend (a two-tailed test) at the α level of significance, hypothesis H0 (no trend) is rejected if the absolute value of |*Z*| is greater than *Z1-α/2*, where *Z1-α/2* is obtained from the standard normal cumulative distribution tables. The M-K test detects trends at four levels of significance: α = 0.001, 0.01, 0.05 and α = 0.1. A significance level of 0.001 means that there is a 0.1% probability that the value of xi is from a random distribution and are likely to make a mistake if we reject hypothesis *H0*. A significance level of 0.1 means that there is a 10% probability that we make a mistake if we reject hypothesis *H0*. If the absolute value of *Z* is less than the level of significance, there is no trend. For the four tested significance levels the following symbols are used in the template:

*** if trend at α = 0.001 level of significance – *H0* seems to be impossible
** if trend at α = 0.01 level of significance
* if trend at α = 0.05 level of significance – 5% mistake if we reject the *H0*
\+ if trend at α = 0.1 level of significance.
Blank: the significance level is greater than 0.1, cannot be excluded that the *H0* is true.

The most significant trend is assigned three stars (***), with a gradual decrease in importance, the number of stars also decreases.

Results and discussion

Analysis of annual maximum runoff volumes V_{tmax} on the Hron River (1931–2020

Based on the mentioned methodologies, the waves that belong to the maximum annual flow were selected. Subsequently, the maximum runoff volumes with *t*-day duration were calculated. The runoff time duration was determined as *t* = 2, 5, 10 and 15 days. The calculated maximum runoff volumes with *t*-day runoff duration for the Hron River at Banská Bystrica and Brehy are illustrated in Figure 7. Considering the 2-days to 15-days maximum runoff volumes, the flood of 1974 was the highest one within the period of 1931–2020 for both analyzed Hron River stations. The lowest one was in 1973 for Hron River at Banská Bystrica. Considering the 2-days and 5-days maximum runoff volumes, the flood of 2012 was the lowest one within the period 1931–2020 for Hron River at Brehy. Considering the 10- and 15-day runoff volumes, the lowest flood was in 1943. A Log-Pearson III theoretical distribution was selected to calculate the T-year maximum runoff volume with the given runoff time duration t. The calculated volumes were plotted on a log-probability scale. Figure 8a–b shows an example of the exceedance probabilities of the maximum runoff volume for a given flow time duration of 2 days and 15 days on the Hron River at Banská Bystrica and at Brehy for the period 1931–2020. From Figure 8, we can see how the slope of the maximum annual runoff volume probability curves changes from positive to negative as the runoff duration increases. The Kolmogorov-Smirnov test showed that we could not

reject the hypothesis that the selected theoretical probability distribution fit well the observed data at 5% significance. The estimated *T*-year maximum flows and *T*-year maximum runoff volumes V_{tmax} for the Hron River at Banská Bystrica and at Brehy the period 1931–2020 are listed in Table 1.

The Mann-Kendall nonparametric test (M-K test) was used for detection of the significance in long-term trends of annual maximum runoff belong to annual maximum flows of the Hron River at Banska Bystrica and Brehy gauging stations for period 1931–2020. The M-K trend test indicates a decreasing long-term trends in annual maximum runoff volumes with t=5-, 10-, 15-days of the waves belong to annual maximum flows of the Hron River at Banská Bystrica for selected period 1931–2020 and we can reject the hypothesis *H0* at significance level α=0.1 (Fig. 9a–c). The M-K trend test indicates a decreasing long-term linear trends in annual maximum runoff volumes with *t*=15-days of the waves belong to annual maximum flows of the Hron River at Brehy gauging station for selected period 1931–2020 and we can reject the hypothesis *H0* at significance level α=0.1 (Fig. 9d).

Analysis of annual maximum runoff volumes V_{tmax} on the Hron River (1931–2020) in dry and wet periods

In this part of the work, we divided the sets of annual maximum runoff volumes with t-days into two sub-sets based on dry and wet multiannual periods. The dry and wet periods we determined on the basis of double 5-year moving averages of the Hron River annual flows at Banská Bystrica and at Brehy stations for the period 1931–2020 (Fig. 10a–b).

The wetness of individual years is different and more or less independent of each other. It is to be understood that the various physical causes also distort the action of the decisive factors to such an extent that we can speak of randomness. According to this, but also from experience, we can say that years of a similar nature usually group together, (Dub, 1957). The limit value for determining the dry and wet periods was the value of the long-term average annual flow Q_a of the Hron River at two selected stations. Due to the fact that we took the period as a result of the moving average, dry and wet years can also occur in it. An average number of 46 years were included in the dry period and a number of 44 years

Fig. 7. Flood wave volume series of the Hron River at Banská Bystrica and at Brehy for flood durations t (2-, 5-, 10-, 15-days) (e.g. V_{2max} means maximal annual runoff volume in 2 days).

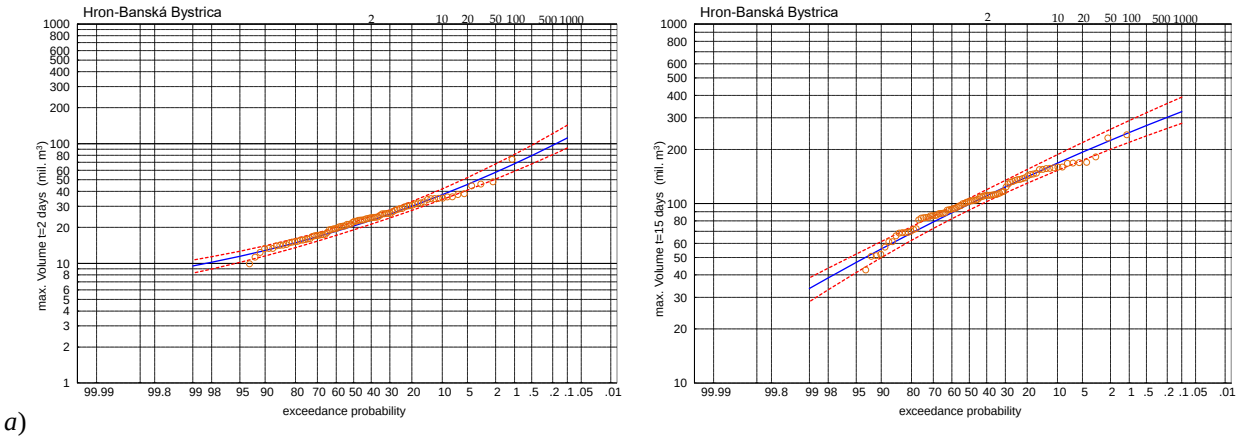

a)

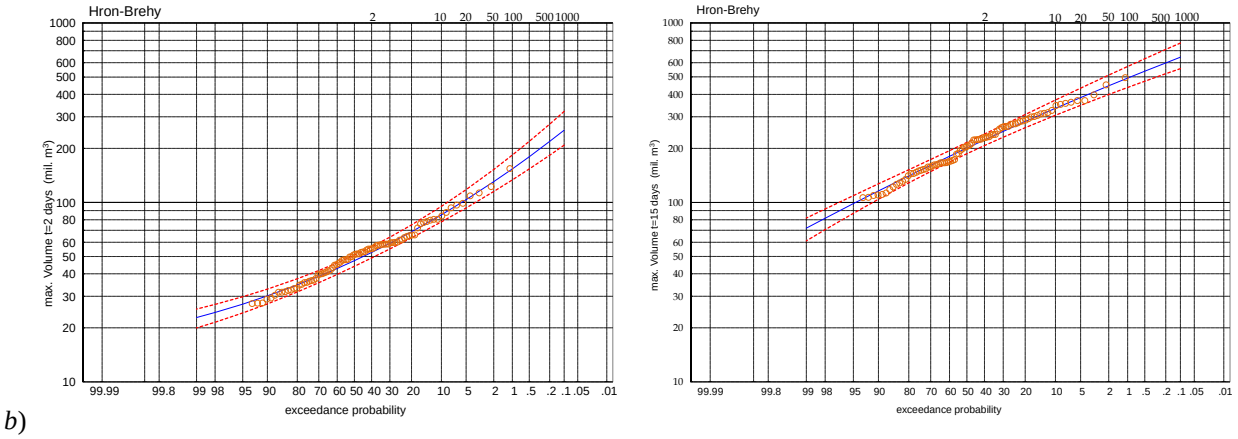

b)

Fig. 8. Examples of the theoretical LPIII exceedance probability curves of the maximum annual runoff volumes with t=2-days and 15-days for the Hron River at Banská Bystrica and at Brehy (1931–2020).

Table 1. T-year maximum flows Q_{max} and *T*-year annual maximum runoff volumes V_{tmax} of the Danube River at Bratislava (1876–2019) (Log-Pearson III) (*P=p*100%, p=1-e-1/T*)

River: Gauging station	Q_T [m^{3}s^{-1}]	*t*=2 days	*t*=5 days	*t*=10 days	*t*=15 days
Hron: Banská Bystrica	Q_{50}	V_{50tmax} [mil. m^3]			
	418	58	112.9	171.8	225.4
	Q_{100}	$V_{100tmax}$ [mil. m^3]			
	493	68	129.2	189.3	248.8
	Q_{500}	$V_{500tmax}$ [mil. m^3]			
	708	97	172.6	231.9	302.7
	Q_{1000}	$V_{1000tmax}$ [mil. m^3]			
	821	112.4	192.9	249.1	325.6
Hron: Brehy	Q_{50}	V_{50tmax} [mil. m^3]			
	1012	130.4	242.4	356.1	447.6
	Q_{100}	$V_{100tmat}$ [mil. m^3]			
	1188	153.1	278.9	398.7	493.6
	Q_{500}	$V_{500tmax}$ [mil. m^3]			
	1669	218.4	375.9	501.2	599.4
	Q_{1000}	$V_{1000tmax}$ [mil. m^3]			
	1911	252.7	422.4	547.5	644.8

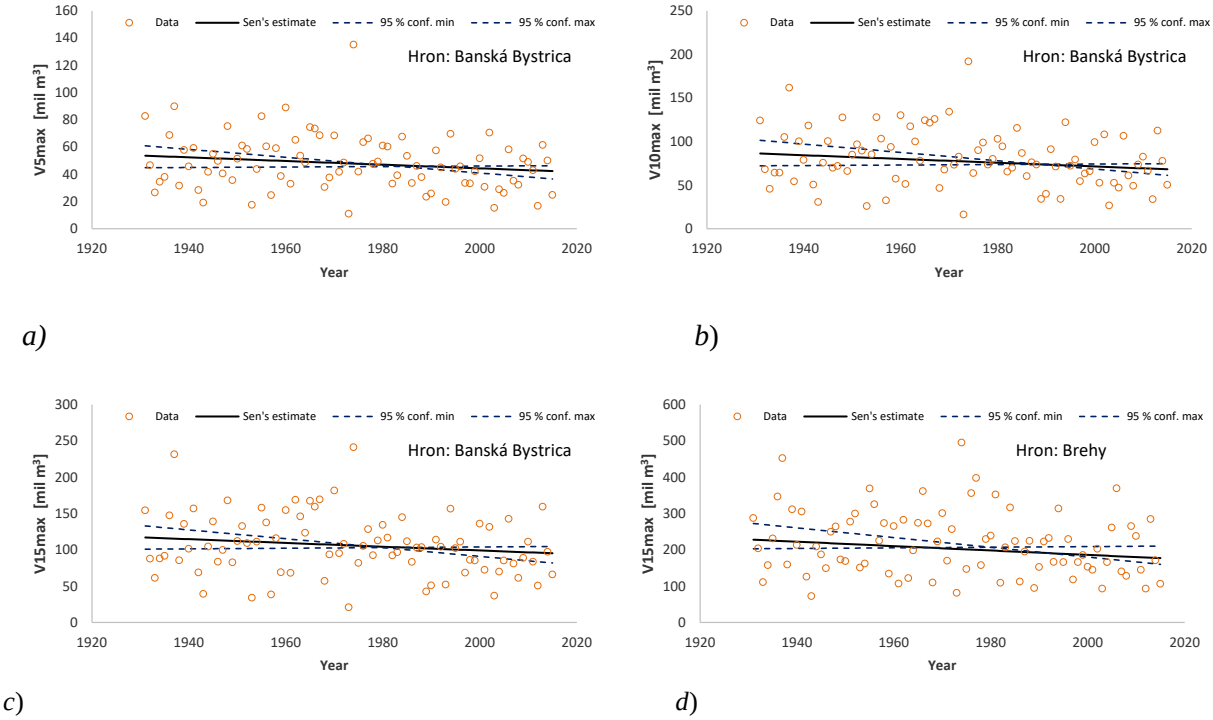

Fig. 9. The Mann-Kendall trend test for annual maximum runoff volumes V_{tmax} with various time duration of the waves belong to annual maximum flows of the Hron River at Banská Bystrica gauging station and at Brehy gauging station (1931–2020).

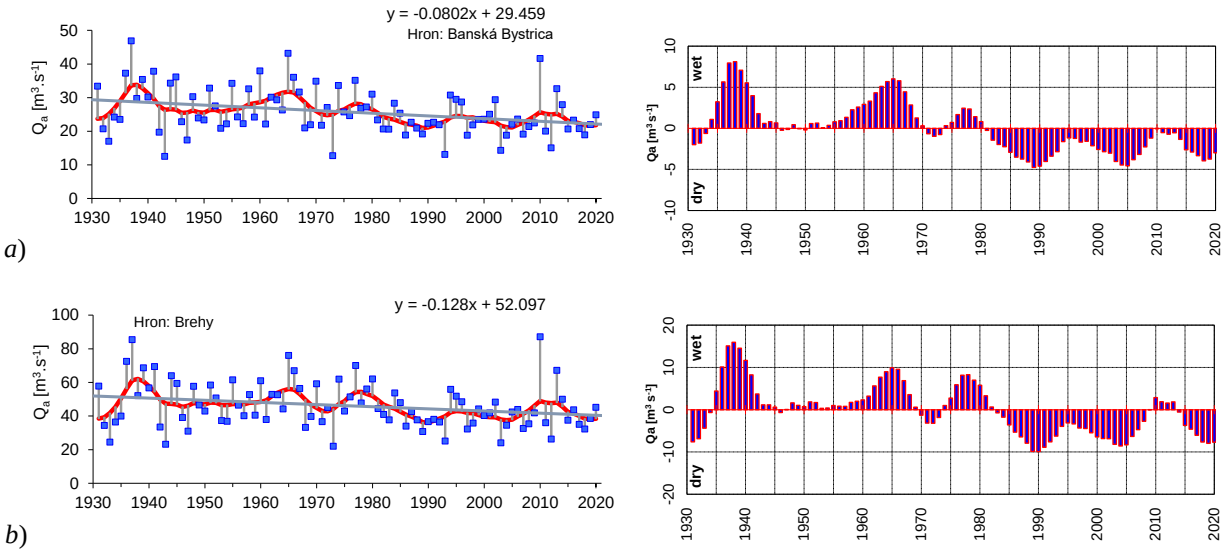

Fig. 10. Course of the a) annual flows, their linear trend and b) dry and wet periods based on double 5-year moving averages of the Hron River a) at Banská Bystrica and b) Brehy gauging stations for the period 1931–2020.

in the wet period (Figure 10). Figure 10 also shows that since 1980 the dry periods prevail.

The M-K trend analysis did not indicate a significant long-term linear trend in annual maximum runoff volumes for dry and wet periods. A Log-Pearson III distribution was used to calculate the *T*-year maximum runoff volume with the given runoff time duration *t* for dry and wet periods.

The example of differences between estimated T-year maximum annual runoff volumes for dry and wet periods are illustrated in Figure 11. In the wet period, with the same probabilities of exceeding, higher values of maximum volumes may occur compared to the dry period. Dividing the period 1931–2020 into dry and wet periods had a greater impact on changes in LPIII exceedance curves of the maximum runoff at higher values of volumes with time duration t=2 and 5-days for wet period.

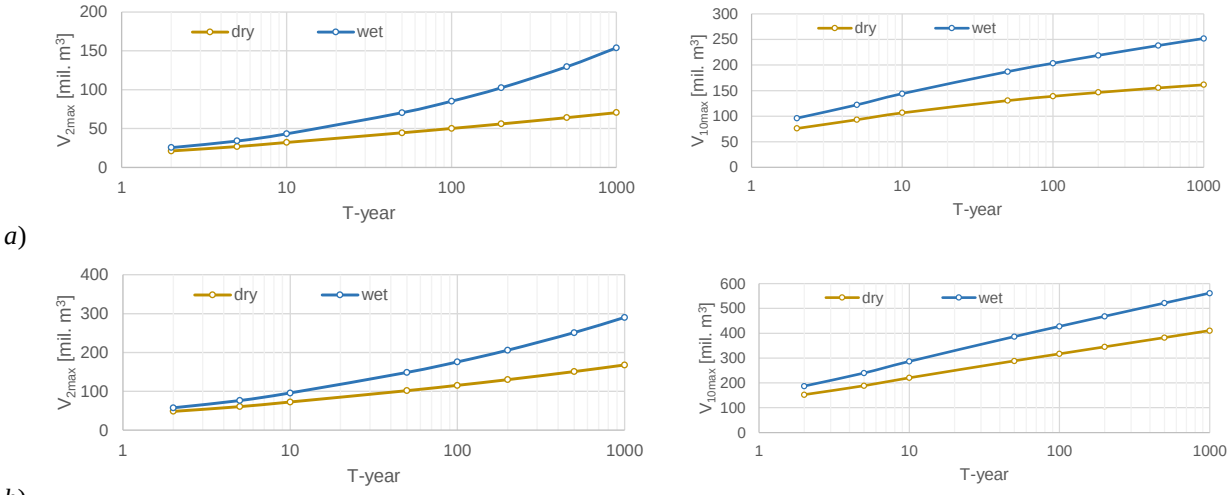

a)

b)

Fig. 11. Example of the differences in estimated T-year maximum annual runoff volumes with time duration t 2-days and 15-days for dry and wet periods of the Hron River a) at Banská Bystrica and b) at Brehy gauging stations (1931–2020).

Conclusion

In the present paper we analyzed, the occurrence of annual maximum runoff volumes with *t*-day durations for a 90-year series of mean daily discharge of the Hron River at Banská Bystrica and at Brehy gauging stations (Slovakia). The statistical methods were used to clarify how the maximum annual runoff volumes of the Hron River at selected gauging stations changed over the period 1931–2020 and over dry and wet periods. The highest number of flow waves belonging to the annual maximum occurs in March and in April. On the Hron River is usually the maximum annual flow occur simultaneously with the annual maximum runoff volume of waves with a given time duration t. However, the corresponding values in terms of significance are not always equivalent. Spring flow waves usually have a larger volume, while summer flow waves have a smaller volume but a higher flow. Based on the exceeding probability curves of the annual maximum runoff volumes, it is possible to determine to the selected volume *V* for different *t* the probability of its exceeding and return period. The M-K tests showed decreasing trend of the annual maximum runoff volumes at significance level α=0.1 for the period 1931–2020 for *t*=5-, 10-, 15-days of the waves belong to annual maximum flows of the Hron River at Banská Bystrica.

The division of the period 1931-2020 into wet and dry periods has shown that the dry periods prevail since 1980 on the Hron River in analyzed gauging stations. Next, probabilities of exceedance of the annual maximum runoff volumes on the Hron at Banská Bystrica and Berhy for selected runoff durations *t*=2-, 5-, 10-, and 15-days in given periods were estimated, plotted and compared. The results suggest that the maximum annual runoff volumes of duration t=2-days, 5-days and 10-days has no significant changes in estimation. In the wet period with the same probabilities of exceeding, higher values of maximum volumes may occur compared to the dry period. Dividing the period 1931–2020 into dry and wet periods had a greater impact on changes in LPIII exceedance curves of the maximum annual runoff volumes with long return period values of volumes with time duration *t*=2-, and 5-days.

The results are useful in water planning, flood protection and can help mapping flood risk areas and developing river management plans in Hron River basin. It would also be good to analyze possible long-term changes in volumes in terms of seasonality during the year. In the future, it would be desirable to confirm the conclusions also on other rivers in Slovakia with satisfactory long runoff data series, or based on reconstructed discharge values by indirect methods (analogy, mathematical runoff modeling, etc.).

Acknowledgement

This work was supported by the project VEGA No. 2/0004/19 "Analysis of changes in surface water balance and harmonization of design discharge calculations for estimation of flood and drought risks in the Carpathian region".

References

ACWD (1982): Guidelines for determining flood flow frequency, Bulletin 17-B. Technical report, Interagency Committee on Water Data, Hydrology Subcommittee. 194 p.

Bačová-Mitková, V., Halmová, D. (2014): Joint modelling of flood peak discharges, volume and duration: a case study of the Danube River in Bratislava. Journal of Hydrology and Hydromechanics, Vol. 62, no. 3, 186–196. DOI: 10.2478/johh-2014-0026

Bačová Mitková, V., Pekárová, P., Miklánek, P., Pekár, J. (2016): Hydrological simulation of flood transformations in the upper DanubeRiver: Case study of large flood

events. In Journal of Hydrology and Hydromechanics, Vol. 64, No. 4, 337–348. https://doi.org/10.1515/johh-2016-0050

Bačová Mitková, V., Halmová, D. (2021): Analizing changes and frequency distribution in maximum runoff volumes with different duration of the Danube river at Bratislava. Acta Hydrologica Slovaca, vol. 22, no. 1, 50–60. doi: 10.31577/ahs-2021-0022.01.0006

Balistrocchi, M., Orlandini, S., Ranzi, R., Bacchi, B. (2017): Copula-based modeling of flood control reservoirs. Water Resources Research, Vol. 53, no. 11, 9883–9900. https://doi.org/10.1002/2017WR021345

Blöschl, G. et al. (2017): Changing climate shifts timing of European floods. Science 357, 588–590. DOI: 10.1126/science.ann2506

Blöschl, G., Hall, J., Viglione, A. et al. (2019): Changing climate both increases and decreases European river floods. Nature 573, 108–111. https://doi.org/10.1038/s41586-019-1495-6

Bobee, B. (1975): The Log Pearson Type 3 Distribution and Its Application in Hydrology. Water Resources Research, Vol. 11, No. 5, 681–689.

Gądek, W. J, Bodziony, M. (2015): The hydrological model and formula for determining the hypothetical flood wave volume in non-gauged basins. Meteorol. Hydrol. Water Manage. Vol. 3, no. 1, 3–10. DOI: https://doi.org/ 10.26491/mhwm/41759

Gilbert, R. O. (1987): Statistical Methods for Environmental Pollution Monitoring. John Wiley & Sons, Inc., New York

Griffis, V. W.; Stedinger, J. R. (2007): The Log-Pearson type III distribution and its application in flood frequency analysis. I: Distribution characteristics. J. of Hydrologic Engineering, 12, 5, 482–491.

Guo, Y., Adams, B. (1998): Hydrologic analysis of urban catchments with event-based probabilistic models 1. Runoff volume. Water Resources Research Vol. 34, no.12, 3421–3431. https://doi.org/10.1029/98WR02449

Halmova D., Pekarova P., Pekar J., Onderka M. (2008): Analyzing temporal changes in maximum runoff volume series of the Danube River. IOP Conf. Series: Earth and Environmental Science 4, IOP Publishing. 1–8. doi:10.1088/1755-1307/4/1/012007.

Hamed, K. H. (2008): Trend detection in hydrologic data: The Mann-Kendall trend test under the scaling hypothesis. Journal of Hydrology, 349(3-4), 350–363.

Huang, K., Fan, Y. R. (2021): Parameter Uncertainty and Sensitivity Evaluation of Copula-Based Multivariate Hydroclimatic Risk Assessment. Journal of Environmental Informatics, (2). Dec2021, Vol. 38 no. 2, 131–144.

Mediero, L., Jiménez-Álvarez, A., Garrote, L. (2010): Design flood hydrographs from the relationship between flood peak and volume," Hydrol. Earth Syst. Sci., 14, 2495–2505.

Mitková, V., Pekárová, P., Kohnová, S. (2004): Comparison of estimates of maximum seasonal flows in the Danube-Bratislava profile. Acta Hydrologica Slovaca. No. 1, 34–40. (In Slovak)

Paquet, E., Garavaglia, F., Garçon, R., Gailhard, J. (2013): The SCHADEX method: a semi-continuous rainfall–runoff simulation for extreme flood estimation. J. Hydrol., Vol. 495, 23–37. https://doi.org/10.1016/j.jhydrol. 2013.04.045

Papaioannou, G., Kohnová, S., Bacigál, T., Szolgay, J., Hlavčová, K., Loukas, A. (2016): Joint modelling of flood peaks and volumes: A copula application for the Danube River. Journal of Hydrology and Hydromechanics, Vol. 64, no. 4, 382–392. DOI: 10.1515/johh-2016-0049

Pawar, U.; Hire, P. (2018): Flood Frequency Analysis of the Mahi Basin by Using Log Pearson Type III Probability Distribution. Hydrospatial Analysis 2(2), 102–112. Dx.doi. org/10.21523/gcj3.

Pekárová, P., Szolgay, J. (eds.), 2005: Scenarios of changes in selected hydrosphere and biosphere components on the Hron and Vah catchment areas due to climate change. Press Bratislava: Veda, 496 p. ISBN 80-224-0884-0. (In Slovak).

Pekárová, P., Bačová Mitková, V. Pekár J., Miklánek P., Halmová D., Liova S. (2018): Historical food on the territory of Slovakia and their importance in hydrology. (In Slovak: Historické povodne na území Slovenska a ich význam v hydrológii.) Bratislava: Veda, SAS, 135 p. ISBN 978 -80-224-1684-9.

Pekárová, P., Miklánek, P. (eds.) (2019): Flood regime of rivers in the Danube River basin. Follow-up volume IX of the Regional Co-operation of the Danube Countries in IHP UNESCO. IH SAS, Bratislava, 215 p. + 527 p. app., DOI: 10.31577/2019.9788089139460.

Pilon, P. J., Adamowski, K. (1993): Asymptotic variance of flood quantile in log Pearson type III distribution with historical information, J. of Hydrol., 143, 3-4, 481–503.

Szolgay, J., Gaál, L., Kohnová, S., Hlavčová, K., Výleta, R., Bacigál, T., Blöschl, G., (2015): A process-based analysis of the suitability of copula types for peak-volume flood relationships. Proc. IAHS, 370, 183–188. doi: 10.5194/piahs370-183-2015.

Zatkalík, G. (1970): Calculation of the basic parameters of the flow waves. PhD. thesis. 71 p. (In Slovak)

Ing. Veronika Bačová Mitková, PhD. (*corresponding author, e-mail: mitkova@uh.savba.sk)
Institute of Hydrology SAS
Dúbravská cesta 9
84104 Bratislava
Slovak Republic

DOI: 10.31577/ahs-2022-0023.01.0006

ACTA HYDROLOGICA SLOVACA

Volume 23, No. 1, 2022, 52 – 61

A methodology for the estimation of control flood wave hydrographs for the Horné Orešany reservoir

Anna LIOVÁ*, Peter VALENT, Kamila HLAVČOVÁ, Silvia KOHNOVÁ, Tomáš BACIGÁL, Ján SZOLGAY

Recent changes in climatic characteristics and consequent changes in the discharges and in the hydrological response of watersheds raise questions about the safety of water structures. Changes in flood wave characteristics (shape, volume, peak flow) may significantly affect the functionality of these structures. The study proposes a methodology for constructing design wave and flood hydrographs using discharge time series. A case study was carried out in the Little Carpathians watershed of the Parná River, above the profile of the Horné Orešany reservoir in Slovakia. The volumes and characteristic shapes of the flood waves with the maximum annual and seasonal discharges were determined using the Floodsep software. Subsequently, the *T*-year annual and seasonal discharges were estimated. Then, for pairs of the *T*-year discharges and the associated volumes of flood waves, a joint probability distribution was constructed by copula functions. The associated volume of the *T*-year peak discharges was selected from the copula, and the probability of exceeding it was determined. Based on this analysis, a set of annual and seasonal control flood waves with the design maximum discharge, the associated volume with the selected probability, and the typical shape of the flood wave was constructed. This research provides satisfactory results for designing control waves necessary for assessing water structures with extreme loads and establishing a functional methodology for assessing other water structures in the region.

KEY WORDS: design flood hydrograph, Horné Orešany reservoir, separation of discharge wave

Introduction

Discharge time series are essential for various hydrology and water resources management activities. They are used to provide valuable information about long-term flow characteristics as well as, to a partial extent, when the analysis of individual extreme events are essential for solving many problems. In the case of floods, flood peak discharges are often sufficient to perform a traditional flood frequency analysis, the results of which can be used to design many engineering structures such as levees, bridges or flood control channels. However, it is sometimes critical to use whole flood hydrographs, as they provide other essential flood characteristics such as volume, duration, gradient, course, etc. These characteristics can be affect by the recent hydrological time series changes (Ďurigová et al., 2020; Mohammadzadeh et al., 2019; Yonus and Hassan, 2022). In practice, these hydrographs are often referred to as design flood hydrographs (DFH), which are often associated with an estimated return period. Hence, the physical properties of a flood event and statistical information about the event's rarity must be united (Serinaldi and Grimaldi, 2011). Design flood hydrographs are used as input for hydraulic simulations that are necessary for the design and safety assessments of critical hydraulic structures, such as dams or retention basins, as well as for the preparation of operational rules and management strategies of existing flood mitigation measures (Goswami, 2020; Yue et al., 2002).

The design of a hydraulic structure is sensitive to all the characteristics of a DFH, which means that it has to be estimated as close to reality as possible (Paquet, 2019). Even slight differences in any characteristic of the DFH may cause significant changes in the cost and efficiency of these structures (Yue et al., 2002). An excellent example of the importance of characteristics other than the flood peak, volume, and duration on the efficiency of retention basins in flood protection is given by Chow et al. (1988). They describe a situation in which two flood waves, differing only in their shapes, result in significant differences in the retention basin's flood peak reduction efficiency. To define a complete DFH, one has to estimate the following characteristics: 1) its peak discharge, 2) hydrograph volume or duration, and 3) the shape of the hydrograph. Estimating the first two characteristics is a traditional task in hydrology. It is backed up by many well-established methods, which are thoroughly described in an extensive literature describing the individual methods and their practical application.

Unfortunately, most of these methods are dedicated to a univariate flood frequency analysis (FFA), which communicates the difficulties of estimating hydrological variables (mostly peak discharges) with very large return periods that are far beyond the range of an available historical dataset (Paquet, 2019). However, the characteristics of flood hydrographs cannot be described by a single variable but must be described by a set of interdependent random variables usually consisting of a flood´s peak, volume and duration (Brunner et al., 2016). This means that the univariate framework of the FFA is not applicable and that a bi- or multivariate approach has to be considered instead of accounting for the dependency between, e.g., flood peaks and flood volumes or flood peaks and flood durations (Gräler et al., 2013; Salvadori and Michale, 2004; Szolgay et al., 2016).
Flood hydrographs often come in different shapes. They differ not only between catchments but also between the individual events influenced by various hydroclimatic factors (e.g., rainfall depths, wetness of a catchment), including the governing processes that determine the flood type (Brunner et al., 2017; Merz and Blöschl, 2003). Yue et al. (2002) summarize the existing methods of constructing unit hydrographs, which can be used to represent the shape of the constructed DFH and group them into the following four classes: traditional unit hydrograph (TUH), synthetic unit hydrograph (SUH), typical hydrograph (TH) and statistical methods (SM). While the TUH methods (Dooge, 1959; Yue and Hashino, 2000) utilize rainfall data and rely on simple rainfall-runoff modelling, the SUH methods (Jena and Tiwari, 2006; Snyder, 1938) try to relate the unit hydrographs to the physiographic descriptors of the catchments and enable their estimation in ungauged catchments as well. The TH methods (Paquet, 2019; Xiao et al., 2009) select the unit hydrograph from the observed flood hydrographs and scale it accordingly, as opposed to the SM methods (Brunner et al., 2018a; Goswami, 2020; Serinaldi and Grimaldi, 2011), which use probability density functions (pdf) of known flexible distributions to model the shape of the unit hydrograph with the significant advantage of the area under the curve being one (1). When constructing a DFH, Brunner et al. (2017) also emphasize the importance of limiting the analysis to the individual flood types such as flash floods, short-precipitation and long-precipitation floods, or snowmelt floods. The authors state that such a flood type-specific design is also advantageous from a statistical point of view as it avoids mixing very different events, which also justifies the assumption made in the FFA that the variables are independent and are randomly and identically distributed. Moreover, the flood type-specific design can also help to identify seasons with different types of flood risks (e.g., large peaks in the summer vs. large volumes in the spring), which can help adjust the existing flood control policies and operational rules of the reservoirs (Gaál et al., 2015; Merz and Blöschl, 2008).
Particular problems in constructing a DFH include developing a sampling strategy and identifying the individual flood events. The sampling strategy influences the sample size used in the analysis, which can often lead to different characteristics of the constructed DFH. Brunner et al. (2018b) investigated annual maxima (AM) and peaks over threshold (POT) sampling strategies and concluded that the latter seems to be a better choice for the estimation of a DFH. However, one should consider that the selection of the sampling strategy influences the apparatus of the methods that can be used in the FFA. Moreover, the automatic selection of the events can extend the flood sample by outliers (man-made floods that should be excluded from the FFA, or multimodal floods that should not be used to estimate the shape of the flood), which have to be manually removed.
Besides selecting the sampling strategy, one must also identify the individual flood events in terms of finding their beginning and end and separating their direct and base runoffs. Thiessen et al. (2019), who developed a method for identifying rainfall-runoff events in discharge time series, states that even though this process might be straightforward for a trained hydrologist, it is complicated to formulate rigid criteria that would enable the reliable identification of flood events. Currently, there is no single accepted method for automating this process, even though it has been the subject of substantial scientific efforts (Oppel and Mewes, 2020).
As the beginning and end of a flood event are often associated with the intersection of baseflow and direct runoff curves, most methods try to separate the baseflow from the discharge time series. The first methods date back to the 1930s (Chow et al., 1988), with the most recent ones utilizing digital filtering techniques, which are currently considered to provide the best results (Gonzales et al., 2009), as the most reliable tracer-based methods often lack input data. To mention a few of these methods, Paquet (2019) identified flood hydrographs by fixing a time from the flood peak (0 h) to the beginning (-24 h) and end (+48 h) of the event. Merz et al. (2006) proposed an iterative approach in which using a digital filter of Chapman and Maxwell (1996), the baseflow was separated from the direct runoff. The event's beginning and end were set at points where the direct runoff became lower than a certain threshold given by the direct runoff at the time of the peak flow. Thiesen et al. (2019) proposed a data-driven approach with different predictors to identify a flood hydrograph at the beginning, peak and end. They found that models using discharges as predictors returned the best results, making them even more attractive, as no additional data is required except for the discharge time series. Finally, Oppel and Mewes (2020) trained several machine learning algorithms to identify the beginning and end of a flood event as given by the position of its peak discharge. Despite the fact that their methods were able to reproduce manually-identified flood hydrographs very well, the process of building, training, and testing the algorithms is far beyond the capabilities of ordinary practitioners. Therefore, multiple authors have often suggested performing some sort of manual control to pick incorrectly identified flood events and exclude oddly-shape events from a flood sample dataset (Gaál et al., 2012; Merz et al., 2006; Paquet, 2019).
This study presents a complete methodology that can be

used to build design flood hydrographs using only discharge time series. Within the methodology, a simple semi-automatic procedure was developed to identify the beginning and end of the pre-selected flood events, thereby enabling any type of sampling strategy. The flood event characteristics such as flood peaks, volumes, and durations are also a subject of a bivariate FFA using copulas to derive a joint probability distribution for dependent variables (either flood peaks and volumes or flood peaks and durations). The shape of the DFH is derived from the identified flood events, which are simplified to maintain the monotonicity of their rising and falling limbs (multimodal to unimodal hydrographs) and smoothed using a smoothed function composed of several normal distributions pdfs. The method enables the DFH construction using a flood´s peak, volume or duration and shape.

Materials and methods

Study area

The design flood hydrograph estimation for the safety assessment of the waterworks was processed for the Horné Orešany reservoir dam in Slovakia, which is located on the Parná river at rkm 25.00. The Parná river, with a length of 38.5 km, is the right-handed tributary of the Trnávka river. The spring of the Parná river is located in the Little Carpathians on the southeastern slopes of the Vápenná hill at an altitude of 560 m a.s.l. The catchment area in the reservoir profile is 45.59 km²; the catchment is fan-shaped; and the average slope of the catchment is 2.5 %. The water structure is classified in II category of water structures, according to the amount of damage that would result from the sudden release of the water held. The dam was built for the purpose of land irrigation, mitigation of peak flows, improvement of minimum flows, sport fishing, and electricity generation. The water reservoir volume is 3.8 mil. m^3 and the flooded area is 0.496 km^2.
As the input data were used the discharge time series in hourly time steps and the maximum annual discharges. Data used in the analysis were provided by the Slovak Hydrometeorological Institute (SHMI) for the 5250 Parná – Horné Orešany gauging station for the period 1.11.1988–31.12.2019. The gauging station is located above the reservoir on the Parná river at rkm 26.8, and has a catchment area of 37.86 km^2. Precipitation and air temperature data were used for a better determination of the flood wave durations. The precipitation in the daily time step was collected from the Dolné Orešany rainfall station for the period 1.11.1988–31.12.2013. The air temperature data in the daily time step were taken from the SHMI Modra – Piesok climatological station for the period 1.11.1988–31.12.2013.

Methodology

Selection of discharge waves based on their seasonal occurrence

To determine the design flood hydrographs, it was necessary to correctly select the discharge waves and identify their volume and shape characteristics. The discharge waves analysed differed significantly not only in their duration but also in their shape and volume. Spring discharge waves are associated with melting snow or a combination of melting snow and rain. A similar wave formation may occur in the winter period. Therefore, these waves have a longer duration and greater volume than summer discharge waves, which often arise from storm events. Summer waves are slimmer in shape with a shorter duration.
For this reason, flood waves were analysed for annual and seasonal maximum discharges for the period 1989–2019, i.e.:

- Seasonal maximum discharges, April to May – Spring season;
- Seasonal maximum discharges, June to October – Summer season;
- Seasonal maximum discharges, November to March – Winter season;
- Annual maximum discharges.

Separation of discharge waves

A discharge wave is characterised by a rising limp, culmination, and subsequent falling limp. The separation of these waves and the calculation of the base flow have been processed by methods used in the FloodSep software (Valent, 2019). An example of separation is shown in Figure 1. The main task o f FloodSep is to

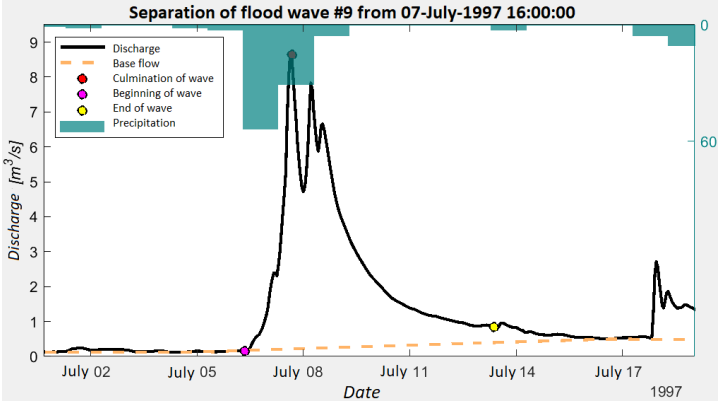

Fig. 1. Example of a flood wave separation in the FloodSep programme (Valent, 2019).

identify individual flood events from a time series of discharges and then analyse their characteristics. Subsequently, it was necessary to determine the flood peaks from a series of hourly discharges for each year. In each group of floods, the peak discharges were manually determined. The separation of the waves then took place in the following steps in each group according to the methods that were programmed in FloodSep:

1 Separation of the base flow: the beginning and end of the wave are determined subjectively.
2 Allocation of the beginning and end of the wave using precipitation and air temperature data.

Selection of the representative shape of the wave

The shape of the flood wave used in the design flood hydrographs was determined using the methods programmed in FloodSep as follows: In the first step, the discharge waves selected were simplified and scaled to an interval <0.1>. Then the multimodal flow hydrographs were transformed into a simple modal form. In the second step, a representative hydrograph was constructed from a set of scaled waves. The hydrographs were centred on the peak position so that the x-axis coordinate at this point was equal to 0. When flood hydrographs are constructed, the important parameter is the percentile, which affects the shape of the representative hydrograph. In this study, the 50%, 70% and 90% percentiles were applied, which resulted in three different shapes of flood hydrographs.

Local estimation of T – year discharges from available measurements

The estimation of the annual and seasonal floods, the selection of the theoretical probability distribution, and the parameters of the method for estimating the theoretical probability distribution were made according to the DVWK (1999) methodology. The following theoretical probability distribution and methods for estimating the parameters were selected according to statistical tests proposed in the DVWK:

- Spring season – 3-parameter lognormal distribution (LN3), the maximum likelihood method;
- Summer season – The Generalized Extreme Value distribution (GEV), the maximum likelihood method;
- Winter season – Pearson type III distribution (P3), the method of probability weighted moments;
- $Q_{an,max}$ – log-Pearson type III distribution (LP3), the moments method.

Volume of flood waves derived by an analysis of the relationship between the culmination and volumes

A joint probability distribution using a copula function was constructed for the pairs of peak discharges and their associated volumes. In this paper, we use the following types of copulas, chosen according to the smallest distance:

- Spring season – Frank copula;
- Summer season – Gumbel copula;
- Winter season – Gumbel copula;
- $Q_{an,max}$ – T copula.

For this study, we used a selected discharge with a probability of exceeding 0.01 and a conditional probability of non-exceedance of 0.5, 0.7, and 0.9.

Results and discussion

Separation of discharge waves

Figures 2 to 4 show the separation of the discharge waves in the spring, summer, and winter seasons. We can see that during the initial separation, some waves had prolonged durations and thus increased their volume. Attention was particularly paid to waves that were outside the range of the majority of the separated waves after the first step of the separation. When determining the duration of waves with more extreme values, whether it involved the peak discharge or volume, the beginning and end of the flow waves were incorrectly determined in the first step using the base flow. After an adjustment in the second step, their volumes decreased.
The results of the separation of the annual maximum discharge waves are shown in Figure 5.
We can see that the wave layout is not homogeneous and consists of several groupings of waves. While winter and spring waves rank towards waves with larger volumes and lower peak discharges, summer waves stand out from this trend and are characterised by a higher discharge and smaller volume, i.e., shorter durations. This redistribution of the waves points to the fact that the selection of waves in each season was an appropriate procedure for the solution and should be taken into account in the design of the design flood hydrographs.

Representative shape of control flood waves

As already mentioned in the previous section, waves with a percentile value of 50, 70 and 90% were selected for each group of floods. Figures 6 to 9 show the separated waves scaled for each group; as an example, only the percentile value of 50% is presented here. The highlighted shape is the representative one, see Figs. 6 to 9 (left). The next step produces a representative smoothed hydrograph using the Gauss composite function. The representative hydrograph defines the shape of the design wave, which is necessary for the correct determination of design flood hydrographs Figs 6 to 9 (right).

Construction of the flood control waves

When the design flood hydrographs were constructed, the design discharge values of the selected probability of exceedance and the corresponding volume and duration of the wave were estimated.
The results of the local estimation of the T – year discharges and conditional volumes of a given 100-year

discharge for each group are shown in the following Tables 1 to 3. As already mentioned in the previous sections, we used the following data for the design flood estimation: the 100-year design discharge, conditional probability of non-exceedance of the volume 0.5, 0.7 and 0.9, and wave duration, which we determined by assigning the conditional volume to the wave shape, using the 50, 70, and 90% percentile shapes.

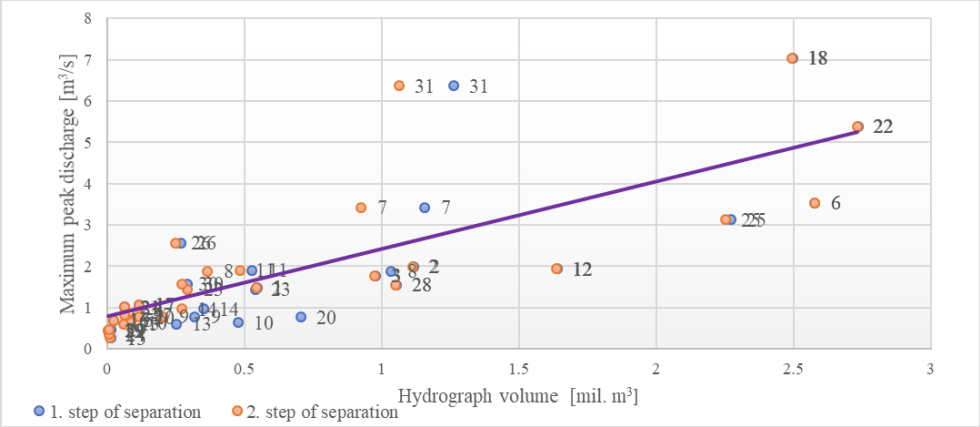

Fig. 2. Relationship between a flood´s volume and peak discharge: results of discharge-wave separation in the Spring season.

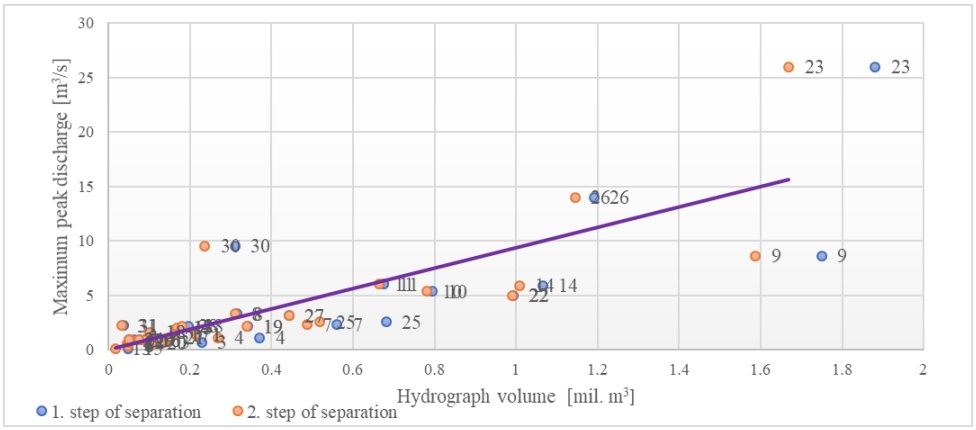

Fig. 3. Relationship between a flood´s volume and peak discharge: results of discharge-wave separation in the Summer season.

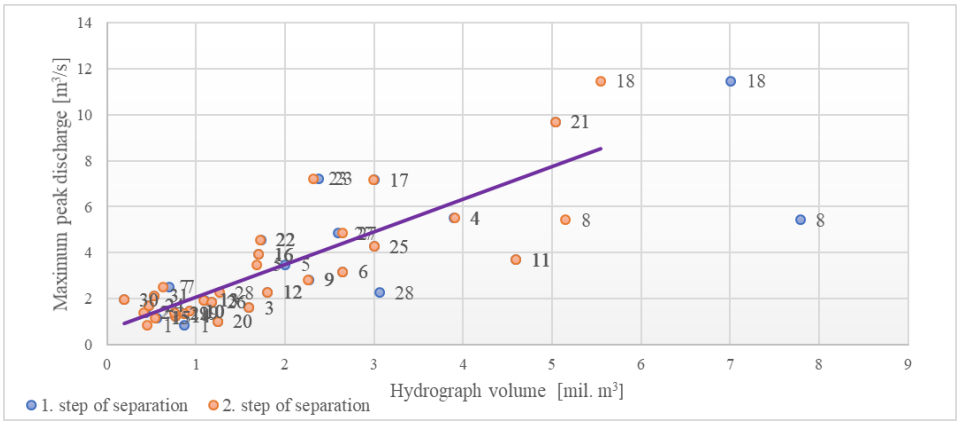

Fig. 4. Relationship between a flood´s volume and peak discharge: results of discharge-wave separation in the Winter season.

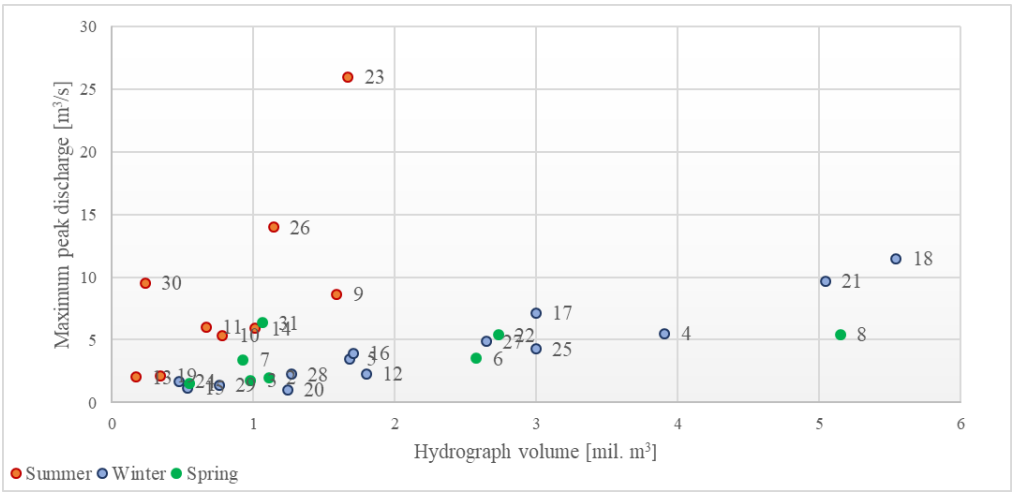

Fig. 5. Relationship between a flood´s volume and peak discharge – annual maximum discharges.

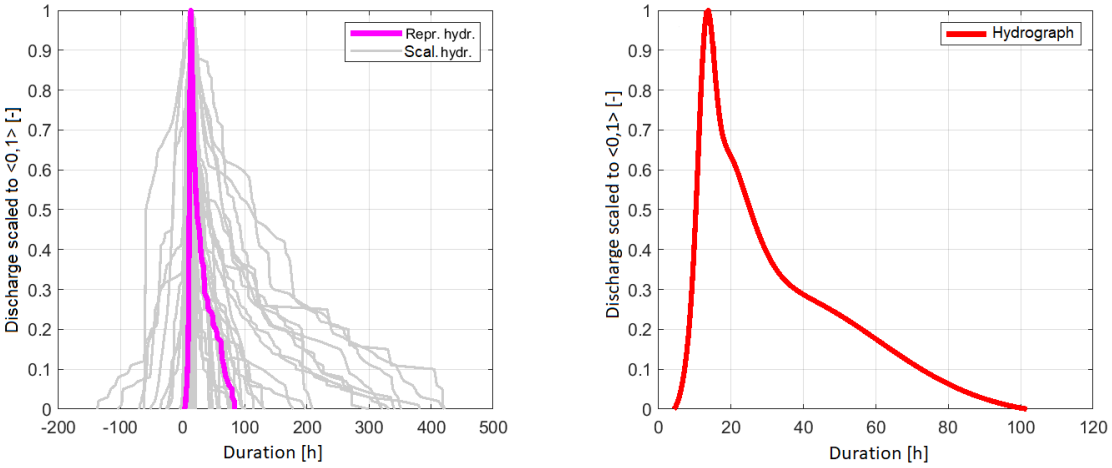

Fig. 6. Representative hydrograph of scaled waves (left) and smoothed representative hydrograph for the spring season (right).

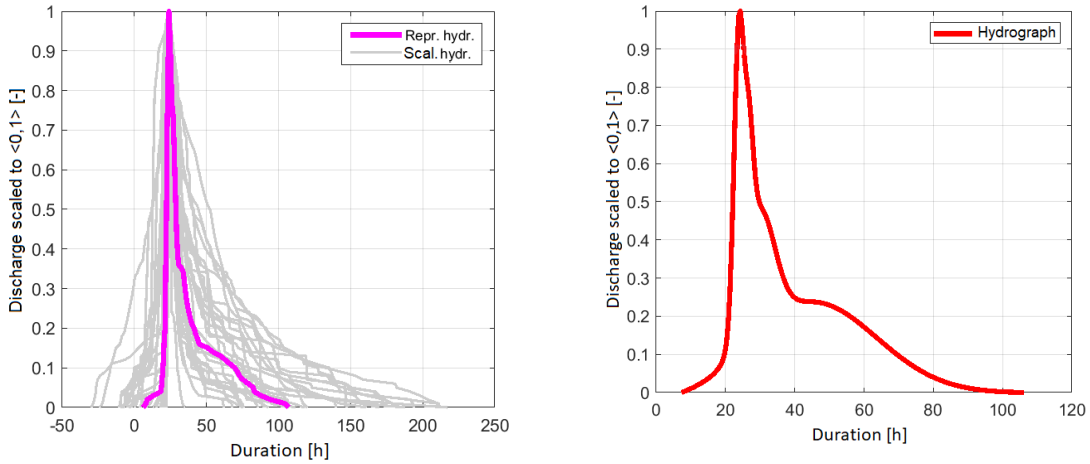

Fig. 7. Representative hydrograph of scaled waves (left) and smoothed representative hydrograph for the summer season (right).

.

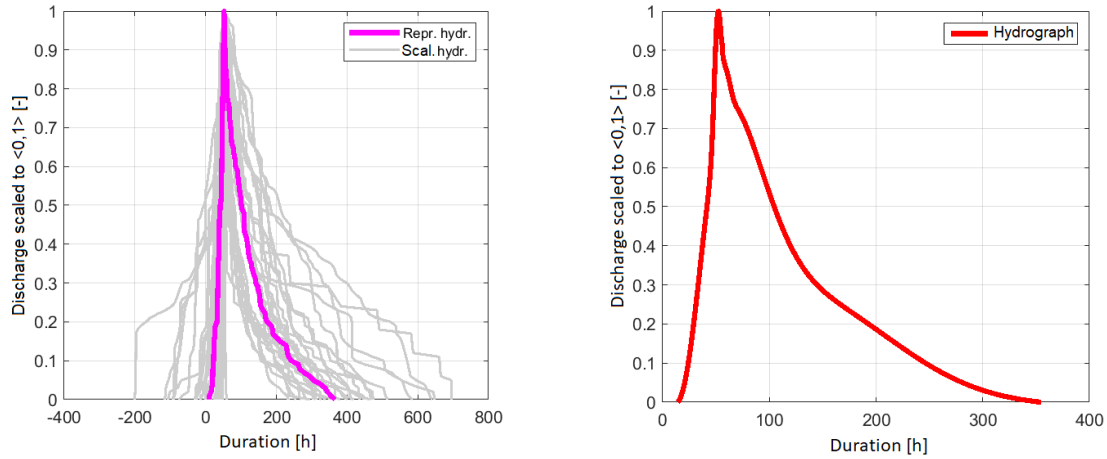

Fig. 8. Representative hydrograph of scaled waves (left) and smoothed representative hydrograph for the winter season (right).

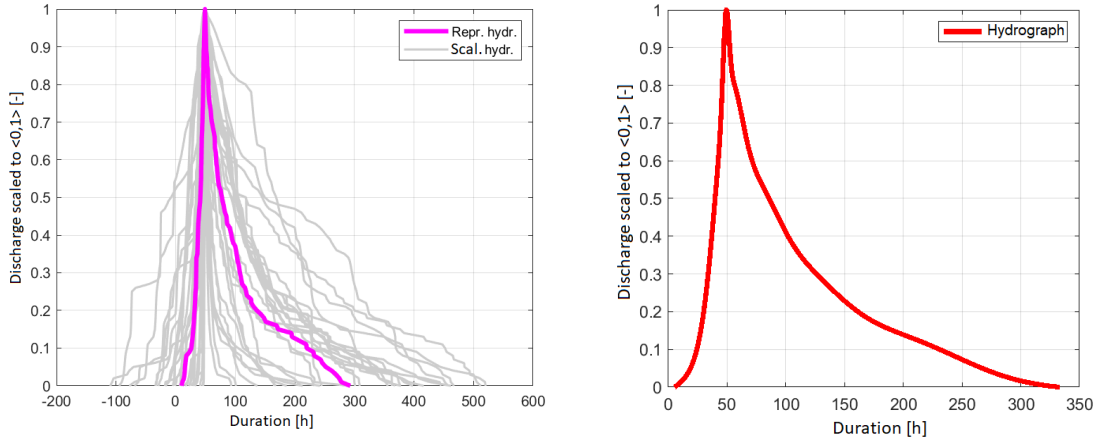

Fig. 9. Representative hydrograph of scaled waves (left) and smoothed representative hydrograph for the annual culminative discharge group (right).

Table 1. *T*-year maximum discharges [m^3 s^{-1}]

N [years]	2	5	10	20	25	50	100	200	500	1000
Spring season	1.2	2.6	4.0	5.6	6.2	8.2	10.7	13.6	18.2	22.3
Summer season	1.8	4.6	8.1	13.7	16.1	26.7	43.7	71.3	135.7	220.5
Winter season	2.5	5.0	6.9	9.0	9.6	11.7	13.7	15.8	18.5	20.6
Annual	3.9	7.7	11.2	15.4	17.0	22.4	28.8	36.5	48.9	60.2

Table 2. Conditional volumes with various non-exceedance probabilities to a given 100-year discharge [million m^3]

P [-]	0.4	0.5	0.6	0.7	0.8	0.9	0.99
Spring season	2.117	2.405	2.724	3.110	3.621	4.460	7.207
Summer season	2.194	2.271	2.345	2.432	2.525	2.671	3.090
Winter season	6.840	7.109	7.374	7.642	7.958	8.415	9.711
Annual	2.713	3.253	3.900	4.736	5.944	8.146	17.219

Table 3. Values of the design flood hydrographs

Group	Q_{100} [m^3.s^{-1}]	V [mil. m^3]			t_c [h]		
		0.5	0.7	0.9	0.5	0.7	0.9
Annual maximum	28.80	3.253	4.736	8.146	132.8	184.8	269.2
Spring season	10.69	2.405	3.11	4.46	222.9	343.1	397.1
Summer season	43.70	2.271	2.432	2.671	82.0	89.2	92.4
Winter season	13.72	7.109	7.642	8.415	506.0	511.2	540.7

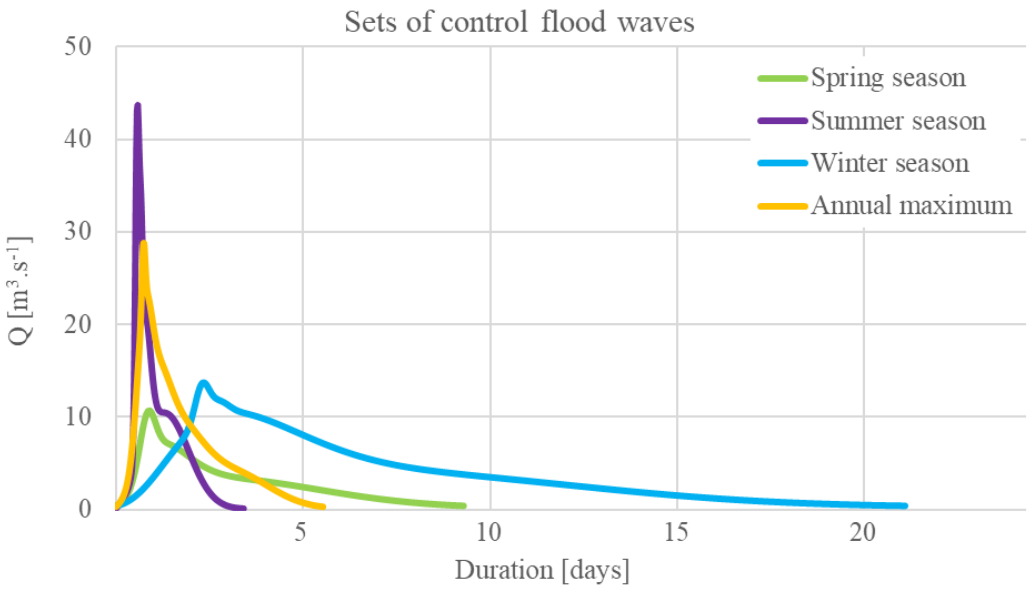

Fig. 10. Design control flood waves for all the seasons analysed.

Conclusion

We have addressed the construction of a set of design flood hydrographs. The design of the flood hydrographs was based on an analysis of the relationship between the culmination, volume, and shape of the flood waves. The project was processed for the Parná River basin in the profile of the Horné Orešany dam. The findings and results can be summarised as follows:

As the discharge waves differ significantly due to their seasonal occurrence, the first step needed to analyse the individual discharge waves in separate groups was to select a group of annual maximum discharges and three seasonal groups i.e., spring, summer, and winter. The next step was the separation of the individual discharge waves, where we took into account the antecedent climatic conditions, i.e., the precipitation and air temperature to determine the beginning and end of each discharge wave. The precipitation data were essential in deciding upon the duration and shape of the rising and falling limp of the flood hydrograph. The temperature data were mainly used in the winter season to estimate the start of the melting snow. The separation resulted in the dataset of the volume and duration of all the flood events identified. Representative shapes of the flood hydrographs were constructed from the separate discharge waves. Finally, we identified the design flood hydrographs with the selected probability of exceedance. In this paper we have shown the results for discharges with the probability of exceeding 0.01. The relationship between the peak discharge and the volumes of the individual flood events has been analysed, and a joint probability distribution was constructed using a copula function. Finally, we calculated the conditional probability of non-exceeding the volume of a given 100-year discharge.

Acknowledgement

This work was supported by the Slovak Research and Development Agency under Contract No. APVV 19-0340, No. APVV 20-0374 and the VEGA Grant Agency No. VEGA 1/0632/19.

References

Brunner, M. I., Seibert, J., Favre, A.-C. (2016): Bivariate return periods and their importance for flood peak and

volume estimation, WIREs Water, 3, 6, 819–833. DOI: 10.1002/wat2.1173

Brunner, M. I., Viviroli, D., Sikorska, A. E., Vannier, O., Favre, A.-C., Seibert, J. (2017): Flood type specific construction of synthetic design hydrographs, Water Resources Research, 53, 2, 1390–1406. DOI: 10.1002/2016WR019535

Brunner, M. I., Furrer, R., Sikorska, A. E., Viviroli, D., Seibert, J., Favre, A.-C. (2018a): Synthetic design hydrographs for ungauged catchments: a comparison of regionalization methods, Stochastic Environmental Research and Risk Assessment, 32, 7, 1993–2023. DOI: 10.1007/s00477-018-1523-3

Brunner, M. I., Sikorska, A. E., Furrer, R., Favre, A.-C. (2018b): Uncertainty Assessment of Synthetic Design Hydrographs for Gauged and Ungauged Catchments, Water Resources Research, 54, 3, 1493–1512. DOI: 10.1002/2017WR021129

Chapman, T., Maxwell, A. (1996): Baseflow Separation, Comparison of Numerical Methods with Tracer Experiments, undefined,

Chow, V. T., Maidment, D., Mays, L. (1988): Applied Hydrology, New York: McGraw-Hill Science/Engineering/Math, 572 pp. ISBN: 978-0-07-010810-3

Dooge, J. C. I. (1959): A general theory of the unit hydrograph, Journal of Geophysical Research (1896-1977), 64, 2, 241–256. DOI: 10.1029/JZ064i002p00241

DVWK 101 (1999): Wahl des Bemessungshochwassers. Empfehlung zur Berechnung der Hochwasser-wahrscheinlichkeit. DVWK Schriften, Heft 101. Verlag Paul Parey, Hamburg.

Ďurigová, M., Hlavčová, K., Poórová, J.(2020): Detection of Changes in Hydrological Time Series During Recent Decades. Slovak Journal of Civil Engineering,28(2) 56–62. https://doi.org/10.2478/sjce-2020-0016

Gaál, L., Szolgay, J., Kohnová, S., Hlavčová, K., Parajka, J., Viglione, A., Merz, R., Blöschl, G. (2015): Dependence between flood peaks and volumes: a case study on climate and hydrological controls, Hydrological Sciences Journal, 60, 6, 968–984. DOI: 10.1080/02626667.2014.951361

Gaál, L., Szolgay, J., Kohnová, S., Parajka, J., Merz, R., Viglione, A., Blöschl, G. (2012): Flood timescales: Understanding the interplay of climate and catchment processes through comparative hydrology, Water Resources Research, 48, 4 DOI: 10.1029/2011WR011509

Gonzales, A. L., Nonner, J., Heijkers, J., Uhlenbrook, S. (2009): Comparison of different base flow separation methods in a lowland catchment, Hydrology and Earth System Sciences, 13, 11, 2055–2068. DOI: 10.5194/hess-13-2055-2009

Goswami, M. (2020): Generating design flood hydrographs by parameterizing the characteristic flood hydrograph at a site using only flow data, Hydrological Sciences Journal, 0, 0, pp. 1–19. DOI: 10.1080/02626667.2020.1843656

Gräler, B., Berg, M. J. van den Vandenberghe, S., Petroselli, A., Grimaldi, S., Baets, B. D., Verhoest, N. E. C. (2013): Multivariate return periods in hydrology: a critical and practical review focusing on synthetic design hydrograph estimation, Hydrology and Earth System Sciences, 17, 4, 1281–1296. DOI: https://doi.org/10.5194/hess-17-1281-2013

Jena, S. K., Tiwari, K. N. (2006): Modeling synthetic unit hydrograph parameters with geomorphologic parameters of watersheds, Journal of Hydrology, 319, 1, 1–14. DOI: 10.1016/j.jhydrol.2005.03.025

Merz, R., Blöschl, G. (2003): A process typology of regional floods, Water Resources Research, 39, 12 DOI: https://doi.org/10.1029/2002WR001952

Merz, R., Blöschl, G. (2008): Flood frequency hydrology: 1. Temporal, spatial, and causal expansion of information, Water Resources Research, 44, 8 DOI: 10.1029/2007WR006744

Merz, R., Blöschl, G., Parajka, J. (2006): Spatio-temporal variability of event runoff coefficients, Journal of Hydrology, 331, 3, 591–604. DOI: 10.1016/j.jhydrol.2006.06.008

Mohammadzadeh, N., Amiri, B., Endergoli, L., Karimi, S. (2019): Coupling Tank Model and Lars-Weather Generator in Assessments of the Impacts of Climate Change on Water Resources. Slovak Journal of Civil Engineering, 27(1) 14–24. https://doi.org/10.2478/sjce-2019-0003

Oppel, H., Mewes, B. (2020): On the Automation of Flood Event Separation From Continuous Time Series, Frontiers in Water, 2, p. 18. DOI: 10.3389/frwa.2020.00018

Paquet, E. (2019): Synthetic hydrograph generation by hydrological donors, Hydrological Sciences Journal, 64, 5, 570–586. DOI: 10.1080/02626667.2019.1593418

Salvadori, G., De Michele, C. (2004): Frequency analysis via copulas: Theoretical aspects and applications to hydrological events, Water Resources Research, 40, 12 DOI: 10.1029/2004WR003133

Serinaldi, F., Grimaldi, S. (2011): Synthetic Design Hydrographs Based on Distribution Functions with Finite Support, Journal of Hydrologic Engineering, 16, 5, 434–446. DOI: 10.1061/(ASCE)HE.1943-5584.0000339

Snyder, F.F. (1938): Synthetic unit-graphs, Eos, Transactions American Geophysical Union, 19, 1, pp. 447–454. DOI: 10.1029/TR019i001p00447

Szolgay, J., Gaál, L., Bacigál, T., Kohnová, S., Hlavčová, K., Výleta, R., Parajka, J., Blöschl, G. (2016): A regional comparative analysis of empirical and theoretical flood peak-volume relationships, Journal of Hydrology and Hydromechanics, 64, 4, 367–381. DOI: 10.1515/johh-2016-0042

Thiesen, S., Darscheid, P., Ehret, U. (2019): Identifying rainfall-runoff events in discharge time series: a data-driven method based on information theory, Hydrology and Earth System Sciences, 23, 2, 1015–1034. DOI: 10.5194/hess-23-1015-2019

Valent, P. (2019): Floodsep: user´s manual, SvF STU in Bratislava

Xiao, Y., Guo, S., Liu, P., Yan, B., Chen, L. (2009): Design Flood Hydrograph Based on Multicharacteristic Synthesis Index Method, Journal of Hydrologic Engineering, 14, 12, 1359–1364. DOI: 10.1061/(ASCE)1084-0699(2009)14:12(1359)

Yonus, M., Hassan, S. (2022): The Impact of Climate Change on Stochastic Variations of the Hydrology of the Flow of the Indus River. Slovak Journal of Civil Engineering,30(1) 33–41. https://doi.org/10.2478/sjce-2022-0004

Yue, S., Hashino, M. (2000): Unit hydrographs to model quick and slow runoff components of streamflow, Journal of Hydrology, 227, 1, 195–206. DOI: 10.1016/S0022-1694(99)00185-7

Yue, S., Ouarda, T. B. M. J., Bobée, B., Legendre, P., Bruneau, P. (2002): Approach for Describing Statistical Properties of Flood Hydrograph, Journal of Hydrologic Engineering, 7, 2, 147–153. DOI: 10.1061/(ASCE)1084-0699(2002)7:2(147)

Ing. Anna Liová (*corresponding author, e-mail: anna.liova@stuba.sk)
Ing. Peter Valent, PhD.
prof. Ing. Kamila Hlavčová, PhD.
prof. Ing. Silvia Kohnová, PhD.
prof. Ing. Ján Szolgay, PhD.
Department of Land and Water Resources Management
Faculty of Civil Engineering
Slovak University of Technology in Bratislava
Radlinského 11
810 05 Bratislava
Slovak Republic

doc. Ing. Tomáš Bacigál, PhD.
Department of Mathematics and Descriptive Geometry
Slovak University of Technology in Bratislava
Radlinského 11
810 05 Bratislava
Slovak Republic

DOI: 10.31577/ahs-2022-0023.01.0007

ACTA HYDROLOGICA SLOVACA

Volume 23, No. 1, 2022, 62 – 72

Post-flood analysis of the flood from the rupture of the stone dam in Rudno nad Hronom on May 17, 2021

Pavla PEKÁROVÁ*, Pavol MIKLÁNEK, Ján PEKÁR, Jana PODOLINSKÁ

The study is aimed at reconstructing the course of the flood from May 17, 2021 breach of the stone dam in Rudno nad Hronom. Firstly, the volume of water in the reservoir before its breach was determined. The reservoir storage volume was estimated to be 14 807 m^3. Then, we focused on the analysis of the hydrological regime in the wider Rudniansky Brook region. In order to derive the flood wave course from the rainfall, a series of 15-minute discharge from neighbouring water gauges measured by the Slovak Hydrometeorological Institute were analysed. In analysing the long-term trends of precipitation and temperature series we used data from the Banská Štiavnica meteorological station (period 1901–2020). In the second part, based on several field measurements after the flood event, we estimated the peak flows of floods from May 17, 2021 above the reservoir and under the reservoir. One hundred meters above the reservoir culmination reached 7.8 $m^3 s^{-1}$, under the reservoir it was between 80 to 100 $m^3 s^{-1}$. Finally, we reconstructed the course of the flood wave from the precipitation above the reservoir by hydrological analogy and by simple rainfall-runoff hydrological model NLC. The course of the breakthrough wave from the reservoir water just below the dam was determined to be triangular in shape so that the peak reached 90 $m^3 s^{-1}$ and the volume was 15,000 m^3.

KEY WORDS: breakthrough wave, rupture dam, Rudniansky Brook, rainfall-runoff NLC model

Introduction

Dams on streams play an important role in the comprehensive development of the landscape. Reservoirs are built for various purposes, e.g. for agricultural irrigation, fishing, recreation, drinking water supply, flood prevention or energy production. Thousands of reservoirs have been built on watercourses around the world over the last 200 years. For example, in China alone, according to statistics from 2021, 98 000 reservoirs have been built, including 4 700 reservoirs with a capacity of between 10 million and 1 billion cubic metres. Hundreds of reservoirs have been built in the Danube basin since the beginning of the 16th century, especially on the upper Danube (ICPDR, 2013).

In Slovakia, according to Bednárová and Dušička (2011), 281 water reservoirs have been built, which fall under the administration of the Slovak Water Management Company. Of these, 231 are small reservoirs and 50 reservoirs are included in the world register of large dams (ICOLD – International Comittee on Large Dams). A total of 1.89 billion m^3 of water can be stored in them. In densely populated areas, a flood due to a dam rupture can cause a devastating disaster with loss of life and property. The time required to warn people living below the reservoir is very short in the event of a flood caused by a dam rupture (Oguzhan, and Aksoy, 2020; Xu et al., 2012).

May 2021 was extremely cold and very wet in Slovakia. From 12 to 17 May 2021 several frontal waves passed eastwards through Slovakia. The dam rupture was caused by persistent rainfall, which peaked in the afternoon of May 17, 2021. This precipitation caused the water levels of several Slovak rivers to rise (SHMÚ Flood Reports No 4, 6 and 7, 2021). In the Hron river basin, peak flows with a probability of being exceeded once in 20 years were assessed in Kalinčiakovo on the Sikenica, and once in 10 years in Jasenie on the Jaseniansky brook, in Harmanec–Papiereň on the Bystrica and in Žiar nad Hronom and Kamenín on the Hron River. As a result of intense rainfall, the watercourses were dammed in many places and flooded local roads as well as the intravillans and extravillans of several municipalities.

On the Rudniansky brook above the village of Rudno nad Hronom on 17.5.2021 at the time after 15.30 a 6 m high unpaved stone dam was washed away by the flowing water. The reservoir above the dam was already full before the precipitation event. The breakthrough wave that occurred after the dam broke damaged bridges, cars, footbridges, fences, flooded houses, covered gardens with mud and caused great material damage in the village of Rudno nad Hronom. Unfortunately, the breakthrough wave also caused one human casualty. In order to document this event, we conducted several

measurements and hydrological analysis of this event in the Rudniansky Brook watershed.
In the first part of the study the volume of water in the reservoir built in 2011 before its breach in 2021 is determined. In the second part, the hydrological conditions of the Rudniansky Brook basin are analyzed, the results of field measurements are described. Finally, in the third part the course of the flood wave is analysed in the profiles upstream and downstream the reservoir.

Material and methods

The Rudniansky Brook is located in central Slovakia in the Hron basin in the western part of the geomorphological unit Štiavnické vrchy, in the subunit Hodrušská hornatina (Fig. 1). It rises below the Lachtriská saddle in the cadastral territory of the Uhliská municipality at an altitude of about 655 m. It flows in a west to north-west direction and after Rudno nad Hronom it flows into the Hron (left-side tributary of the Hron) at an altitude of 200 m. The river network is leaf-shaped. According to the classification of Gravelius, the Rudniansky brook is a stream of the 3rd order. The length of the stream is 8.2 km, the gradient of the stream is 450 m and the average slope of the stream is 5.3%. The catchment area of the Rudnianský Brook is 17.86 km^2, the average elevation of the catchment area is 495 m, and the average slope of the catchment area is 19.4°. According to the vertical structure, the area is characterised as a lower mountainous area.
The subsoil of the basin is made up of volcanic rocks and occasional deluvial sediments. Fluvial sediments are found along the watercourses. The entire catchment area is covered by Cambisols modal (brown forest soils). Potential natural vegetation would be mainly represented by Carpathian oak-hornbeam forests, foothill beech forests and maple-lime forests at lower elevations. At present, 90 % of the catchment area is covered by forests. Almost half of the forests are made up of beeches, followed by oaks and hornbeams. Maples, ash, spruces, larches, and firs are less abundant (LGIS, 2021).

Description of the historical ponds (tajchy) near Rudno nad Hronom

More than 50 water reservoirs – taichs – were built in the Štiavnické vrchy mountains in the 16th– 9th centuries in order to obtain energy for pumping groundwater from mining tunnels, but also to obtain water supplies for the mining industry (Weis et al., 2017). This unique water management system, together with the town of Banská Štiavnica, was inscribed by UNESCO on the list of cultural heritage of humanity in 1993. Two taichs have been built in the Rudniansky Brook basin above the village of Rudno nad Hronom: the Old/Upper Taich (325 to 345 m a.s.l.) and the New/Lower Taich (276 to 293 m a.s.l.) (Hrdý and Weis, 2020; Pekárová et al., 2021a). These were valley reservoirs that were built by damming the valley with an earthen dam. The Old taich existed until the 19th century. In 1926, the dam of the New Taich near the left bank of the safety spillway partially broke and the water from the breakthrough caused a catastrophic flood in the village of Rudno. In the 1970's, the dam was breached to the bottom of the reservoir for safety reasons and for the passage of forestry equipment. Several solid stone dams were built in the village to trap sediment. These were regularly cleaned (Fig. 2a).
In December 2011, a permeable unpaved stone dam was completed in the place of the original dam of the ruptured New Tajch just above the village of Rudno nad Hronom (Fig. 2 a–b). This was intended to catch extreme flood waves. The crown elevation of the dam was 280 m. The catchment area above the reservoir is 12 km^2. According to the available information, the new retention area of the dry polder was ca. 29 680 m^3 in front of a stone dam 10 m wide, 6 m high, and 22 m long with a DN 800 bottom outlet 32 m long (Hríb, 2012). The stone dam broke and washed away on 17.5.2021 at the time after 15.30 hrs. by the flow of water from the continuous rain. The breakthrough wave that occurred after the break of the dam in the village Rudno nad Hronom caused great material damage (Fig. 2c, d).

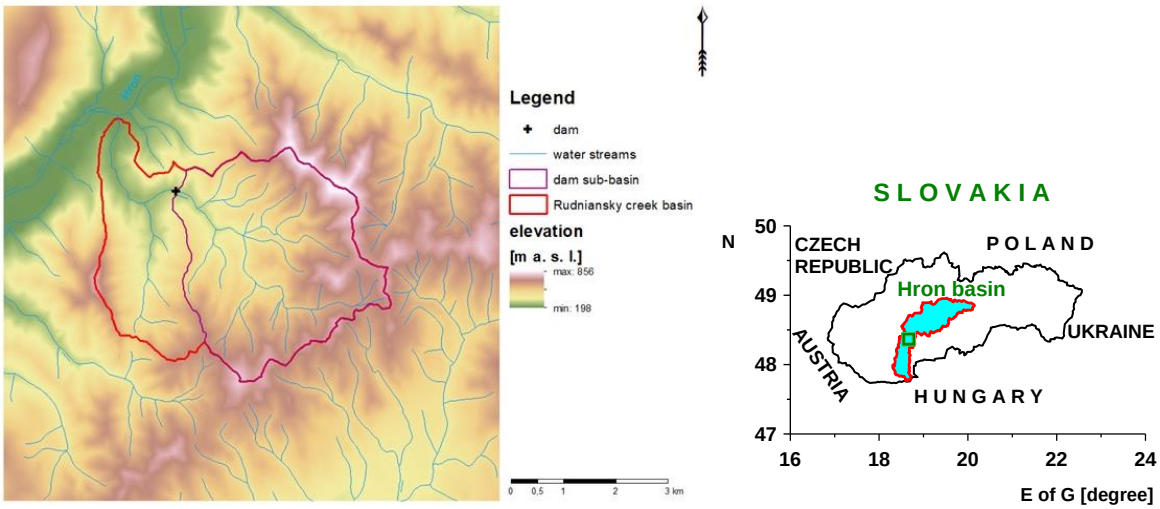

Fig. 1. Position of the Rudniansky Brook basin in the Hron basin (right) and the small reservoirs in the Rudniansky Brook basin (left) upstream the village Rudno nad Hronom.

Fig. 2. a) Two concrete stone dams downstream the reservoir near Rudno nad Hronom. b) Unpaved permeable 6 m high stone dam built in 2011 in the place of the former 17 m high dam of the New tajch, picture taken from the side of the reservoir (Photo Hríb, 2012). c–d) Flood damages in the village Rudno nad Hronom. The water level height of the flood on 17. 5. 2021 at 18.15 hrs. is visible on the house wall (Photo https://www.youtube.com/watch?v=5SWMHLeao1s).

Data used

There is neither a rain gauge station nor a water gauge station on the Rudniansky Brook to record water levels. Therefore, average monthly rainfall totals from the Banská Štiavnica rainfall gauging station from 1901 to 2020 were used to evaluate the long-term trend of annual rainfall totals. The maximum daily rainfall was evaluated from a series of daily rainfall totals for the period 1961–2020 and compared with the values according to Šamaj et al. (1985). The long-term trend of annual mean flows was analysed at the station Plášťovce Krupinica, where flow measurements since 1931 have been evaluated.

As the May 17, 2021 rainfall event also affected the adjacent valleys of Rudniansky Brook with similar intensity, we assume that the course of the flood waves was similar. In order to derive the flood wave course from the rainfall, a series of 15-minute/hourly discharge Q from neighbouring stations measured by the Slovak Hydrometeorological Institute (SHMI) were analysed.

1. Plášťovce: Krupinica (area: 302.79 km^2, measured since 1931).
2. Kalinčiakovo: Sikenica (area: 217.84 km^2, measured since 1970);
3. Žarnovica: Kľak (area: 131.95 km^2, measured since 1958);
4. Pečenice: Jabloňovka (area: 51.36 km^2, measured since 1986);
5. Bzenica: Vyhniansky potok (area: 37.75 km^2, measured since 2008).

In the analysis of the maximum annual flows, the series of peak flows Q_{max} evaluated for the hydrological year (from November 1 to October 31 of the following year) were used.

Methods and NLC model

To simulate flood waves, a conceptual non-linear NLC (non-linear cascade model) rainfall-runoff model was used (Pekárová et al, 2021b). The NLC model is a rainfall-runoff model with lumped parameters to simulate isolated rainfall-runoff events. Its use is aimed at simulating extreme summer floods in small basins (flash floods). The resulting outflow is formed by the superposition of simulated direct runoff (surface and so-called hypodermic runoff), and groundwater runoff. The first component is simulated by a cascade of linear or non-linear reservoirs in series, the second component by a single linear reservoir. The input into the model represents the precipitation during the simulation period and the index of antecedent precipitation at its beginning. The schematic model structure is shown in Fig. 3.

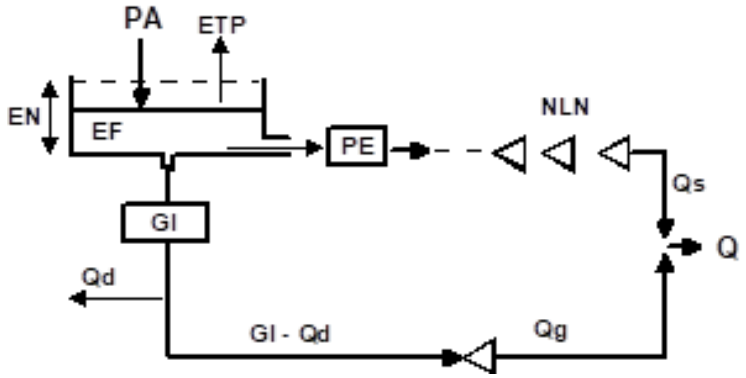

Fig. 3. Schematic representation of the NLC model structure. (PA – input precipitation, PE – effective precipitation, ETP – evapotranspiration, Qs – direct runoff, GI – groundwater input, Qg – groundwater runoff, Q – total runoff, Qd – deep percolation, EN and EF are storage parameter and actual water content of the unsaturated zone).

Results

In order to obtain the necessary hydrological data on the course and height of the catastrophic flash flood wave of May 17, 2021, the staff of the Slovak Hydro-meteorological Institute (SHMI) and the Institute of Hydrology of the Slovak Academy of Sciences (IH SAS) carried out a number of independent expeditionary measurements in the Rudniansky Brook catchment (Fig. 4). According to photographs and information from local residents, the reservoir was filled to the crown of the dam before the breach, with water flowing over the crest in two erosion gullies. During the first measurements, the peak flood flow from the rainfall above the reservoir was reconstructed by hydrometry and the peak flow of the breakthrough wave below the reservoir was estimated. Traces of the flood in the basin upstream the reservoir were documented. During further measurements, the sediment elevation in the reservoir was measured.

Determination of the volume of water in the reservoir

In the flood wave volume calculations, it was necessary to find the volume of water that flowed out of the reservoir after the dam broke (Pekárová et al, 2021a). It was not possible to work with the 2011 reservoir volume figure (ca. 30 000 m^3), as the bottom of the reservoir has been covered with sediment for more than 10 years (Fig. 5). The thickest sediment deposits we measured in the field were about 1–1.7 m high.

The volume of the reservoir was calculated using the Digital Model of Relief (DMR) via the ZBGIS Map Client application. The DMR was imaged by airborne laser scanning between November 16, 2018 and March 27, 2019. At least 5 points per m^2 were scanned with a height accuracy of 0.06 m. The water reservoir in Rudno nad Hronom was empty at the time of scanning. The DMR section was processed in ArcGIS 10 software. Contours with an interval of 0.5 m were derived from the DMR section using the Contour tool. The DMR section was clipped with a contour with an elevation of 280 m (Fig. 6). We obtained the DMR of the empty water reservoir. With the Surface Volume tool, the reservoir storage volume in 2019 was calculated to be 14 807 m^3, which is about half of the volume given by the project author more than 10 years ago.

Runoff variability at the station Plášťovce on the Krupinica River

Variability analysis of precipitation, air temperature and runoff

The analysis of the results of the long-term evolution of annual precipitation totals at the Banská Štiavnica station is presented in Figure 7. From 1901 until 1980 the long-term trend was decreasing, since 1994 the annual precipitation totals have increased. In the decade 2001–2010, the highest variability of annual precipitation totals (c_v = 0.26) was calculated; both the lowest (2003–491 mm) and the highest (2010–1296 mm) annual precipitation totals for the whole period since 1901 were measured in this decade.

At this station, the highest 24-hour rainfall in the period 1961–2020 was 70.8 mm on 29 October 1990. But in the past, a rainfall of 82.5 mm was measured on 5 May 1908 (Šamaj et al., 1985). The *100*-year 24-hour rainfall is 88 mm in the period 1961–2018, the same *100*-year rainfall was calculated by Šamaj et al. (1985) for the period 1901–1980.

Similarly, as in the case of precipitation, the runoff of the Krupinica River at Plášťovce station has been decreasing from 1931 to 1993. The decade 1931–1940 was the wettest, the decade 2011–2020 the driest (Fig. 7). Despite the increase in annual precipitation in the last two decades, Krupinica flows have been declining. This is mainly due to higher air temperatures, but also to the increasing amount of wood in forests and the resulting higher evaporation. Average daily discharges are highest in March-April and lowest in August–September.


a)–b) Surface runoff after the breakthrough wave on May 17, 2021 at 18.15 hrs. (Photo from https://www.youtube.com/watch?v=d2bixIHpRbs)


c) Surface runoff on May18, 2021 at 16.20 hrs. d) Clogged pipe from the bottom drain on June 8, 2021. (Photo Mészáros, Pekárová)

Fig. 4. Runoff from the rainfall wave downstream the reservoir after the breakthrough wave.

Fig. 5. Thickness of 10 years sediments at the reservoir bottom at Rudno nad Hronom. (Photo Pekárová, 8. 6. 2021).

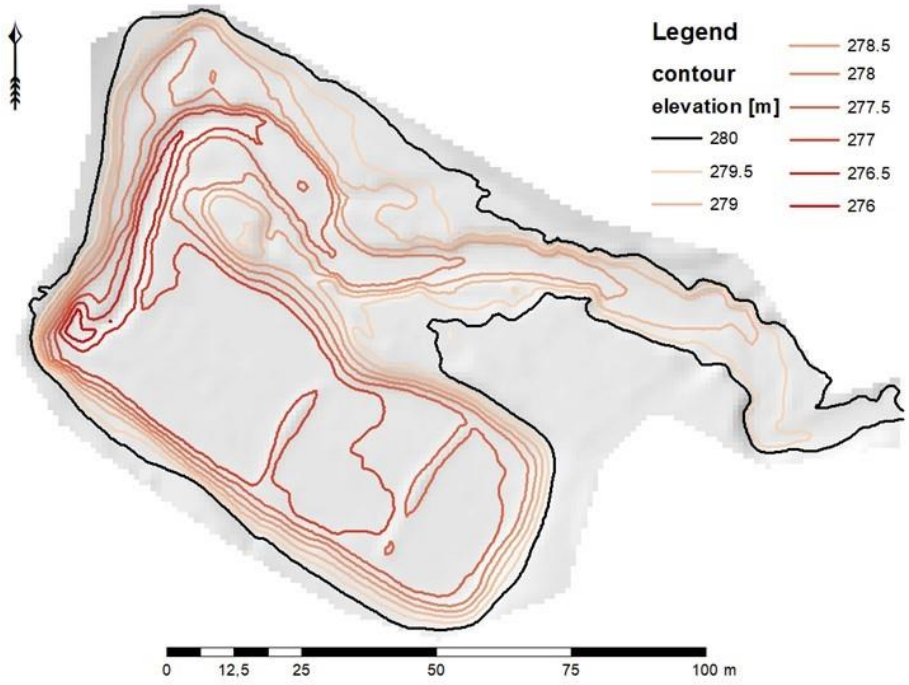

Fig. 6. Water reservoir in 2019.

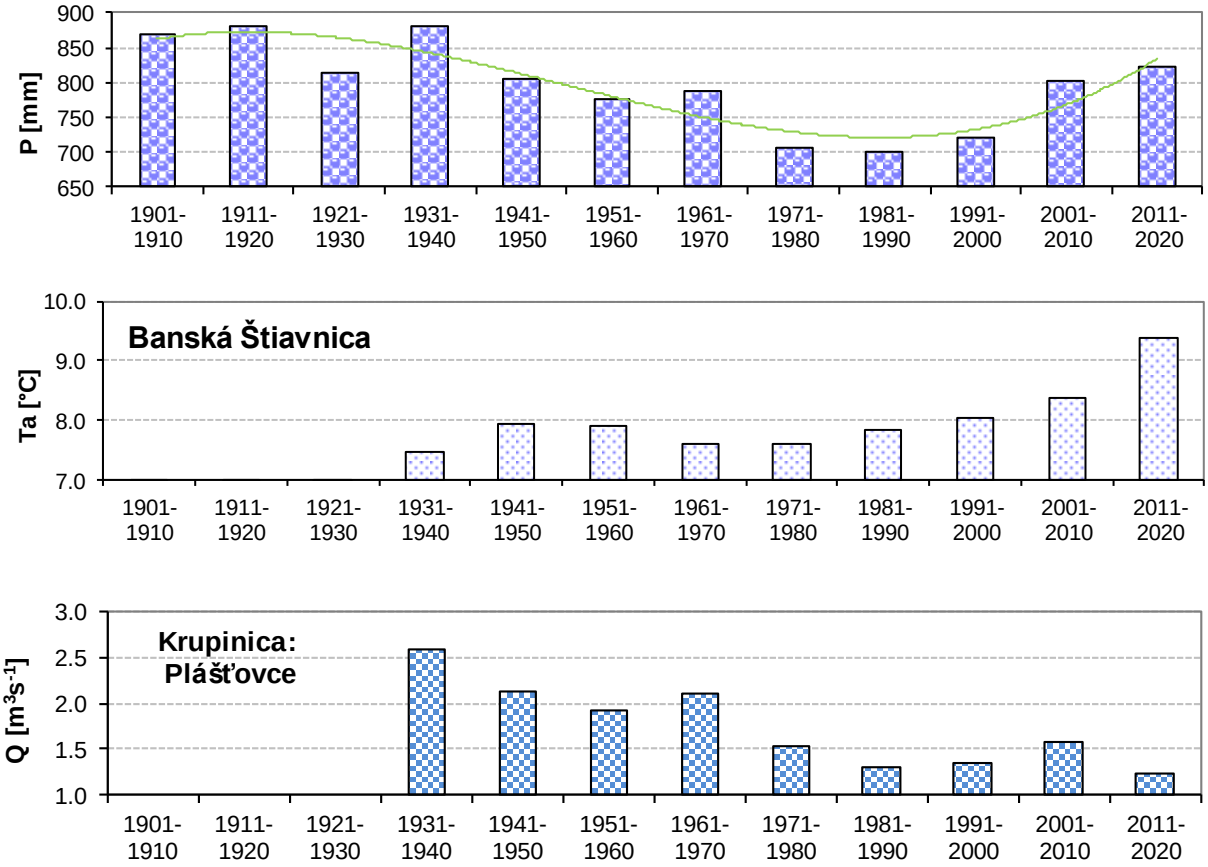

Fig. 7. Development of the 10-year average air temperature and precipitation depth, the meteorological station Banská Štiavnica (1901–2020), and 10-year average discharge at Plášťovce on the Krupinica River.

Analysis of the maximum annual discharge of the streams in the Rudniansky Brook surroundings

According to the SHMI data, the peak flow of the flood wave on May 17, 2021 at 5.15 p.m. CEST reached 38.5 $m^3 s^{-1}$ at Kľak in Žarnovica. In Bzenica on the Vyhniansky Brook, the flood wave from rain peaked at the same time at a discharge of 7.452 $m^3 s^{-1}$. The *T*-year return period of the flood at Kľak was only at the level of 2 years.

For the Rudniansky brook we could use the *T*-year values of the specific runoff from the Vyhniansky brook. The q_{max} series from Vyhniansky brook, however, is only observed since 2008. Therefore, we analyzed the distribution functions of *T*-year specific runoff (q_{max}) from stations in the wider area.

The LP3 distribution was used to estimate the *T*-year specific runoff (Fig. 8). The smaller catchment area leads to the higher gamma skewness parameter (the line turns upwards more). The estimated values of *T*-year specific runoff for the two streams are shown in Table 1. As the catchment area of Rudniansky Brook above the reservoir is only 12 km^2, and Vyhniansky Brook 37.75 km^2, the distribution function will have a much higher skewness parameter and the *T*-year specific discharges with small return period on Rudniansky Brook are likely to be much higher (95% upper limit of *100*-year discharge may reach 40 $m^3 s^{-1}$. The uncertainty in determining this value by statistical methods is very high. According to the SHMI, the *100*-year discharge in this profile (12 km^2) is estimated at 30 $m^3 s^{-1}$.

Analysis of the flood event on 17. 5. 2021 at Rudno nad Hronom

Description of the meteorological situation in May 2021

The months of April and May 2021 in the Hron basin were cold and rainy. On 16 May 2021, a cold front associated with a large-scale pressure low centred over the British Isles moved eastwards across the basin. On 17 May, a frontal wave associated with a shallow pressure low influenced weather in the Rudniansky Brook watershed. This caused numerous persistent precipitation events in the catchment areas of the Hron, Ipeľ and Slaná rivers. From 1 to 16 May at 11 p.m., the rainfall total reached 50.1 mm at the Banská Štiavnica station.

On 16 May it rained 9.1 mm at station Banská Štiavnica. Such rainfall could have fallen over the entire catchment area of the Rudniansky brook up to the reservoir, i.e. 109 000 m^3 of water fell on the catchment area. On 17 May, from 1.00 a.m. until the dam in Rudno nad Hronom broke, the rainfall depth at station Banská Štiavnica was 41 mm. The daily rainfall from 1.00 a.m. to 12 p.m. was 46.4 mm.

Estimation of the peak discharge of the rain flood wave upstream the reservoir

The profile 100 m above the reservoir (48.4191300N, 18.7049519E) was selected to determine the peak discharge by hydrotechnical calculation (Fig. 9). In this profile (Fig. 10a), the flow area at the estimated

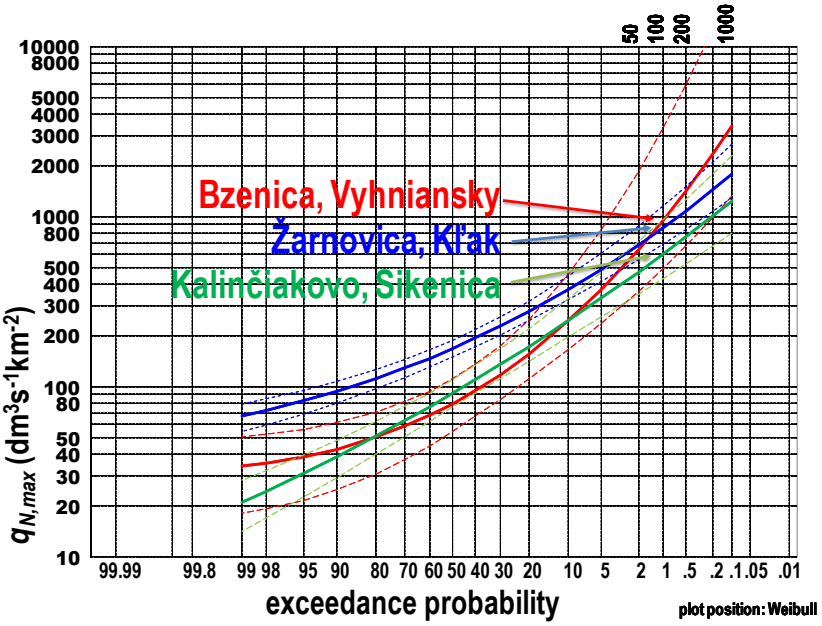

Fig. 8. T-year specific discharge q in l $s^{-1}km^{-2}$ and 95% lower and upper limits of confidence interval. Bzenica Vyhniansky Brook, Žarnovica Kľak and Kalinčiakovo Sikenica, log-Pearson distribution type III.

Fig. 9. Traces of the flood (Photo Mészáros, 1.6. 2021).

(Photo Podolinská, 25. 5. 2021

Photo Podolinská, 25. 5. 2021)

(Photo Miklánek, 1. 6. 2021

Photo Pekárová, 8. 6. 2021)

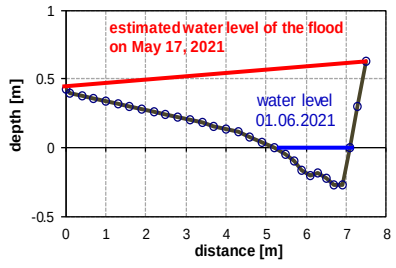

a) Rudniansky brook

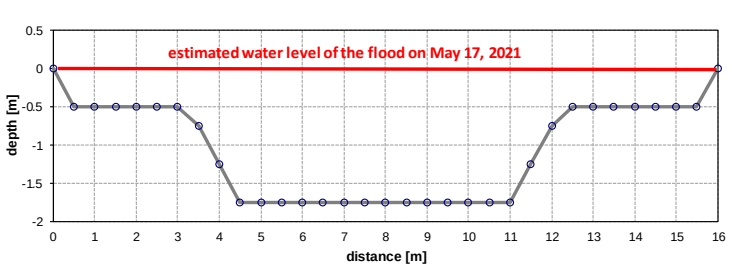

b) Rudniansky brook

Fig. 10. a) Cross-section of the Rudniansky Brook based on field measurements, 100 m upstream the reservoir. (Roughness coefficient = 0.028; stream slope 0.023). b) Cross-section of the Rudniansky Brook about 70 m downstream the reservoir dam.

Table 1. ***T*-year specific discharge of the Kľak and Vyhniansky Brook in l s^{-1} km^{-2}**

T	p	Kľak			Vyhniansky Brook		
		q	*q(5)*	*q(95)*	***q***	*q(5)*	*q(95)*
1000	0.001	**2055**	3180	1478	**3251**	20549	1270
500	0.002	**1624**	2419	1201	**2248**	11849	959
200	0.005	**1181**	1670	907	**1370**	5671	656
100	0.01	**921**	1252	728	**935**	3221	489
50	0.02	**712**	931	580	**633**	1814	360

maximum flood water level of May 17, 2021, the longitudinal slope of the predicted water level, which corresponded to the slope of the stream channel in that profile, was measured.

The flow velocity was calculated using the Chezy formula with Manning roughness coefficient, and continuity formula that was then used to calculate the peak flow.

$$v = C.(R.i)^{1/2} \quad (1)$$

$$C = 1/n \,.\, R^{1/6} \quad (2)$$

$$Q = F.v, \quad (3)$$

where

v is average velocity [m s^{-1}];
C is Chezy's coefficient [m$^{1/2}$ s^{-1}];
R is hydraulic radius [m];
i is hydraulic gradient [m m^{-1}];
n is Manning's roughness coefficient,
F is the water-filled area of cross section [m^2].

The peak discharge of the May 17, 2021 rainfall flood event in the profile 100 m above the reservoir was estimated to be 7.8 m^3 s^{-1}, i.e. 650.2 l s^{-1} km^{-2}. Similar to the neighbouring streams, the flood wave from the rain peaked around 17.00 hrs. CEST. In determining the average profile speed, we were based on the assumption of steady uniform water movement, in which the slope of the water level is parallel to the slope of the bottom.

Estimation of the breakthrough flood wave peak discharge

The profile of the old solid concrete and stone dam below the destroyed spillway was selected to determine the peak discharge from the breakthrough wave below the dam (Fig. 10b). The peak flow was estimated based on the surveyed cross-sectional area and the estimated water velocity to be 90 m^3 s^{-1}.

Reconstruction of the combined rainfall and breakthrough flood wave in Rudno nad Hronom in the profile downstream the reservoir

The temporal development of the rain flood wave upstream the reservoir was derived by two approaches (Fig. 11):

1. hydrological analogy according to temporal development of the rain flood wave in the station Pečenice: Jabloňovka Q_{HA};
2. rainfall-runoff model NLC, Q_{sim}.

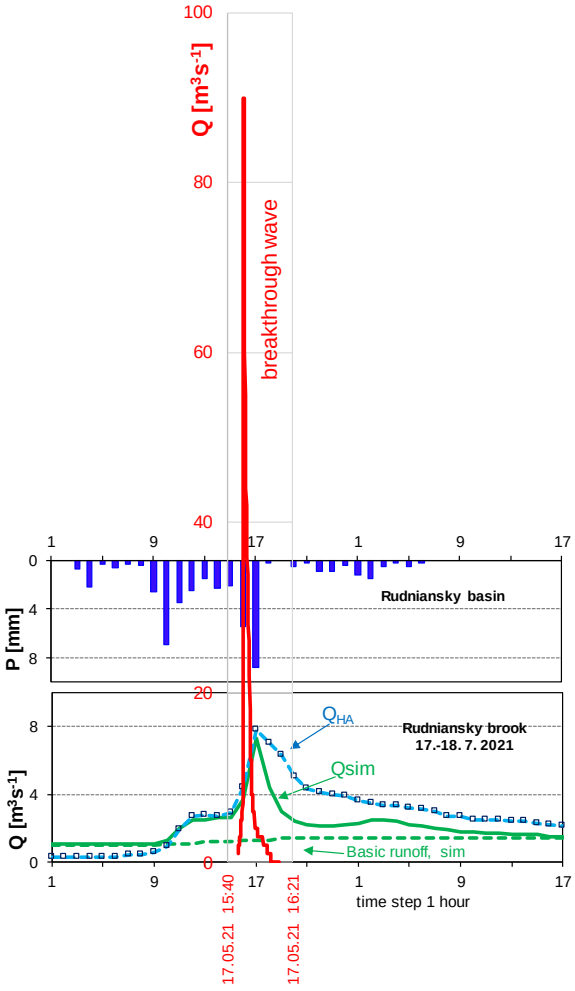

Fig. 11. Scheme of the reconstructed rain flood wave Q_{HA} – by hydrologic analogy (blue) and simulated Q_{sim} – by NLC model (green) downstream the reservoir on 17. 5. 2021. The breakthrough wave (red). The breakthrough wave and the rain flood wave have different scales on both x and y axes.

The course of the breakthrough wave from the reservoir water just below the dam was determined to be triangular in shape so that the peak reached 90 m^3s^{-1} and the volume was 15,000 m^3. The breakthrough wave has an extremely high flow rate on the one hand and a very short duration on the other. Its course is schematically indicated in red in Figure 11.

On 17 May, the daily rainfall from 1.00 to 24.00 hrs on the Rudniansky Brook catchment up to the dam above the village was estimated at 43.2 mm. It means that 481,000 m^3 of water fell on the saturated catchment before the breach of the dam in Rudno nad Hronom. The rainfall for May 17-18, 2021 on the catchment was 47.3 mm, i.e. 568,800 m^3 of water. For two days, 447,480 m^3 of water (78.8%) flowed out based on the hydrological analogy, or 334,520 m^3 of water (60.6%) according to the NLC model.

Discussion and conclusion

The results of the study clearly show that the damage to property in the village of Rudno nad Hronom was caused by the breakthrough wave from the ruptured dam above the village. The breakthrough wave reached a flow rate of 80–100 $m^3 s^{-1}$, while the wave from the rain over the reservoir reached a peak flow rate of about 8 $m^3 s^{-1}$. In the village the discharge would have been maximally two times higher.

The average annual rate of dam failures in the world since 1900 (excluding those caused by war) is 0.02%. The most common causes of dam failure include:

- Non-standard construction materials/techniques;
- Error in the design of the safety spillway;
- Geological instability caused by poor geological investigation;
- Landslide of soil into the reservoir;
- Poor maintenance especially of outlet culverts;
- Extreme inflow into the reservoir;
- Human, computer or design error;
- Internal erosion in earthen dams;
- Earthquakes.

The most important reasons for failure of earthen dams are overtopping problems, outlet blockage problems, and problems associated with improper foundation of the dam. This was also the case with the dam on Rudniansky Brook.

Acknowledgement

This work was supported by the project APVV-20-0374 DETECTIVES – "Regional detection, attribution and projection of impacts of the climate variability and climate change upon the runoff regime in Slovakia", and by the project VEGA No. 2/0004/19 "Analysis of changes in surface water balance and harmonization of design discharge calculations for estimation of flood and drought risks in the Carpathian region".

Dedicated to the memory of our young PhD. student, colleague and friend RNDr. Jakub Mészáros (29. 01. 1991 Levice – 04. 09. 2021 Budapešť).

References

Bednárová, E., Dušička, P. (2011): Water reservoirs and dams since the past till – and how to proceed? Publisher EuroStav, s.r.o. https://www.uzemneplany.sk/sutaz/nadrze-a-priehrady-od-minulosti-po-sucasnost-a-ako-dalej. (In Slovak.)

Hrdý, T., Weis, K. (2020): 3D reconstruction of the abandoned tajch. Geografická Revue. [online]. Banská Bystrica, 16, 2, 51–66. Available at internet https://doi.org/10.24040/GR.2020.16.2.51-66 (In Slovak.)

Hríb, M. (2012): Measures and experience of the contractorin the Government of SR Programme „Revitalisation of the land and the integrated management of the basins in SR". Pdf, Vodales. (In Slovak.)

ICPDR (2013): Assessment Report on Hydropower Generation in the Danube Basin. ICPDR – International Commission for the Protection of the Danube River. 127 p. www.icpdr.org

LGIS (2021): Forestry geographic information system [online]. [cit. 2021-07-20]. (In Slovak.)

Map client ZBGIS [online]. [cit. 2021-06-26]. Bratislava: Ústav geodézie, kartografie a katastra SR, 2021. Available at internet https://zbgis.skgeodesy.sk/mkzbgis/sk/teren. (In Slovak.)

Pekárová, P., Mészáros, J., Miklánek, P. (2021a): Určenie akumulačnej kapacity vodnej nádrže na Rudnianskom potoku pred pretrhnutím kamennej prehrádzky [Accumulation volume assessment of the water reservoir on the Rudniansky creek before the rupture of the stone dam]. In Hydrological Processes in the Soil–Plant–Atmosphere System – Book of peer-reviewed papers [elektronický zdroj]. Bratislava: Institute of Hydrology, Slovak Academy of Sciences, 184–194. ISBN 978-80-89139-50-7.

Pekárová, P., Mészáros, J., Miklánek, P., Pekár, J., Siman, C. and Podolinská, J. (2021b): Post-flood field investigation of the June 2020 flash flood in the upper Muráň River basin and the catastrophic flash flood scenario J. Hydrol. Hydromech., 69, 3, 288–299. https://doi.org/10.2478/johh-2021-0015

SHMÚ Flood Report No. 4. (2021): Flood report: Western Slovakia streams in May 2021, SHMÚ, (editor: A. Blahová. authors: A. Blahová, Ing. T. Masár, Mgr. P. Smrtník, N. Hrušková), 21 pp. (In Slovak.)

SHMÚ Flood Report No. 6. (2021): Flood report: Streams in the Hron, Ipeľ and Slaná basins in May 2021, SHMÚ, (editors: D. Lešková, K. Hrušková, authors: M. Halaj, K. Hrušková, T. Trstenský), 24 pp. (In Slovak.)

SHMÚ Flood Report No. 7. (2021): Flood report: Streams in the upper and middle Váh basin in May 2021, SHMÚ, (editors: D. Lešková, K. Matoková, authors: M. Zvolenský, Soňa Liová, Ivan Machara, Dorota Simonová), 22 pp. (In Slovak.)

Šamaj F., Valovič Š., Brázdil R. (1985): Daily precipitation with exceptional depths in ČSSR in the period 1901–1980. In: Zborník prác SHMÚ 24. ALFA, Bratislava, 9–112. (In Slovak.)

Weis, K., Kubinský, D., Fuska, J., Petrovič, F. (2017): Analysis of changes of the accumulation capacity of the selected artificial water reservoirs within the Banskoštiavnický water management system. Nitra, Univerzita Konštantína Filozofa, 117 pp. (In Slovak.)

Oguzhan, S., Aksoy, A. O. (2020): Experimental investigation of the effect of vegetation on dam break flood waves. J. Hydrol. Hydromech., 68, 2020, 3, 231–241, DOI: 10.2478/johh-2020-0026

Xu, F., Zhou, H., Zhou, J., Yang, X. (2012): A Mathematical

Model for Forecasting the Dam-Break Flood Routing Process of a Landslide Dam. Mathematical Problems in Engineering, vol. 2012, Article ID 139642, 16 pp. https://doi.org/10.1155/2012/139642

RNDr. Pavla Pekárová, DrSc. (*corresponding author, e-mail: pekarova@uh.savba.sk)
RNDr. Pavol Miklánek, CSc.
Institute of Hydrology SAS
Dúbravská cesta 9
841 04 Bratislava
Slovak Republic

RNDr. Ján Pekár, PhD.
Comenius University in Bratislava
Faculty of Mathematics, Physics, and Informatics
Department of Applied Mathematics and Statistics
Mlynská dolina
842 48 Bratislava
Slovak Republic

RNDr. Jana Podolinská
Slovak Hydrometeorological Institute
Regional office Banská Bystrica
Zelená 5
974 04 Banská Bystrica
Slovak Republic

DOI: 10.31577/ahs-2022-0023.01.0008

ACTA HYDROLOGICA SLOVACA

Volume 23, No. 1, 2022, 73 – 81

Comparison of mean daily discharge data for under-mountain and highland-lowland types of rivers

Wael ALMIKAEEL*, Lea ČUBANOVÁ, Andrej ŠOLTÉSZ

Most Slovak rivers have increasing spring flow followed by a period or two of low flow in the summer, autumn, and, in some cases, winter. The flow rate fluctuations in two different streams in Slovakia are being investigated in this study. The study focused on an under-mountain and a lowland-highland river to investigate the low and peak flow periods and to identify the trends in monthly and annual mean flows for both rivers. Analysing daily mean discharge data from two different types of streams requires the use of a robust normalization approach to verify the comparability between the chosen streams. On both streams, a broad statistical low-flow analysis was performed over different study periods, as well as a hydrological drought analysis utilizing the water-bearing coefficient approach over the period 2010–2020. The evaluation for the foothill river in Slovakia demonstrates that snow melting has a significant impact on annual runoff in the spring months, and both rivers have a low flow period in August, September, and October. Despite the considerable variations in the catchment area, geographical, and hydrological characteristics, drought analysis for the years 2010 to 2020 found a lack of normality and a dry hydrological situation in both streams.

KEY WORDS: drought, hydrological analysis, under-mountain river, highland-lowland river, water-bearing coefficient

Introduction

The surface runoff regime in Slovakia is characterized by increased spring runoff. Due to later snow melting in mountainous areas with higher altitudes, the increased spring runoff is manifested in later months compared to the situation in lowland streams (Fendeková and Blaškovičová, 2018). In most Slovak streams, the summer-autumn period represents the period of low water content (especially the months of August to October which is an important period of the growing season (Velísková et al., 2017). The winter low water period is quite significant in mountainous regions (especially the months of December to February). The low-water winter season is associated with snowfall, which does not contribute to immediate runoff during periods of low temperatures (below freezing) caused by partial or complete freezing of the stream (Fendeková and Blaškovičová, 2018).

Low flow is defined as a period when the flow is equal to or less than the expected threshold discharge (Tokarczyk, 2012). Low flow has always been associated with hydrological drought (Van Loon, 2015) because hydrological drought can be characterized by a series of low flows. In many cases, drought studies have discovered that the dry seasons in summer or fall were anticipated by the absence of regular runoff at the time, most particularly the significantly decreased runoff in the normally wet spring months (Fendeková and Blaškovičová, 2018). However, low flows are typically identified by annual minimum series, which may not always imply a streamflow drought (Hisdal et al., 2004). Many authors associate the concept of hydrological drought with the concept of low flow in rivers, although one hydrological drought may consist of several periods of low flows (Almikaeel et al., 2022).

This study focuses on low-flow indices in two different rivers with different characteristics to evaluate the low flow seasons on both streams. Two rivers from the Slovak territory are selected to represent under-mountain and highland-lowland types of rivers. Gidra and Topľa Rivers are chosen for this study to conduct the comparison.

Hydrological drought consists of low flow periods, but the continuous seasonal appearance of low flow is not necessarily a hydrological drought, although many researchers define hydrological drought as a prolonged period of low flow in the river (Tokarczyk, 2012). Furthermore, hydrological drought is defined as a random event characterized by a duration and deficit volume (Tokarczyk, 2012). Drought should not be confused with low flow, aridity, water scarcity, desertification, or related hazards such as heatwaves and forest fires. Low flows are often characterized by annual minimum series, which do not in all years reflect a streamflow drought.

The water-bearing coefficient is a method used to assess drought based on the annual mean discharge and the long-term mean discharge of the river. The water-bearing coefficient is utilized to assess hydrological drought on in Gidra and Topľa Rivers based on the analysis of the annual discharge data governed by the Slovak Hydrometeorological Institute (WMO, 2008). It is also used to distinguish between low flow characteristics and streamflow drought characteristics (Hisdal et al., 2004).

Material and methods

Several hydrological variables are considered while assessing surface water content. The hydrological regime of discharges is assessed over various time steps and periods. Minimum/maximum mean daily discharges (in monthly or annual steps, for the entire study period), *M*-daily discharges (the flow duration curve of mean daily discharges), minimum/maximum monthly and annual discharges (with the date of occurrence), which are then statistically processed (GWP Slovakia, 2013).

The mean daily discharge is a basic parameter of surface water hydrology and it is obtained using the flow that corresponds to the mean daily water stage as calculated by the valid rating curve (WMO, 2008). In the event of significant variations in water levels over the day, it is calculated as the mean value of discharges corresponding to water levels across appropriately chosen shorter time intervals (e.g. 3 hours) (Výleta et al., 2018). The Slovak Hydrometeorological Institute (SHMI) provides water stage measurements, and flow characteristics are compared to long-term values for the reference period 1961–2000. (determined since 2006 for surface waters). To make the comparison between mean discharge values and the long-term mean Q_a threshold more convenient, the exceedance rate will be introduced and used in this study. It is defined as the percentage of the years in which the monthly or annual mean discharge values of a specific month surpassed the long-term mean across the study period.

Comparing discharge data between different rivers with a variety of sizes, characteristics and annual mean discharge is not possible without using relative values. Relative values ensure the comparability of different watercourse discharges data by introducing a reference period. The long-term mean discharge is computed over the reference period for each stream and then utilized to normalize the annual mean discharge (Q_{mean}) i.e. the percentage ratio of mean annual discharge (Q_{mean}) and long-term mean discharge for the reference period 1961–2000 (Q_a) for individual discharge gauging stations (Fendeková and Blaškovičová, 2018).

The daily mean discharge of the Topľa and Gidra Rivers was analysed in this study. SHMI provided data for the Gidra and Topľa Rivers from 1961 to 2020 and from 1988 to 2020, respectively. SHMI also provides the long-term mean for both streams for the same reference period of 1961 to 2000.

Hydrological drought analyses of the chosen period are based on the assessment of discharge characteristics of low flow. Low-flow information of annual, seasonal, and different periods typically relied on estimating statistics from all available data. For many purposes, grouping data by months, series of months, or certain seasons may be more appropriate. Both annual minimum and flow-duration analyses can be performed for individual months or groups of months (WMO, 2008). Low flow statistics, namely mean flow is used as the general parameter in this study. The mean discharge is calculated monthly and annually for both Gidra and Topľa Rivers.

The long-term mean Q_a over the period 1961–2000 is used as a threshold to characterize periods of deficient streamflow as anomalies from the daily, monthly, and annual flow range. However, the selected threshold discharge should classify the low-flow events from the analysed time series. The criterion for differentiating hydrological droughts from a sequence of low flow occurrences was based on the classification by Dracup et al. (1980) (Tokarczyk, 2012).

Hydrological drought analyses of the chosen period are based on the assessment of discharge characteristics of low flow. The water-bearing coefficient is used to assess the hydrological status of a given river by comparing the mean discharge value of any year with the long-term mean value (which represents the normal status) (GWP Slovakia, 2013). Thus, the ratio between annual mean discharge value and long-term mean discharge is compared to standard values which define the normal, wet, and dry hydrological status of the river (GWP Slovakia, 2013).

Analysis and Results

The Gidra River

Gidra River was selected as a typical foothill stream. It springs below Baďurka in the Little Carpathians, at an altitude of about 470 m above sea level. It is a right-hand tributary of the Dudváh River and it is 38.5 km long. In the media, the Gidra River was mentioned in connection with the catastrophic flood in 2011. The only water gauging station is located above the village of Píla at an altitude of 270.04 m a. s. l., and rkm 33.30 (Fig. 1), where available measured data on water stages are since 1961, the catchment area is 32.95 km^2 to the profile of the water gauging station (SHMÚ, 2019). The mean daily discharges for the period 1961–2020 were analysed, which means 59 years, while the long-term mean annual discharge for the period 1961–2000 reported by SHMI is $Q_{a\ 1961–2000} = 0.298$ m$^3 \cdot$s^{-1}.

The mean values of discharges were evaluated on a monthly basis (Fig. 2, Tab. 1), and an increasing trend is observed starting from November till April where the peak is usually reached in April or March for the whole study, the period is clearly confirmed. The monthly mean discharges start decreasing from April to reach their minimum in August, September, or October which complies with the summer-autumn low water period of the Slovak streams – months of August and September. The winter season can also be considered a low water period, especially the month of December. Generally, five monthly mean discharges surpass the threshold of $Q_{a\ 1961–2000}$ which are January, February,

March, April, and May. Therefore, the normal and wet period for the Gidra River is taking a place between January and May, while the period from June till December tends to be below normal or dry as it is lower by at least 0.04 $m^3 \cdot s^{-1}$from the Q_a threshold.

Table 1 shows the minimum, maximum, and mean daily discharge values for each month over the period 1961–2020. Analysing the values of maximum daily mean discharge values distributed over monthly periods may indicate that large discharge values are more likely to occur from January till July (winter and spring seasons). Thus, the maximum daily mean discharges could be interpreted as a result of heavy rain or as a result of snow melting in the spring season (Fendeková and Blaškovičová, 2018). Large Maximum daily mean discharges are always indicators of floods of different types (usually flash and pluvial floods) (Sauquet and Lang, 2017). The daily minimum values of each month range between 0.02 $m^3 s^{-1}$ in August up to 0.61 $m^3 s^{-1}$ in April.

Comparing monthly mean discharges of March and April with the Q_a value confirms that discharge values in most cases surpass the Q_a threshold (Fig. 3). The exceedance rate of March mean discharges is 73% which is higher compared to the 65% exceedance rate in April. As a result, in the Gidra River, the monthly mean discharge

Fig. 1. Map of Slovakia with areas of interest – Gidra and Topľa River.

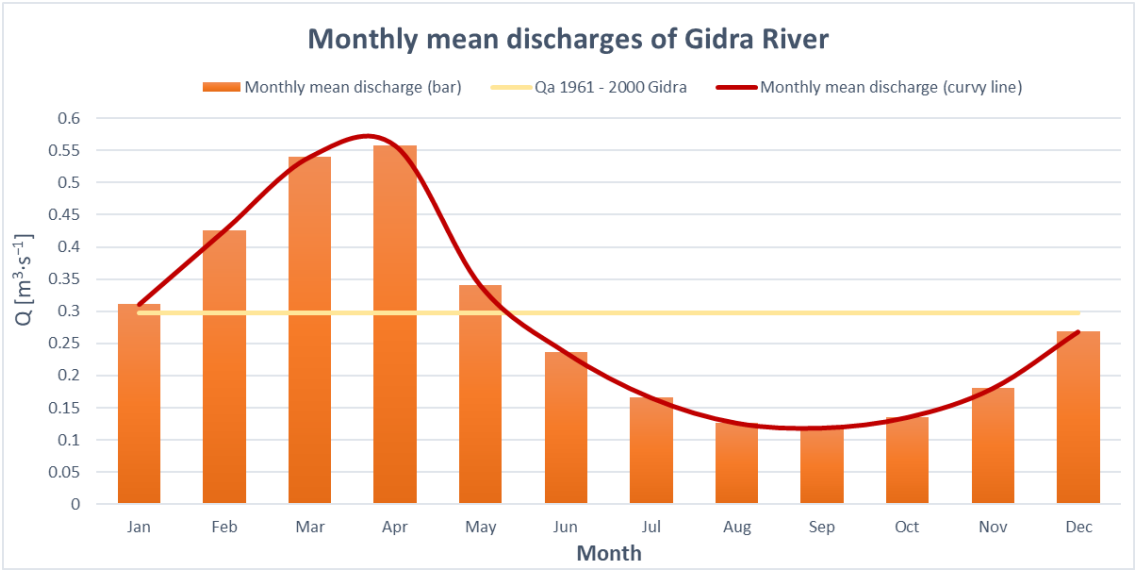

Fig. 2. Evaluation of the mean monthly discharges for the whole assessed period 1961–2020.

Table 1. Monthly mean discharges for the study period 1961–2020

month	I.	II.	III.	IV.	V.	VI.	VII.	VIII.	IX.	X.	XI.	XII.
Q_{min}	0.040	0.050	0.040	0.061	0.050	0.042	0.024	0.020	0.020	0.028	0.040	0.020
Q_{max}	4.974	4.090	6.473	4.810	4.060	4.880	5.552	2.210	2.546	3.651	1.627	3.698
Q_{mean}	0.310	0.432	0.540	0.554	0.340	0.236	0.165	0.126	0.118	0.135	0.181	0.267

in March is more likely to exceed the Q_a level than in April, making the March mean discharge value an indicator of the hydrological situation's normality.
Comparing the discharge values for August, September, and October over the period 1961–2020 (Fig. 4), the exceedance rates of these months are 7%, 5%, and 5%, respectively. In September and October, the monthly mean discharge values surpass the Q_a threshold only in three years, while the monthly mean discharges in August surpassed the Q_a threshold four times. These results confirm the finding of Fendeková (Fendeková and Blaškovičová, 2018), that most Slovak watercourses have a period of low flow in the summer and autumn (usually from August to October).
The trend of monthly mean discharges in the Gidra River over the period 1961–2020 is decreasing (Fig. 5), where the Gidra River basin is included among the highly vulnerable areas of Slovakia (GWP Slovakia, 2013). As well as the observation of the inhabitants of Malá Mača village in the lower section of the Gidra River (in the area above the confluence with Dudváh River). In 2017, a completely dry Gidra riverbed was recorded by them in the summer months. The previously mentioned information provides an insight into the hydrological situation in the Gidra River and indicates a real change in the hydrological regime.

The Topľa River

The spring of the Topľa River (Fig. 1) is located in the Čergov Mountains, under Minčol peak with an altitude of 975 to 1070 m a. s. l. The total length of Topľa River is 129.8 km, the basin area is 1 506 km² and it is a right-hand tributary of the Ondava River. Topľa was chosen as the representative of the highland-lowland stream (Frandofer and Lehotský, 2014). In the profile of the town of Bardejov in 103.50 rkm, where measured data on water stages since 1967 are available, the catchment area is 325.80 km² (SHMÚ, 2019).
The mean daily discharges for the period 1988–2020

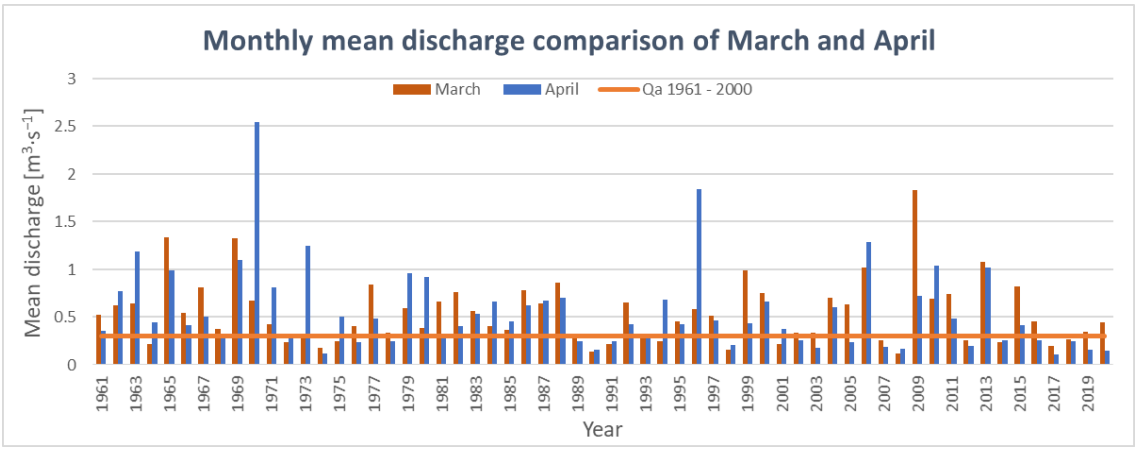

Fig. 3. Comparison of the monthly mean discharges of the most significant months – March and April from the viewpoint of the water content for the period 1961–2020.

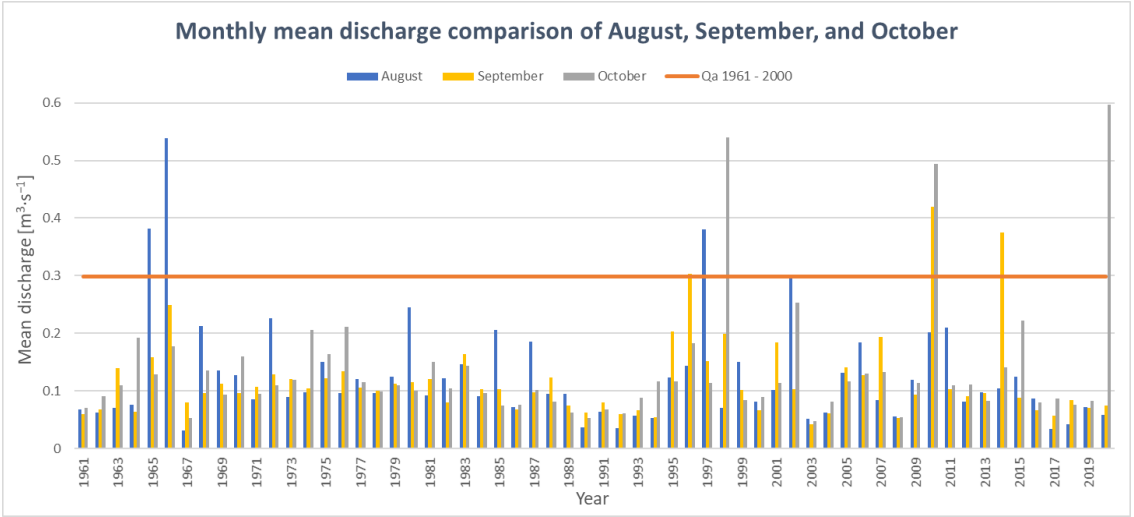

Fig. 4. Comparison of the monthly mean discharges of the driest months – August, September and October for the period 1961–2020.

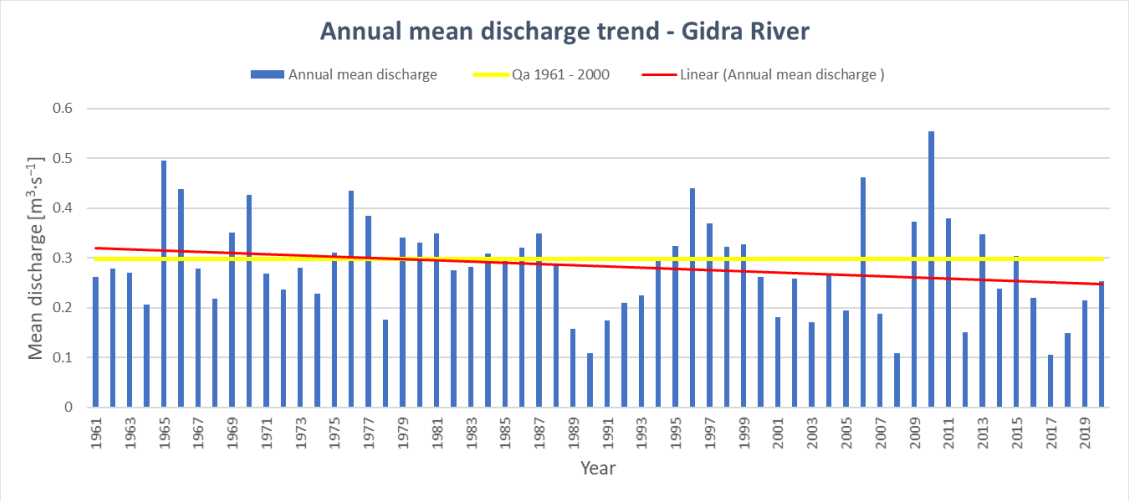

Fig. 5. Evaluation of the annual mean discharges for the period 1961–2020 with decreasing flow trend.

were analysed, which means 32 years, while the long-term mean annual discharge for the period 1961–2000 reported by SHMI is $Q_{a\ 1961–2000}$ = 2.978 $m^3 \cdot s^{-1}$.

The first Gerlachov gauging station is located in Topľa, 118.6 rkm, at an altitude of 358.39 m a. s. l., with a catchment area of 139.4 km^2. The second water gauging station is located in the town of Bardejov at an elevation of 265.05 m a. s. l., 103.5 rkm, and with a catchment area of 325.8 km^2 (Bačova Mitkova and Pekarova, 2019).

The daily mean discharges over the period 1988–2020 are utilized to extract the monthly mean discharge over the period 1988–2020 as shown in Fig. 6. Monthly mean discharges are represented in two different ways, the first one is a bar chart represented in blue and the other representation was a curvy line colored in orange. The long-term mean of the Topľa River over the period 1961–2000 is also plotted to compare the monthly discharges with the long-term mean which can be an indicator of the expected flow relative to Q_a threshold. The peak value of monthly mean discharge is mostly reached in March or April and there are three significant trends on the monthly mean discharges graph. The increasing discharge starts in January to reach a peak in March or April. then the decreasing trend appears starting from April till August or September where the steady trend of monthly discharges continues till December/ January. In the steady trend, we can notice that the discharge values range between 1.5–2 $m^3 \cdot s^{-1}$.

Only four monthly mean discharges surpass the threshold of $Q_{a\ 1961–2000}$ which are March April May and June while monthly mean discharges in February and July are usually ranged closely to the Q_a threshold. Therefore, the normal and wet period for the Topľa River is taking a place between February and July, while the period from August till January tends to be below normal or dry as it is lower by at least 1 $m^3 \cdot s^{-1}$ from the Q_a threshold.

Table 2 shows the minimum, maximum, and mean daily discharge values for each month over the period 1988–2020. Analysing the values of maximum daily mean discharge values distributed over monthly periods may indicate that flood events in Topľa River are likely to happen each month of the year. The maximum discharge value in June supports the findings of Fendeková that spring floods typically have larger volumes because they are usually the result of melting snow or, in some cases, a mixture of melting snow and rain (Fendeková et al., 2018).

As mentioned before, large maximum daily mean discharges are generally indicators of various types of floods (Sauquet and Lang, 2017). The daily minimum values of each month range between 0.21 $m^3 \cdot s^{-1}$ in June up to 1.195 $m^3 \cdot s^{-1}$ in April.

Comparing monthly mean discharges of March and April with the Q_a value confirms that discharge values in most cases surpass the Q_a threshold (Fig. 7). Where the exceedance rate of March mean discharges is 88% which is a higher rate compared to the 70% exceedance rate in April. The significant exceedance rate of March matches a high rate of exceedance in the Gidra River with a different magnitude.

Observing the discharge values of August, September, and October over the period 1988–2020 (Fig. 8) shows that the exceedance rates are 15%, 12% and 12% respectively. In September and October, the monthly mean discharge values surpass the Q_a threshold only in three years, while the monthly mean discharge in August surpassed Q_a threshold five times.

These findings support Fendeková's observation that the highest runoff occurs in the spring, and peak discharges likewise occur in the spring, primarily in March (Fendeková and Blaškovičová, 2018). Also, the increasing spring flow is also vital for runoff levels in the later months of each year (Hanus et al., 2021). There are two concentrated periods of low flow in the year – the summer-autumn depression inflow, which has its lowest point between August and October, and secondary winter depression, which has its lowest point usually in January (Fendeková and Blaškovičová, 2018).

The trend of monthly mean discharges in the Topľa River over the period 1988–2020 is slightly increasing which

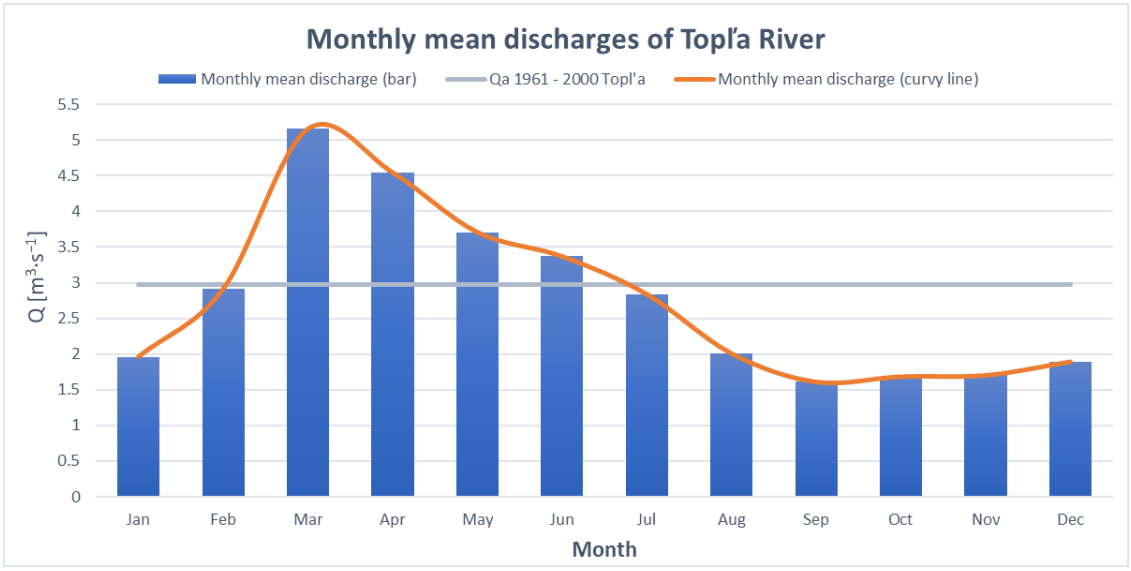

Fig. 6. Evaluation of the mean monthly discharges for the whole assessed period 1988–2020.

Table 2. Monthly mean discharges for the study period 1988–2020

month	I.	II.	III.	IV.	V.	VI.	VII.	VIII.	IX.	X.	XI.	XII.
Q_{min}	0.42	0.39	0.54	1.20	0.57	0.21	0.28	0.36	0.36	0.30	0.44	0.37
Q_{max}	15.81	48.01	97.63	33.53	65.40	173.57	80.77	42.38	31.50	22.43	18.74	19.11
Q_{mean}	1.96	2.91	5.16	4.54	3.71	3.37	2.84	2.01	1.61	1.68	1.70	1.89

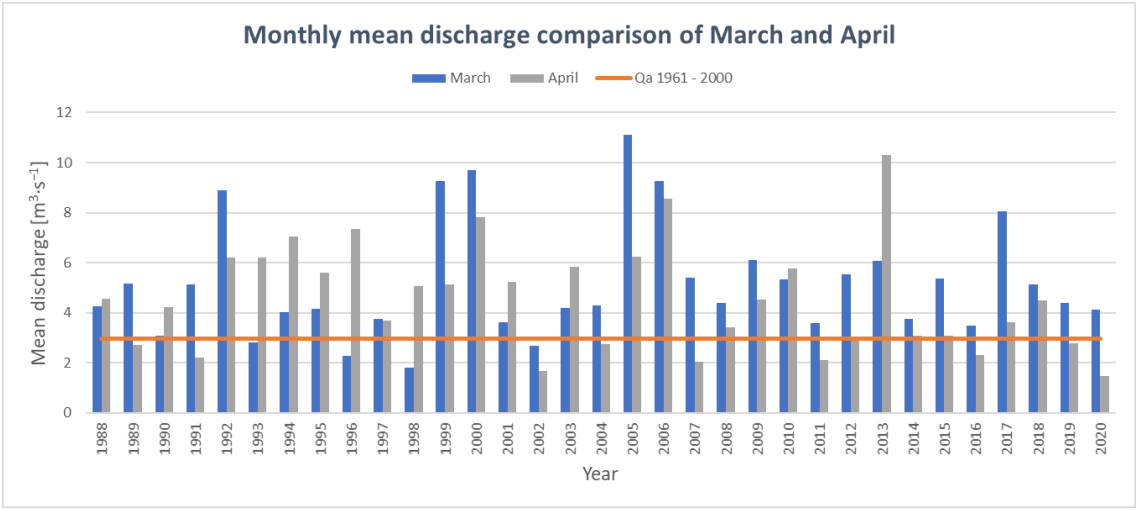

Fig. 7. Comparison of the monthly mean discharges of the most significant months – March and April from the viewpoint of the water content for the period 1988–2020.

can be interpreted as a result of floods events (Fig. 9). However, to reduce the effect of the megaflood that happened in 2010 on the annual mean discharge linear trend, the value of the annual mean discharge of 2010 was substituted by the mean discharge value over the period 1988–2020. The resulting linear trend incline decreased and the trend of the annual mean discharges is approximately steady.

Drought analysis:

Hydrological drought is characterized by low flow periods and is caused by decreasing river discharges. There are numerous indices for measuring and identifying drought, but the availability of different data kinds is the most important factor in determining which index to utilize. The water-bearing coefficient is used to

assess the hydrological situation of each year because the daily mean discharge is the only data type used in this study (Almikaeel et al., 2022; GWP Slovakia, 2013).

The water-bearing coefficient is the ratio of annual mean discharge to the long-term mean discharge. This ratio is compared to standard intervals of dry, normal, wet to evaluate the hydrological situation of a stream. Standard water-bearing coefficient values describe the proportion of mean discharge in a certain period compared to the long-term mean, as shown in standard intervals. The standard intervals are classified into three groups (determine whether the year is dry, normal, or wet). The intervals are set as (10%–89%) for dry situations, (90%–110%) for normal situations, and (111%–more) for wet situations (GWP Slovakia, 2013).

The water-bearing coefficient is computed over the period 2010–2020 for both rivers using the annual mean discharge of a given year and the long-term mean given by SHMI (GWP Slovakia, 2013). As a result, the ratio of yearly mean discharge value to long-term mean discharge is compared to standard values that describe the river's normal, wet, and dry hydrological status.

Table 3 shows the evaluation of the hydrological situation using the water-bearing coefficient for the period 2010 to 2020. In the second column of the table, Q_{mean} represents the annual mean discharge of the corresponding year (first column), Q_{mean}/Q_a is the water-bearing coefficient for each river, and status is the corresponding value of the hydrological situation. The status is chosen based on the previously specified intervals to represent the hydrological situation using the water-bearing approach.

In both Gidra and Topľa Rivers, the last ten years were generally dry which confirms the findings of multiple studies (Almikaeel et al., 2022; Repel et al., 2021). Seven years over the period 2010–2020 are classified as dry years according to the water-bearing coefficient method. In the Gidra River, three years are considered as wet years and only one year as a normal year over the period 2010–2020.

A similar situation is observed in the Topľa River, where

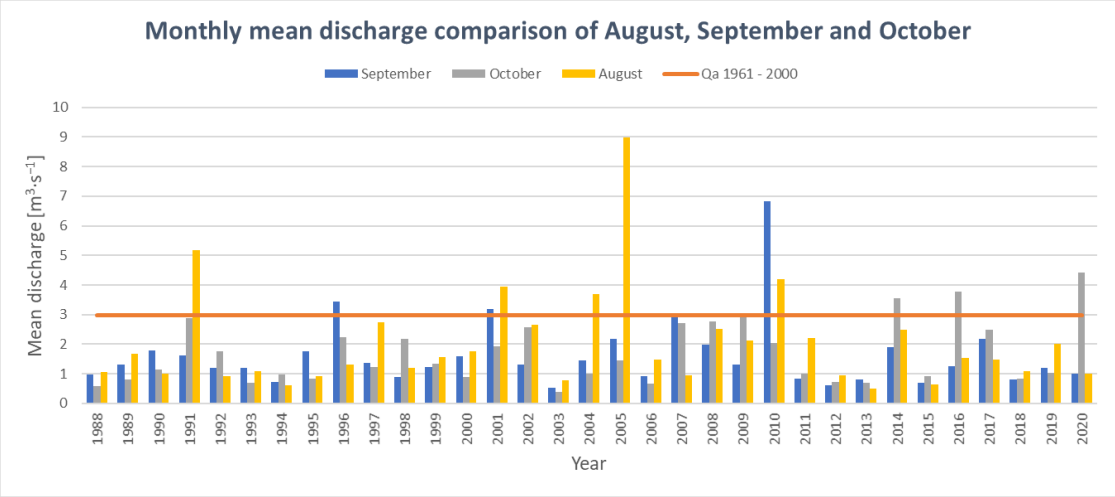

Fig. 8. Comparison of the monthly mean discharges of the driest months – August, September and October for the period 1988–2020.

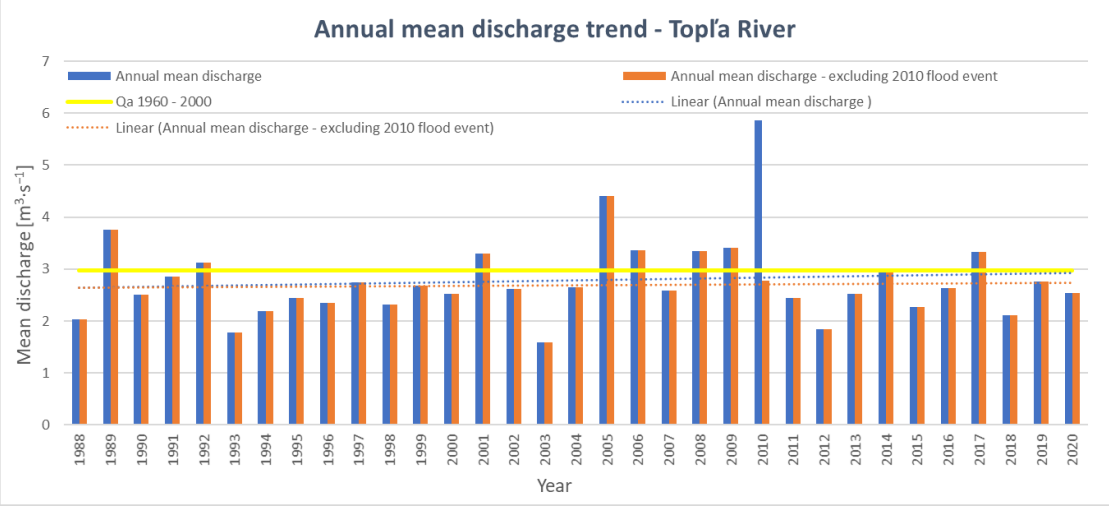

Fig. 9. Evaluation of the annual mean discharges for the period 1988–2020 with a steady (or slightly increasing) flow trend.

Table 3. The hydrological drought assessment of Topľa and Gidra Rivers over the period 2010–2020

	Gidra River			Topľa River		
year	Q_{mean}	Q_{mean}/Q_a	**Status**	Q_{mean}	Q_{mean}/Q_a	**Status**
2010	0.55	186%	Wet	5.86	197%	Wet
2011	0.38	127%	Wet	2.44	82%	Dry
2012	0.15	51%	Dry	1.84	62%	Dry
2013	0.35	117%	Wet	2.53	85%	Dry
2014	0.24	80%	Dry	2.98	100%	Normal
2015	0.30	102%	Normal	2.27	76%	Dry
2016	0.22	74%	Dry	2.63	88%	Dry
2017	0.11	35%	Dry	3.33	112%	Wet
2018	0.15	50%	Dry	2.11	71%	Dry
2019	0.21	72%	Dry	2.76	93%	Normal
2020	0.25	85%	Dry	2.54	85%	Dry

two years are considered as wet and also two years are classified as normal years. The water-bearing coefficient values of the Gidra River range from 35% up to 186% while the range for the Topľa River is located between 62%–197%. This means that drought situations in the Gidra River are more severe compared to the Topľa River over the period 2010–2020.

Normal years mean that the annual mean discharge in both rivers is 90% up to 110% of the long-term mean. The lack of normality is observed in both rivers in the last 10 years raises many questions about the main reason for facing such a dry period.

Conclusion and discussion

Based on the findings of previous analysis, both rivers have the typical characteristics of the under-mountain stream and highland-lowland river in terms of the increased spring runoff. The wetted period (increased run-off) of the Gidra River is generally occurring between January and May which is represented as the area under the mean discharge curve and above the corresponded Q_a threshold. The wetted period (increased run-off) of the Topľa River is generally occurring between February and July which is represented as the area under the mean discharge curve and above the corresponded Q_a threshold.

The Gidra river's runoff trend has been decreasing over the study period, implying a change in flow regime due to a variety of factors. Many researchers correlate the changing of discharge regime in mountainous regions directly to climate change. Snow evapotranspiration in mountainous regions is accelerated by climate change (Dankers and Christensen, 2005), which occurs in the season of snow accumulation and melting process. As a result, the predicted flow from snow melting is decreasing, causing a low rate of discharge in rivers (Meira Neto et al., 2020).

In the Topľa River, the trend of annual discharge is slightly increasing due to multiple flood events. Maximum daily mean discharge analysis of Topľa River includes relatively high values in each month of the year. Discharges in March in both rivers tend to exceed the Q_a more often than any other month in the analysis of both rivers.

Finally, some similarities and differences have been addressed in this study regarding both types of rivers, under-mountain and highland – lowland rivers. The results are presented as follow:

The similarities:

- Monthly mean discharge peak values are recorded in March and April.
- The highest exceedance rate of monthly mean discharge is recorded in March.
- The lowest level of monthly discharge values is observed in the summer and autumn seasons (August, September, October).

The differences:

- Maximum values of daily mean discharges are more likely to occur in any month for Topľa River, while large daily mean discharges of the Gidra River are more likely to occur in the first half of the year.
- The trend of annual mean discharge is decreasing in the Gidra River, while it is slightly increasing for the Topľa River.
- The mean wet period where the exceedance rate is high is slightly different for both rivers, January to May for the Gidra River, March to June for Topľa River, which confirms the findings of Fendeková.

Despite all the differences between Topľa and Gidra Rivers in terms of location, catchment size, type, and hydrological situation, drought and lack of normality were the dominant situations of both rivers over the period 2010–2020. There are a large number of factors that cause the different trends and behaviours we observe nowadays in terms of river flows and most of them are directly related to climate change. However, characterizing those changes or predicting them in advance may contribute to designing better water management decisions for all the problems that are associated with drought and low flow (Sýs et al., 2021).

Acknowledgement

This contribution was developed within the framework and based on the financial support of the APVV-19-0383 project, "Natural and technical measures oriented to water retention in sub-mountain watersheds of Slovakia", together with APVV-20-0023 project, "Research on hydraulic characteristics of fish passes with regard to ichthyological requirements"and Vega project No.1/0728/21 "Analysis and prognosis of impact of construction activities on ground water in urbanized territory".

References

Almikaeel, W., Čubanová, L., Šoltész, A. (2022): Hydrological drought forecasting using machine learning – Gidra river case study. Water, 14(3), 387. https://doi.org/10.3390/w14030387

Bačova Mitkova, V., Pekarova, P. (2019): Analysis of maximum runoff volumes with different time durations of flood waves: A case study on Topľa river in Slovakia. IOP Conference Series: Earth and Environmental Science, 362(1), 012013. https://doi.org/10.1088/1755-1315/362/1/012013

Dankers, R., Christensen, O. B. (2005): Climate change impact on snow coverage, evaporation and river discharge in the sub-arctic tana basin, Northern Fennoscandia. Climatic Change, 69(2–3), 367–392. https://doi.org/10.1007/s10584-005-2533-y

Dracup, J. A., Lee, K. S., Paulson Jr., E. G. (1980): On the definition of droughts. Water Resour. Res. 16,2, 297–302, DOI: 10.1029/WR016i002p00297.

Fendeková, M., Blaškovičová, L. (2018): Prognosis of hydrological drought development in Slovakia. Bratislava, 2018. ISBN 978-80-223-4673-3, 182 p.

Fendeková, M., Horvát, O., Blaškovičová, L., Danáčová, Z., Fendek, M., Bochníček, O. (2018): Prognosis of climate change driven drought in the Poprad, Torysa and Topľa River Basins. Acta Hydrologica Slovaca, 19(2), 234–243. 2644-6291 (printed until 2018).

Frandofer, M., Lehotský, M. (2014): Morfologicko-sedimentová diferenciácia horského vodného toku a jeho odozva na povodňové udalosti. Geomorphologia Slovaca Et Bohemica, Bratislava, vol. 14, issue 1, ISSN 1337–6799, http://www.asg.sav.sk/gfsb/v0141/GSeB_1_2014.pdf

GWP Slovakia (2013): Guidelines for Drought Management Plan Milestone 2: Slovak case study report. Retrieved April 29, 2021, from http://www.shmu.sk/File/Hydrologia/Projekty_hydrologia/projekt11_Slovak_case_study_report_IDMP.pdf

Hanus, S., Hrachowitz, M., Zekollari, H., Schoups, G., Vizcaino, M., Kaitna, R. (2021): Future changes in annual, seasonal and monthly runoff signatures in contrasting alpine catchments in Austria. Hydrology and Earth System Sciences, 25(6), 3429–3453. https://doi.org/10.5194/hess-25-3429-2021

Hisdal, H., Tallaksen, L. M., Clausen, B., Peters, E., Gustard, A. (2004). Hydrological drought characteristics – ipb university. Retrieved April 29, 2021, from http://mtaufik.staff.ipb.ac.id/files/2015/07/Ch05_final_Elsevier-Text book-Hydro-Drought-Tallaksen-Van-Lanen-2004.pdf

Meira Neto, A. A., Niu, G.-Y., Roy, T., Tyler, S., Troch, P. A. (2020): Interactions between snow cover and evaporation lead to higher sensitivity of streamflow to temperature. Communications Earth & Environment, 1(1). https://doi.org/10.1038/s43247-020-00056-9

Repel, A., Zeleňáková, M., Jothiprakash, V., Hlavatá, H., Blišťan, P., Gargar, I., Purcz, P. (2021): Long-term analysis of precipitation in Slovakia. Water, 13(7), 952. https://doi.org/10.3390/w13070952

Sauquet, E., Lang, M. (2017): Flood regimes: Recent development and future under climate change. Floods, 299–309. https://doi.org/10.1016/b978-1-78548-268-7.50018-3

SHMÚ (2019): Hydrologická ročenka, povrchové vody 2018. SHMÚ, Bratislava, p. 195.

Sýs, V., Fošumpaur, P., Kašpar, T. (2021): The impact of climate change on the reliability of Water Resources. Climate, 9(11), 153. https://doi.org/10.3390/cli9110153

Tokarczyk, T. (2012): Classification of low flow and hydrological drought for a river basin. Acta Geophysica, 61(2), 404–421. https://doi.org/10.2478/s11600-012-0082-0

Van Loon, A. F. (2015): Hydrological drought explained. WIREs Water, 2(4), 359–392. https://doi.org/10.1002/wat2.1085

Velísková, Y., Dulovičová, R., Schügerl, R. (2017): Impact of vegetation on flow in a lowland stream during the growing season. Biologia, 72(8), 840–846. https://doi.org/10.1515/biolog-2017-0095

Výleta, R., Kohnová, S., Valent, P. (2018): Riešené úlohy z hydrológie I. Povodie, zrážky, prietok a hydrologická bilancia. Spektrum STU, p. 83, ISBN 978-80-227-4887-2

World Meteorological Organization (WMO). (2008): Manual on low-flow estimation and prediction | e-library. Retrieved April 29, 2021, from https://library.wmo.int/index.php?lvl=notice_display&id=7978

Ing. Wael Almikaeel (*corresponding author, e-mail: wael.almikaeel@stuba.sk)
Ing. Lea Čubanová, PhD.
prof. Ing. Andrej Šoltész, PhD.
Department of Hydraulic Engineering
Faculty of Civil Engineering
Slovak University of Technology in Bratislava
Radlinského 2766/11
810 05 Bratislava
Slovak Republic

DOI: 10.31577/ahs-2022-0023.01.0009

ACTA HYDROLOGICA SLOVACA

Volume 23, No. 1, 2022, 82 – 88

Influence of forest dieback on the overland flow and isotopic composition of precipitation

Ladislav HOLKO*, Martin JANČO, Michal DANKO, Patrik SLEZIAK

Small mountain catchments in the highest part of Slovakia are undergoing significant forest changes related to windfalls and bark beetle infestations and resulting forest dieback, wood removal at some places and subsequent natural regeneration or reforestation. Natural forest changes started after 2010 also in the Jalovecký Creek catchment (The Western Mountains, area 22.2 km^2, mean altitude 1500 m a.s.l.). Coniferous forest dominated by the Norway spruce, that used to cover 44% of catchment area consequently dries, the trees defoliate, break after some time and the natural regeneration starts. These changes affect also the hydrological cycle, e.g. interception, snow cover, water infiltration to the soil and runoff formation. We present the first results of the overland flow measurements in the alive and dead forest in summer season 2021 (June to September) and compare the isotopes of oxygen and hydrogen in precipitation and soil water. The results show that the overland flow in the forest is not uncommon, although it constitutes only several per cent of the rain. About a half of 55 rainfall events registered in the open area resulted in the overland flow in the forest (21–30 events at different sites). The overland flow represented on average 4% to 7% of the open area rainfall, but maxima for individual events exceeded 10%. Throughfall in the alive forest was isotopically heavier than the open area rainfall and dead forest throughfall. Isotopic composition of the soil water was distinctly different from precipitation until the mid-July, documenting the influence of the snowmelt water.

KEY WORDS: runoff generation, changing forest, stable isotopes

Introduction

The highest mountain ranges in Slovakia, i.e. the Tatra Mountains and the Low Tatra Mountains were in the previous decades covered by dense forests. These forest were always affected by natural disturbances (windfalls, bark beetles) and human activities (forest management, mountain resorts development). However, compared to the past, the last decade brought visible deforestation at much greater areas, often initiated by windfalls and bark beetle infestations. Forest changes occur also in the Jalovecký Creek catchment that is studied since the end of the 1980' as representative for the hydrological cycle of the highest Slovak mountains. Because the catchment is part of the protected area of the Tatra National Park, its forests have been little affected by human activities during our research period. Forests, dominated by Norway spruce (*Picea abies*) used to cover 44% of the catchment while additional 31% of the catchment was covered by the dwarf pine (*Pinus mugo*), e.g. Holko and Kostka (2006). Although intensive past human activities that ended several decades ago, decreased the natural forest line almost in the entire catchment, most of the forest was recently classified as natural (Celer, 2015). However, the majority of the forest was old (over 100 years); the largest forest area was in the age class 121 to 140 years (Celer, 2015). Therefore, Celer (2015) noted that due to its age, forest breakdown and regeneration can be expected in the near future. In fact, this process started or was intensified by several windfalls and bark beetle outbreaks already before Celer's evaluation, e.g. in 2012 (Bartík et al., 2016).

Forest dieback and regeneration span over the period of many years. Defoliation after the death of the trees appears relatively quickly. The ongoing defoliation can be accompanied by the growth of lichens on trees branches and a rapid development of the forest floor vegetation. Finally, the branches and trunks break and their decomposition starts. Simultaneously, the regeneration continues by growth of pioneering species that use the chance of having more light and nutrients and less competition from the trees when the gaps and large openings form in the previously continuous mature forest.

Recent large-scale forest disturbances in Europe were evaluated e.g. by Mezei et al., 2014; 2017; Seidl et al., 2011. Senf and Seidl (2021) reported that 17% of Europe's forest area was disturbed by anthropogenic and/or natural causes between 1986 and 2016. They also concluded that although the trends in disturbance size were highly variable, disturbance frequency consistently increased and its severity decreased. Hydrological

consequences of changes in forest structure can include e.g. changes in snow accumulation and melt (Bartík et al, 2019), soil moisture, hydrological connectivity and runoff generation. They were often analysed before in studies related to the effects of forest management (deforestation, afforestation). Natural forest dieback, e.g. due to bark beetle infestation takes over longer time than the dieback caused by climatic factors such as windfalls, extreme temperatures or drought. The objective of this study was to investigate the overland flow formation in a forest undergoing the natural dieback/regeneration processes and the effects of the various stages of forest dieback on the isotopic composition of precipitation.

Material and methods

Precipitation amount and isotopic composition, overland flow, soil moisture and isotopic composition of soil water were measured in the open area, alive and dead Norway spruce (*Picea abies*) forest stands in summer 2021 (June to September) in the Jalovecký Creek catchment. The site is located at the forest line (altitude 1450 m a.s.l.). Forest dieback started there in summer 2012 as a result of the bark beetle infestation (*Ips typographus*). It continued in 2016 after a large windfall that occurred in May 2014 and destroyed about 50 hectares of the forest within the distance of about 1 km from the site and a warm and dry weather in 2015 and 2016. An increased dieback at the site is observed since 2017. Our measurements were conducted in the remaining small alive forest stand that is about 130 years old and in the dead forest that died in 2012 in which the regeneration has already started. Precipitation was measured by the tipping bucket rain gauges with automatic registration of the time of each tip corresponding to precipitation depth of 0.2 mm. One tipping bucket rain gauge was installed in the forest gap, two other were installed in the dead forest. Additional data (precipitation from a weighing gauge, radiation, air temperature and humidity, soil moisture at depths 5 cm, 10 cm and 20 cm) were measured every 10 minutes at the nearby (400 m) meteorological station located in the open area at altitude 1500 m a.s.l. (Fig. 1). Monthly precipitation and air temperature in the study period compared to their long-term values measured at the meteorological station (Fig. 2) indicate that June 2021 was comparatively dry and warm while August 2021 was wet and cooler. Precipitation in August 2021 and air temperature in July 2021 were the highest on record.

The overland flow was measured at runoff plots with the area of 1 m^2 (length 2 m, width 0.5 m) by deluometers developed by foresters for the overland flow and erosion research (Midriak, 1986). A deluometer is a covered tin flume the outflow from which can be collected in a vessel. We have measured the outflow from deluometers by tipping bucket rain gauges (Fig. 3). Three deluometers were installed in both the alive and dead forest. Soil moisture of the upper 10 cm of the soil was measured every 15 minutes close to each runoff plot.

Cumulative precipitation samples for the analysis of stable isotopes of oxygen and hydrogen were collected manually once per week from three standard rain gauges (orifice area 500 cm^2) located in forest gap, alive and dead forest. Four suction cup soil lysimeters (two in both the alive and the dead forest) were installed to provide weekly samples of the soil water collected at the depth of 20 cm. However, the usable data were obtained only from two soil lysimeters in the dead forest and one soil lysimeter in the alive forest. One soil lysimeter in the dead forest provided samples covering almost the entire study period (18 June to 1 October) while other

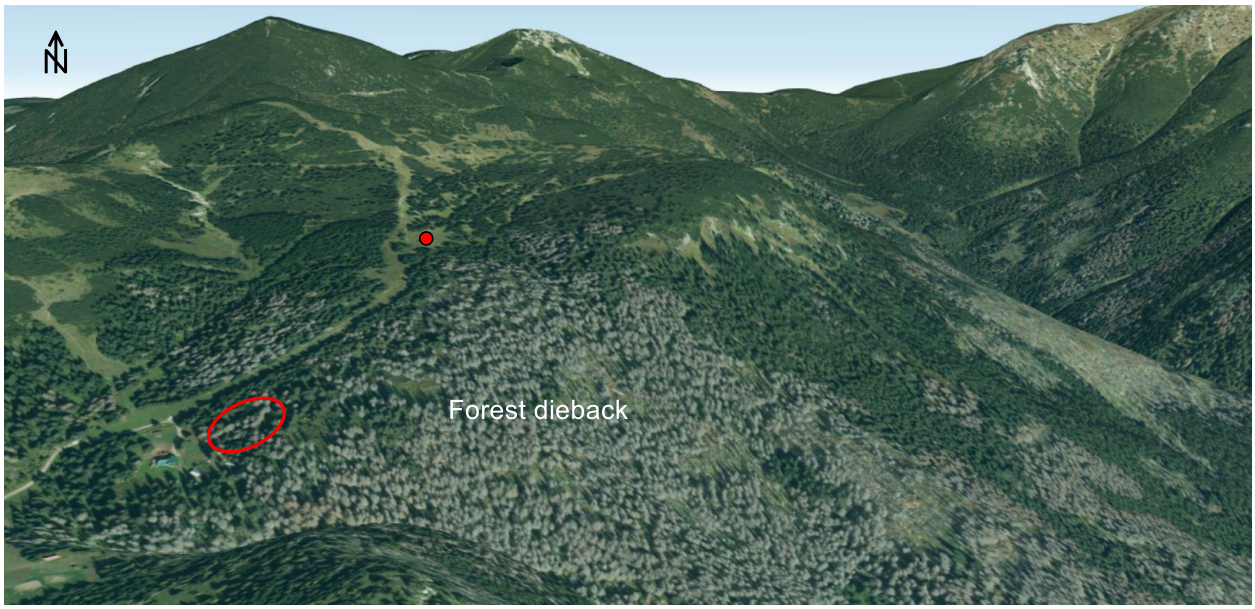

Fig. 1. Part of the Jalovecký Creek catchment showing the study area (the red ellipse), meteorological station (the red dot) and the area affected by forest dieback in 2018 (https://zbgis.skgeodesy.sk).

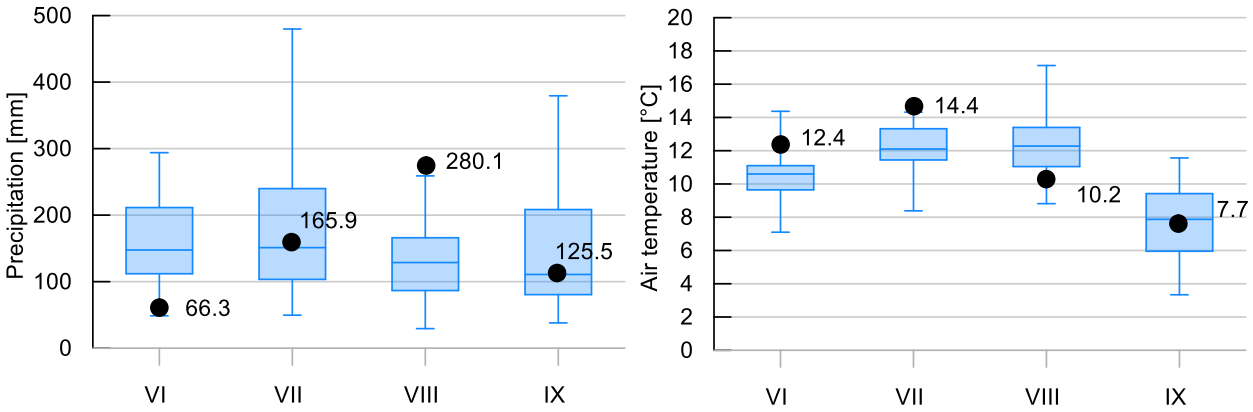

Fig. 2. Monthly precipitation and air temperature in the study period (June to September 2021) denoted by the black dots and numbers and their long-term variability (1989–2020) at the meteorological station close to the study site; the whiskers in boxplots show minimum and maximum, the boxes show upper and lower quartiles and medians.

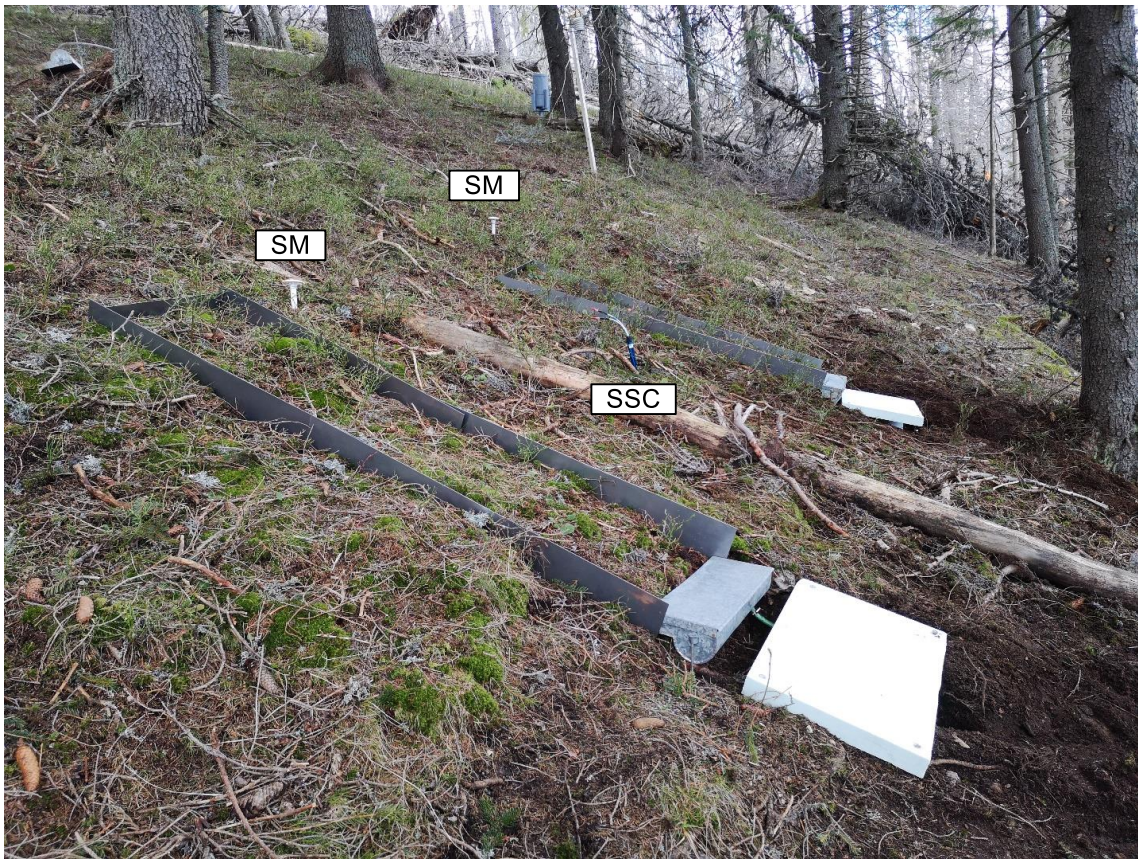

Fig. 3. Runoff plots with deluometers, soil moisture probes (SM) and a suction cup soil lysimeter (SSC) in the alive forest; the tipping bucket gauges measuring the overland flow were protected from the rain by the polystyrene covers.

two lysimeters collected enough water for the isotopic analyses only from July and August (in the dead forest) or at the end of August and in September (in the alive forest). Water samples were analysed ourselves by the Picarro 2130 laser analyzer according to a protocol presented in Holko (2015), The results are expressed in δ-values related to the international reference VSMOW2. Analytical accuracy was better than ±0.2‰ for $\delta^{18}O$ and ±1.0‰ for $\delta^{2}H$. Deuterium excess d (d= $\delta^{2}H$-8x $\delta^{18}O$) was used to check if the sampled water was not evaporated.

The obtained data allowed comparison of precipitation amount and its isotopic composition among the sites, amount and timing of the overland flow, its relation to the soil moisture and rainfall characteristics (total amount, intensity, maxima) and the relationships

between the isotopic composition of precipitation at different sites in the forest and in the soil water. The precipitation-overland flow data analysis was conducted for rainfall events. The events were determined from hourly precipitation data whereby a break after the last hour with rain or the occurrence of overland flow not longer than 5 hours was allowed to attribute the following rainfall to the same event.

Results and discussion

Measured data are shown in Fig. 4. Precipitation and soil moisture document the occurrence of two wet periods at the beginning and end of August and a drier period between the end of June and mid-July. The soil moisture data indicate that soil profile could have been saturated at the beginning and end of August, i.e. favourable conditions for the overland flow generation occurred. Five episodes of higher overland flow in the forest were observed. Except the above mentioned wet periods they occurred also after greater rainfalls in the middle and at the end of July and in the middle of September. 55 rainfall events were identified in the study period while the overland flow at different plots was registered for 21 to 30 of them. The data did not indicate a clear threshold, i.e. the minimum rainfall amount that generated the overland flow. However, rainfall events in the open area exceeding 4 mm always produced an overland flow in the forest. Event precipitation in the dead forest was on average 82% and 74% of that in the forest gap (Fig. 5). Precipitation in the dead forest was sometimes higher than that in the forest gap (in 3 and 7 events out of 29 events for which the was the overland flow registered). Similar results were reported for the site in the warm periods of the years 2013, 2014 and 2018–2020 by Bartík et al. (2016) and Jančo (2020).

Although the overland flow occurrence in the forest was common, it represented on average only a few per cents of the open area precipitation (Fig. 5). It was greater at one plot in the alive forest where it represented on average about 7% of the forest gap precipitation while at other plots (in the dead as well as alive forest) it represented on average 4% to 5% of precipitation. The variability of the overland flow amount during individual events was quite great and ranged from less than 1% to more than 10% (Fig. 5). Jančo (2020) reported similar seasonal values of the overland flow amount at the study site for June to October 2017–2019; the overland flow at different plots varied in his study between less than 1% to more than 7% (the data on individual events were not available).

Total overland flow for individual events correlated very well with precipitation in the forest gap; the coefficients of determination of linear regressions ranged from 0.85 to 0.96. Therefore, it was possible to derive the coefficients relating the overland flow and the forest gap precipitation (Table 1) that can serve as the starting values to be examined by further research.

We have analysed 10-min data for selected eight events with greater overland flow. Maximum 10-min precipitation during about a half of events occurred within the first 30 minutes of the rainfall. Other events had longer rainfall durations and the maxima occurred later (about two hours after rainfall beginning or later). Although the number of the analysed events is small, the data indicate that the overland flow as well as its maximum occurred mostly within the first 30 minutes of the rain at all sites and during all events. There was not a big difference between the dead and alive forest in this characteristic. Maximum 10-min overland flow rate was best correlated with maximum rainfall amount (correlation coefficients for different sites varied from 0.71 to 0.99) and it mostly occurred in the same time interval or 10-20 minutes later.

Stable isotopes of oxygen and hydrogen in water samples serve as tracers that can indicate different origin of water. Fig, 4 shows that $\delta^{18}O$ of precipitation in the forest gap during the study period was relatively stable with the drop at the turn of August and September caused by the change in the air masses origin which is common in the study area at the end of summer. The isotopic composition of throughfall can differ from that of the open area rainfall although the observed differences in the Jalovecký Creek catchment comparing the open area rainfall and throughfall in the alive forest were rather small in the past (Holko et al., 2011). The differences between the forest gap, dead and alive forest rainfalls in summer 2021 are shown in Table 2. Throughfall in the alive and dead forest represented on average 56% and 79% of the forest gap rainfall. The differences in isotopic composition of precipitation were greater than in the past years. Precipitation in the forest gap had always the lowest concentrations of heavy isotopes while precipitation in the alive forest was mostly isotopically heavier than in the dead forest, presumably as a result of greater interception in the alive forest. Great differences

Table 1. Coefficients (C) of equations correlating the overland flow (OF) in the forest and forest gap precipitation during an event (P); OF = P x C; R^2 is coefficient of determination, n is the number of events used to determine C

Site	C	n	R^2
Dead forest 1	0.0581	30	0.921
Dead forest 2	0.0625	21	0.820
Dead forest 3	0.0519	22	0.960
Alive forest 1	0.0968	21	0.902
Alive forest 1	0.0588	25	0.908

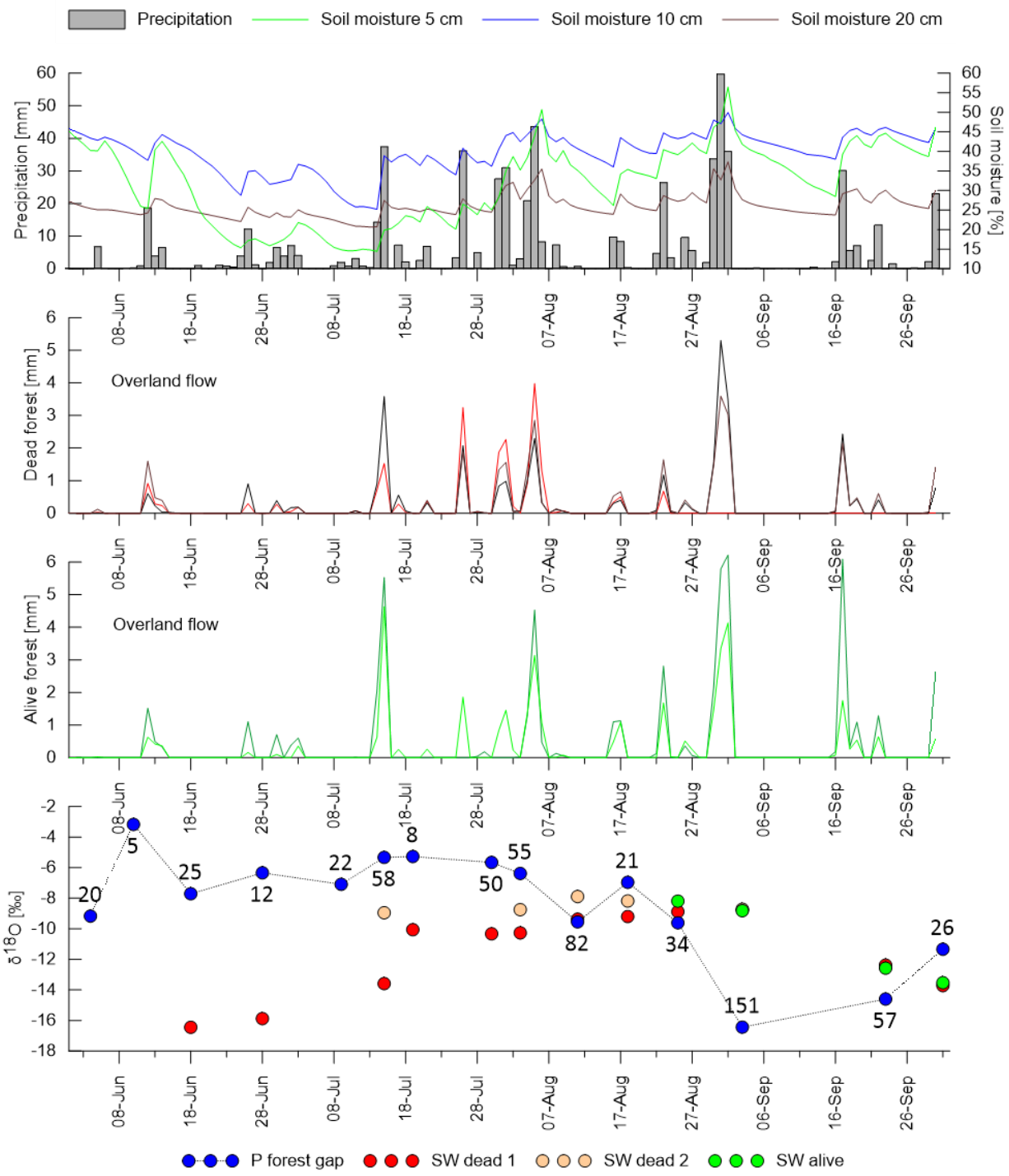

Fig. 4. Daily precipitation totals and average soil moisture at different depths at the meteorological station, daily overland flow totals in the dead and alive forest and isotopic composition of precipitation (P) in the forest gap and of the soil water (SW) in the dead and alive forest; the numbers in the lowermost panel show weekly precipitation amounts [mm] rounded to integer numbers.

in isotopic composition of precipitation were observed in the last sample collected on 1st October. Almost all precipitation collected on that day fell on September 30 as a long lasting rain (duration of about 13 hours) with smaller intensity (average 0.3 mm/10 min) falling at high relative humidity of the air (100%). Greater contribution of fog in the alive and dead forest could thus be the reason of the great difference in the isotopic composition of throughfall.

The isotopic composition of soil water was very different from that of precipitation until August (the bottom panel in Fig. 4). Isotopically light water was observed in

the dead forest until the mid-July. On the basis of our previous measurements (Holko et al., 2013) we conclude that soil until the mid-July contained a significant amount of the snowmelt water that has $\delta^{18}O$ values similar to those, presented for the soil water until the mid-July in Fig. 4. The assumption about greater influence of snowmelt in the dead forest is supported by findings of Bartík et al. (2019) who reported a significant increase in the amount of water stored in the dead forest compared to the alive forest. The soil water became isotopically similar to precipitation in August while the isotopically very light precipitation from the end of August was reflected in the isotopic composition of the soil water with the time delay of at least one week.

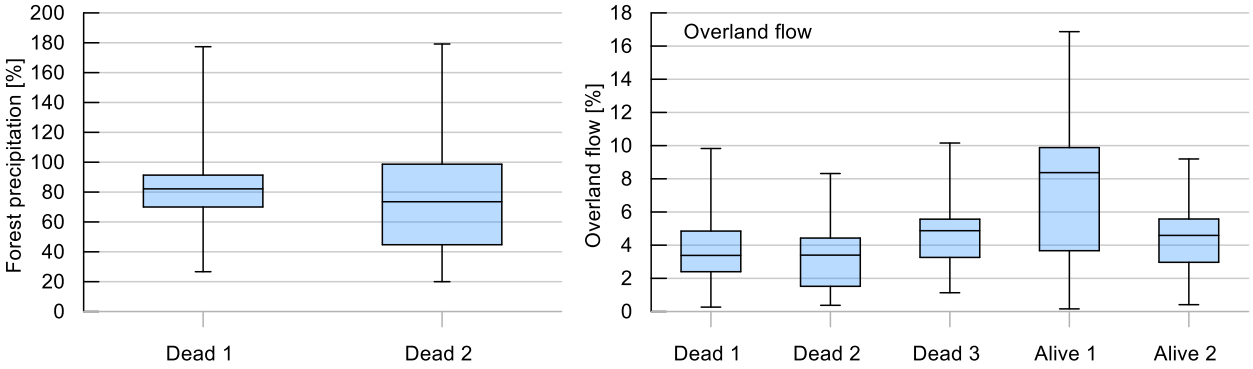

Fig. 5. Left – event throughfall in the dead forest (Dead 1, Dead 2) as a percentage of precipitation in the forest gap for the rainfall events during which the overland flow was observed (data from the tipping bucket rain gauges); right – overland flow in the dead and alive forest during the events over the entire study period (as a percentage of precipitation in the forest gap); the whiskers show minimum and maximum, the boxes show the upper and lower quartiles and medians.

Table 2. Precipitation amounts and isotopic composition of weekly precipitation in the forest gap, alive and dead forest in summer 2021; d is the deuterium excess; the red values represent evaporated samples (presumably due to small rainfall amounts and longer storage in the rain gauge)

Sampling date	Forest gap				Alive forest				Dead forest			
	P [mm]	$\delta^{18}O$ [‰]	$\delta^{2}H$ [‰]	d [‰]	P [mm]	$\delta^{18}O$ [‰]	$\delta^{2}H$ [‰]	d [‰]	P [mm]	$\delta^{18}O$ [‰]	$\delta^{2}H$ [‰]	d [‰]
4-Jun	20.4	-9.2	-60	13.1	5.8	-8.7	-56	13.3	10.6	-9.5	-63	13.4
10-Jun	5.0	-3.2	-16	9.6	1.0	-0.5	-3	1.4	3.0	-1.9	-10	5.1
18-Jun	25.4	-7.7	-50	12.4	15.6	-6.8	-44	11.2	19.2	-7.5	-48	12.0
28-Jun	12.4	-6.3	-39	11.8	3.4	-6.2	-36	13.1	7.9	-6.1	-38	11.5
9-Jul	22.4	-7.1	-47	10.1	3.6	-4.5	-33	3.7	14.0	-6.6	-43	9.5
15-Jul	58.2	-5.3	-27	15.7	49.2	-5.3	-26	16.5	56.8	-5.3	-26	16.4
19-Jul	8.0	-5.3	-32	10.5	4.4	-4.5	-25	11.2	5.5	-4.8	-28	11.0
30-Jul	50.4	-5.7	-32	13.7	25.2	-5.4	-28	16.0	45.2	-5.7	-30	15.3
3-Aug	55.2	-6.4	-37	14.2	30.4	-6.1	-35	13.9	37.0	-6.2	-35	14.5
11-Aug	81.6	-9.6	-63	13.4	61.2	-9.2	-60	14.1	88.2	-9.7	-64	13.5
18-Aug	20.8	-7.0	-41	15.0	9.2	-6.5	-37	15.6	14.6	-6.6	-39	14.3
25-Aug	33.6	-9.6	-63	13.6	25.6	-9.0	-58	14.5	26.4	-8.8	-57	14.1
3-Sep	150.6	-16.4	-117	14.6	165.6	-15.8	-112	14.5	182.4	-15.9	-113	14.5
23-Sep	57.2	-14.6	-106	10.8	40.4	-13.5	-97	10.5	52.0	-14.5	-105	11.6
1-Oct	26.0	-11.3	-80	10.6	15.6	-8.7	-57	12.6	20.4	-9.7	-66	11.3

Conclusion

The first results of the overland flow and isotopic measurements in the changing forest of the Jalovecký Creek catchment indicate that proposed experimental setup can provide useful data on the influence of forest changes on hydrological cycle. Future research can be accompanied by measurements of vegetation characteristics such as the leaf area index. Sampling of the snowmelt water before the summer period and of the overland flow could help in better identification of the soil water sources during the season and contribution of rain and soil water to the overland flow.

Acknowledgement

This work was supported by the grants of the Slovak Academy of Sciences (project VEGA No. 2/0065/19 and MVTS COST CA19120) and Slovak Research and Development Agency (project APVV No. 19-0340).

References

Bartík, M., Holko, L., Jančo, M., Škvarenina, J., Danko, M., Kostka, Z. (2019): Influence of mountain spruce forest dieback on snow accumulation and melt. Journal of Hydrology and Hydromechanics., vol. 67, no. 1, 59–69.

Bartík, M., Jančo, M., Střelcová, K., Škvareninová, J., Škvarenina, J., Mikloš, M., Vido, J., Waldhauserová, P. D. (2016): Rainfall interception in a disturbed montane spruce (Picea abies) stand in the West Tatra Mountains. Biologia, vol. 71, no. 9, 1002–1008.

Celer, S. (2015): Forests in the Jalovecká dolina valley. In Slovak, in: Divočina pod Salatínom (Eds. M. Ballo and L. Holko), REPROservis – DTP štúdio & tlačiareň, Liptovský Mikuláš. 123–146.

Holko, L. (2015): Syringe life and memory effects in isotopic analyses performed by liquid water isotopic analysers – a case study for natural waters from central Europe. Isotopes in Environmental and Health Studies, DOI: 10.1080/10256016.2015.1090987

Holko, L., Danko, M., Dóša, M., Kostka, Z., Šanda, M., Pfister, L., Iffly, J. (2013): Spatial and temporal variability of stable water isotopes in snow related hydrological processes. Die Bodenkultur, 64, 3–4, 39–45.

Holko, L., Kostka Z., Šanda, M. (2011): Assessment of Frequency and Areal Extent of Overland Flow Generation in a Forested Mountain Catchment. Soil and Water Research, 6, 1, 43–53.

Holko, L., Kostka, Z. (2006): Hydrological research in a high-mountain catchment of the Jalovecký Creek. Journal of Hydrology and Hydromechanics., vol. 54, no. 2, 192–206.

Jančo, M. (2020): Interception and selected hydric functions in climax spruce after the bark beetle infestation. In Slovak. PhD. Thesis, Technical University in Zvolen, Zvolen, 141 p.

Mezei, P., Jakuš, R., Pennerstorfer, J., Havašová, M., Škvarenina, J., Ferenčík, J., Slivinský, J., Bičárová, S., Bilčík, D., Blaženec, M., Netherer, S. (2017): Storms, temperature maxima and the Eurasian spruce bark beetle Ips typographus – An infernal trio in Norway spruce forests of the Central European High Tatra Mountains. Agricultural and Forest Meteorology, vol. 242, 85–95.

Mezei, P., Grodzki, W., Blaženec, M., Škvarenina, J., Brandýsová, V., Jakuš, R. (2014): Host and site factors affecting tree mortality caused by the spruce bark beetle (Ips typographus) in mountainous conditions. Forest Ecology and Management, vol., 331, 196–207.

Midriak, R. (1986): Comments to methods of measurements of both surface flow and erosive soil losses in forest stands and above the timberline. In Slovak, Vodohospodársky časopis, vol. 34, no. 6, 653–657.

Seidl, R., Schelhaas, M. J., Lexer, M. J. (2011): Unraveling the drivers of intensifying forest disturbance regimes in Europe. Global Change Biology, vol. 17, 2842–2852.

Senf, C. Seidl, R. (2021): Mapping the forest disturbance regimes of Europe. Nature Sustainability, vol. 4, 63–70.

RNDr. Ladislav Holko, CSc. (*corresponding author, e-mail: holko@uh.savba.sk)
Ing. Martin Jančo, PhD.
Ing. Michal Danko, PhD.
Ing. et Ing. Patrik Sleziak, PhD.
Institute of Hydrology SAS
Dúbravská cesta 9
84104 Bratislava
Slovak Republic

DOI: 10.31577/ahs-2022-0023.01.0010

ACTA HYDROLOGICA SLOVACA

Volume 23, No. 1, 2022, 89 – 98

Observations from the Western Carpathians and Pannonian Plain show that rainfall return levels need to be adjusted to account for rising dew-point temperature

Milan ONDERKA*, Jozef PECHO

Rainfall records from a total of 526 rain gauges located in the western part of the Carpathian Mountains and the adjacent Pannonian Plain were analyzed. Estimation of extreme rainfall totals with various return periods is essential for reliable design of hydraulic infrastructure. The ongoing climate change brings additional challenges to the estimation of rainfall return levels. In this paper, we compared stationary vs. non-stationary generalized extreme value distributions (GEV) for 2-, 5-, 10-, 25-, 50-, and 100-year return levels of 24-h rainfall determined from annual maxima series. The fundamental question we seek to answer in this paper is whether the stationarity-based design concept is adequate under changing climate conditions because the statistical parameters of probability distribution become dependent on dew-point temperature. Our analyses revealed that the projected return levels tend to increase with decreasing return periods. For instance, the 100-year return levels need an adjustment by ~6.64% (CI: -1.03% +14.95%), while the stationary 5-year return periods of 24-h precipitation totals need to be adjusted by up to ~10.5% (CI: -3.61% +21.24%). Our investigations showed that in ~60% of the analyzed sites the current return levels might need an adjustment to account for the rising dew-point temperature. The presented results may have implication for regional water management planning and flood risk assessment.

KEY WORDS: rainfall, non-stationarity, GEV, return period, return level

Introduction

Climate extremes, including heavy precipitation and extreme air temperatures have substantially increased in the past few decades (Onderka and Pecho, 2021; Lakatos et al., 2020; Alexander et al., 2006; Vose et al., 2005). Global warming increases average air temperature, which in turn enhances atmospheric water holding capacity (Onderka and Pecho, 2021). It is now recognized that these changes are responsible for higher frequency and/or intensity of extreme rainfall (Ganguli and Coulibaly, 2017; Agilan and Umamahesh, 2016). Rainfall extremes and their statistical properties are important for proper estimations of design values in numerous engineering infrastructures such as urban drainage systems, bridges, railways, highways, rain harvesting systems and road culverts can be designed more economically when the frequency of extreme rainfall is known (Yan et al., 2021; Lakatos et al., 2020; Onderka et al., 2020; Bara et al., 2009; Faško et al., 2000). Rainfall extremes can studied at a range of spatial and temporal scales (AghaKouchak et al., 2013; Diffenbaugh and Giorgi, 2012; Jakob, 2013; Kharin et al., 2007). A substantial reduction in the return period of an annual maximum precipitation amount with frequent occurrence of extreme rainfall events is predicted by the end of the 21st century (IPCC 2012). O'Gorman (2015) found a dependency between mean and extreme precipitation on air temperature. This dependency has been ascribed to physical relation known as the Clausius–Clapeyron relation (O'Gorman and Schneider, 2009; Wasko and Sharma, 2015; 2017; Onderka and Pecho, 2021), according to which, increased water-holding capacity of warmer air intensifies heavy rainfall at a rate of approximately 7–8% °C −1 of warming. Lenderink et al. (2017) found that in the Netherlands, extreme precipitation of sub-hourly up to the 6-h durations have increased above the Clausius–Clapeyron relation. Similar results are reported by other authors in Switzerland (Ban et al., 2015), Germany (Berg et al., 2013), the UK (Blenkinsop et al., 2015), in Australia (Schroeer and Kirchengast, 2018; Wasko and Sharma, 2015; 2017), North America (Shaw et al., 2011) and in China (Miao et al., 2015). This pattern of increasing annual extremes with air temperature is not valid for every place on the Earth. Observations published in relevant literature suggest that this relation is region-specific. For instance, in India (Ali and Mishra, 2017) and northern Australia (Jones et al., 2010) negative rates have been reported. Consequences of climate change often lead to altered intensity, duration or frequency of all rainfall extremes. Cheng and AghaKouchak (2015)

showed that a stationary climate assumption may lead to underestimation of extreme precipitation by as much as 60%, and that such underestimation ultimately may increase the risk of floods and failure of infrastructure. For example, the return level with a T-year return period represents an rainfall amount that has a 1/T chance of occurrence in any given year (Lakatos et al., 2020; Cooley et al., 2007). However, infrastructure design concepts still rely on stationary return levels, which assume no change in the frequency of extremes over time (Cheng and Aghakouchak, 2015; Agilan and Umamahesh 2018; Sarhadi and Soulis 2017). The concept of frequency analysis inherently implies mutually independent rainfall events.

The frequency of rainfall extremes has been changing and is likely to continue to change in Slovakia in the future (Onderka et al., 2020). Therefore, concepts and models that can account for non-stationary analysis of climatic and hydrologic extremes are needed (e.g. Cooley 2013; Parey et al., 2010; Salas and Obeysekera, 2014). Katz et al. (2002) present non-stationarity in extremes in terms of changing quantiles (also termed "effective return levels"), which vary as a function of time to keep a constant probability of an extreme event. Alternatively, Rootzén and Katz (2013) introduced the concept of "Design Life Level" to quantify the probability of exceeding a fixed threshold during the design life of a project.

To our best knowledge, non-stationarity of 24-h rainfall annual maxima induced by changing climate has not been considered in Slovakia so far. Thus our intention here is to present the first results obtained from non-stationary modeling of return levels of 24-h rainfall with respect to rising air and dew point temperatures with an emphasis placed on a comparison with a stationary set up.

Material and methods

Data sources

Our investigations are based on data collected at 526 rain gauges located throughout the investigated region (Slovakia), i.e. encompassing the northern part of the Pannonian Plain and the adjacent western Carpathian Mountains. The rain gauges are located throughout a broad range of altitudes ranging from 97 up to 2634 m a.s.l. The average distance between the rain gauges is 9.2 km. The analyzed time series span over 40 years and cover the time period 01/1981–12/2020 (Table 1). The choice of rain gauges was based on the length of the available time-series and their quality so that we did not have to fill in missing data nor remove suspicious observations. The 24-h rainfall totals were measured in standard rain gauges operated by the national weather service (Slovak Hydrometeorological Institute). The amount of precipitated water in the rain gauges is measured on a daily basis at 0600 UTC. The capture area of a rain gauge is 500 cm^2. The auxiliary data on near surface dew-point and dry-bulb temperatures were downloaded from the reanalysis ERA5 database in the form of monthly averages of near surface dew-point and dry-bulb air temperatures. The ERA5 data were downloaded from the Copernicus Climate Data Store via the Application Programme Interface CDS API (https://cds.climate.copernicus.eu).

Identification of return levels under stationary and non-stationary conditions

The term return level refers to the magnitude of the daily rainfall event. The return period is the frequency of

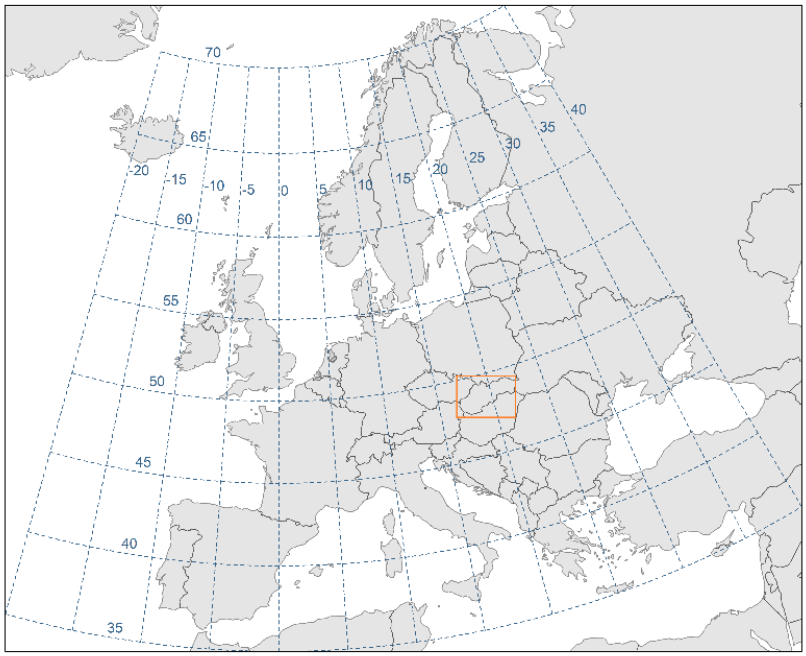

Fig. 1. Location of the investigated region – the rectangle encompasses the western part of the Carpathians Mountains and the adjacent Pannonian Plain.

the event. Return periods are usually identified by analyzing rainfall annual maxima series (AMS), where the largest event of one year is considered to be independent of the largest event from any other year (Bedient et al., 2008). In a purely statistical sense, extremes in rainfall or any other natural phenomenon can be broadly categorized either as stationary and non-stationary (Ragno et al., 2019; Cheng et al., 2014; Cheng and Aghakouchak, 2015). In a stationary model, the mean, variance, and distribution of extremes do not change over time or with respect to other covariates. In a stationary model, observations are assumed to have a probability distribution function with constant parameters. On the contrary, when non-stationarity of the extremes is assumed, the parameters of the underlying probability distribution function change in response to a given covariate (Ragmo et al., 2019). First, we identified annual maxima of 24-h rainfall in each of the time series. This was accomplished by identifying the highest 24-h rainfall total for each calendar year of the record. As the investigated period covers the years 1981-2020, each rain gauge provided 40 maximum 24-h rainfall totals. The time-series of annual maxima from each of the 526 rain gauges were then analyzed to detect non-stationarity with respect to time and dew-point temperature. In this paper, we applied the generalized framework named Process-informed Non-stationary Extreme Value Analysis (ProNEVA) Software Package, Version 2.0 developed by Cheng et al. (2014) and further described with practical applications in Regno et al. (2019). A non-stationarity component is often defined as a temporal dependence of the observed extremes on another physical variable. Incorporating a physical control into the statistical analysis is possible when there is strong evidence (empirical or theoretical) that the physical covariate can alter the statistics of the extremes. Since it is recognized that increasing air temperature intensifies the development of convective storms (Onderka and Pecho, 2021) the temporal trend in near-surface dew point temperature is considered here as a plausible physical covariate for explaining non-stationarity of rainfall extremes. For a stationary model, the cumulative distribution function of the GEV is defined as

$$F_{GEV}(x) = exp\left[-\left(1+\xi\left(\frac{x-\mu}{\sigma}\right)\right)^{-1/\xi}\right] \qquad (1)$$

where F_{GEV} is defined for $\{x: 1+(\xi(x-\mu)/\sigma) > 0\}$, $-\infty < \mu < \infty$, $\sigma > 0$. and $-\infty < \xi < \infty$, where μ is the location parameter, σ is scale parameter, and ξ is the shape parameter (Cheng and Aghakouchak 2015; Smith et al., 2001). The stationary GEV model can be extended to a non-stationary GEV by allowing the parameters of the distribution function in Eq. 1 to vary with a chosen physical covariate x_{cov} or simply with time t. Then, the non-stationary probability density function can be defined as

$$F_{GEV}(x|x_{cov}) = exp\left[-\left(1+\xi(x_{cov})\left(\frac{x(x_{cov})-\mu(x_{cov})}{\sigma(x_{cov})}\right)\right)^{-1/\xi(x_{cov})}\right] \qquad (2)$$

where μ is the location parameter, σ is scale parameter, and ξ is the shape parameter are assumed to be dependent on the covariate x_{cov}. Here, we allowed only the location parameter μ to be covariate-dependent. As pointed out by Ragno et al. (2019), it is difficult to precisely estimate the shape parameter ξ even for the stationary GEV distribution, in this paper only the location parameter μ was allowed to depend on a covariate. The location parameter is therefore defined as a linear function of the covariate.

$$\mu(x_{cov}) = \mu_0 + \mu_1 x_{cov} \qquad (3)$$

where x_{cov} is a covariate and μ_0 and μ_1 are estimated parameters. The parameters of the selected non-stationary GEV distribution were estimated using the Bayesian approach described e.g. in Ragno et al. (2019), AghaKouchak et al. (2013) or Cheng et al. (2014).

Covariate selection – time vs. dew point temperature

Time is the most frequently used covariate in non-stationary modeling of rainfall extremes (Yan et al., 2021; Agilan and Umamahesh, 2016; Ragno et al., 2019). An important advantage of using time as a covariate in non-stationary GEV is that we can project the return levels for a projected time horizon. However, before blindly applying time as a covariate in our analyses it is necessary to justify its utilization as a covariate in non-stationary distribution functions. Our hypothesis was that time can be considered as a covariate only if another physically plausible covariate (e.g. dew-point temperature) co-varies linearly with time (Ganguli and Coulibaly, 2017; Onderka and Pecho, 2021; O'Gorman and Schneider, 2009; Wasko and Sharma, 2015; 2017). If a non-linear temporal trend in dew-point temperature was detected, the parameters in Eq. 3 would need to be adjusted to account for a non-linear temporal evolution of the physical covariate (e.g. using higher order polynomials). In such cases, time as a single covariate could not be used. Therefore, a linear temporal trend in the covariate series is a pre-requisite for using time as a covariate in the non-stationary distribution function. It is well a known fact that summertime rainfall extremes are physically linked to the atmosphere's water holding capacity (Zhang et al., 2019; Onderka and Pecho, 2021; Wasko and Sharma, 2015; 2017). A dependency between the frequency and intensity of extreme rainfall and mean near-surface air and dew-point temperatures has been observed in a growing number of studies (e.g. Ganguli and Coulibaly, 2017; Onderka et al., 2021; O'Gorman and Schneider, 2009; Wasko and Sharma, 2015; 2017). This dependency is physically explained by the relationship between saturated vapor pressure and air temperature, known as the Clausius–Clapeyron relation. Because extreme rainfall apparently scales with dew-point temperature better than with dry-bulb temperature (Zhang et al., 2019; Onderka and Pecho, 2021) in this paper we focused on the temporal evolution of dew-point temperature first.

Various approaches have been proposed to relate annual rainfall extremes to increasing dew-point temperatures (or another appropriate variable). For instance, Westra et al. (2013) use a global approach, i.e. they applied the global mean temperature to scale global rainfall extremes. Poschlod and Ludwig (2021) used the average temperature of the European continent to account for the fact that the sources of water attributing to rainfall in Europe originate from regional moisture transfers (Keune and Miralles, 2019); local temperatures have been used by Onderka and Pecho (2021) in event-based analyses of rainfall intensities (Onderka and Pecho, 2021). Bisselink and Dolman (2008) described a dynamic rainfall recycling model using re-analyses data from ERA40. Based on their investigations for the Central European region, the recycling ratio for the summertime season (J- J-A) is a function of spatial scale.

However, the principle sources of rainfall water for atmospheric precipitation are the evaporated water from the land surface and water bodies such as lakes and oceans. The proportion these two sources of precipitation water contribute to the observed rainfall in an investigated area is usually unknown. For instance, it is estimated that only some 10 to 20 % of rainfall water falling on the Central European region comes from the same area where the rainfall is observed. This implies that the origin of rainwater is mostly attributable to soil moisture evaporated from land surface outside the vicinity of an investigated rain gauge (Poschlod and Ludwig, 2021; Keune and Miralles, 2019; Bisselink and Dolman, 2008).

In this paper we averaged the temporal trends calculated for near surface dew-point temperature series (ERA5 reanalysis data) over a rectangle encompassing the entire investigated region of the western Carpathians and the most northern part of the Pannonian Plain (bottom left corner coordinates: longitude 16.75, latitude 47.75; upper right corner coordinates: longitude 22.75, latitude 49.75, see Fig. 1). First, the temporal trend was calculated separately for each grid point of the ERA5 reanalysis dew-point temperature data. Trends were esimated only on summertime data (JJA). A global trend was then constructed by averaging the individual local (grid point) trends. The global average trend was used as a proxi covariate in the non-stationary GEV analyses for each of the 526 rain gauges.

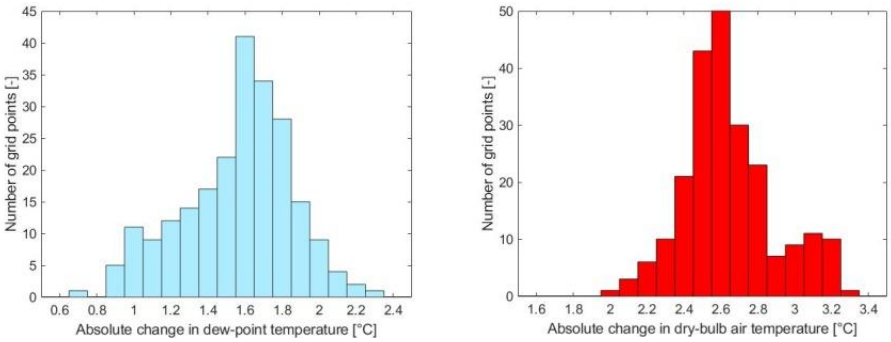

Fig. 2. Histograms of temporal changes (period 1981–2020) in summertime (JJA) near surface dew-point temperature (left) and dry-bulb temperature (right) determined from ERA5 data (n = 225 grid points). The median absolute change in summertime dew-point temperature over the investigated period is 1.6°C, and the median change in summertime dry-bulb temperature is 2.6°C.

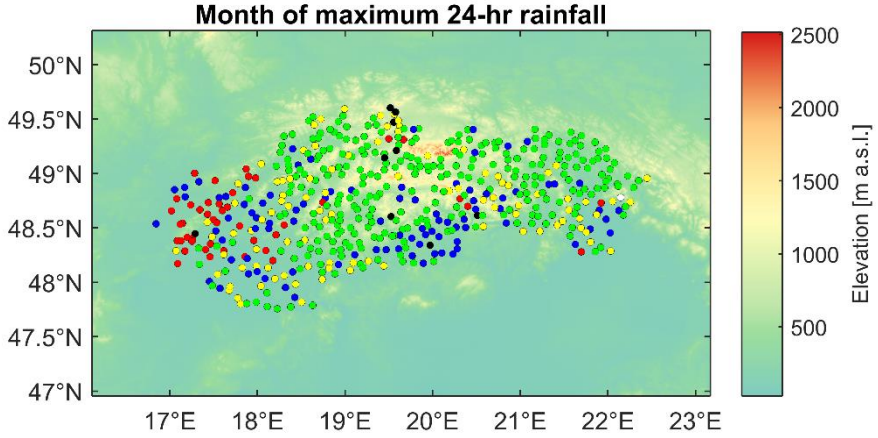

Fig. 3. Distribution of months (median values) with the highest rate of annual 24-h maxima. The following color-coding was applied to distinguish between months: black = May; blue = June; green = July; yellow = August; red = September.

Goodness of fit

Four goodness-of-fit measures were calculated to test the performance of the models. The tests were used to facilitate the selection a parsimonious model, i.e. a model showing a sufficient level of performance efficiency with the minimum number of parameters. The models were compared based on the Akaike Information Criterion (AIC), Bayesian Information Criterion (BIC) and the Root Mean Square Error (RMSE). The Akaike Information Criterion (AIC) is formulated as

$$AIC = 2(D - L) \qquad (4)$$

where D is the number of parameters of the statistical model and L is the log-likelihood function. The model associated with a lower AIC is considered a better fit. The Bayesian Information Criterion (BIC) is defined as

$$BIC = D\ ln(N) - 2L \qquad (5)$$

where N is the length of records. Similar to AIC, the model with lower BIC results a better fit. In addition to AIC and BIC, the Root Mean Square Error (RMSE) was calculated. A time series was declared non-stationary if AIC, BIS and RMSE concurrently satisfied the three following conditions: $AIC_{NonStat} < AIC_{Stat}$; $BIC_{NonStat} < BIC_{Stat}$; $RMSE_{NonStat} < RMSE_{Stat}$. As summarized in Table 2, we used all three criteria to identify non-stationary series of annual rainfall maxima. First we compared the percentage of rain gauges with stationary and non-stationary series based on comparison of the Akaike Information Criterion (AIC), Bayesian Information Criterion (BIC) and the root mean squared errors (RMSE). Note that the last column in Table 1 indicates the percentage of rain gauges satisfying the condition that all three criteria of non-stationarity are satisfied concurrently. The further statistical analyses are based on the concurrent satisfaction of the three criteria.

By analyzing the temporal aspects when a rainfall maximum occurs we found that the annual maxima occur mostly in the summer months between June and September, as shown in Fig. 3 with an apparent spatial pattern. In the south-western portion of the investigated region the annual maxima occur predominantly in May and September, whereas the month of July dominates in the rest of the region. Therefore the trend analysis of the ERA5 near surface dew point temperature series was conducted only for the summer months (June, July and August). The trend analysis of dew point temperature revealed that, over the period 1981–2020, the average near surface dew-point temperature increased linearly by 1.6°C (Fig. 2). The use of time as a covariate in non-stationary GEV analysis is therefore justified. Recalling the C-C scaling rate of ~7% per every degree of dew-point temperature, the 1.6°C increase in dew point should roughly correspond to 11.2% increase in rainfall extremes. Table 2 summarizes the comparison of the stationary and non-stationary approach. The corresponding histograms of changes in return levels between the stationary estimates (1981–2020) and the non-stationary estimates projected for the time horizon 2040 are shown in Figure 4. The 2-year return levels increased by 13.39% and the 100-year return levels increased by 6.64%. In general, the return levels tend to increase with decreasing return period. Similar results were obtained by Ganguli and Coulibaly (2017) who compared intensity-duration-frequency curves constructed for non-stationary conditions with current design standards in Canada. They found that return periods (10 years or less), which are values typical for urban drainage design require an update of up to ~7%. For longer recurrence intervals (50–100 years) the authors conclude that updates ranging from 2 to 44% are needed. Figure 5 shows the overall distributions (histograms) of the simulated 2-, 5-, 10-, 20-, 50- and 100-year return levels. The percentage changes in return levels are shown in maps (Fig. 6).

Table 1. Percentage of rain gauges with stationary and non-stationary annual maxima series based on comparison of the Akaike Information Criterion (AIC), Bayesian Information Criterion (BIC) and the root mean squared errors (RMSE). The last column indicates the percentage of rain gauges satisfying the condition that all three criteria of stationarity are satisfied concurrently, i.e. AIC, BIC and RMSE of the stationary models are lower than for the non-stationary models

	$AIC_{stat}<AIC_{NonStat}$	$BIC_{stat}<BIC_{NonStat}$	$RMSE_{stat}<RMSE_{NonStat}$	$AIC_{stat}<AIC_{NonStat}$ and $BIC_{stat}<BIC_{NonStat}$ and $RMSE_{stat}<RMSE_{NonStat}$
Stationary AMS [%]	69.96	84.22	48.29	32.70
	$AIC_{Nonstat}<AIC_{Stat}$	$BIC_{Nonstat}<BIC_{Stat}$	$RMSE_{Nonstat}<RMSE_{Stat}$	$AIC_{Nonstat}<AIC_{Stat}$ and $BIC_{Nonstat}<BIC_{Stat}$ and $RMSE_{Nonstat}<RMSE_{Stat}$
Non-stationary AMS [%]	30.04	15.78	51.71	59.86

Table 2. **Percentage change [%] of stationary vs. non-stationary return levels simulated for the time horizon 2040. The statistics was calculated for rain gauges satisfying the non-stationarity criteria**

Return period	2-year	5-year	10-year	25-year	50-year	100-year
Min	-27.44	-23.86	-22.84	-22.21	-22.09	-22.19
Max	49.03	40.34	36.71	33.58	32.03	35.50
Kurtosis	0.21	0.69	1.11	1.64	1.92	2.23
Skew	-0.31	-0.53	-0.65	-0.68	-0.54	-0.27
P10	-4.18	-3.61	-2.31	-1.82	-1.53	-1.03
P50	13.39	10.49	9.25	7.81	6.92	6.64
P90	28.83	21.24	18.30	16.05	15.09	14.95
St.Dev.	13.44	9.99	8.58	7.53	7.26	7.43
Average	12.94	9.76	8.49	7.47	7.03	6.79

Table 3. **Global statistics of return levels (maximum likelihood values) calculated for the ensemble of stationary and non-stationary models for the time horizon 2040. The values are indicated in mm**

Return period	2-year	5-year	10-year	25-year	50-year	100-year
Min	27.35	36.72	42.66	50.04	53.65	56.35
Max	78.83	103.41	119.76	140.51	155.97	171.37
Kurtosis	2.57	4.43	5.30	5.11	4.09	2.88
Skew	1.30	1.57	1.64	1.54	1.35	1.15
P10	35.60	45.93	52.03	59.42	64.66	69.25
P50	41.36	52.30	59.85	69.31	76.84	84.35
P90	52.97	65.01	73.42	85.49	95.44	105.30
St.Dev.	7.61	8.59	9.52	11.28	13.20	15.77
Average	43.31	54.20	61.63	71.38	78.93	86.75

Table 4. **Return levels of the 24-hr rainfall [mm] projected for the time horizon 2040. The projections were performed for both the stationary and non-stationary conditions. ML stands for maximum likelihood estimates; the confidence interval of the ML estimates is defined as the 5th and 95th percentiles (P05 and P95). The percentage change (% change) was calculated as a 100*(RL2040/RLstat)**

	Return levels [mm]					
Rain gauge location	**2-years**	**5-years**	**10-years**	**25-years**	**50-years**	**100-years**
Bratislava – Koliba						
ML	46.74	56.95	64.11	73.64	81.08	88.79
P05	36.46	47.96	55.62	64.35	70.01	75.17
P95	56.6	69.18	79.04	95.55	108.54	125.04
% change	19	14.9	13.2	11.9	11.4	11.1
Bratislava – Airport						
ML	40.31	52.23	61.10	73.54	83.77	94.83
P05	28.78	41.36	49.99	61.34	68.27	74.53
P95	48.54	63.40	77.93	102.78	130.61	164.08
% change	21.2	14.3	11.3	8.6	7.1	6

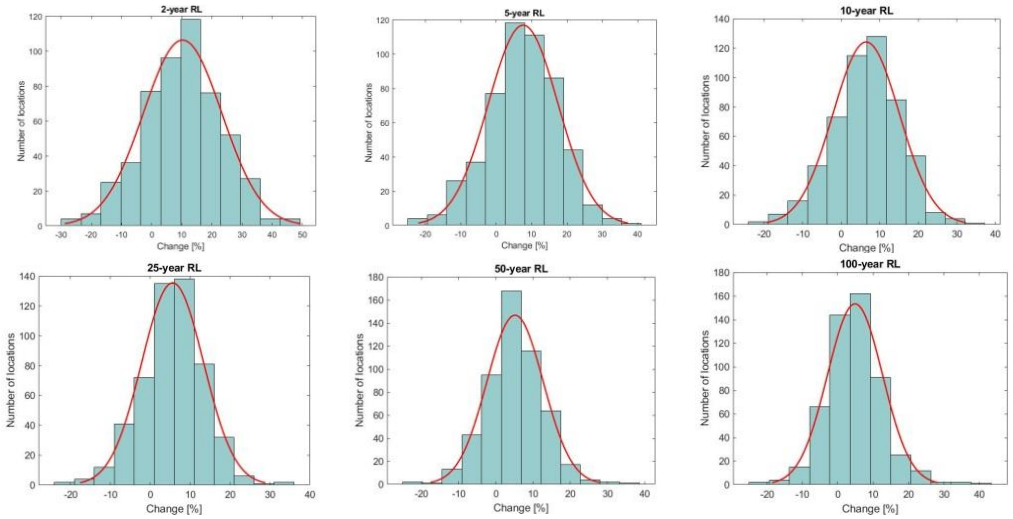

Fig. 4. Histograms with their normal pdf functions constructed for the changes in return levels. The percentage changes indicate the change between the stationary estimates (1981–2020) and the non-stationary estimates projected for the time horizon 2040.

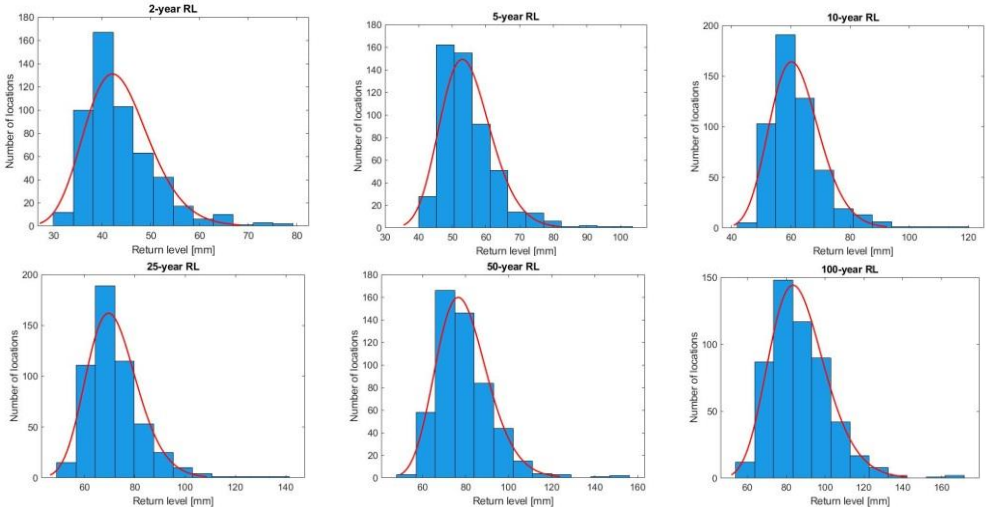

Fig. 5. Histograms with their log-normal pdf functions constructed for the 2-, 5-, 10- , 20-, 50-, and 100-year return levels (maximum likelihood estimates) simulated for the time horizon 2040.

It is important to note that in this study we related non-stationarity only to one physical driver, i.e. dew-point temperature.

In terms of other physical drivers related to convective precipitation that could be potentially used as a covariate in non-stationary GEV analyses, convergence, vorticity and vertical wind shear changes should be considered (Onderka and Pecho, 2021).In addition to these physical drivers, there are reports from other parts of the globe where atmospheric circulation modes, global and regional changes in air temperature, global carbon dioxide trends and the level of urbanization are recognized as being capable of affecting the non-stationary behavior of rainfall extremes in the future (Agilan and Umamahesh, 2016; Yan et al., 2021).

First, we focused on the appropriateness of using time as a single covariate to describe the non-stationary behavior of rainfall annual maxima series. To justify the use of time as a covariate, we used the temporal trend in summertime dew-point temperature as a plausible physical variable controlling the occurrence of summertime rainfall extremes.

Based on the presented analyses we can conclude that the stationarity-based concept may not be adequate for the design of hydraulic infrastructures under changing climate conditions because the parameters of probability distribution change with time.

In fact, an update of the present-day stationary estimates of rainfall return levels is needed to account for the rising dew-point temperature.

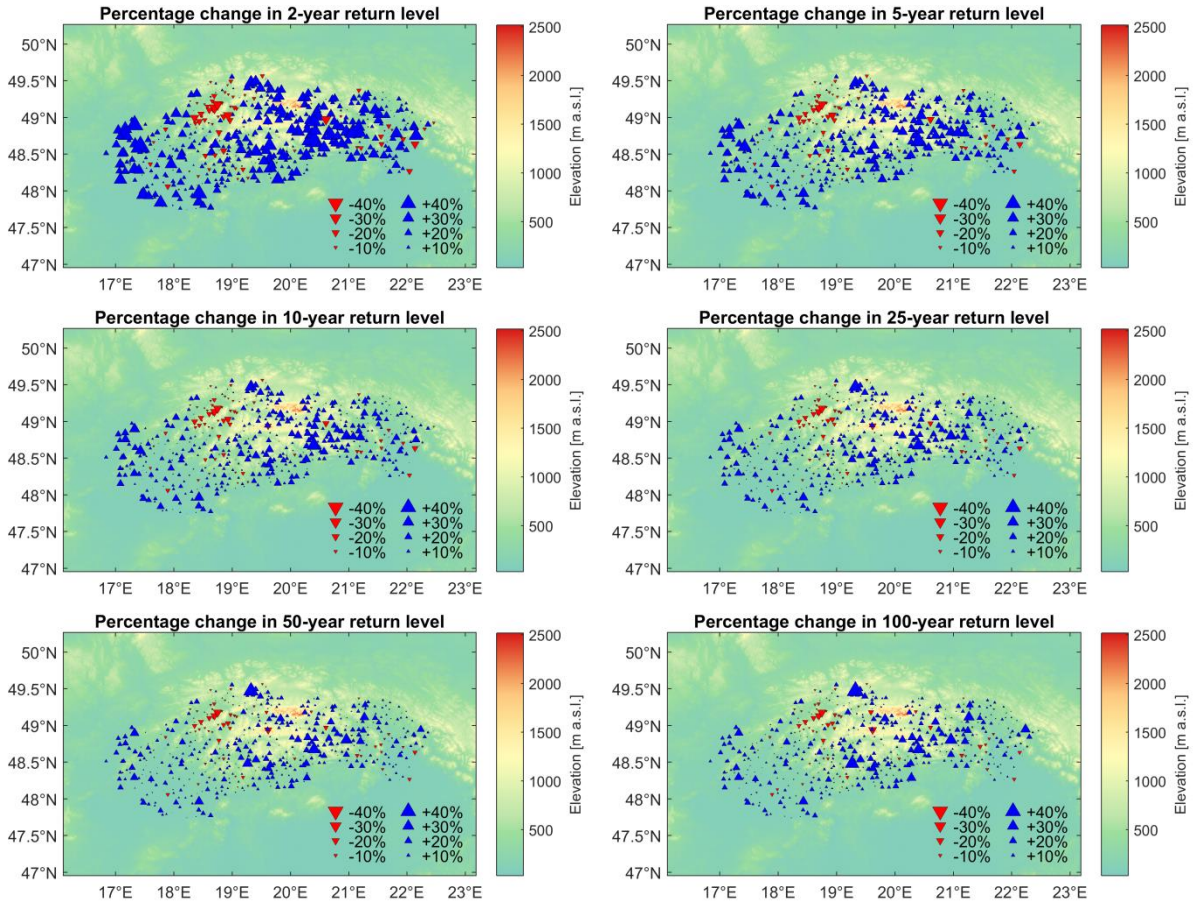

Fig. 6. Spatial distribution of the percentage changes in return levels. The percentage changes indicate the change between the stationary estimates (1981–2020) and the non-stationary estimates projected for the time horizon 2040.

Conclusions

The following conclusions can be drawn from this paper:

- Over the period 1981–2020, the average summertime near surface dew-point temperature in the investigated region increased by ~1.6°C
- Up to 60% of the investigated sites showed non-stationarity in rainfall annual maxima
- Changes in the projected return levels tend to increase with decreasing return periods
- By 2040, the 100-year return levels are likely to increase by ~6.64%
- The 2-year return levels might rise up to 13.39% by 2040

Acknowledgement

The research presented in this paper could not be accomplished without the following grants: „Scientific support of climate change adaptation in agriculture and mitigation of soil degradation (ITMS2014+ 313011W580), supported by the Integrated Infrastructure Operational Programme and funded by the ERDF; and the national VEGA grant No. 2/0003/21 "Complex analysis of the effects of rising air temperature on rainfall extremes in Slovakia".

References

AghaKouchak, A., Easterling, D., Hsu, K., Schubert, S., Sorooshian, S. (2013): Extremes in a Changing Climate: Detection, Analysis and Uncertainty. Dordrecht: Springer. ISBN 978-94-007-4479-0.

Agilan, V., Umamahesh, N. V. (2016): Is the covariate based non-stationary rainfall IDF curve capable of encompassing future rainfall changes? Journal of Hydrology, 541, 1441–1455. doi: 10.1016/j.hydrol. 2016.08.052

Agilan, V., Umamahesh, N. V. (2018): Covariate and parameter uncertainty in non-stationary rainfall IDF curve. Int J Climatol; Vol.. 38, 365–83. Online ISSN:1097-0088.

Alexander, L. V., Zhang, X., Peterson, T. C., Caesar, J., Gleason, B., et al. (2006): Global observed changes in daily climate extremes of temperature and rainfall. J Geophys Res, Vol. 111, p. D05109. ISSN: 2156-2202.

Ali, H., Mishra, V. (2017): Contrasting response of rainfall extremes to increase in surface air and dewpoint temperatures at urban locations in India. Sci Rep; Vol. 7, p. 1228. ISSN 2045-2322.

Ban, N., Schmidli, J., Schär, C. (2015): Heavy rainfall in a changing climate: Does short-term summer rainfall

increase faster? Geophys Res Lett, Vol. 42, 1165–72. ISSN 1944-8007.2015EDHIGHLIGHTS.

Bara, M., Kohnová, S., Gaál, L., Szolgay, J., Hlavčová, K. (2009): Estimation of IDF curves of extreme rainfall by simple scaling in Slovakia. Contrib to Geophys Geod; Vol. 39, 187–206. ISSN: 1338-0540.

Bedient, P., Huber, W., Vieux, B. (2008): Hydrology and Floodplain Analysis: International Edition. Pearson Education (US). ISBN10 0132422867

Berg, P., Moseley, C., Haerter, J. O. (2013): Strong increase in convective rainfall in response to higher temperatures. Nat Geosci, Vol. , 181–5. ISSN 1752-0908.

Bisselink, B., Dolman, A. J. (2008): Rainfall recycling: Moisture sources over Europe using ERA-40 Data. American Meteorological Society. doi: 10.1175/ 2008JHM962.1

Blenkinsop, S., Chan, C., Kendon, E. J., Roberts, N. M., Fowler, H. J. (2015): Temperature influences on intense UK hourly precipitation and dependency on large-scale circulation. Environ. Res. Lett., 10 (5), doi:Artn 05402110.1088/1748-9326/10/5/054021

Cheng, L., AghaKouchak, A., Gilleland, E., Katz, R. W. (2014): Non-stationary extreme value analysis in a changing climate. Clim Change Vol. 27, 353–69. ISSN: 0165-0009.

Cheng, L., AghaKouchak, A., (2015): Nonstationary Rainfall Intensity-Duration-Frequency Curves for Infrastructure Design in a Changing Climate. Sci Rep, Vol. 4, p. 7093 https://doi.org/10.1038/srep07093

Cooley, D. (2013): Return Periods and Return Levels Under Climate Change, Springer, Dordrecht. p. 97–114. ISBN: 978-94-007-4479-0.

Diffenbaugh, N. S., Giorgi, F. (2012): Climate change hotspots in the CMIP5 global climate model ensemble. Clim Change, Vol. 114, 813–22. ISSN: 0165-0009.

Faško, P., Lapin, M., Šťastný, P., Vivoda, J. (2000): Maximum daily sums of rainfall in Slovakia in the second half of the 20th century. Prace Geograficzne, Vol. 1008, 131–8. ISSN 1644-3586

Ganguli, P., Coulibaly, P. (2017): Does nonstationarity in rainfall require nonstationary intensity–duration–frequency curves? Hydrol. Earth Syst. Sci., 21, 6461–6483, doi: 10.5194/hess-21-6461-2017

Jones, R., Westra, S., Sharma, A. (2010): Observed relationships between extreme sub-daily precipitation, surface temperature, and relative humidity. Geophysical Research Letters. 37. 22805-. 10.1029/2010GL045081.

IPCC (2012): Managing the Risks of Extreme Events and Disasters to Advance ClimateChange Adaptation. A Special Report of Working Groups I and II of theIntergovernmental Panel on Climate Change [Field, C. B., V. Barros, T. F. Stocker,D. Qin, D. J. Dokken, K. L. Ebi, M. D. Mastrandrea, K. J. Mach, G.-K. Plattner, S. K. Allen, M. Tignor, and P. M. Midgley (eds.)]. Cambridge University Press, Cambridge, UK, and New York, NY, USA, p. 582. ISBN 978-1-107-02506-6 HardbackGanguli P., Coulibaly P., 2017. Does Nonstationarity in Rainfall Requires Nonstationary Intensity- Duration-Frequency Curves? Hydrol Earth Syst Sci, 1–31. ISSN 1027-5606.

Jakob, D. (2013): Nonstationarity in Extremes and Engineering Design. Extremes in a changing climate: Detection, Analysis and Uncertainty. Springer. Vol. 65, 363–417. ISBN: 978-94-007-4479-0.

Katz, R. W., Parlange, M. B., Naveau, P. (2002): Statistics of extremes in hydrology. Advances in Water Resources, Vol. 25, 1287–304. ISSN 0309-1708.

Keune, J., Miralles, D. G. (2019): A rainfall recycling network to assess freshwater vulnerability: Challenging the watershed convention. Water Resources Research, doi: 10.1029/2019WR025310

Kharin, V. V., Zwiers, F. W., Zhang, X., Hegerl, G. C. (2007): Changes in temperature and rainfall extremes in the IPCC ensemble of global coupled model simulations. Journal of Climate, Vol. 20, 1419–44. ISSN: 0894-8755.

Lakatos, M., Izsák, B., Szentes, O., Hoffmann, L., Kircsi, A., Bihari, Z. (2020): Return values of 60-minute extreme rainfall for Hungary. Quarterly Journal of the Hungarian Meteorological Service, 124 (2), 143–156. doi:10.28974/idojaras.2020.2.1

Lenderink, G., Barbero, R., Loriaux, J. M., Fowler, H. J. (2017): Super-Clausius–Clapeyron Scaling of Extreme Hourly Convective Rainfall and Its Relation to Large-Scale Atmospheric Conditions. Journal of Climate Vol. 30, 6037–52. (ISSN: 0894-8755.

Miao, C., Ashouri, H., Hsu, K. L., Sorooshian, S., Duan, Q., Miao, C., et al. (2015): Evaluation of the PERSIANN-CDR Daily Rainfall Estimates in Capturing the Behavior of Extreme Rainfall Events over China. Journal of Hydro-meteorology, Vol. 16, 1387–96. ISSN: 1525-755X.

O'Gorman, P. A. (2015): Rainfall Extremes Under Climate Change. Current Climate Change Reports, Vol.1, 49–59. ISSN: 2198-6061.

O'Gorman, P. A., Schneider, T. (2009): The physical basis for increases in rainfall extremes in simulations of 21st-century climate change. Proceedings of the National Academy of Sciences of the United States of America, Vol. 106, 14773–7. ISSN 1091-6490.

Onderka M, Markovič L., Nejedlik P., Pecho J. (2020): Are rainfall extremes becoming non-stationary due to global warming? A case-study from Slovakia. Meteorologické Zprávy, Vol. 73(5), 138-145. ISSN: 0026-1173.

Onderka, M., Pecho, J. (2021): Sensitivity of selected summertime rainfall characteristics to pre-event atmospheric and near-surface conditions. Atmospheric Research, 259, doi: 10.1016/j.atmosres.2021.105671

Parey, S., Hoang, T. T. H., Dacunha-Castelle, D. (2010): Different ways to compute temperature return levels in the climate change context. EnvironmetricsVol. 21, 698–718. ISSN: 1099095X.

Poschlod, B., Ludwig, R. (2021): Internal variability and temperature scaling of future sub-daily rainfall return levels over Europe. Environ.Res.Lett., 16, 064097, doi: 10.1088/1748-9326/ac0849

Ragno, E., AghaKouchaka, A., Cheng, L., Sadegh, M. (2019): A generalized framework for process-informed nonstationary extreme value analysis. Advances in Water Resources, 130, 270–282, doi: 10.1016/j.advwatres. 2019.06.007

Rootzén, H., Katz, R. W. (2013): Design Life Level: Quantifying risk in a changing climate. Water Resources Research, Vol. 49, 5964–72. 1944-7973. Rosbjerg D., Madsen H., 1998. Design with uncertain design values. In Hydrology in a Changing Environment, Volume III. Wiley, 155–163

Salas, J. D., Obeysekera, J. (2014): Revisiting the Concepts of Return Period and Risk for Nonstationary Hydrologic Extreme Events. Journal of Hydrological Engineering, Vol. 19, 554–68. ISSN: 1943-5584.

Sarhadi, A., Soulis, E. D. (2017): Time-varying extreme rainfall intensity-duration-frequency curves in a changing climate. Geophysical Research Letters. 2454–2463. ISSN: 1944-8007.

Schroeer, K., Kirchengast, G. (2018): Sensitivity of extreme rainfall to temperature: the variability of scaling factors from a regional to local perspective. Climate Dynamics, Vol. 50, 981–94. ISSN: 1432-0894.

Shaw, S. B., Royem, A. A., Riha, S. J., et al. (2011): The Relationship between Extreme Hourly Rainfall and Surface Temperature in Different Hydroclimatic Regions of the United States. Journal of Hydrometeorology, Vol. 12, 319–25. ISSN: 1525-755X.

Smith, B., Prentice, I. C., Sykes, M. T. (2001): Representation of vegetation dynamics in the modelling of terrestrial ecosystems: comparing two contrasting approaches within European climate space. Global Biology and Biogeography, Vol. 10, 621–37. ISSN: 1466-8238.

Vose, R. S, Easterling, D. R., Gleason, B. (2005): Maximum and minimum temperature trends for the globe: An update through 2004. Geophysical Research Letters, Vol. 32. ISSN: 1944-8007.

Wasko, C., Sharma, A. (2015): Steeper temporal distribution of rain intensity at higher temperatures within Australian storms. Nature Geoscience, Vol. 8, 527–9. ISSN: 1752- 0894.

Wasko, C., Sharma, A. (2017): Continuous rainfall generation for a warmer climate using observed temperature sensitivities. Journal of Hydrology, Vol. 544, 575–90. ISSN: 0022-1694.

Westra, S., Alexander, L., Zwiers, F. (2013): Global Increasing Trends in Annual Maximum Daily Precipitation. Journal of Climate. 26. 7834-. 10.1175/JCLI-D-12-00502.1.

Yan, L., Xiong, L., Jiang, C., Zhang, M., Wang ,D., Xu, C-Y. (2021): Upadating intensity-duration-frequency curves for urban infrastructure design under a changing environment. WIREs Water. doi: 10.1002/wat2.1519

Zhang, W., Villarini, G., Wehner, M. (2019): Contrasting the responses of extreme precipitation to changes in surface air and dew point temperatures. Climate Change 154, 257–271. doi:10.1007/s10584-019-02415-8

Mgr. Milan Onderka, PhD. (*corresponding author, e-mail: milan.onderka@savba.sk)
Earth Science Institute, SAS
Department of Atmospheric Physics,
Dúbravská cesta 9
814 38 Bratislava
Slovak Hydrometeorological Institute
Jeséniova 17
833 15 Bratislava
Slovak Republic

Mgr. Jozef Pecho
Slovak Hydrometeorological Institute
Jeséniova 17,
83315 Bratislava
Comenius University
Faculty of Mathematics, Physics, and Informatics
Mlynská dolina F1
842 48 Bratislava
Slovak Republic

DOI: 10.31577/ahs-2022-0023.01.0011

ACTA HYDROLOGICA SLOVACA

Volume 23, No. 1, 2022, 99 – 108

Impacts of excessive nutrients load in aquatic ecosystem

Viera KOVÁČOVÁ*

The mechanisms of water eutrophication are not fully understood, but excessive nutrient loading into surface water system is considered to be one of the major factors. This paper reviews nutrient inputs to surface water; the role of nutrients in the eutrophication of surface water; the response of biota to nutrient enrichment; monitoring of changes due to eutrophication and the management. The major influencing factors on water eutrophication include nutrient enrichment, hydrodynamics, environmental factors such as temperature, salinity, carbon dioxide, element balance, microbial and biodiversity. With regards of international and national legislative for the ecological status assessment ecological potential, chemical status, biological quality elements, supporting physical-chemical and hydro-morphological quality elements have been investigated. The aim of this paper is to analyse eutrophication and salinization problem, factors affecting this process, its consequences and possibilities of prevention. The partial aim is to evaluate eutrophication state of surface water in Žitný ostrov channel network following the assessment physical-chemical and microbiological indicators in monitored period.

KEY WORDS: surface water, eutrophication, nitrogen, phosphorus

Introduction

Eutrophication of a water body occurs when nutrients, specifically nitrogen and phosphorus, accumulate in the water column and bottom sediments. If eutrophication is accelerated through human activity it can become detrimental to ecosystem. High nutrient levels promote blooms of photosynthetic life, which will eventually die and become food for aerobic bacteria. The proliferation of bacteria that follows can lead to decreased dissolved oxygen levels and a consequential drop in biodiversity. This nutrient enrichment can lead to highly undesirable changes in ecosystem structure and function (Rathore et al., 2016). The nutrients of main concern are nitrogen (N) and phosphorus (P), and an oversupply of either nutrient can cause changes in the structure and function of aquatic ecosystems, although is probably the more important in surface water impacted by agriculture (Withers and Lord, 2002; Smith et al., 1999).

Water eutrophication has become a worldwide environmental problem in recent years. Understanding the mechanisms of water eutrophication will help for prevention and remediation of water eutrophication. In this paper, recent advances in current status and major mechanisms of water eutrophication, assessment and evaluation criteria, and the influencing factors were reviewed. Eutrophication as excessive plant growth resulting from nutrient enrichment (mainly nitrogen and phosphorus compounds) by human activity is the primary problem relating most surface waters today.

Ingrowth of water stream by vegetation is very often surface water problem, above all in lowland area. Presumption of its grow is mainly vegetation period. Water vegetation reduces flow profile of water streams, deforms velocity profile and by that affect too transport processes in the surface flow. Additionally, surroundings of water flow in the downland areas of offtentimes markedly agricultural managed with used manorial, what results in a nutrient concentrations of increasing of grow. Salinization is an increasing environmental problem in ecosystems. The assessment of total dissolved solids (TDS), pH, electrical conductivity (EC), exchangeable sodium percentage (ESP), alkalinity and the concentrations of main ions makes possible to identify salinization degree. The saltaffected groundwater occur in the south-east part of Žitný ostrov, where the dry and mild summer climate, evaporation soil water regime and mineralized groundwater create conditions for salinization of surface water. Five localities with highly-mineralized groundwater were monitored to evaluate salinity in the period 1989–2019. Evaporative residues (salt content) reached value 0.1–0.2%. In 2019 dry evaporative residues (salt content) was higher than 0.2%, EC was higher than 250 mS m^{-1}. The mentioned data allow us to state that salinization of soils and surface water is developing.

Eutrophication is the term applied to the observable effects of increased nutrients on an aquatic system.

If eutrophication is accelerated through human activity it can become detrimental to ecosystems. The limiting factors – namely concentrations of nitrogen (N) and phosphorus (P), temperature, pH, light, dissolved oxygen and CO_2 level - are known to affect eutrophic water bodies. The need to reduce anthropogenic nutrient inputs to aquatic ecosystems in order to protect drinking-water supplies and to reduce eutrophication. Developing the appropriate nutrient management strategy is very important. Nitrogen (N), needed for protein synthesis and phosphorus (P), needed for DNA, RNA, and energy transfer, are both required to support aquatic plant growth and are the key limiting nutrients in most aquatic ecosystems. (Conley et al., 2009). The external supplies of N and P to aquatic ecosystems are derived from a wide variety of sources, including groundwater, fluvial, and atmospheric inputs. The sum of these three sources can be termed the external load. As can be seen the external supplies of nutrients to a water body can originate both as point sources, which are localized and more easily monitored and controlled, and as nonpoint sources, which are diffuse and much more difficult to monitor and regulate. The relative contributions of these two types of sources can differ substantially from watershed to watershed, depending upon local human population densities and land use. N and P exports from point and nonpoint sources can have profound effects upon the quality of receiving waters (Conley, 1999; Smith et al., 1999).

Agriculture and urban activities are major sources of phosphorus and nitrogen to aquatic ecosystems. Atmospheric deposition further contributes as a source of N. These nonpoint inputs of nutrients are difficult to measure and regulate because they derive from activities dispersed over wide areas of land and are variable in time due to effects of weather. In aquatic ecosystems these nutrients cause diverse problems such as toxic algal blooms, loss of oxygen, loss of biodiversity. Nutrient enrichment seriously degrades aquatic ecosystems and impairs the use of water for drinking, industry, agriculture, recreation, and other purposes. (Fiala, 2016). Nitrogen (N), needed for protein synthesis, and phosphorus (P), needed for DNA, RNA, and energy transfer, are both required to support aquatic plant growth and are the key limiting nutrients in most aquatic and terrestrial ecosystems. Massive increases in fixed N additions to the biosphere, largely through the production of fertilizers and increases in fossil fuel emissions. P levels have also significantly increased because of fertilizer use, as well as from municipal and industrial wastewater. Most researchers have concluded that no single factor is responsible, but rather interactions between two or more factors control the rates. (Carpenter et al., 1998). Nitrogen has clearly been established as the nutrient limiting spring phytoplankton production; it is the sinking spring bloom that sends organic matter to bottom waters, which partly sustains hypoxia. The excess P in the water column leads to summer blooms of cyanobacteria, some of which are N_2 fixers that increase N concentrations in surface waters when they are abundant. P limitation, N limitation, and colimitation, and what nutrient is most limiting can change both seasonally and spatially. At the transition between fresh and saline water, P can often be the limiting nutrient during the spring, with N limitation commonly occurring during summer months. Algal production during summer is supported by rapidly recycled P within the water column or released from sediments. (Schneider and Melzer, 2003).

Lampman et al., (1999) developed a simple model that used point source N loading (sewage inputs) combined with fertilizer and NO. (inorganic oxides of N) They found that their model explained $N0_3^-$N export well, with about 20% of fertilizer plus NOy deposition inputs exported in rivers as $N0_3$ -N. These types of studies and improved understanding of nonpoint pollution are needed because human inputs of N and P are greatly increasing worldwide. Losses of nitrogen (N) and phosphorus (P) in land run-off and drainage from agricultural land can impair river water quality and may pose a potential health hazard. Losses of P are up to an order of magnitude smaller than those of N, but may be more significant with respect to freshwater eutrophication. At the field scale, research suggests that rates of nutrient loss are sensitive to both nutrient and land management, in particular, where nutrient inputs continuously exceed production requirements and where farming methods increase land vulnerability to run-off and erosion. A clear distinction can be made between N and P in the timescales over which inputs of these nutrients are buffered by terrestrial ecosystems against loss, which has implications for control strategies. (Harper, 1992; Nash et al., 2021).

At the river basin scale, any targets for reducing nutrient loss are best guided by site-specific information on their likely ecological impact, but this information rarely exists for rivers affected by eutrophication, and only general guidelines are available. True management of the environment requires integrated approaches which include both N and P taking account of differences in their source areas and delivery mechanisms, the vulnerability of land use and adoption of safe management options in relation to landscape characteristics and the sensitivity of the watercourse along its reach. For P, the identification of vulnerable zones represents a step forward to the management of the river basin in smaller definable units, which can provide a focus for safe management practices. This requires a better understanding of the linkages between nutrient sources, transport and impacts is considered an urgent research priority (Withers et al., 2002).

Based on our review, we are certain that (1) eutrophication is a widespread problem in rivers, lakes, estuaries, and coastal oceans, caused by over enrichment with P and N; (2) nonpoint pollution, a major source of P and N to surface waters, results primarily from agriculture and urban activity, including industry; (3) inputs of P and N to agriculture in the form of fertilizers exceed outputs (4) nutrient flows to aquatic ecosystems are directly related to animal stocking densities, and under high livestock densities, manure production exceeds the needs of crops to which the manure is applied; (5) excess fertilization and manure production cause a P surplus to accumulate in soil, some of which is transported to aquatic ecosystems; and (6) excess

fertilization and manure production on agricultural lands create surplus N, which is mobile in many soils and often leaches to downstream aquatic ecosystems, and which can also volatilize to the atmosphere, redepositing elsewhere and eventually reaching aquatic ecosystems (James et al., 2004; Meisinger and Delgado, 2002). If current practices continue, nonpoint pollution of surface waters is virtually certain to increase in the future. Such an outcome is not inevitable, however, because a number of technologies, land use practices, and conservation measures are capable of decreasing the flow of nonpoint P and N into surface waters.

From our review of the available scientific information, we are confident that: (1) nonpoint pollution of surface waters with P and N could be reduced by reducing surplus nutrient flows in agricultural systems and processes, reducing agricultural and urban runoff by diverse methods, and reducing N emissions from fossil fuel burning; and (2) eutrophication can be reversed by decreasing input rates of P and N to aquatic ecosystems, but rates of recovery are highly variable among water bodies. Often, the eutrophic state is persistent, and recovery is slow.

Excess nutrients cause eutrophication of freshwaters all over the world. Decision-support tools are needed to assess nutrient discharges from catchments. This paper used 28-year nutrient-discharge, hydroclimate and land-use history of small rural catchments to calibrate a simple nitrogen (N) and phosphorus (P) runoff model. (Pärn et al., 2012; Pärn et al., 2018). Nutrient pollution is a growing problem for water bodies. This nutrient enrichment, or eutrophication, can lead to highly undesirable changes in ecosystem structure and function. Water chemistry is of great importance to freshwater systems. It has an effect on species composition and can influence which species might have competitive advantages over others to become dominant. Therefore, the growth of phytoplankton populations is limited by their access to phosphorus and nitrogen for metabolic processes. On the other hand, if these nutrients are present in excess, populations can flourish (Khan and Ansari, 2005, Schneider and Melzer, 2003).

Mechanisms and assessment of water eutrophication investigated (Rathore et al., 2016; Yang et al., 2008). Water eutrophication has become a worldwide environmental problem in recent years, and understanding the mechanisms of water eutrophication will help for prevention and remediation of water eutrophication. Recent advances in current status and major mechanisms of water eutrophication, assessment and evaluation criteria, and the influencing factors were reviewed. The need to reduce anthropogenic nutrient inputs to aquatic ecosystems in order to protect drinking-water supplies and to reduce eutrophication (Pärn et al., 2012). Developing the appropriate nutrient management strategy is very important. Nitrogen (N), needed for protein synthesis and phosphorus (P), needed for DNA, RNA, and energy transfer, are both required to support aquatic plant growth and are the key limiting nutrients in most aquatic ecosystems. (Conley et al., 2009).

Massive increases in fixed N additions to the biosphere, largely through the production of biosphere, largely through the production of fertilizers and increases in fossil fuel emissions P levels have also significantly increased because of fertilizer use, as well as from municipal and industrial wastewater. The question of whether one or both nutrients should be controlled to reverse the detrimental effects of eutrophication. Most researchers have concluded that no single factor is responsible, but rather interactions between two or more factors control the rates (Devlin et al., 2011; Harper, 1992; Hessen, 1999; Gentry at al., 1998; Lampman, 1999). P is rapidly recycled between sediments and water. Ecosystems that have been heavily loaded with nutrients can display P limitation, N limitation, and colimitation, and what nutrient is most limiting can change both seasonally and spatially. At the transition between fresh and saline water, P can often be the limiting nutrient P is also often limiting during the spring, with N limitation commonly occurring during summer months (Conley, 1999).

Algal production during summer is supported by rapidly recycled P within the water column or released from sediments. Also, although much of the P in freshwater systems is not biologically available because it is adsorbed by clay and other particles, a considerable, fraction of the P desorbs as readily available, dissolved phosphate under saline conditions. Thus, as the summer progresses, available P increases as N declines and is not effectively compensated by N_2 fixation. The hypoxic conditions also result in injection of large amounts of P back into surface waters during deep winter mixing. Impact of vegetation on flow in a lowland stream during the growing season investigated (Velísková et al., 2017; Dulovičová et al., 2016; Schügerl et al., 2018). The purpose of these studies was to determine how aquatic vegetation influences flow resistance, water depth and discharge in the Komárňanský channel at the Žitný ostrov area. Eutrophication as excessive plant growth resulting from nutrient enrichment (mainly nitrogen and phosphorus compounds) by human activity is the primary problem concerning most surface waters today.

Non-point pollution of surface waters from N and P inputs is well established with agricultural and urban activities constituting the major sources. This has lead to wide-spread eutrophication of surface waters, causing degradation of aquatic ecosystems and problems such as toxic algal blooms, loss of oxygen, fish kills, and loss of biodiversity (David and Gentry, 2000). Non-point sources of N and P are difficult to measure and regulate because of the large land areas involved and extreme temporal variability due to weather. Recently, many efforts have been made to construct N and P balances for watersheds of various sizes in attempts to relate inputs to non-point contributions to surface waters (Carpenter et al., 1998; Maistone and Parr, 2002; Wang et al., 2001).

Much of this increase was estimated to be from fertilizer applications. In order to understand these sources and sinks, we have conducted studies linking N and P export to surface waters with agricultural activities both at the field (Gentry and David, 2000) and small watershed scale. Agricultural non-point sources are important contributors of N and P to surface waters. We determined

N and P net anthropogenic inputs for Žitný ostrov region, examining changes during the last 30 years and linkages to surface water export of N and P. Inputs (fertilizer, atmospheric deposition, and N_2 fixation) were compared to exports (grain export, after accounting for animal and human consumption, plus animal product export) from 1987 through 2019 using state-reported data on fertilizer sales, crop production, and human and animal populations. Large inputs of N were found about 1987, coinciding with increased N fertilizer applications. For P, a different pattern was found for state net anthropogenic inputs with a large input from 1987 to 1990.

Animal and human consumption therefore are currently a small part of N budget, due to the decreasing populations of animals and low human population compared with the amount of agricultural production in the state. These changes in inputs and outputs of N have led to large, but variable, net inputs of N and P each year. The net anthropogenic inputs were greatest during the 1980s. State P net anthropogenic inputs are not similar to N, suggesting that each fertilizer must be examined independently. Phosphorus fertilizer use did follow that of N, however, with large increases through the 1970s and 1980s. Nitrogen has clearly been established as the nutrient limiting spring phytoplankton production; it is the sinking spring bloom that sends organic matter to bottom waters, which partly sustains hypoxia. The excess P in the water column leads to summer blooms of cyanobacteria, some of which are N_2 fixers that increase N concentrations in surface waters when they are abundant. This new N helps to sustain the springtime production and eutrophication. Models suggest that, here, too, reductions in the inputs of both P and N are required for significant improvements in dissolved oxygen concentrations, transparency, and other water-quality conditions. It is prudent, and in most cases essential, to implement a dual–nutrient-reduction strategy when developing measures to control eutrophication (Vahtera, 2007; Wang et al., 2001).

The Žitný ostrov is one of the most productive agricultural areas of Slovakia, situated on the Danube Lowland. Under its surface is the richest water reservoir of Slovakia. For this reason, it is very important to deal with quantity and quality of water resources in this region. The channel network at the Žitný ostrov area was built up for drainage and also to provide irrigation water. There are three main channels of this network: Chotárny channel, Gabčíkovo-Topoľníky channel and Komárňanský channel (Fig.1).

The Žitný ostrov is one of the most productive agricultural areas of Slovakia, situated on the Danube Lowland, where is the richest drinking water reservoir of Slovakia. For this reason, it is very important to deal with quantity and quality of water resources in this region (Kobza and Gáborík, 2008; Western, 2001; Khan and Ansari, 2005). The channel network at the Žitný ostrov area was built up for drainage and also to provide irrigation water. There are three main channels of this network: Chotárny channel – is the P1M water body type (partial river-basin Váh, code SKW0029), Gabčíkovo-Topoľníky channel – is the P1M water body type (partial river-basin Váh, code SKW0023), Komárňanský channel – is the P1M water body type (partial river-basin Váh, code SKV0226).

Fig. 1. Žitný ostrov region – channel network (Chotárny channel, profile Ňárad – 1, channel Gabčíkovo-Topoľníky, profile Vrakúň – 2, Komárňanský channel, profile Okoličná na Ostrove – 3).

Material and methods

Factors influencing water eutrophication

Water eutrophication is mainly caused by excessive loading of nutrients into water bodies like N and P. Excessive nutrients come from both point pollution such as waste water from industry and municipal sewage, and non-point pollution like irrigation water, surface run water containing fertilizer from farmland, etc. Increased nutrient load to water body is now recognized as a major threat of water quality degradation (Yang et al., 2008).
Excessive total nitrogen (TN) and total phosphorus (TP) in water was considered as the only factors inducing water eutrophication. At present nutrient enrichment is only the necessary but not the sufficient condition for algal boom. Eutrophication is not likely to occur if both TN and TP in water are low, but eutrophication may not occur in water high in TN and TP if other conditions such as temperature and current speed are not favorable. The influencing factors of water eutrophication include: (1) excessive TN and TP, (2) slow current velocity, (3) adequate temperature and favorable other environmental factors, and (4) microbial activity and biodiversity.

(1) Nutrient enrichment
(2) Hydrodynamics
(3) Environmental factors
(4) Microbial and biodiversity

(1) The relationship of nutrient enrichment to water eutrophication and algal bloom: (a) When P concentration in water is low, it may be the limiting factor for inducing water eutrophication and algal bloom; (b) When P concentration in water increases rapidly, other may become a new limiting factor, such as pH, water depth, temperature, light, wave, wind or other biological factors. N and P input and enrichment in water are the most primary factors to induce water eutrophication.
(2) Hydrodynamics is not related to disturbing water itself but is influenced indirectly by changing light and nutrient status. In shallow water, increased frequency of disturbance could increased the P release from the sediment, especially at high temperature.
(3) Temperature and salinity are the two important factors to induce alga bloom. Alga bloom always occurs at temperature between 23°C and 28°C, salinity between 25% and 30%. The variation of temperature and salinity also affect algal bloom, and an important condition for algal bloom is that temperature increases and salinity decreases faster than ever in short time. Statistical analysis shows that the influence of temperature on algal growth rate is the largest, followed by salinity and their interaction. Change of salinity is also influenced by the concentration of nutrition. Research shows that salinity is negatively related with $N\text{-}NO_3^-$ and $P\text{-}PO_4^{3-}$, but positively related with $N\text{-}NH_4^+$ and however, it is not very related with $N\text{-}NO_2^-$.
(4) Light plays an important role in the growth, diversity and density of aquatic flora. Algal growth has been reported to increase with light intensity, and luminescence of 4000 lux was found most favorable. There are other factors like pH and dissolved oxygen affecting water eutrophication. The direct relationship between phytoplankton and dissolved oxygen content has been observed by a number of researchers. The change in pH is directly related to the availability and absorption of nutrients from solution. Ionization of electrolytes or the valence numbers of different ion species are influenced by changes in pH. High pH values promote the growth of phytoplankton and result in bloom.

Assessment of surface water quality

Historically are important year 1991, when was passed Directive 91/271/EHS regard cleaning urban waste-water and Directive 91/676 EHS regard nitrate agricultural source pollution and year 2000, when was passed Water Framework Directive (WFD) 2000/60/ES. The ecological status, ecological potential and chemical status assessment the biological quality elements (phytoplankton, phytobenthos and water macrophytes, benthic invertebrates), supporting physical-chemical and hydromorphological quality elements as well as the specific substances have been investigated. Ecological status/potential assessment has been type specific, it has reflected reference conditions, the species diversity, quantity (abundance or biomass) and sensitive species have been included as well. The classification schemes have been already harmonized in the process of European intercalibration.
Makovinská et al. (2015) and Hucko et al. (2013) proposed assessment of the trophic state of water bodies according to following methodics:

a) Assessment of the trophic state of surface water with regards of the Supplement No.1 Directive of Government SR No. 269/2010 – monitored indicators are: total nitrogen, total phosphorus, ammonia nitrogen, nitrite nitrogen, nitrate nitrogen concentrations and phytoplankton biomass (chlorophyll-a) (Table 1).
b) The trophic assessment of surface water trophic state is necessary to use average summer concentrations of nitrates, phosphates and total phosphorus and maximum summer concentration for chlorophyll-a (summer period means months april–september) (Table 2).
c) Assessment of the trophic state of backwaters with regards of OECD methodic (annual average of total phosphorus and nitrogen concentrations, chlorophyll-a concentrations.

Monitoring of surface water in Žitný ostrov channel network has been provided in terms of requirements Supplement No.1 Directive of Government SR No. 269/2010, Part A (general indicators) and Part E (hydrogeological and microbiological indicators) in the period of 1987–2019. For assessment of sensitive sites and identification of eutrophication endangered places the Supplement No. 12 and No. 13 are used. Monitoring and assessment of following indicators were performed – total nitrogen (N_{TOT}), nitrate nitrogen ($N\text{-}NO_3^-$), nitrite nitrogen ($N\text{-}NO_2^-$), ammonia nitrogen

Table 1. Evaluation of trophic state of surface water according to Supplement No.1 Directive of Government SR No. 269/2010

Indicator	Symbol	Unit	Limit value
Ammonia nitrogen	$N\text{-}NH_4^+$	mg l^{-1}	1
Nitrite nitrogen	$N\text{-}NO_2^-$	mg l^{-1}	0.02
Nitrate nitrogen	$N\text{-}NO_3^-$	mg l^{-1}	5
Nitrogen total	N_{TOT}	mg l^{-1}	9
Phosphorus total	P_{TOT}	mg l^{-1}	0.4
Phytoplankton biomass (chlorophyll-a)	CHL_a	μg l^{-1}	50

Table 2. Evaluation of trophic state– Directive 91/676/CEE – Surface water – rivers

Indicator	Unit	State				
		I Ultraoligotrophic	II Oligotrophic	III Mezotrophic	IV Eutrophic	V Hypereutrophic
Nitrates (average summer concentration)	mg l^{-1}	< 2	< 10	< 25	< 50	> 50
Phosphates (average summer concentration)	mg l^{-1}	< 0.1	< 0.5	< 1	< 2	> 2
Phosphorus tot. (average summer concentration)	mg l^{-1}	< 0.05	< 0.2	< 0.5	< 1	> 1
Chlorophyll-a (max.summer conc.)	μg l^{-1}	< 2.5	< 8	< 25	< 75	> 75

($N\text{-}NH_4^+$), total phosphorus (P_{TOT}), phosphate phosphorus ($P\text{-}PO_4^{3-}$) according the Supplement No.1 Directive of Government SR No. 269/2010, Part A and biomass of phytoplankton (CHL_a) according Part E.

The external supplies of N and P to aquatic ecosystems are derived from a wide variety of sources, including groundwater, fluvial, and atmospheric inputs. The sum of these three sources can be termed the external load. The external supplies of nutrients to a water body can originate both as point sources, which are localized and more easily monitored and controlled, and as nonpoint sources, which are diffuse and much more difficult to monitor and regulate. The assessment of water eutrophication has been advanced from simple individual parameters like total phosphorus, total nitrogen, etc., to comprehensive indexes like total nutrient status index. The major influencing factors on water eutrophication include nutrient enrichment, hydrodynamics, environmental factors such as temperature, salinity, carbon dioxide, element balance, microbial and biodiversity. The occurrence of water eutrophication is a complex function of all the possible influencing factors (Yang et al., 2008).

Generally, the physical and chemical evaluation parameters were used to assess water eutrophication, mainly nutrient concentration (N and P), algal chlorophyll, water transparency and dissolved oxygen. Although there are many different assessment parameters, the concentrations of total nitrogen and phosphorus are the two basic ones. (Cheng and Li, 2006) used total nutrient status index (TNI) to assess eutrophication status of surface water. The calculation of total nutrient status index is as follows:

$$TNI = \sum W_j TNI_j,\ W_j = r_{ij}^2 / \sum r_{ij}^2 \quad (1)$$

where

TNI is the sum of indexes of all nutrient parameters,
TNI_j is the TNI of *j* parameter,
W_j is the proportion of *j* parameter in the TNI,
r_{ij} is the relation of chlorophyll a (Chla) to other parameters.

The available parameters concerned include total nitrogen (TN), total phosphorus (TP), Chla, dissolved oxygen (DO), chemical oxygen demand by K_2MnO_4 oxidation method (COD_{Mn}), biological oxygen demand (BOD_5), etc., and TN, TP and Chla are selected for calculating the TNI (Cheng and Li, 2006; Yang et al., 2008). Table 1, 2 shows the limiting values of TN, TP and TNI in various eutrophicated water.

Results and discussion

The results of nitrogen and phosphorus amounts reported in this study are the best indicators of the level of eutrophication. The major influencing factors on water eutrophication include nutrient enrichment, hydrodynamics, environmental factors such as

temperature, salinity, carbon dioxide, element balance, microbial and biodiversity.

This paper investigated surface water to determine their trophic status, measured by water chemistry and biological indicators and briefly review the process, the impacts, and the potential management of eutrophication in freshwater, ecosystems. The limiting factors – namely concentrations of nitrogen (N) and phosphorus (P), temperature, pH, light, dissolved oxygen and CO_2 level - are known to affect eutrophic water bodies. The results of nitrogen and phosphorus amounts reported in this paper are the best indicators of the level of eutrophication (Pavlidou et al., 2015; Nedwell et al., 2001; Newman et al., 2005; Smith et al., 1999; Rathore et al., 2016).

The present paper evaluated the ecological consequences of increased nutrient loading to freshwaters in the context of providing information on the effects of implementing international and national legislative for the ecological status assessment. The limiting factors – namely concentrations of nitrogen (N) and phosphorus (P), temperature, pH, light, dissolved oxygen and CO_2 level - are known to affect eutrophic water bodies. The results of nitrogen and phosphorus amounts reported in this study are the best indicators of the level of eutrophication (Cheng and Li, 2016; James et al., 2004; Jickells, 2005).

The net anthropogenic inputs were greatest during the 1980s. State P net anthropogenic inputs are not similar to N, suggesting that each fertilizer must be examined independently. Phosphorus fertilizer use did follow that of N, however, with large increases through the 1970s and 1980s. The nutrient level in surface water has decreased after 1990th in response to decreased discharge of domestic wastes and non-point pollution from agricultural practices and urban development. However we observe slight increasing in Komárňanský channel during last 5 years. We observed exceeded the limit values not only in some months, but average annual values for nitrates and phosphates, too. For the evaluation the water quality we used the data obtained on Institute of Hydrology SAS during the 1987–2019. Monitored localities was chosen so that they be the most representative area-covering (Fig. 2, 3).

The study was focused on identification of the long-term trends in the surface water quality on Žitný ostrov channel network. Fig. 2, 3 shown changes in measured values of nitrates and phosphates in particular channels in years 1987–2019. It was shown the channel water quality has been changed significantly during the period 1987–1990, after 1990 was slightly decreased. However we observe slight increasing in some profiles of Komárňanský channel with major agricultural activities during last few years. Regarding the eutrophication, the WFD intends to improve the ecological status, including eutrophication status, of all European surface waters of which many are considered to be eutrophic (Jickells, 2005). The present work focus on the assessment of the eutrophication state of surface water in Žitný ostrov region. The values from monitoring in 1987–2019 were evaluated according to Supplement No.1 Directive of Government SR No. 269/2010, part A (general indicators) and part E (hydrogeological and microbiological indicators). In terms of N, nitrate-N concentrations is the limit value 5 mg l^{-1} $N\text{-}NO_3^-$. Nitrite-N concentrations is the limit value 0.02 mg l^{-1} $N\text{-}NO_2^-$. For phosphorus is the limit value 0.4 mg l^{-1} P_{TOT}. In general, the rate of increase the external supplies of N and P has slowed down in Žitný ostrov area during the monitoring period, but slight increasing in some profiles of Komárňanský channel with major agricultural activities during last few years. The limiting factors – namely concentrations, temperature, pH, light, dissolved oxygen and CO_2 level – are known to affect eutrophic water bodies. The results of nitrogen and phosphorus amounts reported in this study are the best indicators of the level of eutrophication (Table. 3).

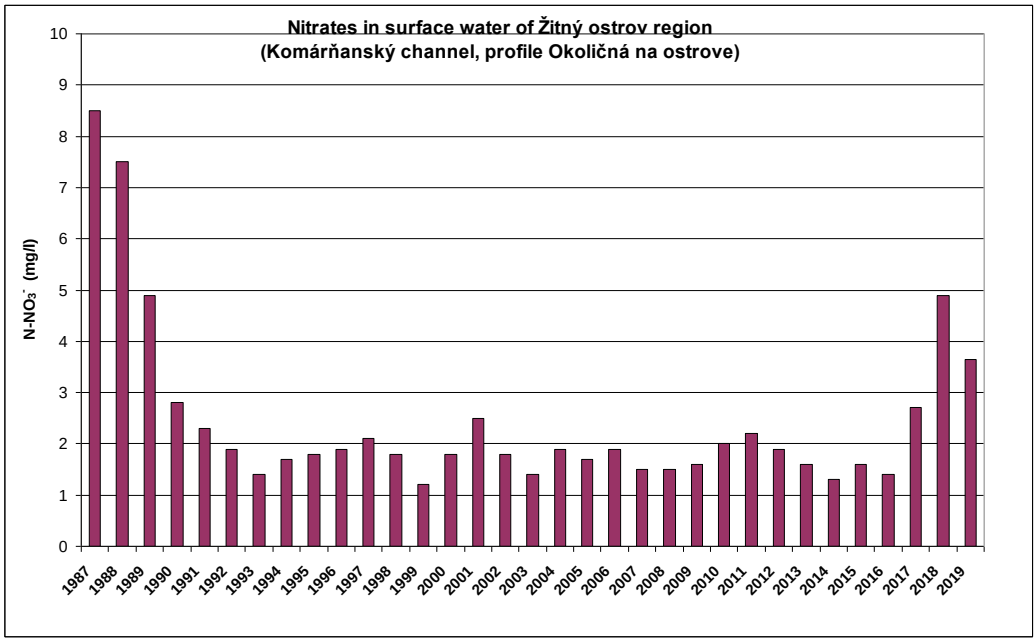

Fig. 2. Nitrates in surface water – Komárňanský channel.

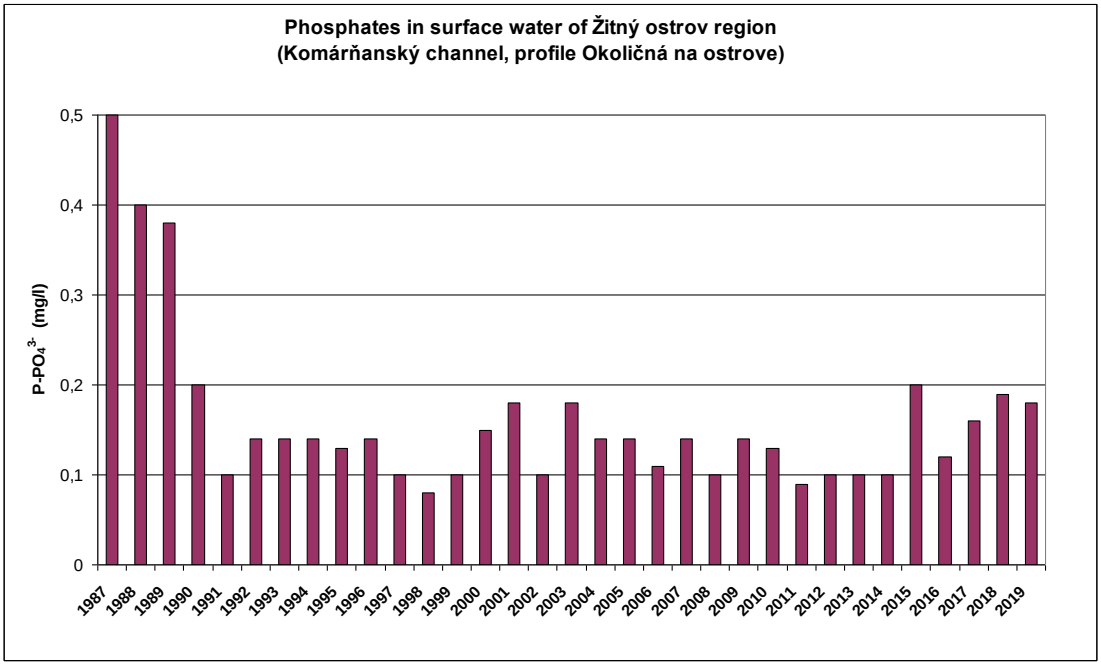

Fig. 3. Phosphates in surface water – Komárňanský channel.

Table 3. Evaluation of trophic state of surface water according to Supplement No. 1 Directive of Government SR No. 269/2010

Place of sampling point: Komárňanský channel Profile: Okoličná na Ostrove			Typ VÚ: P1M Code VÚ: SKV0226				Partial whatershed Váh Monitoring: 2019	
Part A – general water quality indicator								
Term of indikator	Symbol	Unit	Number statements	Min.	Max.	Average	P90/10	Value according to NV 269/2010	Meet/Does not meet
Dissolved oxygen	O_2	mg l^{-1}	12	8.4	14.0	10.8	8.5	> 6.0	M
Temperature	t	ºC	12	3	21.6	11.4	20.3	< 27	M
Chemical consump. oxygen	CHSKCr	mg l^{-1}	12	5.0	18.0	7.7	10.8	< 25	M
Reaction	pH	-	12	6.39	8.19	7.93	8.16	8.5	M
Conductivity	EC	µS cm^{-1}	12	349	543	420	50.1	≤ 700	M
Specific conductivity	SPC	µS cm^{-1}	12	370	933	548	62.2	700	M
Total dissolved solids	TDS	mg l^{-1}	12	284	630	405	0.19	800	M
Ammonia nitrogen	N-NH4	mg l^{-1}	12	0.05	0.9	0.34	0.16	1	M
Nitrate nitrogen	N-NO3	mg l^{-1}	12	2.7	5.2	3.68	3.61	5	N
Total nitrogen	Ntot	mg.l^{-1}	12	2.2	9.4	7.23	3.17	9	N
Phosphate phosphorus	P-PO4	mg l^{-1}	12	0.17	0.42	0.30	0.32	0.35	N
Total phosphorus	Ptot	mg l^{-1}	12	0.18	0.43	0.35	0.38	0.4	N
Turbidity	T	NTU	12	14	64	42	38	100	M

The nutrient level in surface water has decreased after 1990th in response to decreased discharge of domestic wastes and non-point pollution from agricultural practices and urban development However we observe slight increasing in Komárňanský channel (Fig. 2, 3) during last few years.

The study is focused on identification of the long-term trends in the surface water quality in channel network at Žitný ostrov region. The paper shows changes in measured values of nitrates and phosphates in particular channels in years 1987–2019. It was shown the channel water quality has been changed significantly during the period 1987–1990, after 1990 obtain around the same level. But we observe increasing in some profiles of Komárňanský channel with major agricultural activities during last few years. Approach to limit value – nitrate nitrogen 5 mg l^{-1}, nitrogen total 9 mg l^{-1}, phosphate phosphorus 0.35 mg l^{-1}, phosphorus total 0.4 mg l^{-1}.

Conclusion

The present paper deals with the studies conducted on the impact of nitrogen and phosphorus amount on eutrophication in surface water on the Žitný ostrov channel network. The review covers the definition and concept of eutrophication and the adverse effects on quality and ecosystem functioning. The eutrophication of several water bodies leads to significant changes in the structure and function of the aquatic ecosystem. Some profiles in this region have recently been found to be eutrophic.

The limiting factors – namely concentrations of nitrogen (N) and phosphorus (P), temperature, pH, light, dissolved oxygen and CO_2 level - are known to affect eutrophic water bodies. The results of nitrogen and phosphorus amounts reported in this study are the best indicators of the level of eutrophication. In terms of N, nitrate-N concentrations has the limit value 5 mg l^{-1}, $N\text{-}NO_3$. $N\text{-}N_2$ concentrations has the limit value 0.02 mg l^{-1} $N\text{-}NO_2$. For phosphorus has the limit value 0.4 mg l^{-1}, Ptot. (Table 3). The paper shows changes in measured values of nitrates and phosphates in particular channels during 1987–2019. It was shown (Fig. 2,3) the channel water quality has been changed significantly during the period 1987–1990, after 1990 it reaches about the same level, but we observe increasing in some profiles of Komárňanský channel with major agricultural activities.

Acknowledgement

This paper was supported by project VEGA 2/0025/19 and project VEGA 1/0085/20.

References

Carpenter, S. R. N., Caraco, N. F. D., Correll, L. R. W., Howarth, A. N., Sharpley, V., Smith, H. (1998): Nonpoint Pollution of Surface waters whit Phosphorus and Nitrogen, Ecological Applications, 559–568.

Conley, D. J., Paerl, H. M., Howarth, R. V., Boesch, D. F., Seitzinger, S. P., Havens, K. E., Lancelot, Ch. (2009): Controlling Eutrophication: Nitrogen and Phosphorus, Science, Vol. 323, 1014–1017.

Conley, D. J. (1999): Hydrobiologia, 410, 87.

David, M. B., Gentry, L. E. (2000): Anthropogenic Inputs of Nitrogen and Phosphorus and Riverine Export for Illinois, USA. J. of Environmental Quality, Vol. 29, no. 2, 494 – 508.

Devlin, M., Bricker, S., Painting, S. (2011): Comparison of five methods for assessing impacts of nutrient enrichment using estuarine case studies. Biogeochemistry 106,177–205.

Directive of Government SR No. 269/2010 Z.z. for accomplish suitable state of water. Governmmet of Slovak republic 25 May 2010, Part 106/2010, validity of directive 15.06.2010.

Directive 91/271/EEC (European directive) regarding cleaning urban waste-water. The European Economic Community, validity of directive from 29 May 1991.

Directive 91/676 EEC (European directive) regarding nitrate agricultural source pollution (preventing nitrates from agricultural sources polluting ground and surface waters and by promoting the use of good farming practices), The Council of the European Comunities of 12 December 1991 No.1/375/1

Directive (WFD) 2000/60/EC (European directive) of the European Parliament and of the Council establishing a framework for Community action in the field of water policy. OJ L327, 22.12.2000. Water Framework Directive

Dulovičová, R., Velísková, Y., Schügerl, R. (2016): Modification of Silts Hydraulic Conductivity along the Lowland Channel Gabčíkovo-Topoľníky (Slovakia). Multidisciplinary Scientific GeoConference SGEM – Conference proceedings. Book 3, vol. 1. Hydrology and Water Resources. – Sofia 521–528. ISBN 978-619-7105-61-2.

Fiala, D. (2016): Boj o fosfor, aneb pracují všichni vodohospodáři na plný výkon? Vodní hospodářství, 5, 2016.

Gentry, L. E., David, M. B., Kovacic, D., Xue, Y. (1998): Kinetics and Modeling of Dissolved Phosphorus Export from a Tile-Drained Agricultural Watershed. Journal of Enviromental Quality, Agriculture, Ecosystems and Environment 68 1998 85–97

Gentry, L. E., David, M. B (2000): Anthropogenic Inputs of Nitrogen and Phosphorus and Riverine Export for Illinois, USA. J. of Environmental Quality, Vol. 29, no. 2, 494–508.

Harper, D. (1992): Eutrophication of Freshwaters: Principles, problems and restoration. Chapman and Hall 1992, ISBN 978-94-011-3082-0, https://doi.org/10.1007/978-94-011-3082-0

Hessen, D. O. (1999): Catchment properties and the transport of major elements. In: Nedwell, D. B., Raffaelli, D. G. (Eds.), Estuaries. Adv. Ecol. Res. vol. 29, 1–41.

Hucko, P., Štetina, M., Luther, S. (2013): Národný prístup hodnotenia povrchových vôd v SR. Vodárenská biologie, Praha.

Cheng, X. Y., Li, S. J., (2006): An analysis on the evolvement processes of lake eutrophication and their characteristics of the typical lakes in the middle and lower reaches of Yangtze River. Chinese Science Bulletin, 51(13): 1603–1613. [doi:10.1007/s11434-006-2005-4]

James, C. S., Birkhead, A. L., Jordanova, A. A., O'Sullivan, J. J. (2004): Flow resistance of emergent vegetation. J. Hydraul. Biologia 72/8, 840–846.

Jickells, T. (2005): External inputs as a contributor to eutrophication problems. J. Sea Res.54, 58–69.

Khan, F. A., Ansari, A. A., (2005): Eutrophication: An ecological vision. The Botanical Review, 71(4):449–482.

Kobza, J., Gáborík, Š. (2008): Súčasný stav a vývoj obsahu makro- a mikroelementov v poľnohospodárskych pôdach Slovenska. VÚPOP Bratislava, 57 s

Lampman, G. G., Caraco, N. F., Cole, J. J. (1999): Spatial and Temporal Patterns of Nutrient Concentration and Export in the Tidal Hudson River. Estuaries Vol. 22, No. 2, 285–296.

Mainstone, C. P., Parr, W., (2002): Phosphorus in rivers-ecology and management. The Science of the Total Environment, 282–283.

Meisinger, J. J., Delgado, J. A. (2002): "Principles for managing nitrogen leaching." Journal of Soil and Water Conservation, vol. 57, no. 6, 2002, p. 485

Makovinská, J., Velická, Z., Hlúbiková, D., Baláži, P., Tóthová, L. (2015): Metodika monitorovania a hodnotenia vodných útvarov povrchových vôd Slovenska. VÚVH, 179 s., ISBN 978–80-89740–02–4.

Nash, D. M., Wheatherley, A. J., Kleinman, P. J. Sharplay, A. N. (2021): Estimating dissolved phosphorus losses from legacy sources in pastures: The limits of soil tests and small-scale rainfall simulators. J. Environ. Qual. 2021; 50:1042–1062.

Nedwell, D. B., Dong, L. F., Sage, A., Underwood, G. J. C. (2001): Variations of the nutrient loads to the mainland UK estuaries: correlations with catchment areas, urbanisation and coastal eutrophication. Est. Coast. Shelf Sci. 56, 951–970.

Newman, J. R., Anderson, N. J., Bennion, H., Bowes, M. J., Luckes, S., Winder, J. (2005): Eutrophication in rivers: an ecological perspective. Centre for Ecology and Hydrology, 37 pp., DOI: 10.13140/2.1.3711.5208

Pavlidou, A., Simboura N., Rousselaki E., Tsapakis M., Pagou, K., Drakopoulou, P., Assimakopoulou, G., Kontoyiannis H., Panayotidis P. (2015): Methods of eutrophication assessment in the context of the water framework directive: Examples from the Eastern Mediterranean coastal areas. Continental Shelf Research, 108, 156–168.

Pärn, J., Pinay, G., Mander, Ű. (2012): Indicators of nutrients transport from agricultural catchments under temperature climate: A review. Ecological Indicators, 22 (2012), 4–15.

Pärn, J., Henided, H., Kasaka, K., Kauere, K., Sohara, K., Tournebozed, J, Uema, E., Välik, K., Mander, U. (2018): Nitrogen and phosphorus discharge from small agricultural catchments predicted from land use and hydroclimate. Land Use Policy, 75, 260–268.

Rathore, S. S., Chandravanshi, P., Jaiswal, K. (2016): Eutrophication: Impacts of Excess Nutrients Inpucts on Aquatic Ecosystem, Journal of Agriculture and Veterinary Science, Vol. 9, 89–96.

Schneider, S., Melzer, A. (2003): The Trophic Index of Macrophytes (TIM) - a new tool for indicating the trophic state of running waters. Hydrobiology, vol. 88, 1 , 49–67, doi.org/10.1002/iroh.200390005

Schügerl, R., Velísková, Y., Dulovičová, R. (2018): Identifikácia zmien prietokových pomerov a rýchlostného profilu pri prúdení s voľnou hladinou. Hydrologický výskum v podmienkach prebiehajúcej klimatickej zmeny. Monografia ÚH SAV. Veda, Bratislava, 391 s.

Smith, V. H., Tilman, G. D., Nekola, J. C. (1999): Eutrophication: impacts of excess nutrient inputs on freshwater, marine, and terrestrial ecosystems. Environmental Pollution, 100, 179–196.

Velísková, Y., Dulovičová, R., Schügerl, R. (2017): Impact of vegetation on flow in a lowland stream during the growing season. Biologia 72/8, 840–846, DOI: 10.1515/biolog-2017-0095.

Vahtera E. Daniel J. Conley B.G. Gustafsson H.K. Tamminen,T. Voss M. Wulfi F. (2007) : Internal Ecosystem Feedbacks enhance Nitrogen-fixing Cyanobacteria Blooms and Complicate Management in the Baltic Sea.. AMBIO: A Journal of the Human Environment, 36(2):186-194.

Wang, J., Fu, B., Qiu, Y., Chen, L. (2001): Soil nutrients in relation to land use and landscape position in the semi-arid small catchment on the loess plateau in China. Journal of Arid Environments, 48, 537–550.

Western, D. (2001): Human-modified ecosystems and future evolution. Proceedings of the National Academy of Sciences of the United States of America, 98(10):5458–5465. [doi:10.1073/pnas.101093598]

Withers , P. J. A., Lord, E. I. (2002): Agricurtural nutrien inputs to rivers and groundwaters in the UK: policy, environmental management and research needs. The Science of the Total Environment 282–283.

Yang, X., Wu, X., Hao, H., He, Z. (2008): Mechanisms and assessment of water eutrophication. J. of Zhejjang Univ. Sci., 9 (3), 197–209.

Ing. Viera Kováčová (*corresponding author, e-mail: kovacova@uh.savba.sk)
Institute of Hydrology SAS
Dúbravská cesta 9
84104 Bratislava
Slovak Republic

DOI: 10.31577/ahs-2022-0023.01.0012

ACTA HYDROLOGICA SLOVACA

Volume 23, No. 1, 2022, 109 – 116

Hydrochemical regime and water quality of the Danubian lake Katlabukh

Valeriya OVCHARUK*, Natalia KICHUK, Dmytro LUTAI, Liliia KUSHCHENKO, Maria MYROSHNYCHENKO

One of the main sources of water supply in the Ukrainian part of the Danube delta is the Danube lakes, one of which is Katlabukh. The main revenue part in the water balance of the adjacent delta Lake Katlabukh is the inflow of Danube water through canals with offtakes. The water levels in the lake are determined with the rules of the use of the reservoir, as well as with the hydrological regime of the Danube. Water exchange is carried out by off takes Hromadsky and Zhelyavsky. The reduction of water exchange processes with the Danube in combination with anthropogenic impact on the catchment area of small rivers flowing into Lake Katlabukh, as well as the negative phenomena associated with climate change; create many environmental, water, and social problems for the lake. One of the main problems is the unsatisfactory state of water quality in terms of hydrochemical parameters, in particular high mineralization, which limits the use of the lake water for water supply. The permanents monitoring and analysis of the hydrochemical state of the lake waters will allow to development of scientifically based recommendations for improving water quality and rational use.

KEY WORDS: hydrochemical regime, pollution, lakes of the Danube delta

Introduction

The Danube lakes existed mainly due to the hydrology of the Danube. At the same time, their geographical location along the banks of the Danube had little effect on their historically established hydrochemical regime (Gopchenko et al, 2011; Romanova et al, 2019). With the intensification of agriculture in the 1970s, the additional use of the floodplains of the Danube began, and to protect them, embankment dams were built along the Danube, which radically changed the hydrological and historical water regime of the Danube lakes. It is for this reason that the geographical location of Lake Katlabukh relative to other upstream lakes has created the conditions under which it has become hostage to the level regime of the Danube. Therefore, in recent decades, the filling of Lake Katlabukh in terms of its damping without forced water supply has significantly affected the deterioration of both the level regime of the lake and its hydrochemical condition. It is the reduction of water exchange processes with the Danube in combination with an anthropogenic load on the catchment area of small rivers flowing into lake Katlabukh, as well as the negative phenomena associated with climate change, create many environmental, water, and social problems for the lake. The hydrochemical state of the lake water has deteriorated, and water salinity has increased 4–5 times, i.e. from 800 mg dm^{-3} to 4.7 g dm^{-3}. Therefore, it is necessary to analyze carefully the hydrological and hydrochemical regime of the lake and the rivers flowing into it, to develop both scientific recommendations and operational measures to improve the condition of Lake Katlabukh and optimal conditions for its operation following the Water Framework Directive 2000/60 / EU (Directive 2000/60/EC, 2000).

Material and methods

According to physical and geographical zoning, the studied area is located in the steppe zone of Ukraine. Heights vary from north and northwest from 300 m to 0.0 m and – 2.0 m – in the Danube floodplain.

Lake Katlabukh is located 10 km northeast of the city of Izmail. It has an area of 68 km^2, the average width is 2 km, and the maximum width reaches 6 km (Fig. 1).

The shores are steep with the exposure of native rocks. In the south they are waterlogged and merge with the floodplains. The studied lake belongs to the western group of Danube reservoirs located on the left bank of the Danube, and is a continuation of the valleys of the rivers Big and Small Katlabukh, Enika, Tashbunar (Fig. 1), which are shallow and dry in summer.

This area is located in the temperate continental climate. The Black Sea, as well as large reservoirs and a large area up to the floodplains have a mitigating effect on the climate. Winter is short and mild with an unstable frosty period, summer is long and hot, autumn is warm. The low frequency of cyclones in this area is one of

the main reasons for the relatively small amount of precipitation – 380–410 mm per year. Evaporation exceeds 800 mm. Droughts of varying duration (up to 30–40 days a year) affect the area every 3–4 years, but in the last 15 years the droughts are more frequent. The greatest amount of precipitation (65–45% of the annual norm) falls in the warm period of the year in the form of showers. Precipitation is extremely uneven both in territory and in time. For the cold period of the year the prolonged precipitation of low intensity is typical. In terms of climate, the area is characterized by very high heat resources and significant humidity deficit, which affects significantly the natural conditions, biodiversity and socio-economic development of the region.

The research aims to study the hydrochemical regime andassess the quality of surface waters by hydrochemical parameters in Lake Katlabukh for many years and per fisheries standards as the most sensitive to changes in the ecological status of reservoirs and rivers using modern calculation methods.

The main revenue part in the water balance of the estuary lake Katlabukh is the inflow of Danube water through canals with regulator sluice Gromadsky and Zhelyavsky (Table 1).

The channels work (the sluices are opened) only during the period of filling the lakes in spring and discharging water into the Danube or its tributaries in autumn.

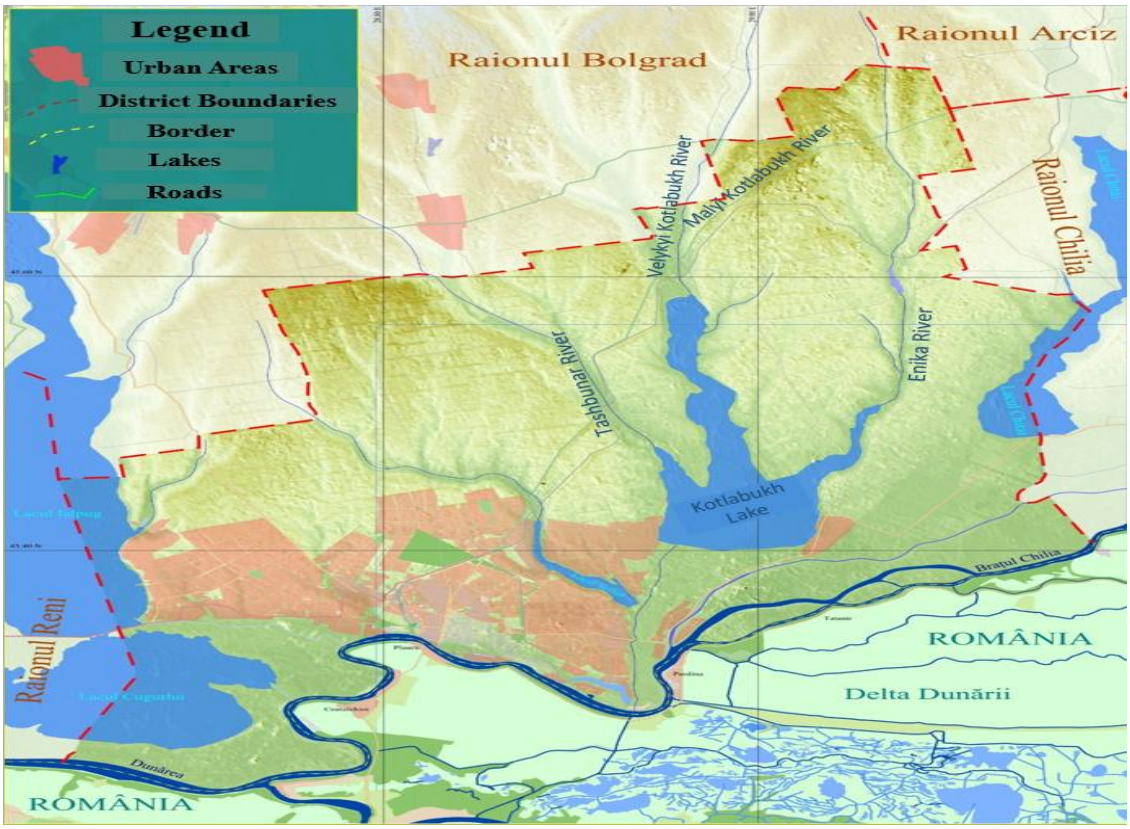

Fig. 1. The Lake Katlabukh location in territory of Ukraine.

Table 1. Information on channels and sluices-regulators of the lake Katlabukh

Sluice	Distance from the estuary to the tributary of Prorva [km]	Channels length [km]		Water-carrying capacity [$m^3 s^{-1}$]	Mark [m BS]			Year of construc-tion	Regulated water body
		Bringing water	Transporting water		Of the sluice threshold	Carriageway	Water level P = 1%		
Hromadsky	78.0	0.150	4.650	55	-0.70	3.60	4.60	1964	Lake Katlabukh
Zhelyavsky	73.2	0.050	3.350	70	-0.70	3.60	4.45	1967	Lake Katlabukh

At other times, the sluices are closed. These channels are self-flowing, so the water exchange depends on the mark differences between the levels in the Danube and the lakes. The operating rules of adjacent lakes admit that the regulatory water exchange processes correspond to natural conditions, ie in spring the lake is filled to the normal headwater level (NHL), in summer they are triggered by water intake and evaporation, and in autumn water from the lake is discharged to the dead storage level (DSL). The water level marks are following: normal headwater level (NHL) = 1.70 m BES, dead storage level (DSL) = 0.70 m BS, active reservoir level (ARL) = 3.00 m BS.

Hydrological features of the estuary area of the Danube are such that the amplitude of fluctuations in water levels decreases from 5–6 m (Reni) to 1.5–2.0 m (Vilkove). The geographical position of Lake Katlabukh, in relation to other upstream lakes, created the conditions under which it became hostage to the level regime of the Danube. Therefore, in recent decades, the filling of Lake Katlabukh in the conditions of dams construction without forced water supply has significantly affected the deterioration of both the level regime of the lake and its hydrochemical state. The water quality in these lakes is largely determined by the water quality of the Danube and small rivers that flow directly into the lakes.

To analyze the hydrochemical regime of Katlabukh Lake for a long period of observations (2000–2018), data from the monitoring gauges of the Danube Regional Water Resources Monitoring Laboratory (which existed until June 2019) were accepted, and state water monitoring was carried out according to the approved monitoring program of the State Agency Water Resources of Ukraine. Currently, all materials of observations on the lake and its tributaries are transferred to the Basin Department of Water Resources of the Black Sea and Lower Danube, and regular hydrological and hydrochemical observations are conducted by the Izmail Department of Water Management. This paper uses information on 4 items of the monitoring network according to the above program, which is shown in Fig. 2, namely:

– Lake Katlabukh PS-2 is on the Suvorov irrigation system, Izmail district;
– small river Tashbunar. The total length of the river is 40.0 km. Located in the Izmail and Bolgrad districts, the river flows into the Katlabukh reservoir. The river flow is regulated; observation point is 1.4 km from the estuary, on the road bridge;
– small river Velykyi Katlabukh. The total length of the river is 49.0 km. Located in the Izmail, Bolgrad, Artsyz districts, the river flows into the Katlabukh reservoir. The river flow is regulated; the observation point is on the road bridge on the route Izmail – Odessa;
– the small river Yenika. The total length of the river is 40.0 km. Located in the Izmail and Artsyz districts, the river flows into the reservoir Katlabukh. The river flow is regulated; the observation point is 0.1 km from the estuary, within village Pershotravneve, Izmail district.

Existing modern methods of water quality assessment are considered as the analysis of compliance of actual values of water parameters with the maximum permissible limits. But the number of regulated parameters is quite large, so there is a need to generalize information about the ecological status of surface waters based on the use of complex indicators that average and smooth the source information (Osadchyy et al, 2013; Kichuk et al 2016; Snizhko 2001).

To assess the water quality of the studied objects, the hydrochemical water pollution index (WPI) was used, which is calculated according to six indicators. Using this index, you can compare the quality of water in different water bodies, even in the presence of different pollutants. Calculations are made according to the formula:

$$WPI = \frac{1}{6}\sum_{i=1}^{6}\frac{C_i}{MPC_i}, \quad (1)$$

where

MPCi – the maximum permissible concentration of the chemical component;
Ci – the actual concentration of the chemical component;
6 – the number of ingredients.

To compare the quality of water in different areas, to determine their dynamics, the classes of water quality are used as criteria (Snizhko 2001; Yurasov et al., 2012), in particular the criterion for assessing the quality of water by WPI (Table 2).

Estimation of water quality according to WPI was performed using 6 chemical indicators for the lake Katlabukh, V. Katlabukh, Yenika, and Tashbunar: oxygen, phenols, oil products, ammonium nitrogen, nitrate-nitrogen, and BOC_5.

To generalize the status of surface waters and to identify possible trends in changes in their quality, in addition to determining the WPI, the assessment of the level of surface water pollution In the first citation, according to the current methodology in Ukraine (KND 211.1.1.106–2003) with the water pollution coefficient (WPC).

Water pollution coefficient (WPC) is a generalized indicator that characterizes the level of pollution and shows the multiplicity of exceeding water quality standards in the parts of MPL. The value of the water pollution coefficient is calculated for ten indicators only. These indicators include indicators exceeding the maximum permissible limits.

The obtained numerical values of the water pollution coefficient allow us to assess the state of water by pollution levels. Indicators of water pollution with the water pollution coefficient are given in Table 3.

The following indicators were used for calculations: BOC_5, ammonium nitrogen, nitrate nitrogen, nitrite nitrogen, copper, zinc; total iron, chlorides, petroleum products, phenols.

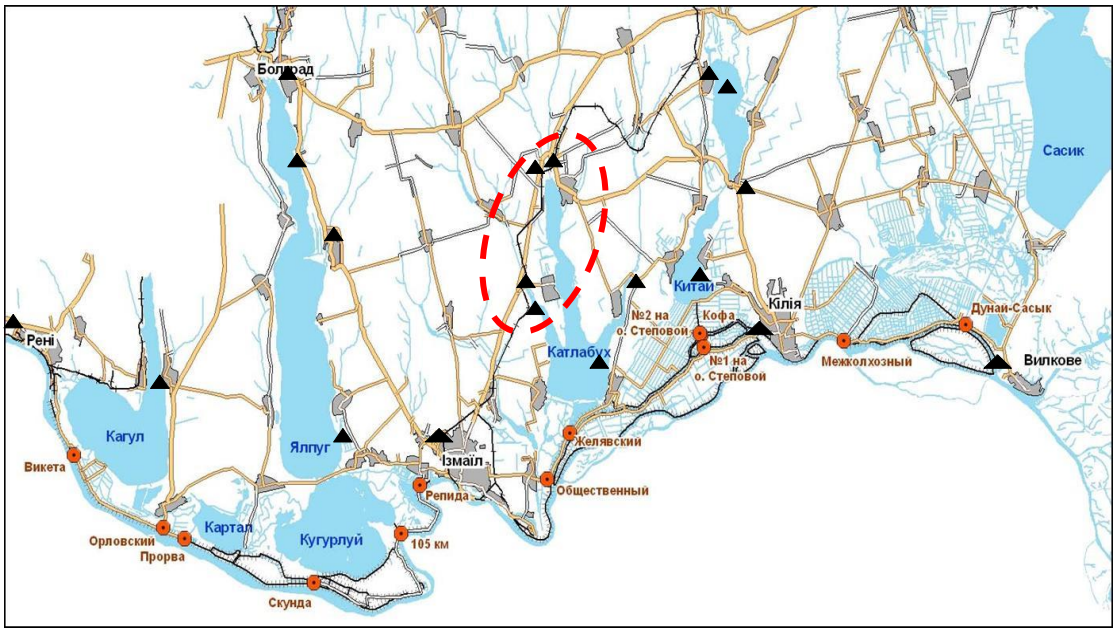

Fig. 2. Water quality monitoring points in the area of activity of the Danube BDWR.

Table 2. Criteria for assessing the quality of water using the WPI

Water quality class	Text description	Value of WPI
I	Very clean	≤ 0.3
II	Pure	> 0.3 – 1.0
III	Moderately polluted	> 1.0 – 2.5
IV	Polluted	> 2.5 – 4.0
V	Dirty	> 4.0 – 6.0
VI	Very dirty	> 6.0 – 10.0
VII	Extremely dirty	> 10.0

Table 3. Indicators of water pollution with the water pollution coefficient

The value of pollution	**1**	**1.01–2.50**	**2.51–5.00**	**5.01–10.0**	**More than 10**
Pollution level	Unpolluted (clean)	Slightly polluted	Moderately polluted	Dirty	Very dirty

Results and discussion

The hydrochemical regime and water quality of lake Katlabukh are influenced by several factors: the volume of runoff of small rivers and its mineralization; the volume of water intake for irrigation and water supply; the amount of precipitation and evaporation from the water surface of lakes; the volume of filling from the Danube and discharge of water into the river (Romanova et al, 2019). Determination of water mineralization was carried out according to the laboratory of the Danube BDWR in such facilities as Lake Katlabukh, Velykyi Katlabukh, Yenika, and Tashbunar.

The dynamics of the average annual mineralization of water bodies for the period 2000–2018 are shown in Fig. 3. The highest mineralization is observed in the Velykyi Katlabukh and Yenika Rivers, which are associated with both natural conditions and anthropogenic pollution.

Lake Katlabukh and the rivers flowing into it are characterized by high water salinity. A significant contribution to such indicators is made, first of all, by sulfate ions, as well as chloride ions, sodium, and potassium ions. To identify the anthropogenic impact on the hydrochemical regime of the studied objects, studies of pollution with nutrients, organic substances, and heavy metals were conducted. To quantify the content of organic matter in the water of Lake Katlabukh and its rivers, the indicators of chemical oxygen consumption (COC) and 5-day biochemical oxygen consumption (BOC_5) were used. In surface waters, the values of BOC_5 vary from 0.5 to 4.0 mg dm^{-3} relative to O_2 and there are seasonal and daily fluctuations (Fig. 4). The highest rates

of organic pollution are characteristics of the Yenika River and Lake Katlabukh, which is associated with water pollution in the Danube.

The significant pollution by heavy metals (manganese, iron), as well as phenols and, to a lesser extent, petroleum products, is also observed in all studied water bodies. Such a significant degree of pollution, in our opinion, is due primarily to the anthropogenic impact on the catchment area of small rivers. The hydrochemical index of water pollution (HIWP) was also used to assess the water quality of the studied objects (Snizhko, 2001). Estimation of water quality according to WPI was performed on 6 chemical indicators for the lake Katlabukh, V. Katlabukh River, Yenika River, Tashbunar River: oxygen, phenols, oil products, ammonium nitrogen, nitrate-nitrogen, and BOC5 based on the data of the Danube BDWR laboratory for 2000–2018. Analysis of the dynamics of the average annual values of HIWP at the observation points for the study period showed that the level of pollutants remains the same, fluctuating up or down depending on the anthropogenic impact. The dynamics of the average annual values of WPI for the studied period are presented in Fig. 5.

The recurrence of pollution classes at the studied water bodies was also calculated. The results of the calculation are given in the table. 4. According to the table, it can be noted that the cleanest water is in Lake Katlabukh, where the values of WPI vary from 0.56 (class II) to 1.87 (class III), but the years with water of the third class for the studied period is only five. The largest value of WPI according to the calculations was observed:

– in V. Katlabukh, in 2012 (WPI – 1.83), the high index was affected by nitrogen nitrite and phenols (3.98 mg dm^{-3}, 3.9 µg dm^{-3}, respectively);
– in Tashbunar, in 2009 (WPI – 1.91), the high index was affected by such an indicator as phenols (2.7 mg dm^{-3});
– in Yenika in 2015 (WPI – 2.26), the high index was affected by such an indicator as phenols (7.00 mg dm^{-3});
– in the lake Katlabukh PS-2 of the Suvorov irrigation system in 2012 (WPI – 1.7), the high index was affected by phenols (7.60 mg dm^{-3}).

The next stage of the study was to assess the quality of water in the studied water bodies and the suitability of these waters for use in fisheries by the water pollution coefficient (WPC).

The results of calculations are shown in Fig. 6.

As can be seen from the graph in Fig. 6, the highest indicators are inherent in the waters of the Yenika River and equal in 2002 -2.88, 2014 - 2.45, 2015 -2.54. These waters are classified as moderately polluted. Also, high values of water pollution coefficient -2.62 in 2009 are characteristics of the waters of the V. Katlabukh River, which allows them to be classified as moderately polluted. This indicates that small river basins are exposed to increasing anthropogenic impact, which is characterized by a fairly high degree of plowing of watersheds, intensification of agricultural production, non-compliance with growing environmental requirements for agricultural production, the presence of powerful sources of pollution in the form of industrial effluents (Kichuk et al 2016; Snizhko 2001).

According to the level of pollution during the studied period of the lake Katlabukh and Tashbunar can be classified as "slightly polluted". The main problem of these water bodies is excessive water pollution with heavy metals, pesticides, phenols, and petroleum products (manganese, iron, sulfates, petroleum products, phenols). The main cause of surface water pollution by these elements is the insufficient level of wastewater treatment coming from municipal, industrial, and

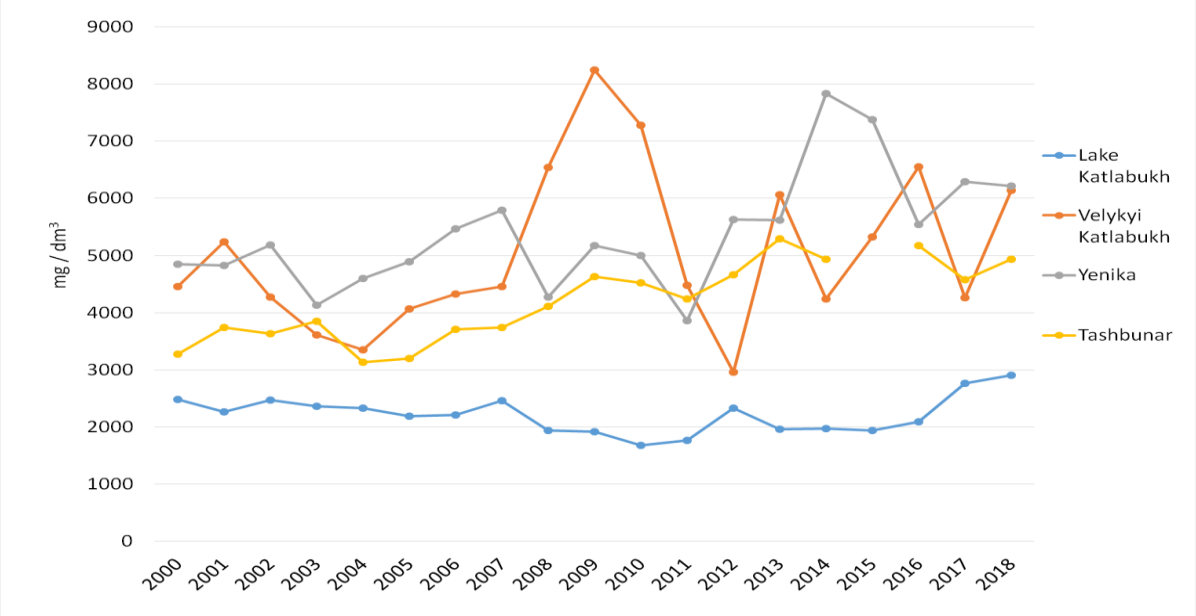

Fig. 3. Average annual values of mineralization of water bodies within the catchment of Lake Katlabukh for the period 2000–2018 [mg dm^{-3}].

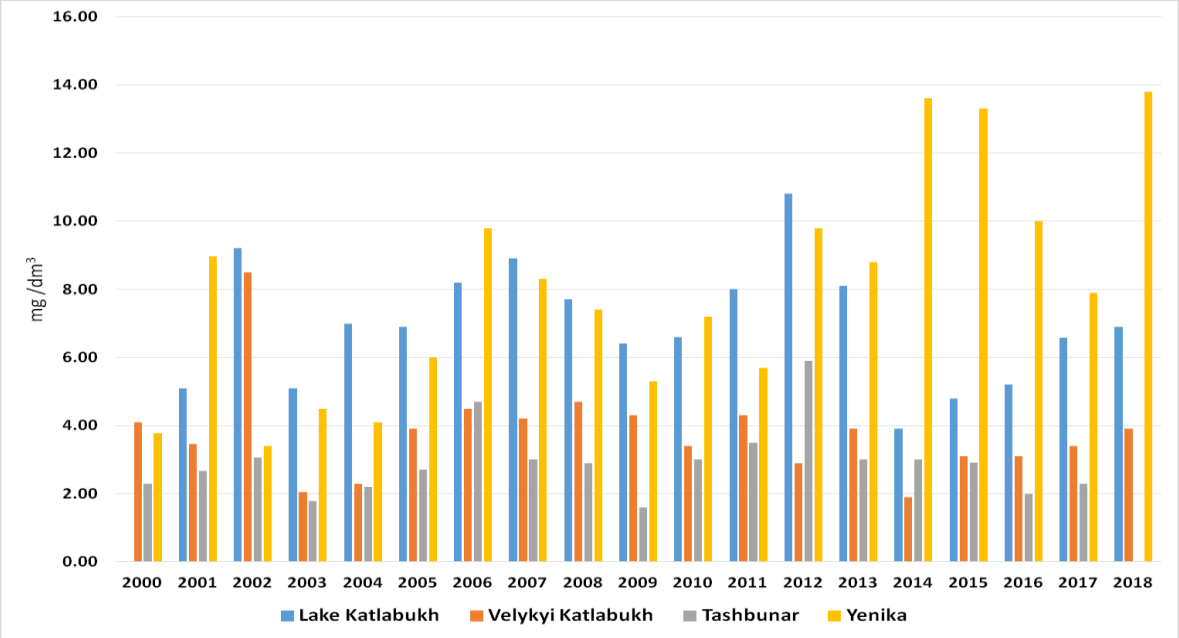

Fig. 4. Average annual values of concentration of BOC_5 of water bodies within the catchment of Lake Katlabukh for the period 2000–2018 [mg dm^{-3}].

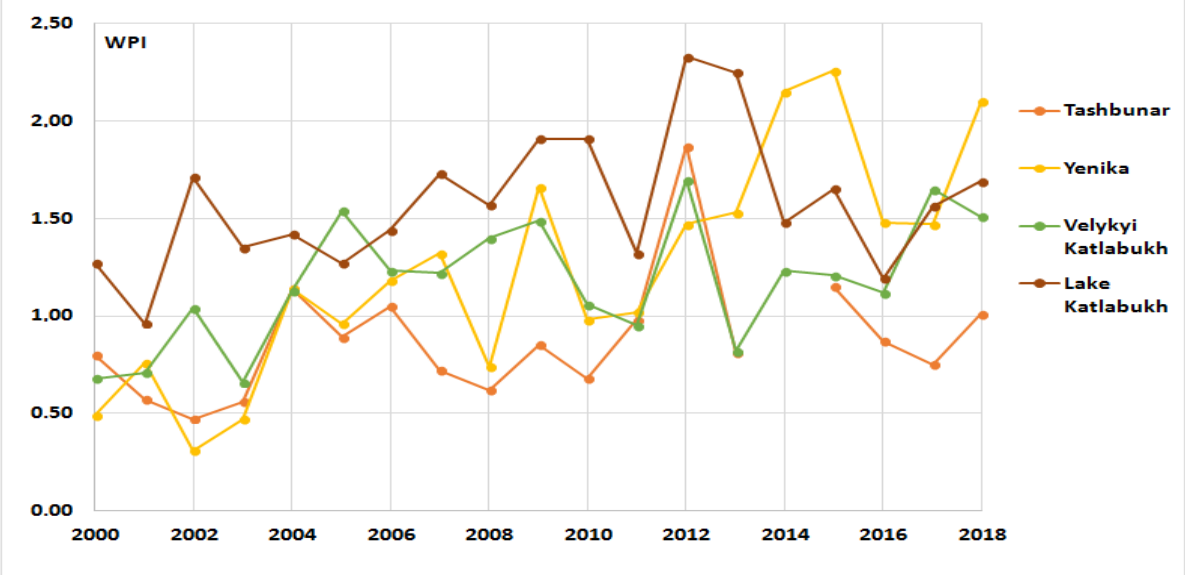

Fig. 5. Dynamics of average annual values of WPI for the studied period.

Table 4. Results of calculation of WPI for the period 2000–2018

Name of water bodies	Classification by water pollution index (WPI)	
	Pollution class	Number of cases [%]
Tashbunar River	**II**	**5**
	III	**95**
Velykyi Katlabukh River	**III**	**79**
	II	**21**
Yenika River	**II**	**37**
	III	**63**
Lake Katlabukh	**II**	**72**
	III	**28**

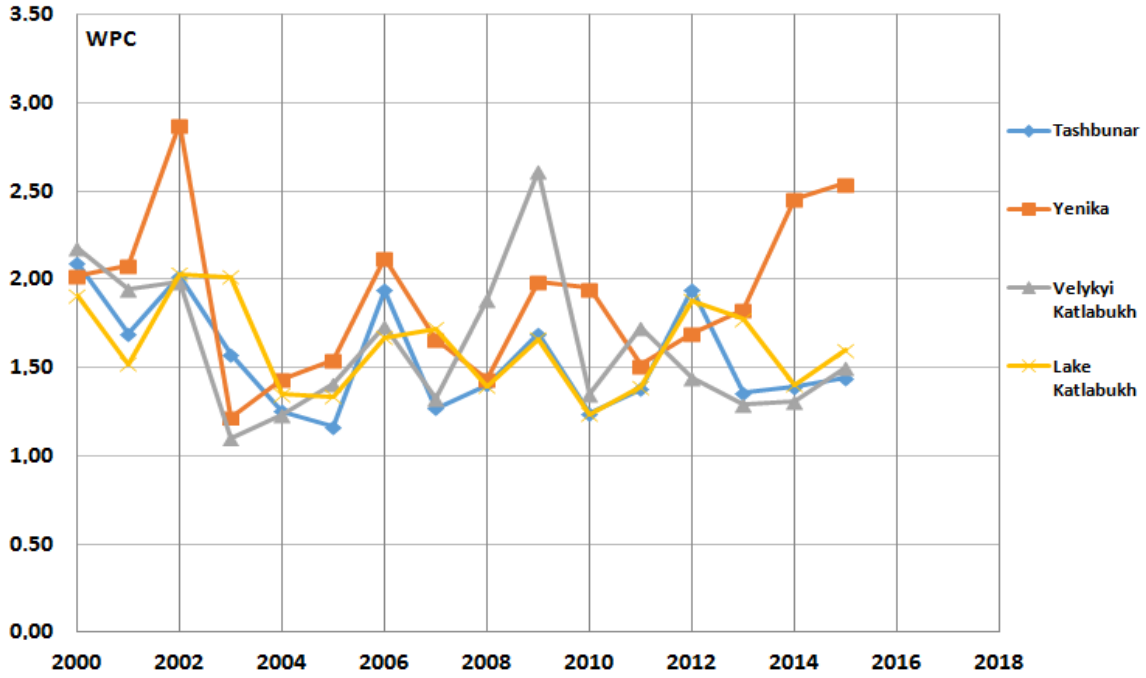

Fig. 6. Dynamics of average annual water pollution coefficient values for the studied period.

agricultural point sources, and with surface runoff.
Further study of the water quality of Lake Katlabukh and the rivers flowing into it according to complex indicators of ecological status is envisaged to state with due probability about the possibility of its use for fisheries and to determine the possible use of the water body for other water users.

Conclusion

The main reason for the unsatisfactory condition of the studied objects is the significant anthropogenic impact on the catchment area of small rivers flowing into Lake Katlabukh, deteriorating the quality of its water resources. One of the main factors in the deterioration of water quality is the lack of water exchange in the lake itself due to many negative factors, including geographical location, the impact of climate change, and imperfect management of operational processes.
To improve the condition of surface waters in Lake Katlabukh it is proposed:

- to conduct a detailed analysis of the impact of human activities and natural factors on the water quality of Lake Katlabukh and the rivers flowing into it;
- both for the lake itself and for the territory of its basin to develop a program of specific measures against water pollution by all possible sources of pollution;
- ensure compliance with environmental legislation by all water users, regulate (restrict) or completely prohibit such activities that affect water quality, in particular, fishery water use.

At the moment, a detailed study of natural and anthropogenic factors affecting the water quality of the lake is being continued in order to create a program of specific measures to improve the current legislation to reduce water pollution not only of the rivers that flow into Lake Katlabukh, but also of the lake itself. In addition, monitoring of compliance with already existing environmental measures of the current legislation is being carried out.

Acknowledgment

The authors express their gratitude to the deputy chief of the Basin Water Resources Department of the Black Sea and the Lower Danube Rivers, Ivan Dmitrievich Kichuk, for consultations and provided materials regarding the monitoring system of surface water quality in the area of the Lower Danube river basin.

References

Directive 2000/60/EC of European Parliament and the Council establishing a framework for the Community action in the field of water policy (EU Water Framework Directive) [Electronic resource]: Act from 23/10/2020. – Access mode: http://eur-lex.europa.eu/resource.html?uri=cellar:5c835afb-2ec6-4577-bdf8-756d3d694eeb.0004.02/DOC_1&format=PDF

Gopchenko, E. D., Ovcharuk, V. A., Kichuk, N. S. (2011): Modern problems associated with the exploitation of the Danube lakes and reservoirs. Black Sea Ecological Bulletin, no.2, 35–41. (in Ukrainian)

Kichuk, N. S., Shakirzanova, Zh. R., Medvedeva, Y. S., Kurilova, I. V. (2016): Formation of hydrochemical regime and assessment of water quality in the Danube lakes. Hydrology, hydrochemistry and hydroecology,

vol. 3, no. 42, 56–63. (in Ukrainian)

Method of calculating the coefficient of pollution of natural waters: KND 211.1.1.106-2003 Organization and implementation of observations of surface water pollution (in the system of mine resources) / Approved. by order of the Minister of Ecology and Natural Resources of Ukraine №89-M of June 4, 2003, Kyiv, 25–30. (in Ukrainian)

Osadchyy, V. I., Nabyvanets′, B. Y., Lynnyk, P. M. (2013): Processes of formation of chemical composition of surface waters. Nika-Center, Kyyiv, 240 p. (in Ukrainian)

Romanova, Ye., Shakirzanova, Zh., Gopchenko, Ye., Medvedieva, Yu. (2019): Water and salt balances of Lake Katlabukh under different operating conditions of the reservoir, Hydrology, hydrochemistry and hydroecology, 4 (55), 23–40, (in Ukrainian)

Snizhko, S. I. (2001): Assessment and forecasting of natural water quality, Nika-Center, Kyyiv, 264 p. (in Ukrainian)

Yurasov, S. M., Safranov, T. A., Chugay, A. V. (2012): Evaluation of natural water quality: a textbook, Ecology, Odessa, 168 p. (in Ukrainian)

Valeriya Ovcharuk, Doctor of Geographical Sciences, Associate Professor (*corresponding author, e-mail: valeriya.ovcharuk@gmail.com)
Natalia Kichuk, Ph.D. in Geography, Associate Professor
Dmytro Lutai, Master of Hydrology
Liliia Kushchenko, Ph.D.-student of the Department of Land Hydrology
Maria Myroshnychenko, Senior Lecturer of the Department of Ukrainian Studies and Social Sciences
Odessa State Environmental University
15 Lvovskaya Str.
Odessa, 65016
Ukraine

DOI: 10.31577/ahs-2022-0023.01.0013

ACTA HYDROLOGICA SLOVACA

Volume 23, No. 1, 2022, 117 – 129

Assessment of surface waters quality of small water reservoirs in agricultural landscape

Jana BOROVSKÁ*, Tomáš RUSŇÁK, Matej MOJSES

In the article are presented results from water quality monitoring of six small water reservoirs situated in agricultural landscape in different Slovak regions. The study period was from June 2020 to September 2021. Studied parameters covered oxygen regime, total dissolved solids, fluorescent dissolved organic matter, turbidity, chlorophyll a, phycocyanin and phycoerythrin. All parameters were measured directly in the field using EXO YSI 2 probe. For interpretation of the measured data the application of different statistical approaches were used. The cluster analysis divided the six monitored water reservoirs in to two clusters. The Kruskal-Wallis test confirmed the significant differences between groups of water reservoirs. Analysis of normalized data revealed main parameters that caused the distribution in to two clusters: chlorophyll a, cyanobacterial photosynthetic pigments phycocyanin and phycoerythrin, turbidity and pH. In the cluster 2 the concentration ranges for these parameters showed large fluctuations. Comparison of the land cover structure of 500 m buffer zones pointed out the importance of buffer zone composition for better water quality. For the cluster 2 the highest proportion belonged to arable soils (63.63–92.00%) and only 1.12–9.33% to forests.

KEY WORDS: surface water, water reservoirs, agriculture, water quality

Introduction

Water, as an important component of the biosphere, provides many functions for humans. Man uses water for personal consumption, in agriculture, industry and energy production, for transport and recreation. Growth of population and rising living standards cause pressure on the amount and availability of quality water resources (Ormerod et al., 2010).

The legal regulations endorse conditions for protection of surface and groundwaters, including aquatic ecosystems and landscape ecosystems directly dependent on water, e.g. the Water Framework Directive, the Council Directive 91/676/EEC, the so-called Water Act, Act no. 364/2004 Coll. on Waters and on Amendments to Certain Acts. This Act also regulates the rights and obligations of natural and legal persons to surface and groundwater and real estate related to them.

Human activities interfere with the natural water cycle and often result in the drainage of water from the natural cycle. In the past, people have tried to compensate for the lack of water in the area and its retention in the country by building water reservoirs. Water reservoirs can serve to variety of purposes. Many are multi-purpose and often cover the requirements of farmers, fisheries organizations, industry, but also perform protective and aesthetic functions in the landscape (Jurík et al., 2015; Szcykowska and Siemieniuk, 2014). Water reservoirs are technical, water management structures and therefore require regular maintenance. Recently, in field research, we often encounter with insufficient maintenance and care of these water works, which also affects the efficiency of their use. Problems of neglected maintenance are visible especially on the dams of reservoirs, their functional objects and on clogging and grounding, especially of small water reservoirs. Mud removal from small water reservoirs consist in removing sediments coming from catchment and from bank abrasion in to reservoir. These sediments create conditions for eutrophication of the reservoir, growth of biomass and its subsequent decaying and sedimentation in the reservoir. A gradual reduction, even impossibility, of water management, biological and ecological functions of small water reservoirs are caused by the clogging (Čistý, 2005; Ignatius and Rasmussen, 2016).

When protecting surface water, it is important to pay attention to the sources of pollution, which can be point and non-point. Natural organic pollution of surface waters is caused by leaching from soils, sediments and by vital products of plants, animals and aquatic organisms. Excessive supply of nutrients and pollutants threatens the quality of ecosystems and human health. Nutrients enter aqueous sources in dissolved ionic form or bound in organo-mineral soil complexes. Insoluble substances are considered the most significant components of surface water pollution by volume. Dissolved substances enter water sources by infiltration of the soil profile with

rainwater or surface runoff. Undissolved substances are transported by soil erosion, mostly by water erosion, in a lesser extent also by wind erosion (Pekárová and Velísková; 1998; Krengel et al., 2018).

Pollution of anthropogenic origin can come from direct and indirect human activity. The most significant impact on the quality of surface waters is the outflow from agricultural areas and the discharge of municipal or industrial wastewater into watercourses and reservoirs (Kriška Dunajský et al., 2018). In the agricultural land, excessive fertilizers, runoff, and soil erosion can lead to an increase in sediment, nutrients, chemical contaminants, and organic matter into water bodies (Huang et al., 2020). Factors that have a significant impact on water quality include river basin and reservoir management, topography and relief of the surrounding landscape, density and species composition of riparian vegetation, the method and intensity of cultivation of adjacent fields, industrial facilities and, last but not least, the presence and size of settlements (Li et al., 2015; Arocena et al., 2018). Smaller villages located in agricultural landscape are often without a built sewerage network and wastewater treatment plants. The absence of wastewater treatment from settlements and agricultural objects, manures and waste dumps results not only in supply of nutrients but also pathogens and hazardous chemicals, which accumulate in the aquatic environment and enter the bio-geo-chemical cycles and food chains.

As a result of global warming also water temperature is rising and this has a significant impact on water chemistry, as well as on development of harmful cyanobacterial bloom. According to the United Nations World Waters Report (UNESCO, 2020), many lakes and estuaries around the world, providing drinking water to millions of people and supporting ecosystem services, are full of harmful substances entering food chains and supporting development of harmful cyanobacterial bloom, which among other things causes hypoxia. Cyanobacterial cells have dimensions of 0.5–60 μm. In their cells, they have photosynthetic pigment chlorophyll a and other pigments, especially phycocyanin and phycoerythrin (Hindák, 2001; Cohen-Bazir and Bryant, 1982). During their evolutionary development, cyanobacteria have adapted to almost all ecological conditions. They often occur abundantly in fresh but also salt waters in free plankton, trapped on various substrates in the littoral, free on the bottom and sometimes as accumulated biomass visible to the naked eye as so-called water bloom. The presence of a cyanobacterial water bloom is often accompanied by an odour, which indicates a deteriorating biological quality of the water (Huisman et al., 2018). The mass occurrence of planktonic cyanobacteria results not only in aesthetically undesirable changes in water reservoirs, but also in the presence of dangerous toxins. Many cyanobacteria excrete toxic substances, especially neurotoxins and hepatotoxins, during the decomposition of their cells, but also alive. Cyanotoxins are dangerous for humans, but they can also cause poisoning of warm-blooded animals, especially cattle, dogs, and birds that have drunk from such water (Hindák, 2001).

The aim of the study was to assess the water reservoirs on the basis of measured water quality parameters.

Research sites

The research sites represent selected small water reservoirs located in the agricultural landscape in Trnava, Nitra and Banská Bystrica districts. Based on the field survey were selected study water reservoirs (WR) in which we monitored changes in surface water quality. The research sites are following: WR Doľany (Trnava district), WR Suchá nad Parnou (Trnava district), WR Dubník 2 (Nové Zámky district), WR Rúbaň 2 (Nové Zámky district), VN Sklabiná (Veľký Krtíš district), WR Želovce (Veľký Krtíš district) (Fig. 1). The monitored water reservoirs belong to the category of small water reservoirs with a ground construction (Table 1).

The water reservoirs Doľany (19 ha) and Suchá nad Parnou (37.6 ha) were built on a stream Podhájský potok, which flows through them. The WR Doľany is situated in area of large agricultural fields. The WR Suchá nad Parnou is situated on the outskirts of the village. It was created to protect the villages from floods. At its southern bank is a cottage area. In addition to irrigation and fishing, it is also used for recreation. The WR Sklabiná (12 ha) is located on a stream Zajský potok and is used for fish farming and recreation. The WR Želovce (3 ha) is situated on a stream Čegovský potok in the area of large agricultural fields. The WR Dubník 2 (14 ha) was built on a stream Parížsky potok. It is located in the area of intensive agriculture. It is used for irrigation and recreational fishing. It is bordered by tree vegetation on the south. The part of its steep bank on the north is collapsing into the water reservoir. The WR Rúbaň 2 (10 ha) is situated on a stream Cegléd. In summer, it is used for irrigation and recreational fishing. The land use and land cover around the water reservoir have the influence on the water quality. Table 2 shows the differences in land cover in the buffer zone of 500 m around the WRs. The monitored water reservoirs belong to the category of small water reservoirs with a ground construction. Important factors influencing the water quality as the amount of precipitation and wind speed are presented in tables 3–5.

Methods

In the period from June 2020 to September 2021, field measurements of surface water quality and monitoring of water levels were carried out at regular monthly intervals. The measurements were carried out from the dams or piers from representative monitoring points selected before. To select the final monitoring point we did monitoring on several point in the WRs and as the results were almost the same we selected the representative ones. One point for each WR. We did monitoring deployments with averaging the datasets. During the months with higher eutrophic state we performed for the control also measurements in additional points to ensure the measured data are representative for the WRs. However, for statistical analysis we used only the data from the selected representative monitoring points. The monitoring depth was 50 cm to allow us to compare

also with another shallow water reservoirs which we study. To avoid differences in measurements caused by the daytime we always kept the sequence of monitoring reservoirs. The monitoring were carried out from 9 am to 2 pm.

The following physico-chemical parameters were selected to evaluate surface water quality: water temperature [°C], conductivity [µS cm^{-1}], total dissolved solids TDS [mg L^{-1}], salinity [psu], optical dissolved oxygen ODO [mg L^{-1}, %sat], water pH, fluorescent dissolved organic matter [RFU], turbidity [FNU], chlorophyll a [µg L^{-1}], phycocyanin BGA-PC [µg L^{-1}] and phycoerythrin BGA-PE [µg L^{-1}]. The measurement of the parameters took place directly in the field using EXO YSI 2 probes. The obtained values were processed by statistical methods.

From June 2021 to September 2021 we also analysed nitrate nitrogen (NO^3-N), ammonium nitrogen (NH_4-N), total nitrogen (TN), total phosphorus (TP) and chemical oxygen demand (COD) by Hach cuvette tests LCK339, LCK304, LCK138, LCK349 and LCI500. These analyses were carried out in the laboratory on spectrophotometer DR5000. The water samples for laboratory analysis of volume 1 L were transported in cold and dark in a portable fridge and analysed imediatelly for content of nitrate nitrogen and ammonium nitrogen and on the other day for content of total nitrogen, total phosphorus and chemical oxygen demand.

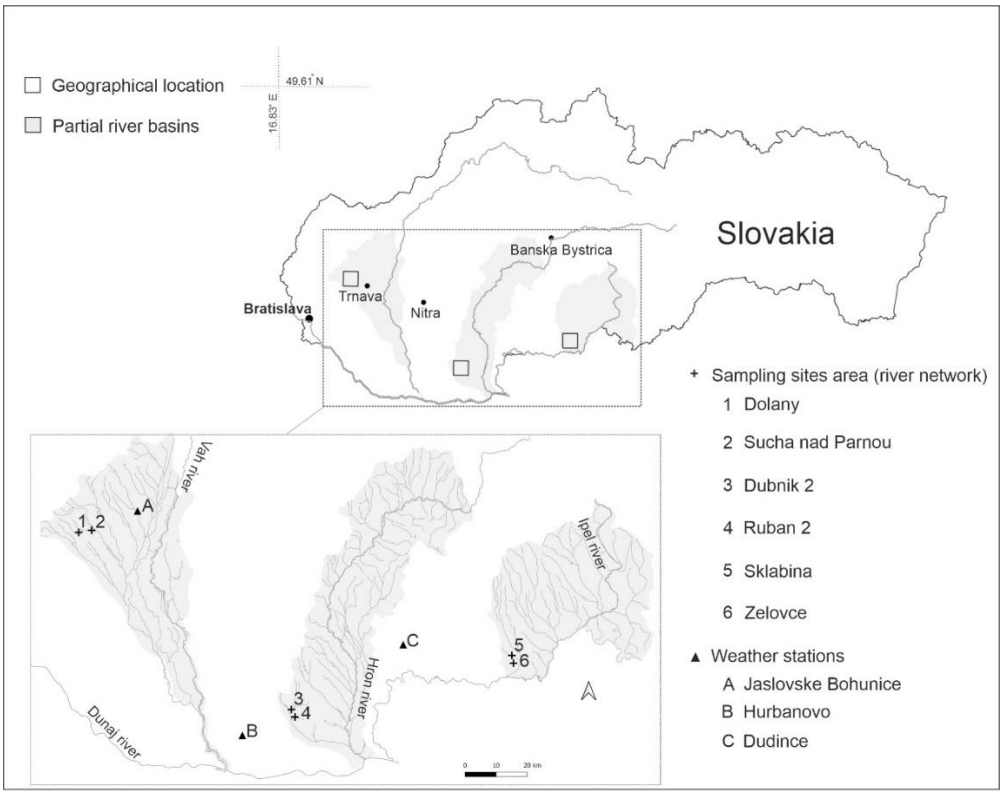

Fig. 1. Location of monitoring water reservoirs and climatic stations (Author: Hubert Hilbert, 2022).

Table 1. Geographical location of the monitoring point (MP) and the water reservoirs´ characteristics

Water Reservoir	MP latitude	MP longitude	Altitude [m]	Area [ha]	Average depth* [m]	Purpose
Doľany	48.373249	17.387733	201	19	6.41	irrigation
Suchá nad Parnou	48.403301	17.41695	174	37.6	5.62	irrigation, fishery, recreational fishing, recreation
Dubník 2	47.946732	18.399433	138	14	3.67	irrigation, fishery, recreational fishing
Rúbaň 2	47.925098	18.417868	144	10	6.91	irrigation, fishery
Sklabiná	48.152451	19.33445	176	12	2.55	irrigation, fishery, recreational fishing, recreation
Želovce	48.129932	19.343233	167	3	3.45	irrigation

**average depth in the monitoring period*

Table 2. **Corine land cover structure of 500 m buffer zone of each water reservoir. Codes: 1 urban areas, 2 industrial, commercial and transport areas, 4 areas with urban vegetation, sport and recreational areas, 5 arable land, 6 permanent crops - orchards and vineyards, 7 meadows and pastures, 9 deciduous forests, 10 mixed forests, 17 marshes and peatlands, 18 water areas, 20 nonspecified forests**

WR	Doľany		Suchá nad Parnou		Dubník 2		Rubáň 2		Sklabiná		Želovce	
Code	[ha]	[%]	[ha]	[%]	[ha]	[%]	[ha]	[%]	[ha]	[%]	[ha]	[%]
1			204153.92	6.23	56197.30	2.42						
2					21920.19	0.95						
4					22297.21	0.96						
5	1561819.82	77.29	1430192.20	43.66	1475502.87	63.63	1133080.61	68.16	1384449.73	70.47	1174993.11	92.32
6	7227.68	0.36	186767.65	5.70	158564.10	6.84	172328.04	10.37				
7	205595.43	10.17	496939.62	15.17	204509.98	8.82	84885.27	5.11	148218.26	7.54	46066.64	3.62
9			504746.22	15.41	216290.56	9.33	184958.43	11.13	147074.32	7.49		
10			85124.24	2.60								
17					720.14	0.03						
18	135151.45	6.69	324617.30	9.91	162722.96	7.02	87171.52	5.24	134391.30	6.84	37400.99	2.94
20	110979.54	5.49	43189.75	1.32					150401.26	7.66	14280.65	1.12
Summary	2020773.92	100.00	3275730.91	100.00	2318725.31	100.00	1662423.88	100.00	1964534.88	100.00	1272741.39	100.00

Table 3. **Monthly means and totals measured at the weather station Hurbanovo: T – temperature, Tmax – maximum temperature, Tmin – minimum temperature, SLP – atmospheric pressure at sea level, H – average relative humidity, PP – total rainfall and/or snowmelt, W – average wind speed, Wmax – maximum sustained wind speed (source: https://en.tutiempo.net/)**

	Hurbanovo							
Parameter	T	Tmax	Tmin	SLP	H	PP	W	Wmax
Date/Unit	[°C]	[°C]	[°C]	[hPa]	[%]	[mm]	[km/h]	[km/h]
VI. 2020	19.8	25.1	14.2	1011.1	70.1	50.5	11.3	20.8
VII. 2020	22.1	28.9	14.8	1015.7	58.4	30.0	9.7	17.2
VIII. 2020	23.0	29.7	16.5	1013.6	61.6	44.5	9.6	17.2
IX. 2020	17.9	24.9	11.6	1017.1	56.9	83.3	9.5	16.8
X. 2020	11.6	15.7	7.7	1014.9	83.0	136.7	11.0	18.0
XI. 2020	5.6	8.9	2.8	1028.0	89.4	17.8	8.0	13.5
XII. 2020	4.0	5.9	1.9	1015.5	87.8	21.3	11.9	19.5
I. 2021	1.8	5.1	-1.3	1012.8	83.6	30.0	11.2	19.0
II. 2021	3.1	8.0	-1.0	1021.5	80.5	22.6	11.0	18.7
III. 2021	5.8	12.7	-0.8	1021.4	58.9	2.0	13.1	24.0
IV. 2021	9.2	15.1	2.7	1017.1	61.2	39.4	14.2	24.7
V. 2021	14.1	19.1	8.0	1013.9	67.6	84.1	13.2	22.3
VI. 2021	22.8	29.4	14.8	1016.2	55.4	10.2	9.0	15.5
VII. 2021	24.0	30.6	17.1	1013.5	59.7	37.9	10.1	18.2
VIII. 2021	20.5	26.8	14.1	1015.0	67.8	34.8	9.1	17.1
IX. 2021	17.1	24.2	10.0	1019.3	66.4	58.4	9.0	15.8

Untill the analyses the samples were kept in a fridge.

We used Shapiro-Wilk test to analyse normality of data with a p-value<0.05 (Shapiro and Wilk, 1965). All data except pH (p-value 0.704) has been not normally distributed. Based on these results we decided to determine the strength and directions of the relationships between water quality parameters with Spearman correlation, which is more suitable for this type of distribution (Spearman, 1904). A cluster analysis (CA) was applied to analyse the similarity of the water reservoirs. Hierarchical agglomerative clustering was chosen. It is the most common approach and is typically illustrated by a dendrogram (McKenna, 2003). The dendrogram provides a visually interpretation of the grouping processes, presenting a picture of the groups and their similarity with a dramatic reduction in dimensionality of the original data (Shrestha and Kazama 2007). CA was performed on the normalized data by

Table 4. **Monthly means and totals measured at the weather station Dudince: T – temperature, Tmax - maximum temperature, Tmin – minimum temperature, SLP – atmospheric pressure at sea level, H - average relative humidity, PP – total rainfall and / or snowmelt, W – average wind speed, Wmax – maximum sustained wind speed (source: https://en.tutiempo.net/)**

Dudince								
Parameter	**T**	**Tmax**	**Tmin**	**SLP**	**H**	**PP**	**W**	**Wmax**
Date/Unit	**[°C]**	**[°C]**	**[°C]**	**[hPa]**	**[%]**	**[mm]**	**[km/h]**	**[km/h]**
VI. 2020	19.4	25.4	13.4	1010.6	73.8	135.9	6.8	13.4
VII. 2020	21.3	28.2	13.5	1015.7	63.8	68.6	6.1	12.1
VIII. 2020	22.2	29.6	15.0	1013.4	65.6	69.6	6.2	12.6
IX. 2020	17.2	24.9	10.2	1016.9	70.6	71.6	5.9	10.8
X. 2020	11.2	15.7	7.0	1014.8	87.1	131.6	5.8	9.3
XI. 2020	4.7	8.1	1.8	1028.1	90.8	16.2	4.5	7.8
XII. 2020	3.8	5.9	1.7	1016.0	88.0	29.5	7.0	11.7
I. 2021	0.5	3.9	-2.8	1012.8	86.0	44.2	6.3	11.9
II. 2021	1.9	6.9	-2.9	1021.7	82.5	33.3	6.0	11.3
III. 2021	4.5	12.3	-2.8	1021.1	61.4	5.6	7.3	14.9
IV. 2021	8.2	15.0	0.6	1016.7	63.4	34.0	8.4	17.2
V. 2021	13.0	19.4	5.8	1013.6	71.3	101.9	8.3	16.7
VI. 2021	22.0	29.3	13.1	1016.0	60.9	32.8	6.0	12.0
VII. 2021	23.2	30.5	15.9	1013.2	64.5	165.4	6.3	12.5
VIII. 2021	19.5	26.4	12.6	1014.6	68.7	40.1	6.7	13.6
IX. 2021	16.1	24.2	8.2	1019.1	65.7	41.9	6.2	12.2

Table 5. **Monthly means and totals measured at the weather station Jaslovské Bohunice: T – temperature, Tmax – maximum temperature, Tmin – minimum temperature, SLP – atmospheric pressure at sea level, H – average relative humidity, PP - total rainfall and / or snowmelt, W - average wind speed, Wmax – maximum sustained wind speed (source: https://en.tutiempo.net/)**

Jaslovske Bohunice								
Parameter	**T**	**Tmax**	**Tmin**	**SLP**	**H**	**PP**	**W**	**Wmax**
Date/Unit	**[°C]**	**[°C]**	**[°C]**	**[hPa]**	**[%]**	**[mm]**	**[km/h]**	**[km/h]**
VI. 2020	18.8	24.1	13.5	1011.2	73.8	71.6	13.7	22.7
VII. 2020	20.5	27.4	13.7	1015.8	65.8	51.3	10.7	19.2
VIII. 2020	22.1	28.9	15.7	1013.6	64.8	38.1	10.7	19.5
IX. 2020	17.0	23.2	11.6	1017.2	71.2	108.7	11.8	19.7
X. 2020	10.9	14.7	7.7	1014.6	85.7	124.5	13.8	24.0
XI. 2020	5.1	7.5	2.9	1027.8	90.4	17.0	10.2	17.4
XII. 2020	3.3	5.0	1.5	1015.1	90.0	36.1	14.7	22.5
I. 2021	0.5	3.2	-2.2	1012.6	86.7	42.9	12.0	21.6
II. 2021	2.3	6.2	-1.1	1021.5	83.2	19.3	12.5	22.2
III. 2021	4.7	11.0	-1.2	1021.6	64.7	8.6	13.7	24.7
IV. 2021	8.1	14.1	2.2	1017.1	63.0	19.3	16.1	28.2
V. 2021	13.0	18.2	7.2	1013.6	70.5	103.9	14.4	25.0
VI. 2021	21.1	28.0	13.2	1016.3	62.7	13.2	10.8	18.7
VII. 2021	23.0	29.5	16.0	1013.5	59.1	51.3	12.8	22.7
VIII. 2021	19.2	24.9	13.8	1015.0	71.0	94.2	11.1	21.0
IX. 2021	16.3	22.8	10.0	1019.4	68.7	26.7	11.4	20.2

means of the Ward´s method, using squared Euclidean distances as a measure of similarity. The Kruskal-Wallis H test was used to analyse whether there was a significant difference between similar groups of the water reservoirs. When the p-unc (uncorrected p-value) is less than 0.05, there were statistically significantly different from each other (Kruskal and Wallis, 1952).

Results and discussion

The measured values at the study sites were influenced by the season and the amount of water in the reservoirs. In the monitoring period from June 2020 to September 2021, we recorded a water temperature in the range of 3.53°C (XII. 2020, Sklabiná) – 27.91°C (VII. 2021, Rúbaň 2). The reaction of water pH ranged from 7.64 (XII. 2020, Sklabiná) to 9.24 (VI. 2021, Želovce). The average pH value for the monitored sites was 8.42. The conductivity ranged from 143.04 µS cm^{-1} (VIII. 2021, Doľany) to 971.16 µS cm^{-1} (VIII. 2020, Dubník 2) with an average of 421.08 µS cm^{-1}. The TDS content ranged from 103.41 mg L^{-1} (VIII. 2021, Doľany) to 647.00 mg L^{-1} (VIII. 2020, Dubník 2) with an average value of 316.20 mg L^{-1}. The fDOM content was from 1.90 RFU (VII. 2021, Suchá nad Parnou) to 28.36 RFU (XI. 2020, Želovce) with an average value of 10.68 RFU. The value of the measured chlorophyll a content ranged from 2.91 µg L^{-1} (II.2021, Rúbaň 2) to 318.23 µg L^{-1} (VI. 2021, Želovce) with an average value of 36.56 µg L^{-1}. High level of variability in selected parameters were also registered by Noskovič et al. (2013) and Ignatius and Rasmussen (2016). According to Sebíň (2007) water quality of water reservoirs in agricultural landscape is more vurnelable to substantial changes than in water reservoirs in forested microcatchment. The measured dissolved oxygen content ranged from 1.88 mg L^{-1} or 22.3%sat (VIII. 2020, Dubník 2) to 22.63 mg L^{-1} or 271.8%sat (VI. 2020, Dubník 2), with an average value of 11.54 mg L^{-1} or 139.66%sat. According to Higgins (2014) extensive experience in the field and testing instrument at the YSI facility, values over 100% air saturation have indeed proven to be quite common. The levels of dissolved oxygen are affected by many water quality parameters and respond to their variations, either directly or indirectly. Kowalczewska-Madura et al. (2022) described the similar supersaturation in Raczyńskie Lake during their study. They measured the oxygen concentration of 23.1 mg L^{-1} in the summer 2019 (270%sat) at the surface level. When analysed the seasonal variability of this parameter, they found out that there was a gradual increase in the mean oxygen concentration in the surface layer, while above the bottom, concentrations varied. Huang et al. (2017) recorded supersaturated DO levels due to low concentrations of oxygen-consuming substances and strong phytoplankton photosynthesis. Proved that algal respiration and photosynthesis rates are proportional to phytoplankton biomass and therefore, the peaks of DO consumption and production by algal respiration and production are synchronized with the peaks of chlorophyll a. In our case, in the period when the maximum DO concentration was measured also turbidity (97.79 FNU), pH (9.06), BGA-PE (284.68 µg L^{-1}) were increased on the site. In the same time were measured the oxygen concentrations of 16.65 mg L^{-1} (192.6%sat) in an upstream WR Jasová and 14.45 mg L^{-1} (171.3%sat) in the WR Rúbaň 2 where the concentration of chlorophyll a reached 60.39 µg L^{-1}.

After processing all measured data by statistical analysis descibed above the water reservoirs were divided in to two clusters on the basis of their similarities. Figure 2 illustrates the emerged clusters in the form of a dendrogram. The water reservoirs Suchá nad Parnou, Rúbaň 2 and Sklabiná represent the first cluster of reservoirs. The second cluster consists of the water reservoirs Dubník 2, Doľany and Želovce.

To find out which monitored parameters caused the division of reservoirs in to the two clusters a normalized data were analysed and produced a bar graph of dissimilarities (Fig. 3).

The main parameters that differ between the two clusters are pH values, turbidity, concentrations of chlorophyll a, cyanobacterial photosynthetic pigments phycocyanin and phycoerythrin and content of fluorescent dissolved organic matter content (Fig. 3). These parameters are noticeably higher in the second cluster of water reservoirs. These results were also confirmed by the Kruskal-Wallis test (Table 6). The most significant difference were in p-values of phycocyanin (5.08E-08), phycoerythrin (1.36E-08), turbidity (4.11E-07) and chlorophyll a (2.00E-6).

In the box plots graphs (Fig. 4 – 6) are presented median, minimum and maximum values, the first and the third quartiles for the water reservoirs of the two clusters during the monitoring period.

The water reservoirs of the group 2 are similar in their character, location and purpose of usage. In these reservoirs we recorded maximum or above-average values of chlorophyll a, phycocyanin and phycoerythrin during the summer months of June, July 2020 and 2021 and September 2020.

The median values for Chl a were 9.69–64.04 µg L^{-1}, the first quartile range from 6.63 to 35.40 µg L^{-1} and the third quartile range from 11.70 to 254.69 µg L^{-1}. An overall concentrations of Chl a ranged from 5.61 to 318.23 µg L^{-1}.

The median values for BGA-PC were 1.47–13.5 µg L^{-1}, the first quartile range from 1.27 to 9.04 µg L^{-1} and the third quartile range from 1.99 to 25.18 µg L^{-1}. An overall concentrations of BGA-PC ranged from 0.75 to 32.94 µg L^{-1}.

The median values for BGA-PE were 11.94–199.76 µg L^{-1}, the first quartile range from 11.21 to 137.78 µg L^{-1} and the third quartile range from 34.61 to 250.82 µg L^{-1}. An overall concentrations of BGA-PE ranged from 10.96 to 284.68 µg L^{-1}. Concentration ranges for Chl a, phycocyanin and phycoerythrin show large fluctuations.

The median values for turbidity were 2.30–57.09 FNU, the first quartile range from 9.59 to 30.14 FNU and the third quartile range from 27.70 to 93.92 FNU. An overall concentrations of turbidity ranged from 2.90

to 117.41 FNU. The median values for pH were 8.19–8.81, the minimum was 7.74 and the maximum was 9.24. The water in the WRs of the cluster 2 is usually coloured to green during the growing season, mainly by the presence of cyanobacteria of the Microcystis species. Cyanobacteria are capable of chromatic adaptation (Chorus and Bartram eds., 1999) and therefore have no problem adapting and changing the ratio of phycocyanin and phycoerythrin in phycobilisomes, thus using a wider part of the solar spectrum (500–650 nm). Dense bloom of cyanobacteria in the WRs of the cluster 2 was accompanied by high contents of chlorophyll a, phycocyanin and phycoerythrin and also by increased pH above 9.

According to Zepernick et al. (2021), this increase in pH provides a competitive advantage to cyanobacteria, such as e.g. Microcystis aeruginosa.

Dense cyanobacterial bloom also affects penetration of light under water surface. When it decreases, it causes die-offs of plants in littoral zones while also lowering the success of predators that need light to pursue and catch prey (Lehtiniemi et al., 2005). In the water reservoirs of the second cluster were also present in substantial number invasive macrophytes Ceratophyllum demersum and Potamogeton pectinatus, but in June 2021 also rare Batrachium sp.

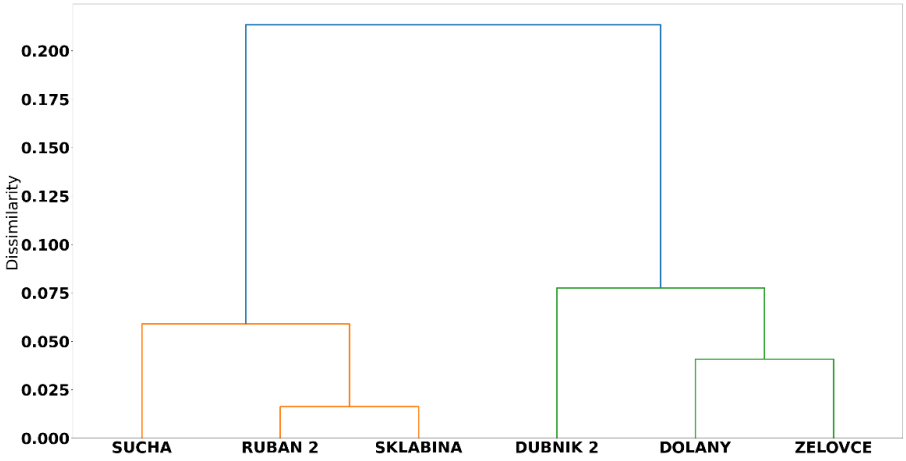

Fig. 2. Dendrogram showing similarities of water reservoirs produced by cluster analysis.

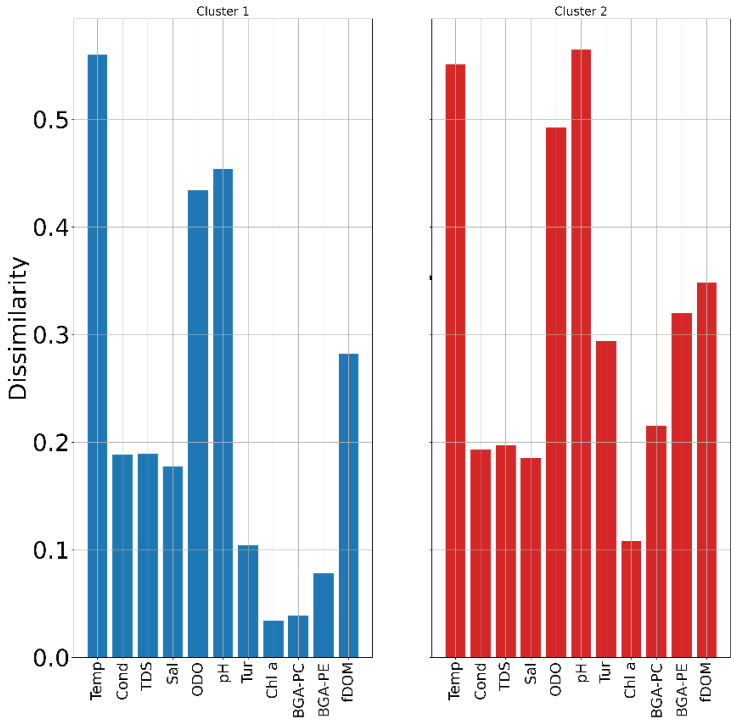

Fig. 3. Bars showing dissimilarities of water quality parameters between clusters.

Table 6. Results of Kruskal-Wallis H test presenting differences

Variable	H-test statistics	p-unc
Temperature [°C]	0.07442	0.78501
Conductivity [µS cm^{-1}]	0.14762	0.70082
TDS [mg L^{-1}]	0.14762	0.70082
Salinity [psu]	0.13629	0.71200
ODO [%sat]	2.72949	0.09851
ODO [mg L^{-1}]	2.29166	0.13007
pH	7.82945	0.00514
Turbidity [FNU]	25.64337	0.00000
Chl a [µg L^{-1}]	22.47904	0.00000
BGA-PC [µg L^{-1}]	29.68556	0.00000
BGA-PE [µg L^{-1}]	32.24752	0.00000
fDOM [RFU]	1.09217	0.29599

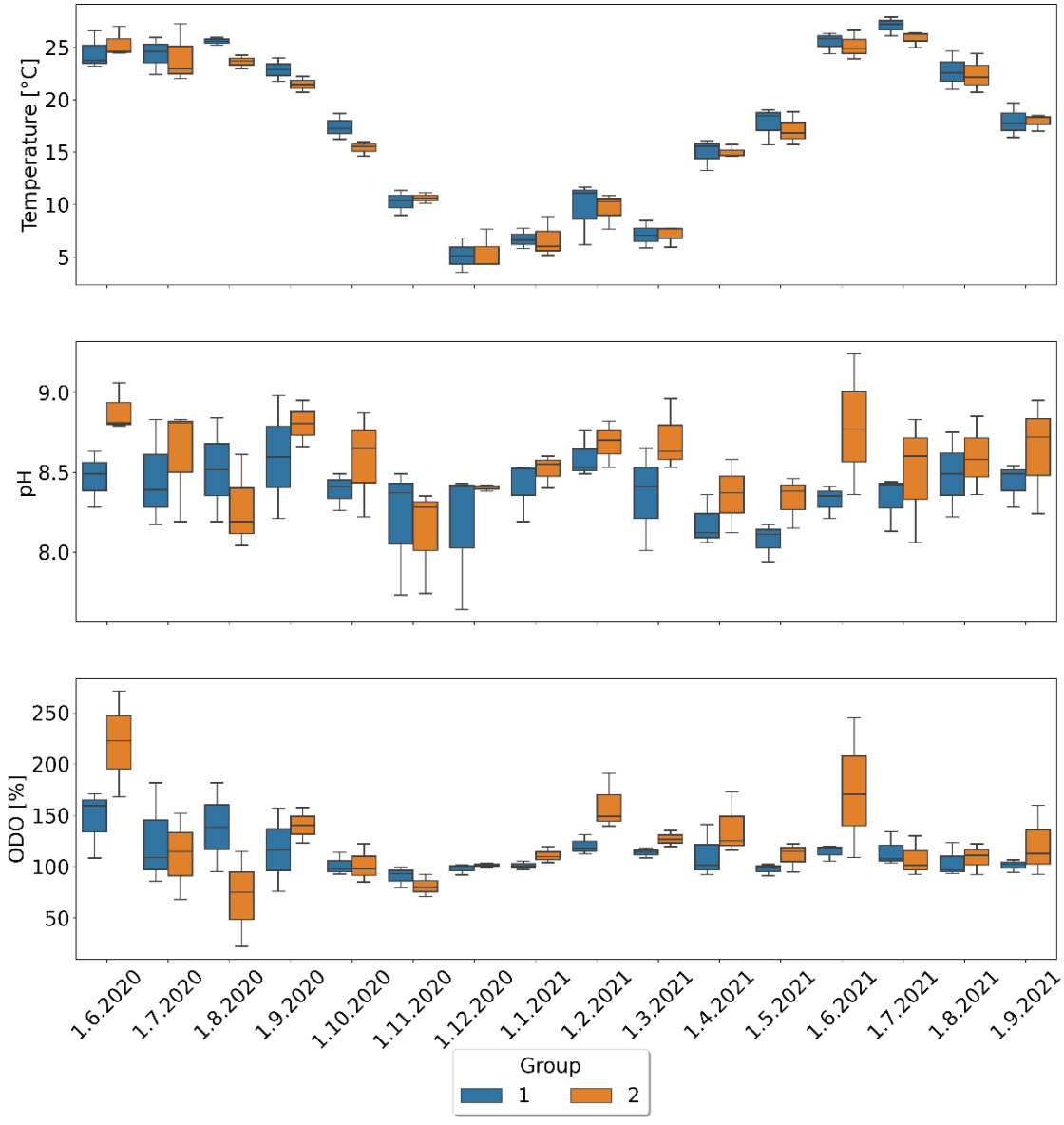

Fig. 4. Box plots showing temporal variations of water quality parameters between clusters: temperature [°C], pH, dissolved oxygen [ODO, %sat].

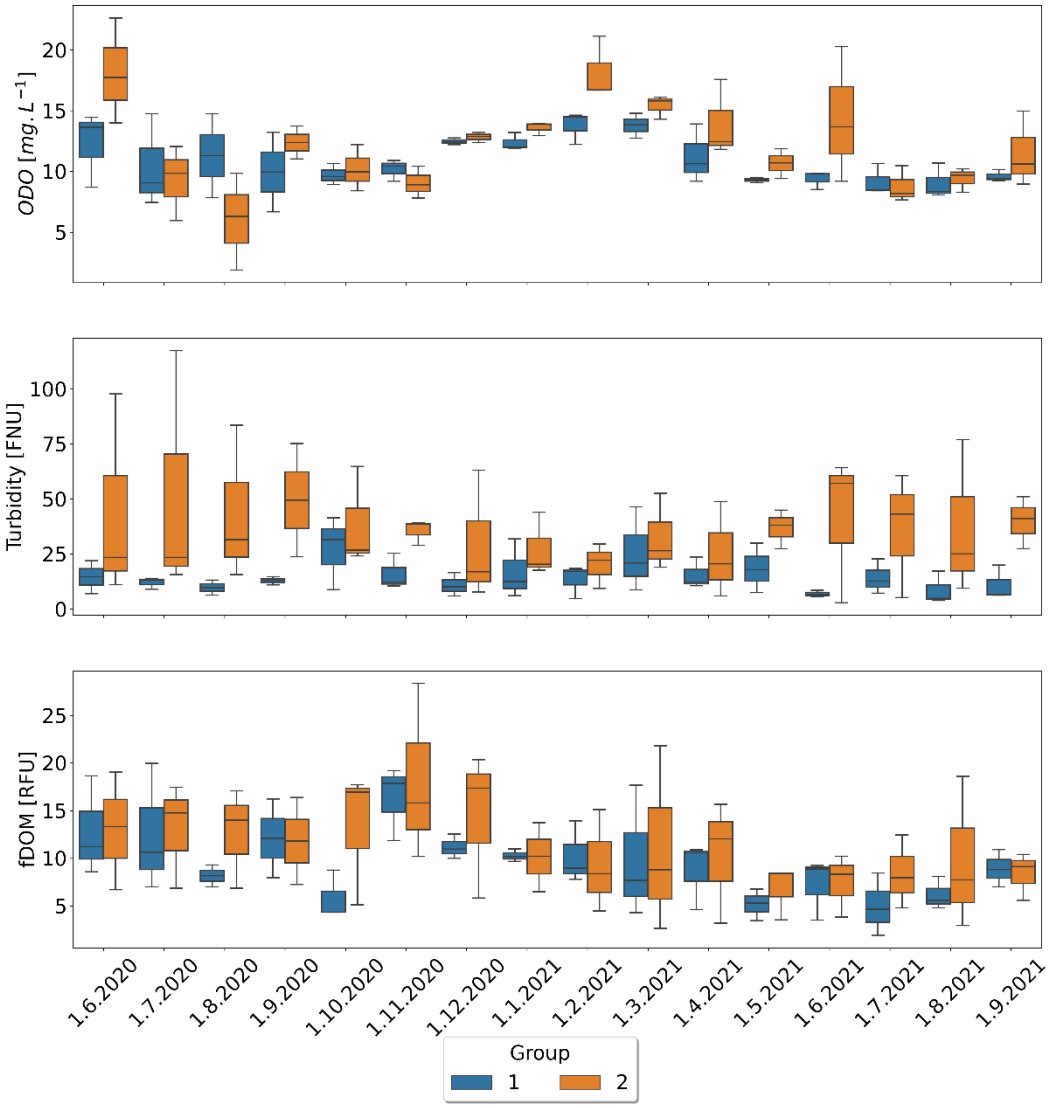

Fig. 5. Box plots showing temporal variations of water quality parameters between clusters: dissolved oxygen [ODO, mg L^{-1}], turbidity [FNU], dissolved organic matter fDOM [RFU].

The land use and land cover in the buffer zone of 500 m around the WRs (Table 2) have the influence on the water quality. For the cluster 2 the highest proportion belongs to arable soils (63.63–92.00%), less to permanent vegetations – orchards and vineyards (0.36 – 6.84 %) and meadows and pastures (3.62–10.17%). Comparing to cluster 1, the cluster 2 has very low coverage of forests ranging from 1.12 to 9,33%. Huang et al. (2020) described a positive affect of forest land buffer zone on water quality indicators. The low percentage of vegetation proper for functioning as buffer zone in cluster 2 contribute to water pollution, mostly by run-off from close arable soils. In cluster 2, the WR Dubník 2 is intensively used for recreational fishing in which fishermen feed fish individually and thereby supply extra nutrients and organic material into the reservoir.

The water reservoirs of the cluster 1 had a better water quality during the observed period, without a harmfull cyanobacterial bloom. Comparing to cluster 2 the median values for Chl a were 5.27–31.32 µg L^{-1}, the first quartile range from 4.23 to 14.78 µg L^{-1} and the third quarlite range from 7.45 to 57.17 µg L^{-1}. An overall concentrations of Chl a ranged from 2.91 to 69.81 µg L^{-1}. The median values for BGA-PC were 0.69–2.37 µg L^{-1}, the first quartile range from 0.53 to 1.89 µg L^{-1} and the third quarlite range from 0.69 to 3.1 µg L^{-1}. An overall concentrations of BGA-PC ranged from 0.17 to 3.15 µg L^{-1}.

The median values for BGA-PE were 13.68–51.43 µg L^{-1}, the first quartile range from 12.35 to 26.30 µg L^{-1} and the third quarlite range from 13.91 to 115.63µg L^{-1}. An overall concentrations of BGA-PE ranged from 8.04 to 137.02 µg L^{-1}.

The median values for turbidity were 4.84–31.52 FNU, the first quartile range from 4.17 to 14.52 FNU and the third quarlite range from 8.06 to 40.10 FNU.

An overall concentrations of turbidity ranged from 3.94 to 46.48 FNU.

The median values for pH were 8.11–8.60, the minimum was 7.64 and the maximum was 8.98.

To compare the land cover (Table 2) with the cluster 2, the WRs of the cluster 1 have lower percentage of arable soils (43.66–70.47%), a little more cover of permanent vegetatations – orchards and vineyards (0.00–10.37%), more meadows and pastures (5.11–15.17%) and higher forests cover ranging from 11.13 to 19.33%. The good water quality makes the water reservoirs of cluster 1, Sklabiná and Suchá nad Parnou, popular recreational localities.

For better interpretation of water quality in the WRs we added from June to September 2021, during the warm season when water quality is mostly endangered by cyanobacterial bloom, analysis of nitrate nitrogen, ammonium nitrogen, total nitrogen, total phosphorus and chemical oxygen demand. Table 7 presents mean values for these parameters for cluster 1 and 2.

All measured concentrations of nutrients presented in the table 7 are higher in WRs of cluster 2. According to the Directive 269/2010 Coll., annex 1A, in any sample wasn´t exceeded the concentration limit for NO^3-N, NH_4- N, TN, and TP. In water reservoirs of the cluster 2 all measured concentrations for COD exceeded limit value of 35 mg L^{-1}. Also according to the annex 2C of the Directive 269/2010 Coll. for the concentration of NH_4-N the recommended (0.15 mg L^{-1}) and the limit (0.8 mg L^{-1}) values for carp zone were not exceeded.

The measured values of the monitored parameters were also statistically processed by Spearman correlation. The obtained correlation matrix expresses the dependences among the individual monitored parameters (Fig. 7).

The values of TDS, conductivity and salinity show

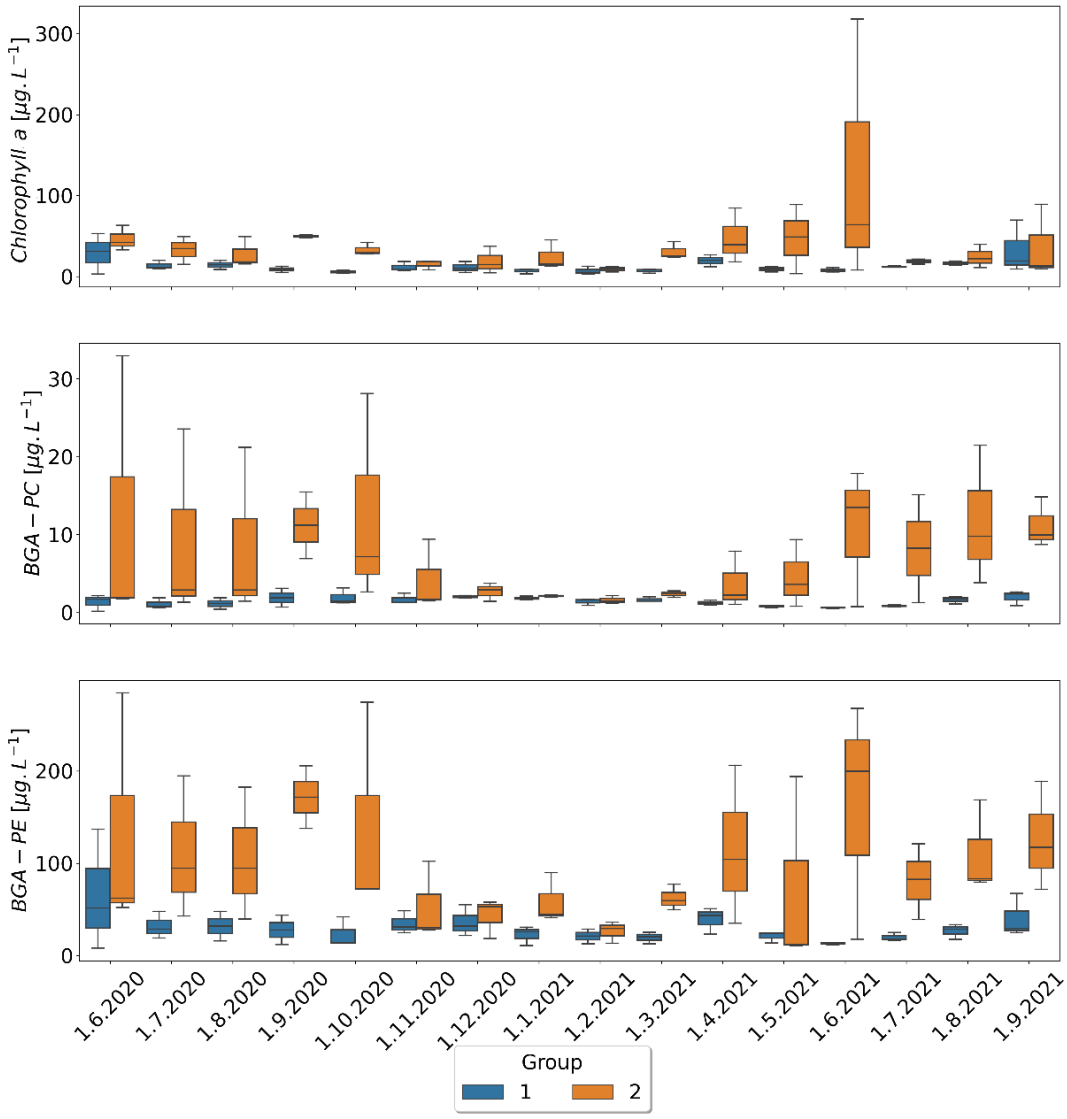

Fig. 6. Box plots showing temporal variations of water quality parameters between clusters: chlorophyll a [µg L^{-1}], phycocyain [BGA-PC, µg L^{-1}], phycoerytrin [BGA-PE, µg L^{-1}].

Table 7. **Mean values of measured concentrations of NO^3-N – nitrate nitrogen, NH_4-N – ammonium nitrogen, TN – total nitrogen, TP – total phosphorus, COD – chemical oxygen demand for cluster 1 and cluster 2**

Date	June 2021				July 2021				
Parameter	NO^3-N	NH^4-N	TN	TP	NO^3-N	NH^4-N	TN	TP	COD
Unit	[mg L^{-1}]	[mg L^{-1}]	[mg L^{-1}]	[mg L^{-1}]	[mg L^{-1}]	[mg L^{-1}]	[mg L^{-1}]	[mg L^{-1}]	[mg L^{-1}]
Cluster 1	0.222	0.018	1.142	0.139	0.192	0.012	1.094	0.069	21.150
Cluster 2	0.267	0.096	3.723	0.202	0.281	0.103	3.193	0.209	65.700

Date	August 2021					September 2021				
Parameter	NO^3-N	NH^4-N	TN	TP	COD	NO^3-N	NH^4-N	TN	TP	COD
Unit	[mg L^{-1}]	[mg L^{-1}]	[mg L^{-1}]	[mg L^{-1}]	[mg L^{-1}]	[mg L^{-1}]	[mg L^{-1}]	[mg L^{-1}]	[mg L^{-1}]	[mg L^{-1}]
Cluster 1	0.160	0.011	1.260	0.175	22.533	0.193	0.047	1.510	0.067	23.900
Cluster 2	0.269	0.058	3.493	0.279	58.833	0.247	0.122	3.380	0.270	76.200

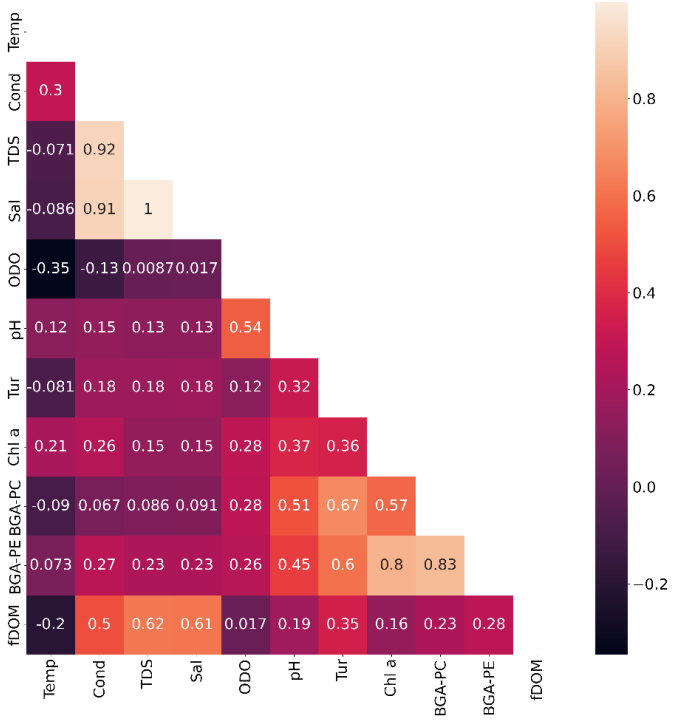

Fig. 7. *Spearman correlation matrix among individual parameters.*

the highest positive correlation. These parameters are interdependent as they are salts, and the Exo sensor uses the measured conductivity data to calculate salinity and TDS. We confirmed a high positive correlation in turbidity parameters with cyanobacterial phycocyanin and phycoerythrin. The development of a cyanobacterial bloom increases turbidity. On the contrary, turbidity with ODO shows the lowest correlation, which confirms that an increase in the number of cyanobacteria is associated with a decrease in dissolved oxygen content (Okogwu and Ugwumba, 2009). We found the highest negative correlations at ODO and temperature, which confirms the fact that with increasing water temperature, the content of dissolved oxygen decreases.

Conclusion

In our study we monitored the water quality of six small water reservoirs in agricultural landscape. To analyze the measured data we used various statistical analysis for the dataset. The cluster analysis divided the six monitored water reservoirs in to two groups (cluster 1 and 2). Analysis of normalized data revieled main parameters that caused the distribution in to two clusters: pH values, turbidity, concentrations of chlorophyll a, cyanobacterial photosynthetic pigments phycocyanin and phycoerythrin and content of fluorescent dissolved organic matter. The Kruskal-Wallis test prooved the significant differences between groups of water

reservoirs.

According to Zhou et al. (2007), Filik Iscen et al. (2008), Pejman et al. (2009) the grouping could facilitate the design of an optimal future monitoring strategy that could decrease monitoring frequency, the number of sampling, and the corresponding costs. For the WRs grouped in one cluster are suitable the same measures of improvement. These measures could be applied on other WRs with the similar characteristics.

In summary, water reservoirs of the cluster 1 had better water quality than water reservoirs of the cluster 2. The major differences were seen in concentrations of Chl a, BGA-PC, BGA-PE, turbidity and pH. The concentration ranges in the cluster 2 for Chl a, phycocyanin, phycoerytrin and turbidity showed large fluctuations. Comparison of the land cover structure of 500 m buffer zone around the water reservois pointed out the importance of buffer zone composition. For the cluster 2 the highest proportion belongs to arable soils (63.63–92.00%). Comparing the forest coverage of the buffer zones, the cluster 1 has forests on 11.13–19.33% of its area and the cluster 2 has forests only on 1.12–9.33% of the area. This agree with Huang et al. (2020) who described a positive affect of forest land buffer zone on water quality indicators.

Position of the WRs in landscape with high quality agricultural soils have a major impact on the intensity of landscape use. Intensive agriculture causes negative effects on the land, water and individual components of the environment. The basic principles of water protection in agricultural landscape require to keep good agrotechnical procedures, good agricultural practices in nutrient management, to apply nutrients only under suitable climatic conditions, to prevent application of fertilizers on steep sloping grounds and to prevent pollution by run-off. Important measure is to maintaine a minimum quantity of vegetation cover during rainy periods. According to our field survey the last requirement was usually not met.

The monitoring reservoirs were build with ground constructions with dams. Reservoirs with dams are ecosystems that accumulate biogenic substancies and various pollutants (Wiatkovski and Paul, 2009, Wiatkovski et al., 2016). Sediments serve as ultimate repository of many pollutants discharged to aquatic systems (Turner et al., 2008). Unfortified banks are one of the significant imperfections that negatively affects the quality and life in water reservoirs. Due to dynamic effect of waves on banks is released soil material and bank areas of reservoirs collapse. This trend was most significant at the WR Dubník 2. The banks of other reservoirs also require protection against the direct effects of waves by technological and biological measures, at least by adjusting the slopes, strengthening the littoral zone with aquatic, especially wetland plants or shrub vegetation. The recommended retention zone of permanent grasslands, which acts as a biological filter for sediments from the environment, should have a minimum width of 15 m (Čistý, 2005).

Reservoirs in agricultural landscape serve during the summer months as sources of water for irrigation, which have a negative impact on the state of water levels. An extra nutrient supply to reservoirs is added via fishermen feeding (corn, grain) that we found in the water. This enriches the reservoir sediments and support the cyanobacterial, algal and macrophytes development. The water in the reservoirs of the cluster 2 is usually coloured to green during the growing season, mainly by the presence of cyanobacteria of the Microcystis species.

Settlements in catchments have also considerable impact on water quality, as many of them still lack public sewerage and efficient wastewater treatment plants.

In order to maintain all the functions of water reservoirs in the landscape, it is necessary to harmonize the management of their active protection and sensitive use. Protection of water resources should become our most important responsibility.

Acknowledgement

This work was supported by the project: VEGA 2/0018/19 Ecological Analyses of Landscape Acculturation in Slovakia since Early Prehistory until Today.

References

Arocena, R., Chalar, G., Pacheco, J. P. (2018): Agriculture and elevation are the main factors for Pampasic stream habitat and water quality. Environ Monit Assess 190, 254. https://doi.org/10.1007/s10661-018-6622-6

Cohen-Bazire, G., Bryant, D. A. (1982): Phycobilisomes: composition and structure. In: N. G. Carr, N. G., Whitton, B. A. (eds.): The Biology of Cyanobacteria. Blackwell Scientific Publications, Oxford.

Council Directive 91/676/EEC of 12 December 1991 concerning the protection of waters against pollution caused by nitrates from agricultural sources. https://eur-lex.europa.eu/legal-content/EN/ALL/?uri=celex%3A31991L0676

Čistý, M. (2005): Rybníky a malé vodné nádrže II. STU Bratislava, Bratislava. ISBN 80-227-2294-4

Directive of the Government of the Slovak Republic No. 269/2010 Coll. defining requirements for achievment of good water status. http://www.zakonypreludi.sk/zz/2010-269

Filik Iscen, C., Emiroglu, Ö., Ilhan, S. et al. (2008): Application of multivariate statistical techniques in the assessment of surface water quality in Uluabat Lake, Turkey. Environ Monit Assess 144, 269–276. https://doi.org/10.1007/s10661-007-9989-3

Hindák, F. (2001): Fotografický atlas mikroskopických siníc. Veda, Bratislava.

Ignatius, A. R., Rasmussen, T. C (2016): Small reservoir effects on headwater water quality in the rural-urban fringe, Georgia Piedmont, USA. Journal of Hydrology: Regional Studies, 8, 145–161. https://doi.org/10.1016/j.ejrh.2016.08.005

Higgins, P. (2014): Environmental Dissolved Oxygen Values Above 100% Air Saturation. https://www.ysi.com/ysi-blog/water-blogged-blog/2014/06/environmental-dissolved-oxygen-values-above-100-air-saturation

Huang, W., Mao, J., Zhu, D.; Lin, C. (2020): Impacts of Land Use and Land Cover on Water Quality at Multiple Buffer-Zone Scales in a Lakeside City. Water 2020, 12, 47. https://doi.org/10.3390/w12010047

Huang, J., Yin, H.; Chapra, S. C.; Zhou, Q. (2017): Modelling

Dissolved Oxygen Depression in an Urban River in China. Water 2017, 9, 520. https://doi.org/10.3390/w9070520

Huisman, J., Codd, G. A., Paerl, H. W., Ibelings, B. W. Verspagen, J. M. H., Visser, P. M. (2018): Cyanobacterial blooms. Nat Rev Microbiol 16, 471–483 https://doi.org/10.1038/s41579-018-0040-1

Chorus, I., Bartram, J. eds. (1999): Toxic Cyanobacteria in Water: A guide to their public health consequences, monitoring and management. WHO. ISBN 0-419-23930-8. doi: https://www.who.int/water_sanitation_health/resourcesquality/toxcyanbegin.pdf

Jurik, Ľ., Húska, D., Halászová, K., Bandlerová, A. (2015): Small water reservoirs – sources of water or problems. Journal of Ecological Engineering, vol. 16, no.4, 22–28. https://doi.org/10.12911/22998993/69348

Kowalczewska-Madura K, Kozak A, Kuczyńska-Kippen N, Dondajewska-Pielka R, Gołdyn R. (2022): Sustainable Restoration as a Tool for the Improvement of Water Quality in a Shallow, Hypertrophic Lake. Water. 2022; 14(7):1005. https://doi.org/10.3390/w14071005

Krengel, F., Bernhofer, C., Chalov, S., Efmov, V., Efmova, L., Gorbachova, L., et al. (2018): Challenges for transboundary river management in Eastern Europe – three case studies. Journal of the Geographical Society of Berlin, 149(2–3), 157–172. https://doi.org/10.12854/erde-2018-389.

Kriška Dunajský, M., Pumprlová Němcová, M., Konečná J., Karásek, P., Podhrázska, J. (2018): Possibilities of Small Water Reservoir Impact Improvement on Surface Water Quality in Agricultural Landscape. Acta Universitatis Agriculturae et Silviculturae Mendelianae Brunensis, 66, 1, 77–87. https://doi.org/10.11118/actaun201866010077

Kruskal, W. H, Wallis, W. A. (1952): Use of ranks in one-criterion variance analysis. Journal of the American Statistical Association. 47 (260): 583–621. doi:10.1080/01621459.1952.10483441

Lehtiniemi, M. et al. (2005): Turbidity decreases anti-predator behaviour in pike larvae, Esox Lucius. Environmental Biology of Fishes 73, 1-8. https://doi.org/10.1007/s10641-004-5568-4

Li, H., Liu, L., Ji, X. (2015): Modeling the relationship between landscape characteristics and water quality in a typical highly intensive agricultural small watershed, Dongting lake basin, south central China. Environmental Monitoring Assessment, 187, doi: 10.1007/s10661-015-4349-1

McKenna Jr., J.E. (2003): An Enhanced Cluster Analysis Program with Bootstrap Significance Testing for Ecological Community Analysis. Environmental Modelling & Software, 18, 205–220. http://dx.doi.org/10.1016/S1364-8152(02)00094-4

Noskovič, J., Babošová, M., Porhajašová, J. (2013): Concetration of oxygen dissolved in Water Nature Reserve Alúvium Žitavy in the southwestern part of Slovak Republic. Folia Oecologica, 40, 1, 78–83

Okogwu, O. I, Ugwumba, A. O. (2009): Cyanobacteria abundance and its relationship to water quality in the Mid-Cross River floodplain, Nigeria. Revista de Biologia Tropical, 57(1–2): 33–43. https://doi.org/10.15517/rbt.v57i1-2.11288.

Ormerod, S.J., Dobson, M., Hildrew, A.G. and Townsend, C.R. (2010): Multiple stressors in freshwater ecosystems. Freshwater Biology, 55: 1–4. https://doi.org/10.1111/j.1365-2427.2009.02395.x

Pejman, A. H., Bidhendi, G. R. N., Karbassi, A. R. et al. (2009): Evaluation of spatial and seasonal variations in surface water quality using multivariate statistical techniques. Int. J. Environ. Sci. Technol. 6, 467–476. https://doi.org/10.1007/BF03326086

Pekárová, P., Velísková, Y. (1998): Modelovanie kvality vody v povodí Ondavy. Veda, Bratislava.

Sebíň, M. (2007): Vplyv využitia krajiny na kvalitu vody v toku v poľnohospodársky využívanom a zalesnenom mikropovodí. Acta hydrologica Slovaca, 8, 1, 22–28

Szczykowska, J., Siemieniuk, A. (2014): The present condition of small water retention and the prospects of its development using the example of the Podlaskie Voivodeship. Journal of Ecological Engineering, vol. 15, no. 3, 90–96. https://doi.org/10.12911/22998993.1109130

Shapiro, S. S.; Wilk, M. B. (1965): An analysis of variance test for normality (complete samples). Biometrika. 52 (3–4): 591–611. https://doi.org/10.1093/biomet/52.3-4.591.

Shrestha, S., Kazama, F. (2007): Assessment of Surface Water Quality Using Multivariate Statistical Techniques: A Case Study of the Fuji River Basin, Japan. Environmental Modelling and Software, 22, 464–475. http://dx.doi.org/10.1016/j.envsoft.2006.02.001

Spearman, C. (1904): The proof and measurement of association between two things. American Journal of Psychol. 15 (1): 72–101. https://doi.org/10.2307/ 1412159

Turner, R. E., Rabalais, N. N., Justic, D. (2008): Gulf of mexico hypoxia: Alternate states and a legacy. Environ. Sci. Technol., 42, 2323–2327

UNESCO, UN-Water (2020): United Nations World Water Development Report 2020: Water and Climate Change, Paris, UNESCO

Wiatkowski, M., Paul, L. (2009): Surface Water Quality Assessment in the Troja River Catchment in the Context of Włodzienin Reservoir Construction. Polish Journal of Environmental Studies. 18. 923–929.

Wiatkowski, M., Rosik-Dulewska, C. (2016): Hydrological and hydraulic conditions for a construction of a pre-dam reservoir in the słup reservoir backwater. Rocznik Ochrona Srodowiska. 18. 468–479.

Zepernick, B. N, Gann, E. R, Martin, R. M, Pound, H. L, Krausfeldt, L. E, Chaffin, J. D., Wilhelm, S. W. (2021): Elevated pH Conditions Associated With Microcystis spp. Blooms Decrease Viability of the Cultured Diatom Fragilaria crotonensis and Natural Diatoms in Lake Erie. Front. Microbiol. 12: 598736. https://doi.org/10.3389/fmicb.2021.598736.

Zhou, F., Liu, Y., Guo, H. (2007): Application of Multivariate Statistical Methods to Water Quality Assessment of the Watercourses in Northwestern New Territories, Hong Kong. Environ Monit Assess 132, 1–13. https://doi.org/10.1007/s10661-006-9497-x

RNDr. Jana Borovská, PhD. (*corresponding author, e-mail: jana.borovska@savba.sk)
Mgr. Tomáš Rusňák, PhD.
Ing. Matej Mojses, PhD.
Institute of Landscape Ecology SAS
Akademická 2, 949 01 Nitra
Slovak Republic

DOI: 10.31577/ahs-2022-0023.01.0014

ACTA HYDROLOGICA SLOVACA

Volume 23, No. 1, 2022, 130 – 139

Estimation of limitations for groundwater recharge using the example of the Sarden site in Syria

Abdulnaser ALDARIR, Thomas FICHTNER, Ian Desmond GWIADOWSKI, René BLANKENBURG, Peter-Wolfgang GRAEBER*

Groundwater is the main source of all renewable water resources for drinking and irrigation water in most arid and semi-arid areas. However, groundwater abstraction by pumping has increased in most areas significantly, leading to a lowering of the groundwater level. Managed aquifer recharge is a measure to prevent or counteract these temporary and permanent groundwater declines and their negative effects.

The work described here deals with the numerical simulation of treated wastewater infiltration for improving the local groundwater balance in the catchment area of Sarden village, Syria. The semi-arid region is characterized by shallow silty clay soils, limestone cliffs and karst aquifers. Different model setups were built up by means of the software PCSiWaPro simulating the effects of different boundary conditions on the saturation conditions in the vadose zone. This should enable an initial assessment of whether and under what conditions the installation of an infiltration system is possible.

Results of the research are showing that the hydraulic conditions in the unsaturated soil zone at the site are influenced most by the groundwater level and the number of trenches used for infiltration, whereas precipitation events are playing a subordinate role. In case of elevated groundwater level and too low number of infiltration trenches, the water can rise up to or in the infiltration trenches.

KEY WORDS: recharge of groundwater, treated wastewater infiltration, infiltration trenches, numerical model

Introduction

At present, an increasing water scarcity in different parts of the world is observed caused by rapid population growth and the consequences of climate change. The supply of freshwater from groundwater and surface water sources is limited and cannot meet the growing demand (Food and Agriculture Organization of the United Nations, 2018; Gleeson et al., 2012; Wada et al., 2010; Yaghi et al., 2016). Furthermore, discharge of urban sewage, the missing sewage network and generally poor living conditions have led to a deterioration in surface and groundwater quality in many developing countries (Wild et al., 2007).

Also in the semi-arid country Syria, high population growth and accelerated urbanization have increased the demand for water and led to a continuous depletion of water resources, which endangers their long-term sustainability (Berndtsson and Mourad, 2012). The results of a study in north Syria, Sarden region showed that groundwater pumping leads to a long-term decrease in groundwater levels, particularly in the dry season (Bananah, 2016).

In this case, managed aquifer recharge or artificial groundwater recharge (MAR) can be used to prevent or counteract temporary and permanent water scarcity problems by infiltrating excess surface waters (Casanova et al., 2016; Dillon et al., 2009). One opportunity here is the use of wastewater treated by preliminary treatment stage. The following infiltration of this water in the course of recharge can reduce the pressure on freshwater resources, such as groundwater, especially in arid and semi-arid areas (Bouwer, 2002; Dillon et al., 2009; Heidarpour et al., 2007).

At the moment, however, large amounts of untreated or inadequately treated wastewater are used in developing countries by farmers for irrigation, which raises concerns about public health and the environment. This situation requires rethinking the way wastewater has to be treated and reused (Manzoor, 2007; Scheffer et al., 2003). Especially in areas where the construction of a sewage collection system is not considered economically viable, reuse of water treated by decentralized treatment systems for infiltration can be an option. As a result, direct infiltration into the ground contributes to controlling the sustainable recharge of an aquifer and attempts to maintain a constant groundwater level. The decentralized wastewater treatment and disposal for rural regions has

been already studied, e.g., in the Kingdom of Jordan (Van Afferden et al., 2015) and many other areas worldwide (Händel et al., 2018).

These sustainable decentralized treatment systems are focusing on the on-site treatment and recycling of resources contained in domestic wastewater (Capodaglio et al., 2017). For the following reuse of treated wastewater various techniques are used (Asano and Cotruvo, 2004). On the one hand, the discharge of treated wastewater occurs into surface waters, such as rivers or streams. On the other hand, the disposal of the treated wastewater effluent takes place by direct infiltration into the soil by means of infiltration elements such as soakaways, trenches, drainage pipes or swales (Sieker, 1998; Shuster et al., 2010). Here, the quality of treated wastewater effluent can be improved before reaching the aquifer by the processes of filtration, absorption and biodegradation in the aerated unsaturated soil zone (Martins et al., 2017; Morales et al., 2016; Nema et al., 2001, Reemtsma et al., 2000; Zhang et al., 2007). However, using the treated wastewater harbours risks, because pollutants can reach the aquifer (Bekele et al., 2018; Burger and Čelková, 2005).

For the planning and dimensioning of such infiltration systems, it is necessary to understand the taking place processes below the infiltration system depending on the geohydraulic properties of the unsaturated and saturated parts of the aquifer as well as operational parameters of the system such as infiltration rates or the infiltration cycle (Alam et al. 2021; Bouwer, 2002; Lyman et al., 1992; Meikle et al., 1995). Especially, the variation of water saturation respectively the aeration in the subsurface zone is of particular importance due to its importance for the purification of the infiltrated water. Optimal conditions can be ensured by avoiding fully saturated conditions in the soil below the infiltration system.

Numerical models can be used to take a closer look at these processes and to assess the influence of different boundary conditions on the hydraulic conditions below the infiltration system (Krug, 2001). Therefore, a large number of scenarios with different boundary conditions for the Sarden site were performed to eliminate some uncertainties regarding the future use of treated wastewater for the application of artificial groundwater recharge.

The results of the study should provide answers to the following questions:

- Is the Sarden site suitable for infiltrating treated wastewater by trenches in terms of quantity?
- How are the hydraulic conditions below the infiltration system influenced by the boundary conditions groundwater level, precipitation and the number of trenches?
- How does the infiltration influence the saturation of the vadose zone below the infiltration system?
- Is the infiltration influencing the groundwater level?

Material and methods

Study area

The study area "Sarden plain" is located in a catchment area covering around 44 km^2, whereby the "Sarden plain" itself covers an area of approx. 7 km^2. It is located in a semi-arid area in north-western Syria (50 km west of Aleppo) between 36° 06'–36° 11' latitude and 36° 33'–36° 38' longitude and represents a secondary catchment area of the Orontes Basin (Fig. 1). According to topographic reliefs, the highest elevation in the basin is 825 m above sea level, the lowest point is at 437 m above sea level. The climate is semi-arid/Mediterranean with hot, dry summers and cool, humid winters (Farahani et al., 2009). The precipitation varies between 290 mm per year in dry years and 750 mm per year in wet years and 564 mm per year as the mean precipitation, which begins in October and extends to April. The potential evapotranspiration is between 1200 mm per year and 1800 mm per year. The natural infiltration rate in the catchment area was estimated at 55% of the average annual precipitation, which corresponds to an annual value of 310 mm (Bananah, 2016).

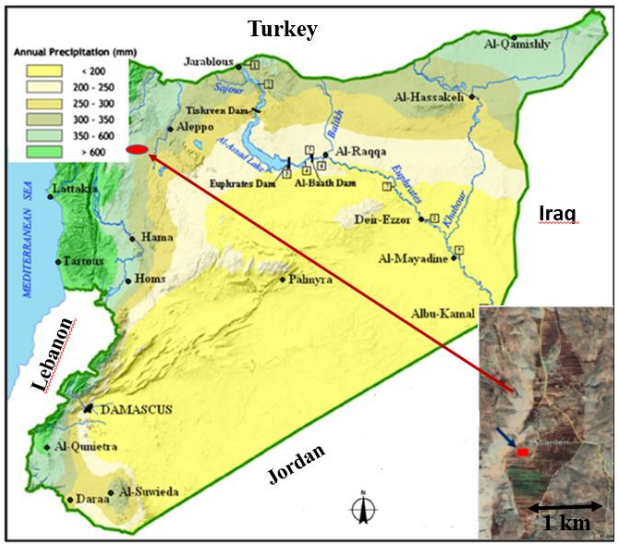

Fig. 1. Study area of the Sarden Plain (Google, 2022).

The dominant type of geological formations in the study area is the Neogene including the middle Helvetians, composed of biogenic sediments along with limestone rocks (Abbas et al., 2015; Brew et al., 2001). The upper soil layer consists of loamy-silt soil and is poor in organic matter (Bananah 2016).

There are three villages in the Sarden plain with a total of about 3600 inhabitants. The village of Sarden, located in the middle of the plain, was chosen as the location for the study. Around 500 people are living permanently in the village. However, in summer (June to August), the population temporarily increases to around 900 people. At the moment, there is no effective wastewater treatment plant in the three villages. However, groundwater recharge by using treated wastewater could be a final step in solving the problems regarding the quantity and quality of water in the Sarden plain.

Numerical investigation

Simulation program PCSiWaPro

The realized simulations were carried out with the help of the simulation software PCSiWaPro, developed at the Technical University of Dresden, Institute for Waste Management and Contaminated Sites Treatment (Gräber et al., 2006). The program is based on the SWMS-2D program, developed by Šimůnek and van Genuchten (1994). The program is accordingly applicable to problems in variably saturated porous media, i.e. under unsaturated to fully saturated conditions. Two-dimensional models can be realized, by applying Richards-equation (Richards, 1931) for unsaturated flow and Mualem-van-Genuchten retention and relative hydraulic conductivity model (Mualem, 1976; Schaap and van Genuchten, 2006).

Model setup

A two-dimensional numerical model with the dimensions of 80.2 m (width) and 30 m (height) was built up for simulating the quantities of treated wastewater and precipitation to be potentially infiltrated in the future (Fig. 2). The cross-section of the trenches and the saturated and unsaturated soil zone is represented by 42,500 nodes in total. Discretization is carried out using the finite element method, with irregular triangular structures being used in the areas with the high pressure gradients to be expected and geometric discontinuities (e.g. trench area) are designed with a correspondingly close mesh.

The thickness of the aquifer is assumed with 30 m. The groundwater level is set at 10 m below ground surface (GWL10m) in a first variant, in another variant the groundwater level is set at 6 m below ground surface (GWL6m).

For the infiltration of the water, 8 infiltration trenches were implemented in the first variant (Fig. 2a), in another variant the infiltration was carried out by means of 17 infiltration trenches (Fig. 2c). The distance between the trenches is 5 m in the model with 8 trenches and 2.5 m for the model with 17 trenches. The height of the trenches is set at 0.5 m and the width at 0.6 m. The model boundary was defined based on estimates of the transverse distribution of the water flow respectively the range of the infiltration front. Thus, the distance between the outer trenches and the boundary of the model is 20.2 m in the system with 8 trenches and 15 m in the system with 17 trenches.

The inflow of treated wastewater and precipitation to the trenches is defined as a boundary condition of the second type with a time-dependent, variable inflow. The area between and around the trenches was also provided with a boundary condition of the second type, only precipitation infiltrates here. The lower border of the model representing the boundary to an impermeable storage layer as well as the lateral borders above the saturated zone are defined as no-flow boundary condition. The outflow from the model is regulated at the left and right border by a boundary condition of the first type.

The amount of treated wastewater to be infiltrated by means of trenches is 80 litres per inhabitant and day, which results is 40,000 l/d for 500 people (September to May) and 72,000 l/d for 900 people (June to August). The simulated period is 365 days in total, which includes the periods of low and high treated wastewater accumulation. The distribution of these volumes over the day occurred according to the hydrograph of the daily water consumption (DIN EN 12566-3, Deutsches Institut für Normung e.V., 2016). The infiltration of the resulting treated wastewater sum in the model was realized every 6 hours, which corresponds to the time step intervals of the model. Thus, a realistic infiltration pattern with increased wastewater accumulation in the morning and evening hours of a day was realized. The precipitation infiltration was implemented as a variable, time-dependent flux boundary condition using the precipitation hydrographs of years with average annual precipitation (560 mm) and years with high precipitation (750 mm) (Syrian Ministry of Agriculture and Agrarian Reforms, 2013).

An evaluation of the infiltration process taking into account the different boundary conditions should be carried out based on the simulated water contents in the implemented observation points and based on the groundwater levels. Therefore, 14 observation points for the model with 8 infiltration trenches and 21 observation points for the model with 17 infiltration trenches were implemented (Fig. 2b and 2d).

The specific soil hydraulic parameters from on-site measurements were not available. Based on large-scale geological maps, it was defined that the upper soil zone consists of loamy silt. The entire soil zone, except the area around the trenches, is assumed to be a homogeneous, isotropic layer with a saturated hydraulic conductivity of around 5×10^{-6} m s^{-1}. The material around the trenches is defined as coarse sand with a hydraulic conductivity of around 2.5×10^{-4} m s^{-1}. The retention parameters of the soils are assumed according to DIN 4220, Deutsches Institut für Normung e.V., 2008 (Table 1).

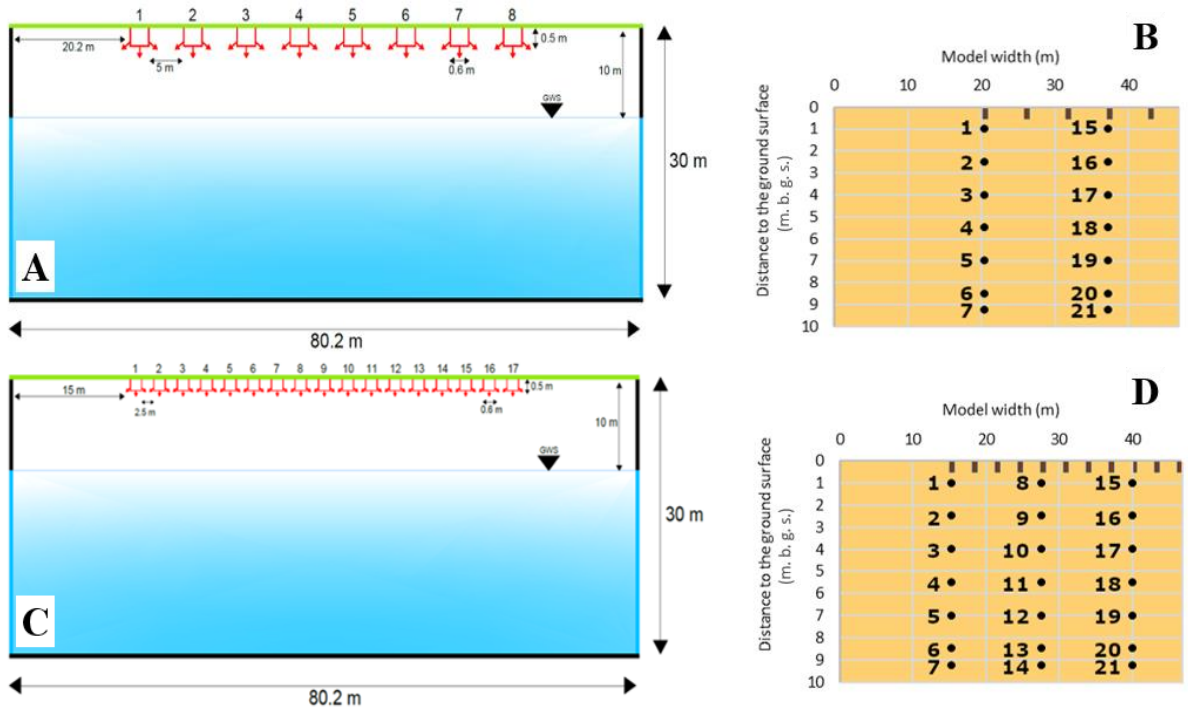

Fig. 2. Conceptual model of the infiltration systems with 8 trenches (a) and 17 trenches (b) for the Sarden site; location of the observation points (MP) in the cross-section of the model below 8 trenches (c) and 17 trenches (d).

Table 1. Hydraulic parameters of the used soil materials

	Aquifer	Area around the trench
Saturated hydraulic conductivity K [m s^{-1}]	5 x 10^{-6}	2.5 x 10^{-4}
Residual water content Θ_r [m³ m^{-3}]	0.05	0.0
Saturated water content Θ_s [m³ m^{-3}]	0.40	0.38
van Genuchten shape parameter n [-]	1.35	1.47
van Genuchten shape parameter a [m^{-1}]	1.70	22.1

The simulation results were first fundamentally checked for plausibility using the information on numerical stability (balance error, iterations per time step) supported by the PCSiWaPro program.

Results and discussion

General insights

Parameter adjustments within different scenarios can lead to significant changes in the simulated water content. During the evaluation, however, it was possible to obtain findings, which apply independently of the simulation variants considered.

All determined water content curves can be divided into four phases (Fig. 3a and 3b). In the short first phase, the short-term settling process of the numerical model can be observed. In the second phase, which begins within the first month November and lasts until the end of May, changes in the water content are caused by the infiltration of water from precipitation events instead of by the inflow of treated wastewater. In the third phase (June to August) the water content is significantly increasing and remaining at a constant level due to the higher inflow of treated wastewater caused by the higher number of inhabitants in summer. Phase four (September to October) shows the same behaviour as phase two.

With the displayed water contents at observation point 15 (Fig. 3a), which is located directly below the central infiltration trench, for the two chosen scenarios in Fig. 3a (8 trenches, GWL6m, increased annual precipitation/17 trenches, GWL10m, average annual precipitation) the full range of water content values and the biggest discrepancy in the water content curves for all scenarios are visualized.

When looking at the groundwater level below the trenches (Fig. 3c), it becomes clear that not only the water content at the observation points increases as a result of the treated wastewater infiltration. By comparing the groundwater levels in the time with reduced (end of May, runtime 211 days) as well as

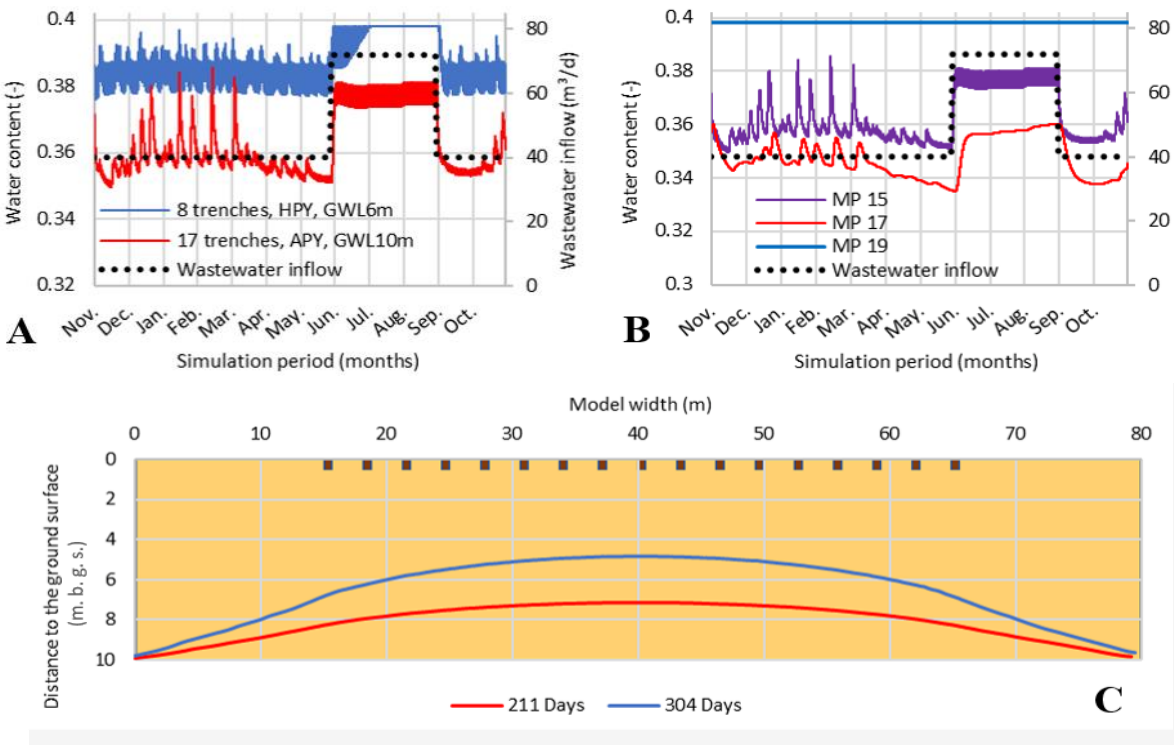

Fig. 3. Water content at observation point 15 for two different scenarios with best and worst-case conditions (a); water content at several observation points (MP15, 17, 19) below the central trench (trench 9 of 17) in the model with 17 trenches during a year with average annual precipitation and assumed groundwater level GWL10m (b); groundwater level below the 17 trenches before the summer (end of May, runtime 211 d) and at the end of summer (end of August, runtime 304 d) with initial groundwater level GWL10m and average annual precipitation (c).

increased treated wastewater infiltration (end of August, runtime 304 days), it can be seen that groundwater level rises up to 2 m below the infiltration system due to the increase in the infiltration of treated wastewater.
Also, the effects of the infiltration process can be observed in the water content curves of the observation points (Fig. 3b). Due to the lateral expansion during the infiltration process, the infiltrated wastewater is distributed over the entire area below the trenches. For this reason, a zone forms in the soil (see MP 17 in Fig. 3b) in which neither the water content of the area directly below the trenches (see MP 15) nor the water content of the saturated zone (see MP 20) is reached.

Influence of groundwater levels

In order to assess the influence of the groundwater level on hydraulics in the unsaturated soil zone, two different scenarios for the model with 17 trenches were performed. In case of the GWL6m scenario, all observation points that are deeper than 6 m below ground surface (Fig. 2d, points 5, 6, 7, 12,13, 14, 19, 20, 21) are located in the groundwater from the start. The difference is also clear at observation points that are above the elevated groundwater level. As can be seen in Fig. 4a, the water content curves differ significantly at observation point 16 (2.5 m below ground surface).
Due to the chosen initial conditions for both model variants, the initial water content in the scenario GWL6m is higher than in the scenario GWL10m. In December, the two hydrographs came closer, because during this period, observation point 16 is not yet influenced by the increased groundwater level in scenario GWL6m. Observation point 16 in scenario GWL6m reaches the maximum water content in December due to intense precipitation events in combination with the infiltration of treated wastewater. At this time, the groundwater level has risen to such an extent, that MP 16 is under the groundwater level. In the scenario GWL10m, there is only a significantly smaller temporary increase in the water content, since the measuring point here is outside the area of direct influence of the groundwater level.
In February, the average water content is differing by around 0.044. This corresponds to a saturation difference of around 11%. The water content decreases again from the middle of March in scenario GWL6m and approaches the water content curve from scenario GWL10m due to lower precipitation amounts and the resulting decrease in the groundwater level.
The groundwater levels rise again in the summer period (June to August) with an increased inflow of wastewater

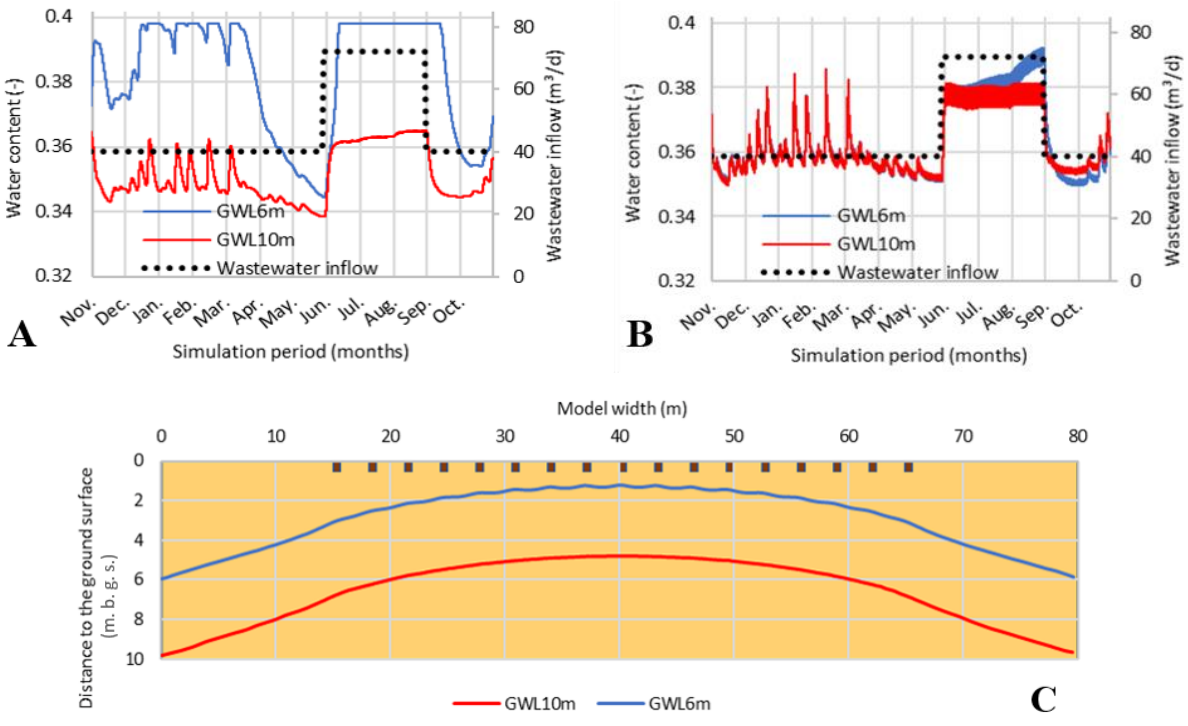

Fig. 4. Water content at observation point 16 for different initial groundwater levels for a year with average annual precipitation (a); water content at observation point 15 for different initial groundwater levels for a year with average annual precipitation 15 (b); groundwater level at the end of summer (end of August, runtime 304 d) for different initial groundwater levels and average annual precipitation (c).

caused by the higher number of inhabitants (Fig. 3c). During this period, the groundwater level in scenario GWL6m rises above observation point 16 (Fig. 4c) causing fully saturated conditions with a constant very high water content until the infiltrated amount of treated wastewater is decreasing in September. In this time, the groundwater level in scenario GWL10m in the center of the system is 4 m lower than in scenario GWL6m, so that the saturation at the observation point does not exceed a value of 92%.

The rise in groundwater during the summer up to around 1.2 m below ground surface is also influencing observation point 15 (Fig. 4b). After the water contents for both scenarios are the same from the beginning in November until June, there is an increase in the water content in scenario GWL6m due to the proximity to the groundwater level. However, fully saturated conditions are not reached.

A rise of the groundwater level up to the trenches was not observed for both scenarios (GWL10m, GWL6m) at any point in time. Nevertheless, the influence of the increased groundwater level on the saturation conditions (Fig. 4a and 4b) and the representative groundwater level (Fig. 4c) can be proven.

Influence of annual precipitation

As previously described, the average annual precipitation in the study area is around 560 mm. However, since up to 750 mm of precipitation must be planned for a year with high precipitation, the influence of the corresponding annual precipitation hydrographs on the hydraulic conditions in the unsaturated zone should be investigated. For this purpose, the water contents at observation point 15 for the model with 17 trenches were evaluated (Fig. 5a).

Despite a difference of around 190 mm per year between the amount of annual precipitation, there are only minor effects on the observed water contents at the observation points. The primary difference is caused by the different distribution of the precipitation over the year due to different precipitation events. This can be observed from the different temporary increases in water content. The water content in the summer months June, July and August is only influenced by the increased sewage inflow, because no precipitation events were recorded in the average year from May to September (Fig. 5b).

Influence of the number of trenches

After examining the influence of the factors precipitation and groundwater level on the hydraulic conditions in the unsaturated soil zone, the two potential infiltration system concepts (8/17 trenches) are compared for a year with high precipitation and an elevated groundwater level at 6 m below the ground surface. The focus here is on

process reliability and thus the question of whether the treated wastewater will rise up in or even above the trenches. It can be shown that the water content for the concept with 8 trenches is constantly above the curve of the system with 17 trenches system (Fig. 6a).

The discrepancy between the mean annual water content

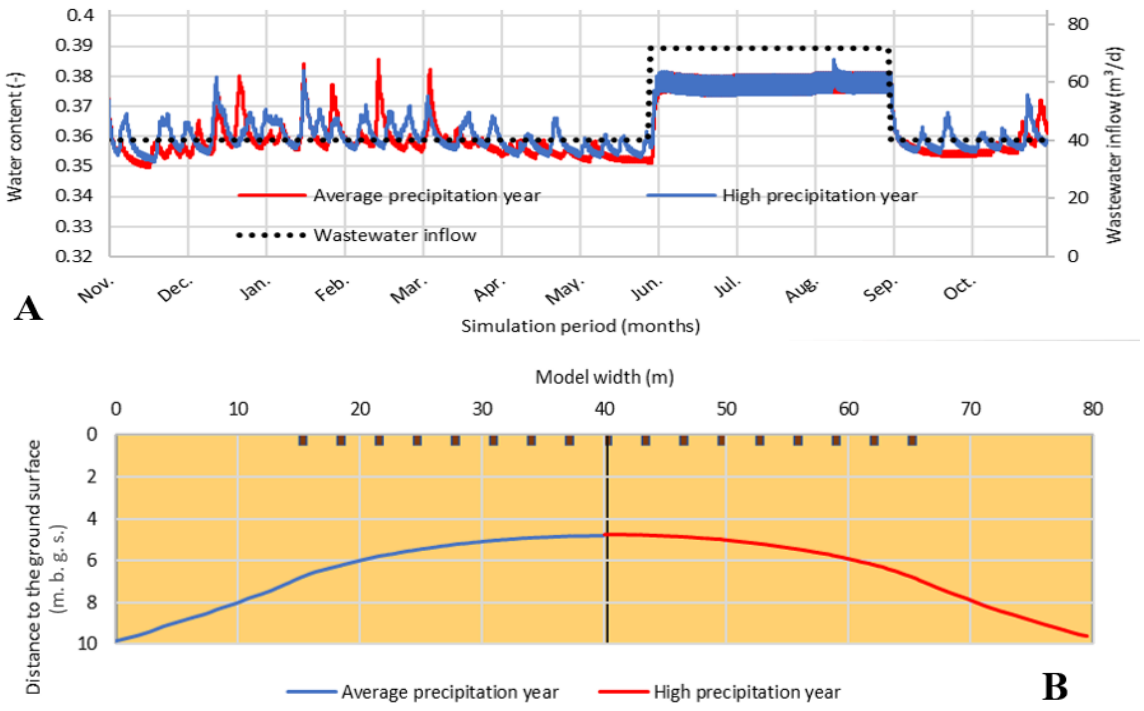

Fig. 5. Simulated water content at observation point 15 for two different annual precipitation hydrographs (a); groundwater level - left: in the average year, right: in the year with high precipitation (b).

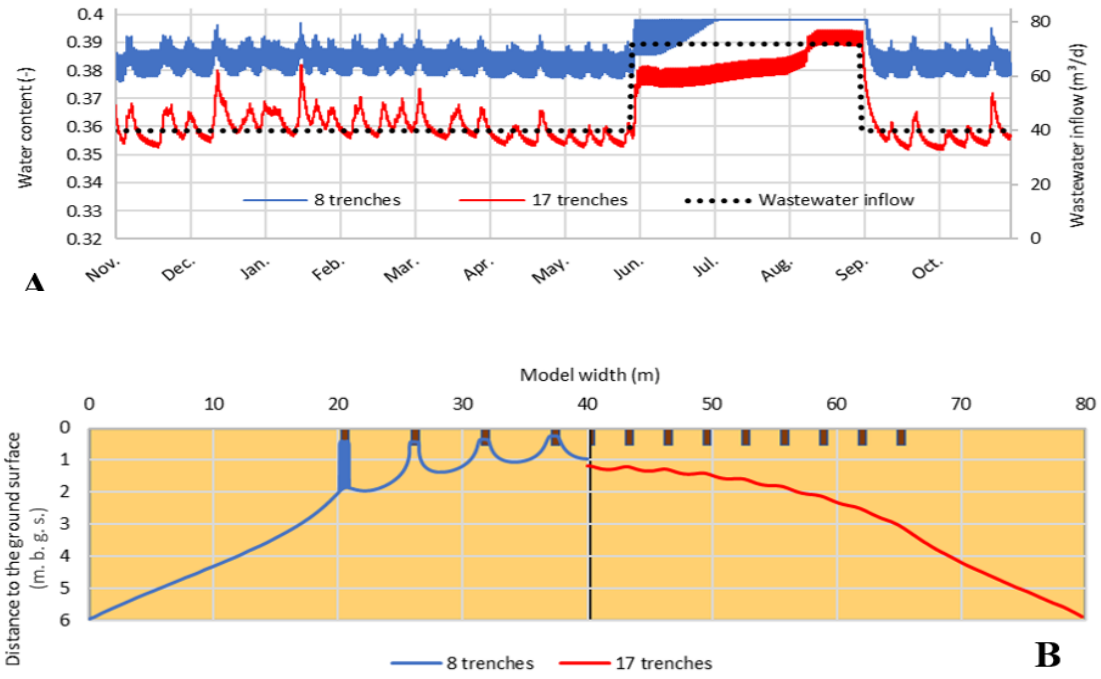

Fig. 6. Simulated water content at observation point 15 using 8 or 17 trenches for infiltration for a year with high precipitation and elevated groundwater level (a); groundwater level at the end of summer (end of August, runtime 304 d) - left: usage of 8 trenches, right: usage of 17 trenches (b).

is around 0.021, which corresponds to a mean saturation difference of around 5.3%. In addition, the maximum water content is constant at the measuring point below the 8 trenches in July and August, while the maximum water content is never reached at the measuring point below the 17 trenches.

There are two reasons for this observation. On the one hand, the inflow per trench is higher in the case of the installation of 8 trenches compared with the 17 trenches system. As a result, the flow in the soil matrix increases directly below the trenches, which is accompanied by an increase in the water content at observation point 15. On the other hand, the 8 trenches system is around 10 m smaller than the system with 17 trenches, despite the increased spacing of the trenches. As a result, the fully saturated area below the trenches increases.

During the summer months with increased treated wastewater inflow, the groundwater rises up to the level of the trenches in the system with 8 trenches (Fig. 6b). In the scenario with 17 trenches, the groundwater level rises up to around 1.2 m below ground surface at the highest point, i.e. remains around 0.7 m below the central trench.

Conclusion

After evaluating the model results, several statements could be made for a potential infiltration system in the village of Sarden:

- The study shows that in principle the infiltration of treated wastewater is possible under the climatic conditions at the Sarden site in terms of quantitative aspects.
- The increased inflow of treated wastewater during the summer months causes a significant increase in the local groundwater level and the water content below the trenches.
- The results indicate that an infiltration system with a higher number of infiltration trenches provide more process reliability and can infiltrate larger volumes of treated wastewater. Infiltration of the treated wastewater via 17 infiltration trenches does not lead to full saturation of the area below the trenches as well as the rise of groundwater level up to or in the trenches can be prevented.
- The initial groundwater level has a big influence on the saturation conditions of the unsaturated soil zone. The simulations indicate that an increased groundwater level can lead to a rise of groundwater up to and in the trenches. For planning such an infiltration system, the groundwater level plays a decisive role and has to be considered.
- The precipitation events, which were simulated and evaluated within the framework of this study, played a subordinate role for the saturation conditions within the unsaturated soil zone. Although the amount of infiltrated precipitation caused a temporary increase in the water content, it did not have any long-term negative effects on the infiltration process.

However, the simulations performed and results obtained are based on limited or assumed data on the subsurface zone and the corresponding hydraulic properties. For a better characterization of the subsurface zone, on-site investigations must be carried out to collect more data, e.g. with the help of pumping tests and drill core analyses. Further scenario analyses, which assume variation widths of the hydraulic model parameters, could also provide further validation of the findings.

Due to the mentioned limitations, the results of the study presented can only be understood as a preliminary planning step due to the complexity of real conditions at the Sarden site and their impact on the infiltration process. Furthermore, it must be noted that the results of this investigation can only be transferred to other areas to a limited extent and cannot be generalized.

Acknowledgements

The Philipp Schwartz Initiative of the Alexander von Humboldt Foundation funded this research.

References

Abbas, J., Aldarir, A., Alsaleh, H., Bananah, M. (2015): The study of the hydrological situation of Chelf Basin and the development of effective solutions to prevent the immersion in winter. R. J. of Aleppo University Agricultural Sciences, Series No. 117.

Alam, S., Borthakur, A., Ravi, S., Gebremichael, M., Mohanty, S. K. (2021): Managed aquifer recharge implementation criteria to achieve water sustainability. Science of The Total Environment, Vol. 768. https://doi.org/10.1016/j.scitotenv.2021.144992.

Asano, T., Cotruvo, J. (2004): Groundwater recharge with reclaimed municipal wastewater: health and regulatory considerations. Water Research 38(8), 1941–1951. https://doi.org/10.1016/j.watres.2004.01.023.

Bananah, M. (2016): The use of mathematical modeling and water harvesting techniques in the management of water resources for karst water shed Chlef (Idlib – Orontes Basin). M. sc. Thesis, Aleppo University.

Bekele, E., Page, D., Vanderzalm, J., Kaksonen, A., Gonzalez, D. (2018): Water Recycling via Aquifers for Sustainable Urban Water Quality Management: Current Status, Challenges and Opportunities. Water 10(4), 457. https://doi.org/10.3390/w10040457.

Berndtsson, R., Mourad K.A. (2012): Water status in the Syrian water basins. Adv Mol Imaging 02(1), 15–20. https://doi.org/10.4236/ojmh.2012.21003.

Brew, G., Barazangi, M., Al-Maleh, K., Sawaf, T. (2001): Tectonic and geologic evolution of Syria. GeoArabia 6(4).

Bouwer, H. (2002): Artificial recharge of groundwater: Hydrogeology and engineering, Hydrogeology Journal 10(1), 121–142. https://doi.org/10.1007/s10040-001-0182-4.

Burger, F., Čelková, A. (2005): Numerical simulation of solute transport by water infiltration into characteristic alluvium quaternary sediment profiles of Danube lowlands. Acta Hydrologica Slovaca 6(1), 11 – 23.

Capodaglio, A. G., Callegari, A., Cecconet, D., Molognoni, D. (2017): Sustainability of decentralized wastewater treatment technologies. Water Practice and Technology 12(2), 463–477. https://doi.org/10.2166/wpt.2017.055.

Casanova, J., Devau, N., Pettenati, M. (2016): Managed Aquifer Recharge: An Overview of Issues and Options, in: Jakeman, A.J., Barreteau, O., Hunt, R.J., Rinaudo, J.-D., Ross, A. (Eds.) Integrated Groundwater Management: Concepts, Approaches and Challenges. Springer International Publishing, Cham, 413–434. https://doi.org/10.1007/978-3-319-23576-9_16.

Dillon, P., Pavelic, P., Page, D., Behringen, H., Ward, J. (2009): Managed aquifer recharge: An introduction (No. 13), Waterlines Report Series. National Water Commission, Canberra, Australia.

DIN 4220 (2008): Pedologic site assessment - Designation, classification and deduction of soil parameters (normative and nominal scaling). DIN Deutsches Institut für Normung e.V., Berlin, Germany, p. 50.

DIN EN 12566-3 (2016): Small Waste Water Treatment Systems for up to 50 PT–Part 3: Packaged and/or Site Assembled Domestic Waste Water Treatment Plants; Deutsches Institut für Normung e.V.: Berlin, Germany, p. 46.

FAO and World Bank (2009): https://openknowledge.worldbank.org/handle/10986/30307 License: CC BY-NC-ND 3.0 IGO.

Farahani, H. J., Izzi, G., Oweis; T. (2009): Parameterization and evaluation of the AquaCrop model for full and deficit irrigated cotton. Agron J 101(3), 469–476. https://doi.org/10.2134/agronj2008.0182s.

Food and Agriculture Organization of the United Nations; World Bank Group (2018): Water Management in Fragile Systems: Building Resilience to Shocks and Protracted Crises in the Middle East and North Africa. Cairo: FAO and World Bank.

Gleeson, T., Wada, Y., Bierkens, M. F. P., van Beek, L. P. H. (2012): Water balance of global aquifers revealed by groundwater footprint. Nature 488, 197–200. https://doi.org/10.1038/nature11295.

Gräber, P.-W., Blankenburg, R., Kemmesies, O., Krug, S. (2006): SiWaPro-DSS-Beratungssystem zur Simulation von Prozessen der unterirdischen Zonen. in: Wittmann, J., Müller, M. (Eds.) Simulation in Umwelt-und Geowissenschaften. Shaker Verlag, Leipzig, Germany, pp. 216, ISBN 978-3-8440-7579-3.

Google (2022): Map of Sarden plain, retrieved 27.04.2022 from https://earth.google.com/web/@35.93286319,37.10464293,282.52485894a,116449.18395979d,35y,9.99338657h,0t,0r.

Händel, F., Engelmann, C., Klotzsch, S., Fichtner, T., Binder, M., Graeber, P. W. (2018): Evaluation of decentralized, closely-spaced precipitation water and treated waste water infiltration. Water 10(10), 1460. https://doi.org/10.3390/w10101460.

Heidarpour, M., Mostafazadeh-Fard, B., Abedi Koupai, J., Malekian, R. (2007): The effects of treated wastewater on soil chemical properties using subsurface and surface irrigation methods. Agricultural Water Management 90(1), 87–94. https://doi.org/10.1016/j.agwat.2007.02.009.

Krug, W. (2001): Modellierung, Simulation und Optimierung für Prozesse der Fertigung, Organisation und Logistik. Gruner Druck GmbH, Erlangen, Germany, pp. 270, ISBN 1-56555-231-8.

Lyman, W. J., Patrick, J. R., Benjamin, L. (1992): Mobility and Degradation of Organic Contaminants in Subsurface Environments. CRC Press: Chelsea, MI, USA, pp. 416, ISBN 978-0-87371-800-4.

MAAR Ministry of Agriculture and Agrarian Reforms, Syrian Arab Republic (2013): Annual Agricultural Statistics, 2013, http://moaar.gov.sy/main/archives/12850

Manzoor, Q. (2007): Sustainable Management of Wastewater for Agriculture, Proceedings of the First Bridging Workshop, 11–15 November, Aleppo.

Martins, T., Leitão, T., Carvalho, M. D. R. (2017): Assessment of Wastewater Contaminants Retention for a Soil-aquifer Treatment System Using Soil-column Experiments. Procedia Earth Planet. Sci. 17, 332–335. https://doi.org/10.1016/j.proeps.2016.12.084.

Meikle, A., Amin-Hanjani, S., Glover, L. A., Killham, K., Prosser, J. I. (1995): Matric potential and the survival and activity of a Pseudomonas fluorescens inoculum in soil. Soil Boil. Biochem. 27(7), 881–892. https://doi.org/10.1016/0038-0717(95)00020-F.

Morales, I., Cooper, J., Amador, J. A., Boving, T. B. (2016): Modeling Nitrogen Losses in Conventional and Advanced Soil-Based Onsite Wastewater Treatment Systems under Current and Changing Climate Conditions. PLoS ONE 11(6): e0158292. https://doi.org/10.1371/journal.pone.0158292

Mualem, Y. (1976): A new model for predicting the hydraulic conductivity of unsaturated porous media. Water Resources Research 12, 513–522. https://doi.org/10.1029/WR012i003p00513.

Nema, P., Ojha, C., Kumar, A., Khanna, P. (2001): Techno-economic evaluation of soil-aquifer treatment using primary effluent at Ahmedabad. Water Research 35(9), 2179–2190. https://doi.org/10.1016/S0043-1354(00)00493-0.

Reemtsma, T., Gnirss, R., Jekel, M. (2000): Infiltration of combined sewer overflow and tertiary municipal wastewater: An integrated laboratory and field study on nutrients and dissolved organics. Water Res. 34(4), 1179–1186. https://doi.org/10.1016/S0043-1354(99)00274-2.

Richards, L. A. (1931): Capillary Conduction of Liquids through Porous Mediums. Journal of Applied Physics 1(5), 318–333.

Schaap, M. G., van Genuchten, M. T. (2006): A Modified Mualem–van Genuchten Formulation for Improved Description of the Hydraulic Conductivity Near Saturation. Vadose Zone Journal 5, 27–34. https://doi.org/10.2136/vzj2005.0005.

Scheffer, B., Aldarir, A. N., Fares, M., Hamo, N. (2003): Einfluss der Bewässerung mit Abwasser auf Grundwasser, Boden und Pflanzen in Madkh Area (Süd Aleppo – Syria), 4th international symposium workshop, Kassel Universität and Jordan University, Irbid, Jordan.

Shuster, W. D., Morrison, M. A., Thurston, H. W. (2010): Seasonal and situational impacts on the effectiveness of a decentralized stormwater management program in the reduction of runoff volume. in: Proceedings of the 7th International Conference on Sustainable Techniques and Strategies for Urban Water Management/Novatech, Cincinnati, OH, USA, 28 June–1 July 2010.

Sieker, F. (1998): On-Site stormwater management as an alternative to conventional sewer systems: A new concept spreading in Germany. Water Sci. Technol. 38, 65–71. https://doi.org/10.2166/wst.1998.0378.

Šimůnek, J., van Genuchten, M. Th. (1994): The CHAIN_2D code for simulating two-dimensional movement of water flow, heat, and multiple solutes in variably saturated porous media. Version 1.1. Research Report No 136. Riverside, Cal.: USDA-ARS U.S. Salinity laboratory.

Van Afferden, M., Cardona, J. A., Lee, M. Y., Subah, A., Müller, R. A. (2015): A new approach to implementing decentralized waste water treatment concepts. Water Sci. Technol. 72, 1923–1930. https://doi.org/10.2166/wst.2015.393.

Wada, Y., Beek, L. P. H., van Kempen, C. M., van Reckman,

J. W. T. M., Vasak, S., Bierkens, M. F. P. (2010): Global depletion of groundwater resources. Geophys. Res. Lett. 37, 5. https://doi.org/10.1029/2010GL044571.

Wild, D., Buffle, M.-O., Hafner-Cai, J. (2007): Water: A market of the future. Sustainable Asset Management (SAM), NY, USA, pp. 48.

Yaghi, T., Aldarir, A., Nangia, V., Oweis, T., Arslan, A. (2016): Impact of Climate Changes on Water Resources Availability in the Orontes River Watershed: Case of Homs Governorate in Syria. Jordan Journal of Agricultural Scences 12(2), 499–519.

Zhang, Z., Lei, Z., Zhang, Z., Sugiura, N., Xu, X., Yin, D. (2007): Organics removal of combined wastewater through shallow soil infiltration treatment: A field and laboratory study. J. Hazard. Mater. 149(3), 657–665. https://doi.org/10.1016/j.jhazmat.2007.04.026.

Abdulnaser Aldarir, Prof. Dr. Agr.
Aleppo University
Department of Rural Engineering
Aleppo
Syria

Abdulnaser Aldarir, Prof. Dr. Agr.
Thomas Fichtner, Dr.-Ing.
Ian Desmond Gwiadowski, BSc.
René Blankenburg, Dr.-Ing.
Peter-Wolfgang Graeber, Prof. Dr.-Ing. habil. (*corresponding author, e-mail: Peter-Wolfgang.Graeber@tu-dresden.de)
Technische Universitaet Dresden
Institute of Groundwater Management
01062 Dresden
Germany

DOI: 10.31577/ahs-2022-0023.01.0015

ACTA HYDROLOGICA SLOVACA

Volume 23, No. 1, 2022, 140 – 146

The effect of different fire temperatures on the water repellency parameters of forest sandy soil under different types of vegetation

Anton ZVALA*, Peter ŠURDA, Slavomír HOLOŠ

Soil under specific tree forest species (e.g. pines) can be naturally water repellent. Forest fire can strengthen or destroy soil water repellency (SWR). Fire induced SWR have many direct or indirect effects, including increased preferential flow rate and risk of ground water contamination, increased surface runoff and soil erosion, increased amount of carbon stored in soil, reduced levels of seed germination and plant growth. Understanding the post-fire hydrologic response of forest soil is paramount for effective risk management and mitigation of post-fire hydrologic hazards.

Three experimental sites were located in the Borská nížina lowland (southwestern Slovakia). Eolian (wind-blown) sand dunes form the central part of the Borská nížina lowland, which make it a specific region within Central Europe. Pines have been planted here for sand dune stabilization since the 18th century and today cover a huge part of the lowland. The first site IL1 represent 100-years-old stand of Scots pine (*Pinus sylvestris*), the second site IL2 is a 30-years-old stand of Scots pine (*Pinus sylvestris*) and the third site LL is a deciduous stand with a predominance of alder (*Alnus glutinosa*). The disturbed mineral soil samples were taken from 2.5–5.0 cm depth of soil horizon. The organic horizon (0–2.5 cm) was sampled separately before mineral soil. In the laboratory, the samples from each site in 5 replicates were placed into a muffle furnace and exposed to a temperature from 50 to 900°C. The persistence of SWR in soil samples was measured using the water drop penetration time (WDPT) test.

Our goal was to quantify the changes of SWR of the naturally water repellent soil induced by different fire temperatures under age and species different forest stands. Forest stands were selected to include different vegetation age and type of litter (surface organic horizon) under the relatively same site conditions (climate, soil and relief conditions).

The measured values of natural background water repellency decreased in order IL1>IL2>LL. The highest value of induced SWR ($WDPT_{max}$) was measured at IL1 and further declined in the order LL>IL2; however increase of SWR after heating, estimated as a difference between maximal induced and natural SWR had different trend (LL>IL2>IL1). Mean value of parameter $WDPT_{max}$-$WDPT_n$ at IL1 was statistically different from values estimated at sites IL2 resp. LL.

The changes in natural and induced SWR that we have found may be attributed partially to the quantity and to the origin of organic material (litter of the plant communities with different age and composition of the species).

KEY WORDS: soil water repellency, soil heating, water drop penetration time, forests

Introduction

Wildfire activity, number of fires, area burned, and fire severity, has increased in many areas of the world in recent decades (Abatzoglou et al., 2013; Reilly et al., 2017; Hološ and Šurda, 2021). These rising trends are projected to continue in some regions due to climate change, increasing population, and fire suppression activities (Flannigan et al., 2013; Moritz et al., 2012; Novák, 2021).

Soil water repellency (SWR) is a natural phenomenon occurring under relatively dry conditions in soils with a wide range of land uses and climatic conditions, which can be intensified by heating the soil during wildfires. In fact, fire creates SWR in previously hydrophilic soils and also maintains or even increases it in previously repellent soils, depending on the specific pre-fire conditions and its severity. Various preceding studies reported that fires can create or increase SWR on forest soils (Certini, 2005; Doerr et al., 2004). An increase in the SWR of the soil due to fire may increase preferential flow rate and risk of ground water contamination, make the soil incapable of infiltrating water and being more susceptible to erosion (DeBano and Krammes, 1966). SWR is considered important for post-fire hydrology, causing reduced infiltration and increased surface runoff and erosion, especially after a fire when vegetation has been removed (Certini, 2005, DeBano, 1981; DeBano, 2000; Doerr et al., 2004, Kettridge et al., 2014).

SWR is induced by the hydrophobic and amphiphilic components of soil organic matter. Some authors (e.g., Buczko et al., 2005; Hrabovský et al., 2020; Zavala et al., 2009) found positive correlation between SWR and soil organic matter; other authors shown that quantity of soil

organic matter alone could not fully explain the changes of SWR (Zema et al., 2021). Dinel et al. (1990) found that the concentration of hydrophobic lipid compounds decreases with increasing efficiency of organic matter decomposition and Cesarano et al. (2016) shown that litter incorporated into the soil can produce a variety of effects on SWR, ranging from a dramatic increase to a null effect depending on the considered litter type.

The increase in forest soil temperature during combustion is significantly influenced by the intensity and duration of the fire, which depends on the quality and humidity of the burning fuel, air temperature and humidity, wind speed and terrain topography (Robichaud and Hungerford, 2000; Campbell et al., 1995). At low fire intensities, forest soil temperatures range from 250°C to 450°C (Janzen and Tobin-Janzen, 2008; Franklin et al., 1997). In the presence of a good amount of fuel, the intensity of the fire increases, the forest soil temperature rises from 500°C to 700°C (DeBano et al., 1998), however fire sites with a recorded forest soil temperature of 850°C have been observed (DeBano, 2000). Some laboratory experiments have revealed that heating the soil below 175°C causes slight changes in SWR. A significant increase in SWR was found at temperatures from 175 to 270°C. Temperatures in the range of 270°C to 400°C destroy hydrophobic substances in the soil and, as a result, suppress SWR (DeBano et al., 1976; Doerr et al., 2004; Varela et al., 2005). The effects of fire on SWR depend on other factors, including the type of plants present and their density, organic matter characteristics, soil structure or the mineralogical composition of the clay fraction (Arcenegui et al., 2007; Mataix-Solera et al., 2008; Sándor et al., 2021). Micromorphological studies have suggested that high temperatures have resulted in increased formation of organic carbon coatings responsible for SWR (Dekker et al., 1998).

Main goal of our study was to quantify the changes of SWR of the naturally water repellent soil induced by different fire temperatures under age and species different forest stands. Our hypothesis was that the effect of fire temperature on SWR depends on initial organic carbon content (existence of positive correlation between C_{ox} and hydrophobic components of soil organic matter) and/or on the origin of organic material (different composition of the litter incorporated into the soil can produce either increase or null effect on SWR). Experimental sites were selected to include relatively high natural background SWR (sandy soils of Borská nížina lowland), different stand age and type of litter (surface organic horizon) under the relatively same site conditions (climate, soil and relief conditions). The locality was also chosen due to the close proximity of three age- and species-different stands.

Material and methods

Research site

The research was conducted near the village of Studienka (48° 31.733' N, 17° 07.315' E) in the Borská nížina lowland (southwestern Slovakia). Most of the area is located on Eolithic sands. The soils of the research sites are classified as Arenosol (WRB, 2014) and have a sandy texture (Soil Science Division Staff., 2017). The climate is mild with mild humidity and winter. The average annual temperature in this area is 9–10°C and the average annual rainfall in the Borská nížina lowland is 600–650 mm (Atlas of the Slovak Republic, 2002). Despite Scots pine is being proven to be a native species here, its current large stands are intensively managed human established plantations with specific undergrowth. Pines have been planted here for sand dune stabilization since the 18th century.

Experimental sites were selected to include relatively high natural background SWR, different stand age and type of litter (surface organic horizon) under the relatively same site conditions (climate, soil and relief conditions). The locality was also chosen due to the close proximity of three age- and species-different stands. Within the group of forest stands, 3 research sites were set aside: a 30-year-old (IL2) and a 100-year-old coniferous tree stand (IL1) and 40-year-old deciduous tree stand (LL) (Fig. 1).

The LL research site represents a younger stand of alder (*Alnus glutinosa*) (30–40 years) in an indistinct terrain depression situated under a sand dune overgrown with monocultures of Scots pine (Pinus sylvestris), in an undergrowth dominated by tall sedges (*Carex elata*) and the presence of other more moisture-loving species.

The IL2 site represent 30 years old Scots pine (*Pinus sylvestris*) stand. The tree layer is very dense without undergrowth. The soil surface is covered with a few centimeters of coniferous litter. The mechanical site preparation was used for forest restoration, while the surface layer of soil with humus was removed, so the pine trees were planted in the bare sand.

The IL1 site is a stand older than 100 years; its purpose is to stabilize the sand dune. The herbaceous undergrowth is dominated by grass, especially sheep fescue (*Festuca ovina* agg) and often covered with bushgrass (*Calamagrostis epigejos* (L.) Roth). Other species are rare, such as the wall hawkweed (*Hieracium murorum* L.), the weed species of the black nightshade (*Solanum nigrum* L.) and allochton species with invasive behavior, such as the pokeweed (*Phytolacca americana* L.), the black cherry (*Prunus serotina* Ehrh.) and horseweed (*Conyza canadensis* (L.) Cronq.). Rare species here are also red-stemmed feathermoss (*Pleurozium schreberi* (Bird.) Mitt.) and neat feathermoss (*Pseudoscleropodium purum* (Hedw.) M. Fleisch).

Soil sampling, determination of basic soil characteristics and heating experiment

The mineral part of the soil from the 2.5 cm depth was sampled into the prepared containers after the organic horizon (0–2.5 cm) was gently removed from the soil surface. Basic soil properties were determined with three replications in the ISO Certified Laboratory of the Soil Science and Protection Research Institute in Bratislava.

In the laboratory of IH SAS, the soil samples were sieved through a 2 mm sieve and dried at 40°C. After reaching

equilibrium, the samples were weighed into ceramic dishes. We weighed 5 ceramic dishes for each temperature. The weight of the mineral part of the soil was 60 g. The samples were heated in a muffle furnace LE 15/11 (Fig. 2) at temperatures of 50, 100, 150, 200, 250, 300, 350, 400, 450, 500, 550, 600, 650, 700, 750, 800, 850 and 900°C for 20 min (a new sample for each temperature). After given time, we pulled the samples out of the oven and allowed to cool to room temperature.

Measurement of soil water repellency

Persistence of SWR was assessed by the WDPT test. It involves placing 50 ± 5 µl of a drop of water from a standard dropper or pipette on the soil surface and recording the time of its complete penetration (infiltration) into the soil. A standard drop release height of approximately 10 mm above the soil surface was used to minimize the crater effect on the soil surface (Doerr et al., 1998; Tinebra, 2019).

The natural background water repellency in our experiment is represented by the mean value of the persistence of SWR, measured without heating ($WDPT_n$). The induced SWR was estimated as mean of WDPT values measured at 20°C (without heating) and after heating of soil samples at temperatures of 50–900°C ($WDPT_i$). $WDPT_{max}$ is the highest value of induced SWR, determined as the highest group average of WDPT measured after heating at a certain temperature. T_{max} is the combustion temperature that induced $WDPT_{max}$.

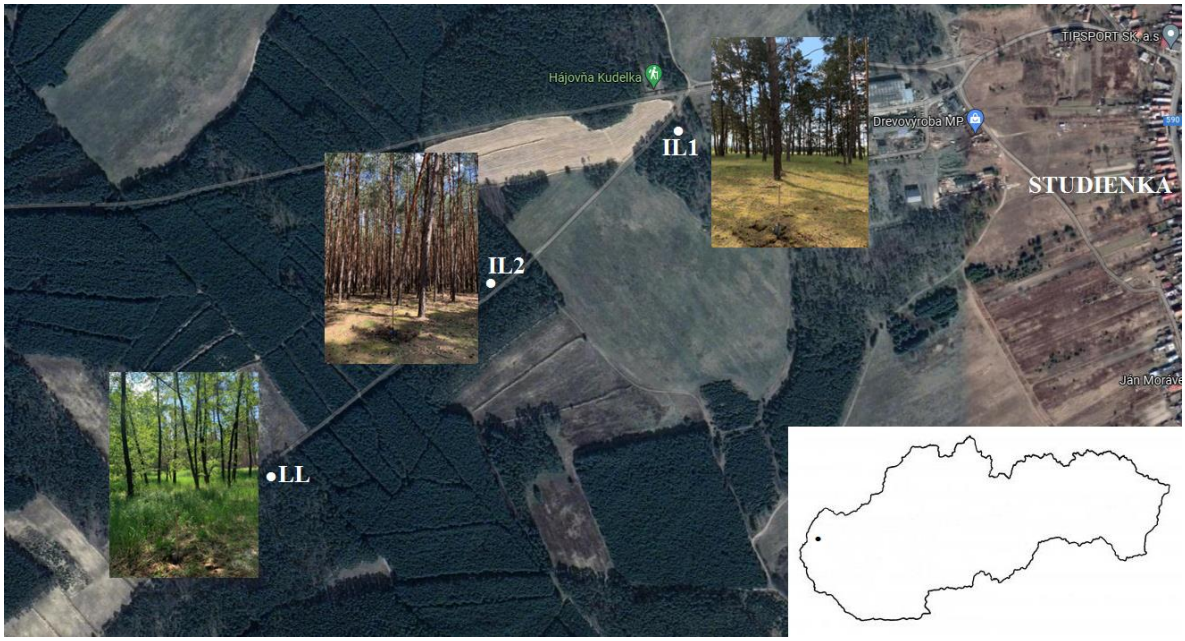

Fig. 1. Map of the experimental area with marked research sites IL1 – 100 years old coniferous forest, IL2 – 30 years old coniferous forest, LL – deciduous forest.

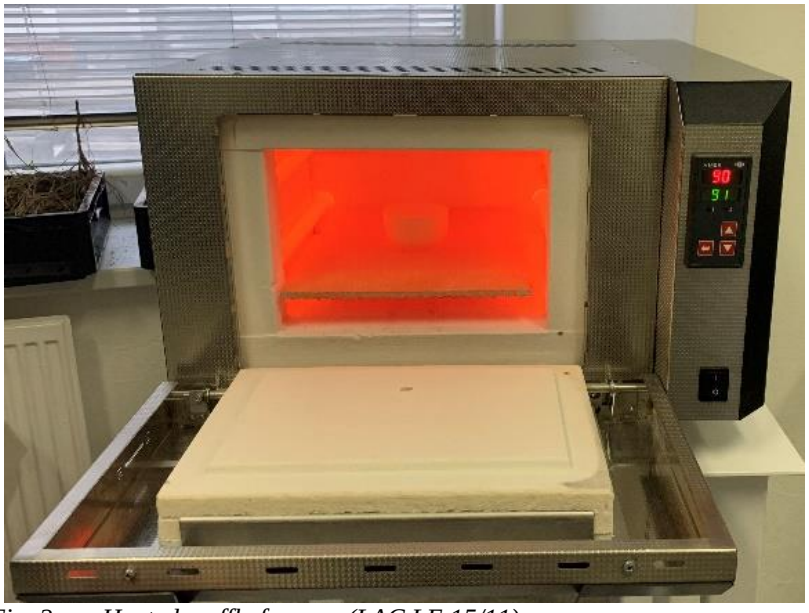

Fig. 2. Heated muffle furnace (LAC LE 15/11).

Statistical analysis

Differences between the parameters estimated in different sites were evaluated using single factor ANOVA with Tukey's Honest Significant Difference (HSD) post-hoc test. The Tukey-Kramer method (also known as Tukey's HSD method) uses the Studentized Range distribution to compute the adjustment to the critical value. The Tukey-Kramer method achieves the exact alpha level (and simultaneous confidence level $(1 - \alpha)$) if the group sample sizes are equal and is conservative if the sample sizes are unequal. The statistical significance in the analysis was defined at $P < 0.05$.

Results and discussion

The basic physical and chemical properties of the upper part of soil horizon at the studied forest stands are in Table 1. The lowest sand fraction was determined at the IL1, which represents a higher stage of succession (100-year-old forest stand) compared to IL2 (approximately 30 years) and LL (approximately 40 years). The older age of the stand is related to the accumulation of plant residues on the soil surface, the decomposition of which increases the proportion of organic carbon and finer grain fraction. The high content of organic carbon per LL, which does not correlate with the age of the stand, may be due to the different composition of the litter - carbon content, C: N ratio (needles vs. leaves).

The water repellency parameters, which were used for analysis of the fire temperature impact on the persistence of SWR at sites LL, IL1 and IL2, are shown in Fig. 3. The natural background water repellency in our experiment is represented by the mean value of the persistence of SWR, measured without heating at 20°C ($WDPT_n$). $WDPT_{max}$ is the highest value of SWR (natural + induced), determined as the highest group average of WDPT measured after heating at a certain temperature. T_{max} is the combustion temperature that induced $WDPT_{max}$. The absolute increase of SWR after heating was estimated as $WDPT_{max}$-$WDPT_n$.

The highest value of $WDPT_n$ was measured on IL1,

Table 1. Physical and chemical properties of the upper part of the soil horizon at the experimental sites IL2, IL1 resp. LL (a 100-year-old and 30-year-old coniferous tree stand, resp. 40-year-old deciduous tree stand). (Cox = organic carbon content)

Attribute	Experimental site		
	IL1	IL2	LL
Sand [%]	89.82	92.31	92.96
Silt [%]	5.81	4.96	3.36
Clay [%]	2.37	2.72	3.68
$CaCO_3$ [%]	<0.05	<0.05	<0.05
Cox [%]	0.75	0.61	1.35

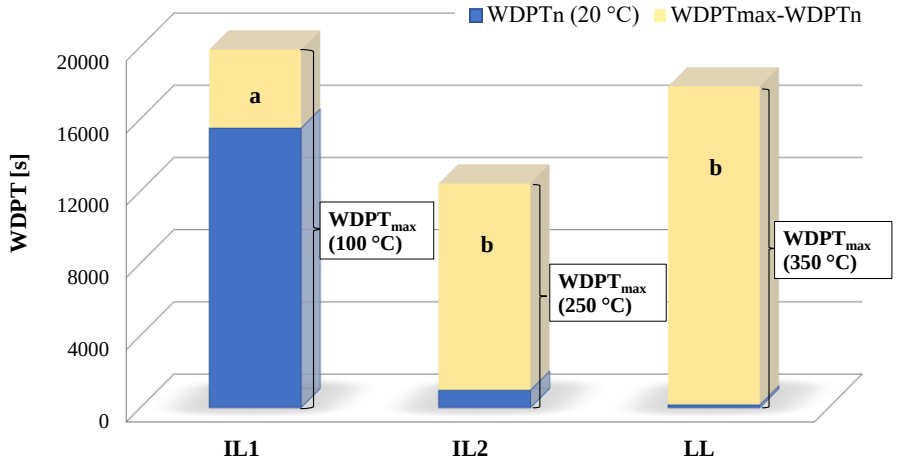

Fig. 3. Water repellency parameters (persistence of SWR at 20°C – $WDPT_n$; highest value of induced SWR, determined as the highest group average of WDPT at a certain temperature – $WDPT_{max}$ at T_{max}, increase of induced SWR as the difference of $WDPT_{max}$ - $WDPT_n$) on the experimental sites IL1 – 100-year-old coniferous forest, IL2 – 30-year-old coniferous forest, LL – 40-year-old deciduous forest. Parameters with the same letter are not significantly different from each other (Tukey's HSD test, $P < 0.05$).

which was caused by the composition of coniferous litter and vegetation cover (especially grasses). The lower value of $WDPT_n$ on IL2 is probably due to the absence of vegetation cover and the lowest value on LL due to the absence of coniferous litter.

The parameter $WDPT_{max}$ decreases in the order of IL1>LL>IL2. Since the proportion of coarse-grained fraction at all the sites is approximately the same and the $WDPT_{max}$ values are not related with C_{ox}, differences in $WDPT_{max}$ can be probably attributed to the different composition of litter.

A different trend was found in the analysis of SWR increase, estimated as a difference between maximal induced SWR and natural SWR. The highest value of $WDPT_{max}$-$WDPT_n$ was measured at site LL and decreased in order IL2>IL1. Mean value of $WDPT_{max}$-$WDPT_n$ at IL1 was statistically different from values estimated at sites IL2 resp. LL.

T_{max} parameter decreases in the order LL>IL2>IL1, which appears to be the same trend as $WDPT_{max}$-$WDPT_n$. The graphical representation of the natural and induced persistence of SWR as a function of temperature (Fig. 4) shows a large degree of variability.

The highest mean value of natural SWR – $WDPT_n$ (15480 s) was measured at the IL1 research site. The heating at 100°C increased the WDPT value to 19650 s. The further increase in heating temperature reduced persistence of SWR and at a temperature of 400°C SWR disappears and does not occur up to the investigated temperature of 900°C. The extreme (natural and induced) SWR of the forest soil from the IL1 site can be caused by the specific type of litter accumulated during 100 years.

The $WDPT_n$ value at the IL2 site was 958 s. The heating to 50°C reduced the WDPT value to 164 s, but further temperature increase to 200°C increased also the WDPT value. We found then a rapid increase in WDPT values in the temperature range from 200°C to 250°C. From 250°C we recorded a decrease in WDPT and at a temperature of 350°C water repellency disappears. The soil remained wettable up to the investigated temperature of 900°C. Site IL2 was covered by a younger forest stand than IL1, which means a shorter accumulation time of litter and the associated lower increase in organic matter content. Induced and natural SWR is also lower than at site IL1. The obtained values of WDPT and T_{max} are in line with results from the study of Novak et al. (2009), who investigated the effect of heating on the persistence of SWR, saturated hydraulic conductivity and soil retention at forest and meadow localities of Borská nížina lowland. Dlapa et al. (2007) at the same locality observed a significant increase in persistence of SWR when the samples were heated for 20 minutes at 150 and 200°C. Water repellency disappeared after heating to 250, resp. 300°C in subsurface and topsoil horizons due to the decomposition of organic matter.

The measured value of $WDPT_n$ at the LL site was 146 s. The heating at 50°C caused an increase in WDPT to 2294 s. We did not measure significant WDPT changes up to heating temperature of 200°C. In the temperature range from 200°C to 350°C, we measured an increase in WDPT to a maximum value of 17796 s. At a temperature of 375°C, water repellency disappears and the soil is wettable up to the last examined temperature of 900°C. The low value of natural background SWR ($WDPT_n$) at LL site was caused by a different type of litter; however, the heating of soil at specific temperature was able to induce extreme SWR – comparable with SWR the site IL1 with the strong natural background SWR. This results are in line with the study of Arcenegui et al. (2007), who investigated the effect of burning temperature (200–500°C), vegetation type (*Rosmarinus officinalis*, *Pinus halepensis* and *Brachypodium retusum*) in two calcareous soils (regosol and luvisol), representing the forest areas of south-eastern Spain. They observed the maximum WDPT values after heating the samples to 300–350°C, while above this temperature the SWR was

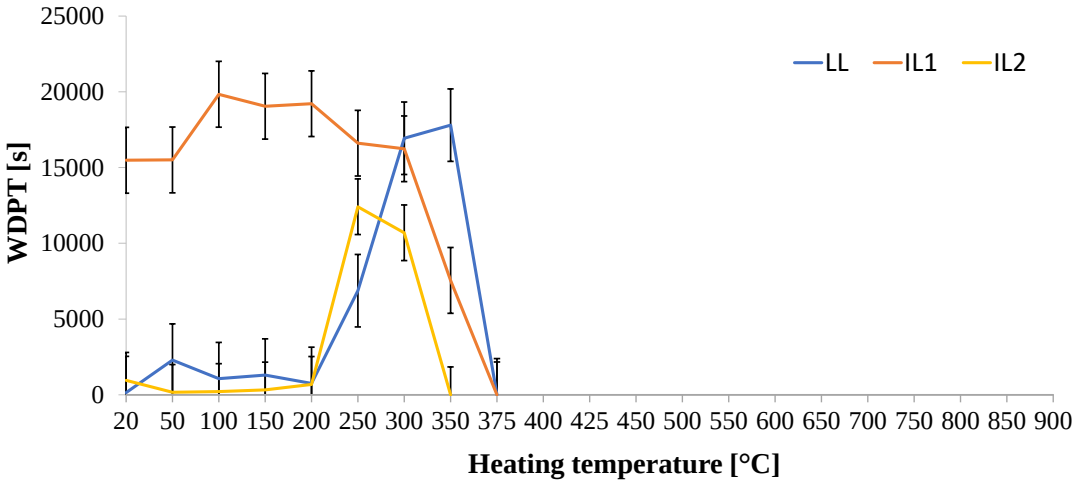

Fig. 4. Persistence of water repellency (as results of WDPT test); natural at 20°C and induced after heating to 50–900 at experimental sites: IL1 – 100-year-old coniferous forest, IL2 – 30-year-old coniferous forest, LL – 40-year-old deciduous forest (bars at each measuring point show the standard deviation).

eliminated. These results show that water repellency caused by combustion can be significantly influenced by environmental factors, such as vegetation type and the amount and properties of litter, and that soil type and its properties also play a crucial role.

Conclusion

Quantity and chemical composition of organic matter from vegetation cover and tree litter affect the natural background SWR. The highest values of natural SWR were measured at site with a 100-year-old Scots pine stand (IL1) and decreased in the order of IL2 (30-year-old Scots pine stand) >LL (40-year-old deciduous forest), which may be due to a longer accumulation of organic matter from coniferous litter and cover vegetation. The highest increase in induced SWR was determined at the LL site and decreased in the order of IL2>IL1, as well as the heating temperature that induced maximal SWR. SWR disappeared at heating temperatures 375, 350 and 400°C at sites LL, IL2 resp. IL1.

Our study did not confirm the positive relation between organic carbon content (C_{ox}) and the maximal value of SWR ($WDPT_{max}$), i.e. value of $WDPT_{max}$ did not increase in same order as value of C_{ox} at study sites. This relation can be applied only for the same vegetation type (IL1 and IL2) – i.e. SWR increases with increasing age and degree of succession only under the same vegetation type (in our study - the Scots pine stand). We found also that with increasing age (succession stage) of the forest stand the proportion of natural background SWR is raising.

The role of the origin of organic material (composition of litter) can be partially confirmed in the conditions of our experiment. The high organic carbon content at LL, which does not correlate with the age of the stand, may be attributed to the different composition of the litter and C:N ratio (needles vs. leaves). However, the highest C_{ox} at LL (compared to IL1 and IL2) did not induce the maximal value of SWR ($WDPT_{max}$), which we assume may be the influence of the different origin of the organic material. The proportion of natural/induced SWR at LL was similar to that at IL2 (parameters were not significantly different from each other), which can be attributed to the similar age of sites. Further research is needed to determine and qualitatively analyze the chemical composition of organic litter at experimental sites.

Acknowledgement

This contribution was supported by the Scientific Grant Agency VEGA Project No. 2/0150/20 „Impact of climate change on rainfall–runoff relationships“ and Project EIG JC2019-074 “Soil Eco-Technology to Recover Water Storage in disturbed Forests”.

References

Abatzoglou, J. T., Kolden, C. A. (2013): Relationships between climate and macroscale area burned in the western United States. Int. J. Wildland Fire 22 (7), 1003–1020. https://doi.org/10.1071/wf13019.

Arcenegui, V., Mataix-Solera, J., Guerrero, C., Zornoza, R., Mayoral, A. M., Morales, J. (2007): Factors controlling the water repellency induced by fire in calcareous Mediterranean forest soils, European Journal of Soil Science, 58 (2007), 1254–1259, 10.1111/j.1365-2389.2007.00917.x

Atlas of the Slovac republic (2002): Ministry of the Environment, Bratislava and Slovak Environment Agency, Banská Bystrica, 2002. 344 s. ISBN 80-88833-27-2.

Buczko, U., Bens, O., Hüttl, R. F. (2005): Variability of soil water repellency in sandy forest soils with different stand structure under Scots pine (Pinus sylvestris) and beech (Fagus sylvatica). Geoderma, 126, 3–4, 317–336.

Campbell, G. S., Jungbauer, J. D., Bristow, K. L., Hungerford, R. D. (1995): Soil temperature and water content beneath a surface fire. Soil Sci 159: 363–374

Certini, G. (2005): Effects of fire on properties of forest soils: a review, Ecologia, Volume: 143, Issue: 1 Pages: 1–10, DOI: 10.1007/s00442-004-1788-8, Published: MAR 2005, Document Type: Review

Cesarano, G., Incerti, G., Bonanomi, G. (2016): The influence of plant litter on soil water repellency: insight from 13C NMR spectroscopy. PLoS One, 11, 3, Article Number: e0152565.

Debano, L., F., Krammes J. S. (1966): Water repellent soils and their relation to wildfire temperatures. International Association of Scientific Hydrology. BulletinVolume 11, Issue 2, Pages 14 – 19June 1966, ISSN 00206024, DOI: 10.1080/02626666609493457

DeBano, L. F., Savage, S. M., Hamilton, D. A. (1976): The transfer of heat and hydrophobic substances during burning, Soil Science Society of America Proceedings, 40, 779–782

DeBano, L. F., (1981): Water repellent soil: a state-of-the-art. USDA, Forest Service General Technical Report, PSW-46.

DeBano, L. F., Neary, D. G., Ffolliott, P. F. (1998): Fire's effects on ecosystems. Wiley, New York, 333p

DeBano, L. F. (2000): The role of fire and soil heating on water repellency in wildland environments: a review. Journal of Hydrology 231–232, 195–206. 29 May 2000, DOI: 10.1016/S0022-1694(00)00194-3

Dekker, L. W., Ritsema, C. J., Oostindie, K., Boersma, O. H. (1998): Effect of drying temperature on the severity of soil water repellency, Soil Science, Volume: 163 Issue: 10 Pages: 780–796, DOI: 10.1097/00010694-199810000-00002

Dinel, H., Schnitzer, M., Mehuys, G. R. (1990): Soil lipids: Origin, nature, content, decomposition, and effect on soil physical properties. In: Soil Biochemistry (eds J.M. Bollag & G. Stotzky), 397–429. Marcel Dekker, New York

Dlapa P., Šimkovic, I., Doerr, S. H., Kanka, R., Mataix-Solera, J. (2007): The effect of site conditions and heating on soil water repellency in aeolian sands under pine forests at Borská nížina lowland (SW Slovakia). Ekológia (Bratislava) 26: 398–407.

Doerr, S. H., Shakesby, R. A., Walsh, R. P. D. (1998): Spatial variability of soil hydrophobicity in fire-prone eucalyptus and pine forests, Portugal. Soil Science. Volume 163, Issue 4, Pages 313–324. April 1998, ISSN 0038-075X, DOI: 10.1097/00010694-199804000-00006

Doerr, S. H., Blake, W. H., Shakesby, R. A., Stagnitti, F., Vuurens, S. H., Humphreys, G. S., Wallbrink, P. (2004): Heating effects on water repellency in Australian eucalypt forest soils and their value in estimating wildfire soil temperatures, International Journal of Wildland Fire, 13 (2) (2004), 157–163, 10.1071/WF03051

Flannigan, M., Cantin, A. S., de Groot, W. J., Wotton, M.,

Newbery, A., Gowman, L. M. (2013): Global wildland fire season severity in the 21st century. For. Ecol. Manage. 294 (S1), 54–61. https://doi.org/10.1016/j.foreco.2012.10.022.

Franklin, S. B., Robertson, P. A., Fralish, J. S. (1997): Small-Scale Fire Temperature Patterns in Upland Quercus Communites. Journal of Applied Ecology, 34(3), 613–630. https://doi.org/10.2307/2404911

Hološ, S., Šurda, P. (2021): Evaluation of Drought – Review of Drought Indices and their Application in the Recent Studies from Slovakia" Acta Horticulturae et Regiotecturae, vol. 24, no.s1, 2021, 97–108. https://doi.org/10.2478/ahr-2021-0015

Hrabovský, A., Dlapa, P., Cerda, A., Kollár, J. (2020): The impacts of vineyard afforestation on soil properties, water repellency and near-saturated infiltration in the Little Carpathians mountains. Water, 12, Article Number: 2550.

Janzen, C., Tobin-Janzen, T. (2008): Microbial communities in fire-affected soils. In Microbiology of Extreme Soils.

Kettridge, N., Humphrey, R. E., Smith, J. E., Lukenbach, M. C., Devito, K. J., Petrone, R. M. (2014): Burned and unburned peat water repellency: implications for peatland evaporation following wildfire, J. Hydrol., 513 (2014), 335–341

Mataix-Solera, J., Arcenegui, V., Guerrero, C., Jordán, M. M., Dlapa, P., Tessler, N., Wittenberg, L. (2008): Can terra rossa become water repellent by burning? A laboratory approach, Geoderma, 147 (2008), 178–184, 10.1016/j.geoderma.2008.08.013

Moritz, M. A., Parisien, M.-A., Batllori, E., Krawchuk, M. A., Van Dorn, J., Ganz, D. J., Hayhoe, K. (2012): Climate change and disruptions to global fire activity. Ecosphere 3 (6), 1–22. https://doi.org/10.1890/ES11-00345.1.

Novák, V. (2021): Ecosystems and Global Changes. Acta Horticulturae et Regiotecturae, vol.24, no.s1, 70–79. https://doi.org/10.2478/ahr-2021-0012

Reilly, M. J., Dunn, C. J., Meigs, G. W., Spies, T. A., Kennedy, R. E., Bailey, J. D., Briggs, K. (2017): Contemporary patterns of fire extent and severity in forests of the Pacific Northwest, USA (1985–2010). Ecosphere 8 (3), e01695. https://doi.org/10.1002/ecs2.1695.

Robichaud, P., R., Hungerford, R., D., (2000): Water repellency by laboratory burning of four northern Rocky Mountain forest soils, Journal of hydrology, Volume231, Page207-219, Special IssueSI, DOI10.1016/S0022-1694(00)00195-5

Sándor, R., Iovino, M., Lichner, L., Alagna, V., Forster, D., Fraser, M., Kollár, J., Šurda, P., Nagy, V., Szabó, A., et al. (2021): Impact of climate, soil properties and grassland cover on soil water repellency. Geoderma 2021, 383, 114780.

Soil Science Division Staff. (2017): Soil survey manual. C. Ditzler, K. Scheffe, and H. C. Monger (eds.). 4th ed. Agriculture Handbook 18. Government Printing Office, Washington, D.C. Retrieved May 26, 2020, from https://www.nrcs.usda.gov/wps/portal/nrcs/detail/soils/ref/?cid=nrcs142p2_054262

Tinebra, I., (2019): Comparing different application procedures of the water drop penetration time test to assess soil water repellency in a fire affected Sicilian area. Catena. Volume 177, 41–48. June 2019, DOI: 10.1016/j.catena.2019.02.005

Varela, M. E., Benito, E., de Blas, E. (2005): Impact of wildfires on surface water repellency in soils of northwest Spain, Hydrological processes, Volume: 19 Issue: 18 Pages: 3649-3657, DOI:10.1002/hyp.5850

WRB, (2014): World Reference Base for Soil Resources (2014), World Soil Resources Reports No. 106. Rome, 192 p.

Zavala, L. M., González, F. A., Jordán, A. (2009): Intensity and persistence of water repellencyin relation to vegetation type and soil parameters in Mediterranean SW Spain. Geoderma, 152, 361–374.

Zema, D. A., Plaza-Alvarez, P. A., Xu, X. Z., Carra, B. G., Lucas-Borja, M. E. (2021): Influence of forest stand age on soil water repellency and hydraulic conductivity in the Mediterranean environment. Science of the Total Environment, 753, Article Number: 142006.

Mgr. Anton Zvala, PhD. (*corresponding author, e-mail: zvala@uh.savba.sk)
Ing. Peter Šurda, PhD.
Ing. Slavomír Hološ
Institute of Hydrology SAS
Dúbravská cesta 9
84104 Bratislava
Slovak Republic

Ing. Slavomír Hološ
Institute of Landscape Engineering
Faculty of Horticulture and Landscape Engineering
Slovak University of Agriculture
Hospodárska 7
949 76 Nitra
Slovak Republic

DOI: 10.31577/ahs-2022-0023.01.0016

ACTA HYDROLOGICA SLOVACA

Volume 23, No. 1, 2022, 147 – 154

Determination of sedimentation speed of soil micro-particles from laser diffraction measurements

Milan GOMBOŠ*, Andrej TALL, Dana PAVELKOVÁ, Branislav KANDRA

In hydropedological research and in various scientific experiments, the determination of the settling rate of soil microparticles is a frequent task. Many laboratory procedures for measuring sedimentation rate are based on the Stokes equation. In recent years, methods based on the principle of laser diffraction can be used to measure grain-size distribution and deposition rate of microparticles. The output of the measurements by a laser diffraction method is statistical distribution of soil texture in the measured sample by particle size expressed in % of volume. Measurements were performed in a wet way by MALVERN Instruments device called Mastersizer 2000. The proposed method is based on measuring the time required for soil particles of certain diameter to pass certan distance. The size of soil microparticles present in space and time is defined by probability. Probability is defined in the form of a grain size distribution function. The advantage of the proposed method is its robustness and elimination of human factor errors. This paper presents the results of theoretical approaches and experimental measurements of the settling rate of soil microparticles. Soil samples were taken in the East Slovakian Lowland. Measurements are performed for the selected sizes of soil microparticles for a probability of occurrence of 90%, i.e for d(90). The results are compared with the results calculated by the Stokes equation.

KEY WORDS: sedimentation rate, soil microparticles, dispersion system

Introduction

Soil microparticles are of particular interest in hydropedological research. They are usually composed of clay particles with a high proportion of clay minerals. Clay particles are defined as particles ≤ 2 μm. Soils with a high proportion of clay particles (> 45%) are called clay soils. Clay minerals can bind water in their structure. When they are saturated with water, their volume increases, and when they are dried, they shrink. During these processes, the retention properties and hydrodynamics of the unsaturated zone of the soil profile change significantly. Knowledge of these properties is essential for the investigation and numerical simulation of the water regime of heavy soils (Gomboš, 2012; Hašková, 2007; Igaz et al., 2011; Skalová et al., 2015; Šoltész et al., 2021; Velísková, 2010; Gomboš et al., 2019; Števulová et al., 2017; Gomboš et al., 2018a; Šoltész et al., 2019; Tall et al., 2019; Dulovičová et al., 2021; Zvala et al., 2021; Taubner et al., 2009). So far, many laboratory procedures for measuring settling rate have been based on sedimentation methods, the theoretical basis of which is the Stokes equation. This is valid for the laminar flow area, for the spherical shape of the particles. The disadvantage of these methods is the fact that as the sedimenting particles are reduced, the dispersion system changes to a colloidal state. The results are influenced by diffusion and thus the validity of Stokes' law is limited to soil microparticle sizes < 2 μm. The settling process in the dispersion system continues until the dynamic sedimentation equilibrium of the system occurs. At sedimentation equilibrium, the sedimentation rate of the dispersed particles equals the rate of their diffusion in the opposite direction. This is especially the case for colloidal dispersions. Diffusion is not measurable in coarse dispersions. Conversely, no measurable sedimentation occurs in analytical dispersions. In recent years, a method based on the principle of laser diffraction has been used for sedimentation analysis (Aydin et al., 2012; Gomboš et al., 2018b; Igaz et al., 2020; Mihalache et al., 2010; Šinkovičová et al., 2017; Yang et al., 2015; Zhu et al., 2016).

This contribution summarizes the basic theoretical background applied to address this issue. The aim of the contribution is to present the methodological procedure and results of experimental measurements of the settling rate of soil microparticles. The velocity calculation is based on the use of sedimentation analysis obtained by the laser diffraction method. Soil samples were taken in the East Slovakian Lowlands. Velocity measurements by the proposed method are performed for

soil microparticle sizes with a probability of occurrence of 90%, i. for d(90), d(50), d(10). The results are compared with the results calculated using the Stokes equation.

Material and methods

Theoretical basis

Sedimentation rate of particles in a disperse system depends on the forces acting on particles. In gravitational field, a settling particle in fluid is under the influence of gravity F_g and the opposing forces, buoyancy F_b and drag force F_D. At the beginning of sedimentation, settling particles increase their speed. At certain speed, drag force increases to such an extent that the forces come into equilibrium. The sedimentation rate is constant if the forces are balanced:

$$F_D = F_g - F_b \quad (1)$$

The equation (1) can be expressed in the form:

$$f.u = V.\rho.g - V.\rho_0.g \quad (2)$$

where
f is the friction coefficient, which depends on the shape and size of particles,
u is the sedimentation rate,
V is the volume of a settling particle,
ρ is the volumetric mass density of a settling particle,
ρ_0 is the volumetric mass density of a dispersion medium,
g is the gravitational acceleration on the surface.

For spherical particles with the radius r, dispersed in a dispersion medium with the viscosity η_0, Stokes derived an equation for the friction coefficient f based on the Navier-Stokes equations:

$$f = 6.\pi.\eta_0.r \quad (3)$$

The combination of equations (2) and (3) gives Stokes` equation (4) describing the sedimentation rate of spherical particles:

$$u = \frac{2}{9}\frac{(\rho-\rho_0).r^2.g}{\eta_0} \quad (4)$$

The equations are valid for spherical particles which are far bigger than the molecules of the surrounding environment, assuming that their surface is smooth without any electric charge and they move at low velocities within laminar flow at low Reynolds number (R_e < 0,5). When calculating the sedimentation rate of soil particles, the deviations from the real conditions are caused by the fact that the conditions of spherical particles and the size of particles are not met. If the particles are not spherical, the equation for Stokes` drag must be modified as follows:

$$F_{D_m} = f_e.u = 3.\pi.\eta_0.d_e.u.K \quad (5)$$

where
d_e is the diameter of a sphere with the same volume as a non-spherical particle, i.e.

$$d_e = \left(\frac{6}{\pi} \times volume\right)^{\frac{1}{3}} \quad (6)$$

K is the correction factor which depends on the shape and size of a particle.

In the experiment, one of the oldest methods of particle size analysis was used – sedimentation analysis. Dispersed phase (i.e. soil particles) in the polydispersed system was statistically divided in the groups of particles of similar size called fractions. In the sedimentation analysis, the distribution of particles was expressed by means of frequency and cumulative distribution functions. Frequency distribution functions $F(r)$ of particle weight express the frequency of the particles of certain size [% of weight] in a dispersed phase:

$$F(r) = \frac{dm_r}{m.dr} \quad (7)$$

where
m_r is the weight of the particles with the size,
r, m is the weight of the whole dispersed phase.

Soil dispersed phase is composed of many fractions. Frequency distribution function $F(r)$ is a continuous distribution curve, assuming that:

$$\int_0^\infty F(r)dr = 1 \quad (8)$$

Cumulative distribution functions $I(r)$ of particle size express the weight proportion of the fractions containing the particles with the size equal or smaller than the defined value e_1:

$$I(r) = \int_0^{r_1} F(r)dr \quad (9)$$

In the measurements based on lased diffraction analysis, the frequency of occurrence of particles of certain size in dispersed phase is expressed in % of volume. Numerically, it is the same value as expressed by % of weight.
Outputs from the measurements by laser diffraction method in the form of frequency of occurrence of particles of a certain size allow the calculation of the particle velocity. During the experiment, suspension (colloid) samples for laser diffraction are taken from the dispersion system at two height levels H_1 and H_2 at selected time intervals. A dependency is analysed for each height:
Outputs from measurements by the laser diffraction method in the form of a number of particles of a certain size allow the calculation of the speed of movement of a microparticle of a certain size. In the actual work procedure, suspension (colloid) samples for laser diffraction are taken from the dispersion system from two

height levels H_1 and H_2 (Fig. 1) at selected time intervals. A dependency is sought for each altitude level:

$$d(P)^{H_1} = f(t)^{H_1} \quad (10)$$

$$d(P)^{H_2} = f(t)^{H_2} \quad (11)$$

where
$d(P)^{H_1}$ and $d(P)^{H_2}$ are functions of time.

These are particle sizes with a diameter d and a probability of occurrence P that pass through the plane of H_1 and H_2 levels at different times t. From equations (10) and (11) it is clear that in order to calculate velocity, it is necessary to find such times t^{H_1}, t^{H_2} at which the left sides of said equations are the same, i. the investigated particle has the same size and probability of occurrence at different heights H_1 and H_2 spaced ΔH apart. It is logical that such a situation occurs at different times from the beginning of sedimentation. Then if

$$d(P)^{H_1} = d(P)^{H_2} \rightarrow \Delta t = f(t)^{H_2} - f(t)^{H_1} \rightarrow speed\ v = \frac{H_1 - H_2}{\Delta t} = \frac{\Delta H}{\Delta t} \quad (12)$$

Some form of analytical expression is preferred for expressing the right-hand sides of equations (10) and (11). In the case of measurements, it is possible to use some interpolation method (linear, cubic), resp. extrapolation. Sometimes it is advantageous to divide the dependences (10) and (11) into intersection intervals and then express each dependence in the form of several equations. Measured speed with speed calculated according to Stokes equation (4).

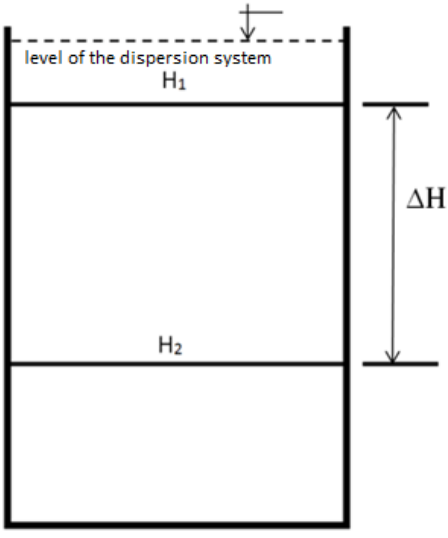

Fig. 1. Experiment scheme.

Description of the experiment

The investigated sites where soil was collected for the sedimentation experiment are located in three localities on the East Slovakian Lowlands (N 48° 39′ 53.41", E 22° 02′ 53.22"; N 48° 28′ 06.41", E 21° 58′ 53.32"; N 48° 39′ 53.41", E 22° 02′ 53.22"). It is an area of tectonic character with a complex structure of decline faults. It consists of Quaternary and especially powerful Neogene sediments. The area is characterized by wetlands, which conditioned the genesis of the local heavy soils. Sampling in the mentioned localities was realized in two soil layers. The basic characteristics of the sampling points are given in Table 1. The particle sizes in μm are given for the individual layers at the beginning of the measurements and at the end of the measurements at the upper sampling level (H_1) above the bottom of the settling vessel.

Soil samples were used to form a dispersed fraction. Subsequently, a dispersion system was created, in which the settling of soil microparticles was investigated. In the experiment, solid dispersed fraction in liquid (distilled water) dispersion system formed a heterogeneous dispersion phase. At the beginning of settling, the dispersed phase formed a coarse suspension $d > 10^{-6}$ m. During settling, a colloidal lyosolic dispersion was formed where the dimensions of particles in disperse phase are defined as 10^{-9} m < d < 10^{-6} m. Depending on the particle shape, a laminar dispersion system with platelet-shaped clay anisometric particles is envisaged. In terms of particle size distribution, it is a polydisperse system consisting of particles of different sizes.

The procedure for the preparation of the dispersion system was as follows: The soil sample was air dried in the laboratory and mechanically crushed. Subsequently, the sample was sieved through a ∅ 2 mm sieve to discard any skeleton. An amount of 0.4 kg was weighed from the sieved soil, and this was mixed with distilled water and a dispersant – a solution of sodium hexameta-phosphate and sodium carbonate in a ratio of 35.7 : 7.9 g per 1 l of distilled water. The resulting suspension was mixed thoroughly and allowed to stand for 24 h. After that, the suspension was boiled for 1 hour with occasional stirring. After cooling, the sample was poured into a sedimentation cylinder and filled with distilled water to complete 5 l. The suspension was then prepared for the experiment.

Prior to the start of the experiment, the suspension in the settling cylinder was thoroughly mixed to form a homogeneous state. From this point on, the sedimentation time was counted. At specified times, a pair of suspension samples at constant heights H_1 and H_2 were taken from the sedimentation cylinder using pipettes. The scheme of the experiment is shown in Fig. 1 where H_2 is 5 cm and H_1 is 15 cm above the bottom of the settling vessel. The investigated path of the soil microparticle ΔH is 10 cm. At the same time, the temperature of the suspension was checked. Sampling time intervals were chosen in a way that their increase in the semi-logarithmic representation was linear. The velocities were calculated based on the particle motion for d (90). A total of 204 samples were analyzed.

The texture of the samples was determined by laser diffraction on a Mastersizer 2000 by MALVERN Instruments. Laser diffraction measures particle size distributions by measuring the angular variation in intensity of light scattered as a laser beam passes through

a dispersed particulate sample. Large particles scatter light at small angles relative to the laser beam and small particles scatter light at large angles. The angular scattering intensity data is then analyzed to calculate the size of the particles responsible for creating the scattering pattern, using the Mie theory of light scattering. The particle size is reported as a volume equivalent sphere diameter. The device is able to work both dry and wet way. The grain size analyses in this work were performed exclusively by the wet method using the Hydro 2000MU dispersion unit. The dispersant was distilled water. Prior to each analysis, the suspension samples exposed to ultrasound for 5 minutes in order to enhance dispersion. The measurement range indicated by the manufacturer is between 0.02 and 2000 µm.

Results and discussion

On the left sides of Figures 2 to 7, the grain distributions in the examined soil layers at the lower H_2 level at the beginning of the experiment and at the end of the experiment are shown. The grain size distributions for the upper sampling levels H_1 are shown on the right. When comparing the grain distribution at the upper and lower sampling point at the start of the experiment (red lines), it is clear that the distributions are the same. The suspension was homogeneous at the start of the experiment. There were no inhomogeneities that could cause errors in measuring the settling rate of soil microparticles. From the comparison of the grain size distribution at the upper and lower sampling point at the end of the experiment (blue lines), some courses are identical (Fig. 4 and Fig. 6). Identical courses indicate that the soil suspension was homogeneous at the end of the experiment. This means that a dynamic sedimentation equilibrium was reached. Small differences in the distribution curves indicate that sedimentation of the smallest particles was still taking place at the end of the experiment. Clearly different course in the left side of Figure 7, i.e. Senné locality, layer 200 to 250 cm under the ground, was probably caused by the agitation of the suspension during sampling at the lower H_2 level.

Table 2 shows the sedimentation rates of soil microparticles from the investigated localities. For comparison, there are also sedimentation rates calculated by the Stokes equation. The sedimentation rates determiend by laser diffraction measurements for d(90) and particle sizes > 2 µm are smaller than the rates calculated by the Stokes equation. The match is higher after introducing an empirical correction factor of 1/5 compared to the original value of 2/9 for the spherical shape of microparticles.

Figure 8 shows a graphical comparison of the soil microparticles settling velocities measured by laser diffraction and Stokes velocities. The graphical comparison shows a good coincidence of the Stokes

Table 1. Basic characteristics of sampling points

Locality	Coordinates		Thickness of the subsoil layer [cm]	Site designation	Soil type	d(10) start of measurements [µm]	d(50) start of measurements [µm]	d(90) start of measurements [µm]	d(10) end of m., upper level [µm]	d(50) end of m., upper level [µm]	d(90) end of m., upper level [µm]
Poľany 1	N 48°39´53.41“	E 22°02´53.22“	0–50	P1(0–50)	clay - loam	3.886	53.968	272.059	0.131	0.168	0.217
			50–100	P1(50–100)	clay	4.389	57.31	218.781	0.133	0.174	0.228
Poľany 2	N 48°28´06.41	E 21°58´3.32“	0–50	P2(0–50)	silt-loam	2.258	16.935	84.432	0.13	0.178	0.249
			100–180	P2(100–180)	sandy-loam	2.062	12.136	41.793	0.131	0.173	0.226
Senné	N 48°39´3.41“	E 22°02´53.22“	100–150	S(100–150)	clay	1.417	5.057	25.456	0.131	0.179	0.250
			200–250	S(200–250)	clay	1.821	10.371	118.514	0.14	0.197	0.311

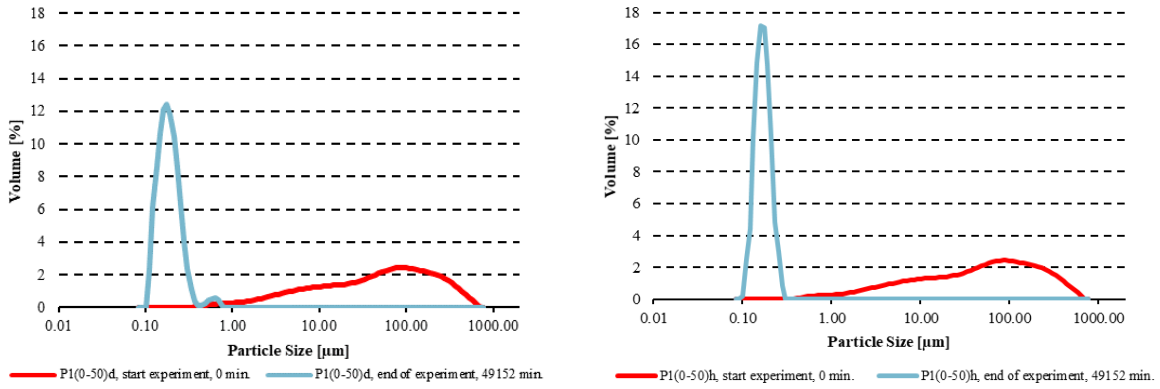

Fig. 2. Grainsize distribution at the lower sampling level H_2 (left) and at the upper sampling level H_1 (right) at the start and at the end of the experiment in the locality Poľany 1, layer 0–50 cm under the surface.

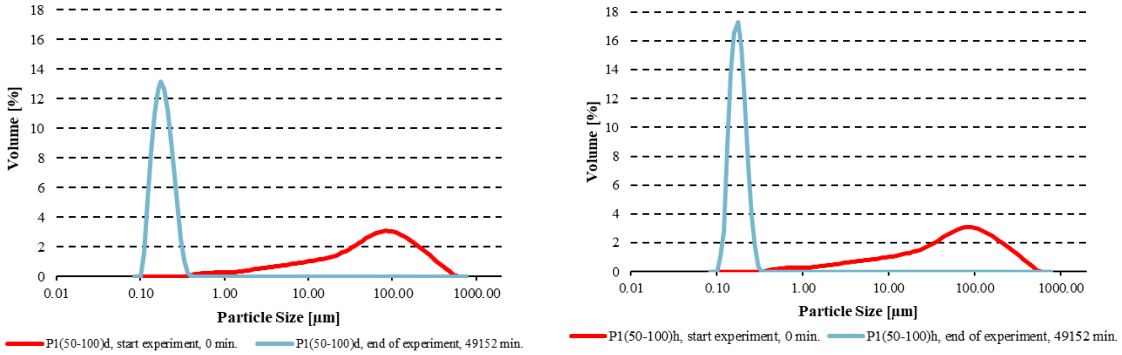

Fig. 3. Grain-size distribution at the lower sampling level H_2 (left) and at the upper sampling level H_1 (right) at the start and at the end of the experiment in the locality Poľany 1, layer 50–100 cm under the surface.

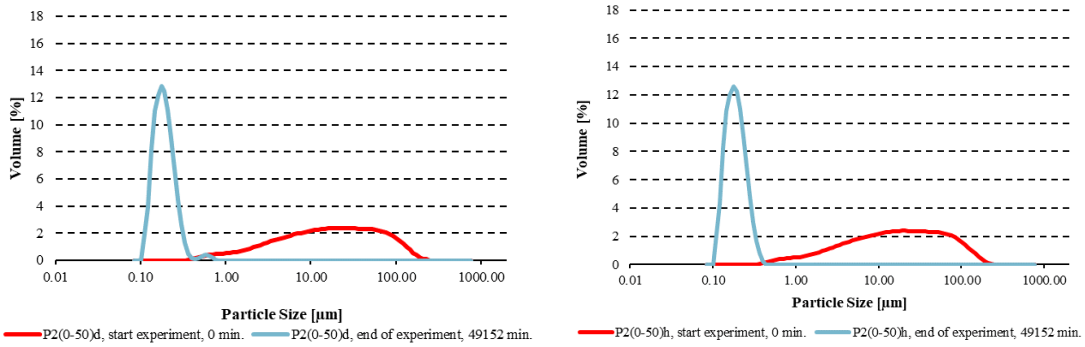

Fig. 4. Grain-size distribution at the lower sampling level H_2 (left) and at the upper sampling level H_1 (right) at the start and at the end of the experiment in the locality Poľany 2, layer 0–50 cm under the surface.

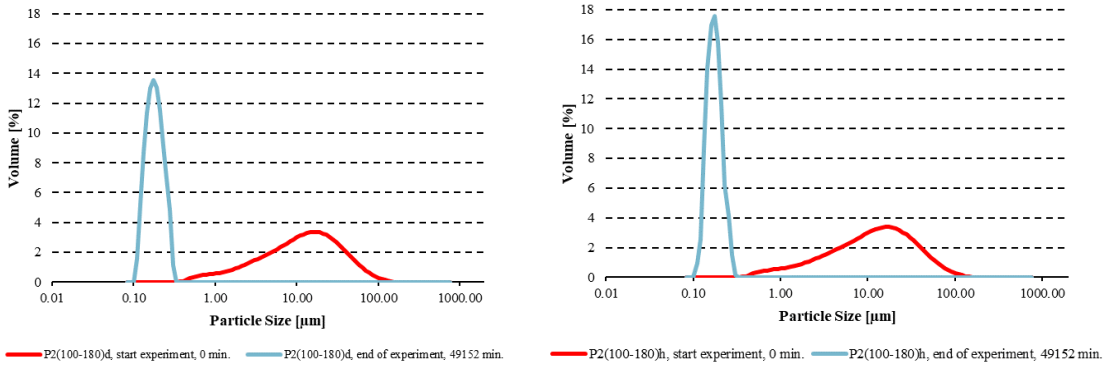

Fig. 5. Grain-size distribution at the lower sampling level H_2 (left) and at the upper sampling level H_1 (right) at the start and at the end of the experiment in the locality Poľany 2, layer 100–180 cm under the surface.

calculations using the empirical correction factor 1/5 with the measured velocities using laser diffraction. High coincidence is only in the interval 2–10 µm. As soil microparticles shrink below 2 µm, the difference between rates calculated by the Stokes equations and laser diffraction analysis increases. From the above, it is assumed that laser diffraction is more accurate for determining settling rates for particles < 2 µm. This is also due to the fact that the diffraction angles decrease as the particle sizes increase. This makes small differences more difficult to detect and the resolution of laser diffraction decreases. Particle shrinkage causes greater intensity in light scattering. This expands the measurement range of laser diffraction and makes it more precise for smaller particle size. The use of traditional methods of grain-size analysis and sedimentation rate

measurement is limited at very small grain sizes. Dispersion system gradually becomes a colloid in which the diffusion effect increases. Under certain conditions, sedimentation equilibrium occurs. Measurements to date have shown that Stokes' law can be applied for soil colloids with particles sized up to 2 μm. For investigating the movement of smaller particles laser diffraction-based techniques are more convenient to be used.

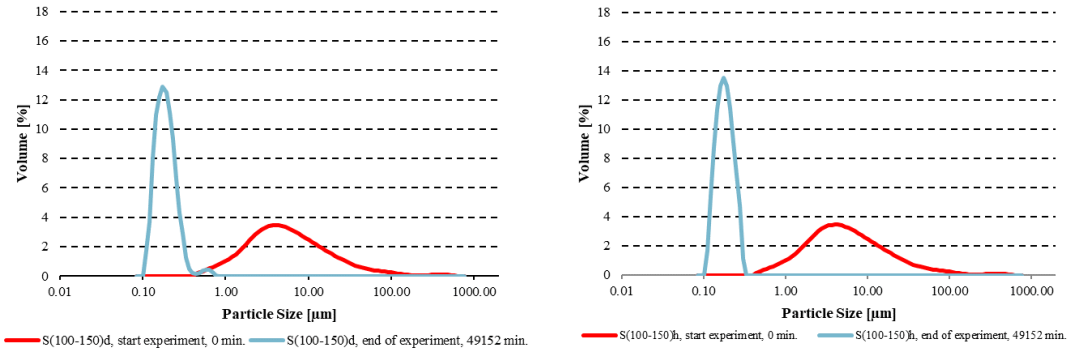

Fig. 6. Grain-size distribution at the lower sampling level H_2 (left) and at the upper sampling level H_1 (right) at the start and at the end of the experiment in the locality Senné, layer 100–150 cm under the surface.

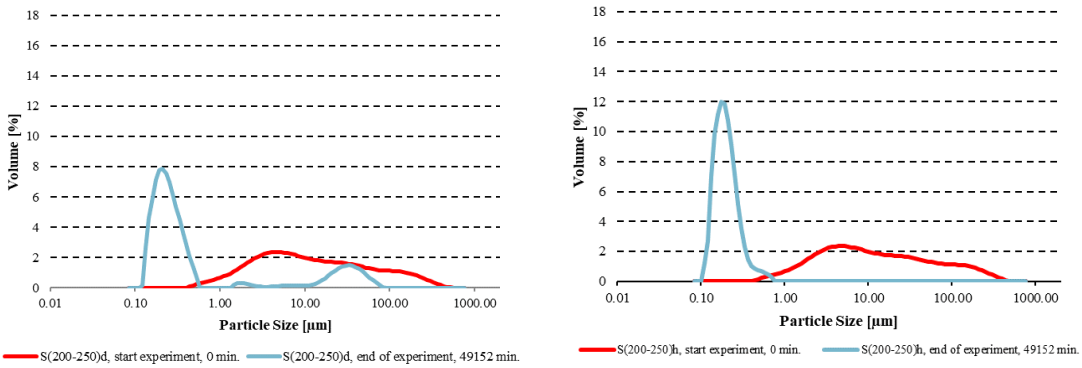

Fig. 7. Grain-size distribution at the lower sampling level H_2 (left) and at the upper sampling level H_1 (right) at the start and at the end of the experiment in the locality Senné, layer 200–250 cm under the surface.

Table 2. Measured settling rates of soil microparticles of different sizes Comparison of sedimentation speed of soil microparticles measured by laser diffraction with speed calculated according to Stokes

soil microparticle size [μm]	10.0	7.0	5.0	3.0	2.0	1.0	0.9	0.8	0.7	0.6	0.5	0.4	0.3
Localities	Settling rate of soil microparticles [μm min^{-1}]												
Poľany P1(0–50)	511.8	304.5	159.3	51.0	30.9	18.3	17.8	17.4	16.9	16.8	12.7	10.2	8.5
Poľany P1(50–100)	1146.1	605.4	279.3	101.8	70.0	37.8	34.2	27.6	21.9	19.0	16.8	15.0	6.3
Poľany P2(0–50)	1030.2	442.3	243.3	75.9	38.1	17.0	16.2	15.5	14.9	11.0	9.3	8.7	8.2
Poľany P2(100–180)	1152.6	605.5	312.4	74.0	51.3	24.6	20.7	17.8	15.7	11.0	9.8	8.9	8.1
Senné S(100–150)	2067.2	1092.2	388.5	95.1	55.0	16.3	14.3	11.4	10.3	9.4	8.7	8.0	4.6
Senné S(200–250)	1918.9	502.3	266.1	80.5	37.8	9.8	8.2	7.5	6.9	5.6	4.2	3.8	---
Stokes K=2/9	5403.4	2647.7	1350.9	486.3	216.1	54.0	43.7	34.6	26.5	19.5	13.5	8.6	4.9
Stokes delta K=1/5	1185.0	580.7	296.3	106.7	47.4	11.9	9.6	7.6	5.8	4.3	3.0	1.9	1.1

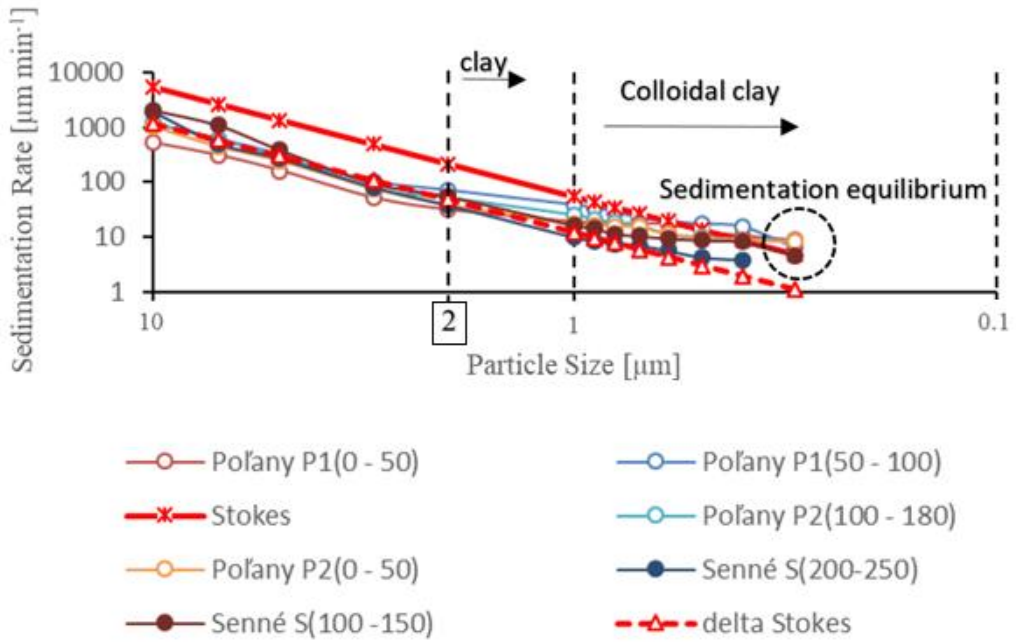

Fig. 8. Graphical comparison of sedimentation rates of soil microparticles measured by laser diffraction with the rates calculated by the Stokes equation.

Conclusion

The availability of modern instruments for research practice opens up new possibilities for research. The contribution summarizes the traditional theoretical background and shows new possibilities for investigating the speed of soil microparticles in water. Previous analysis has been gained on the MALVERN Instruments Mastersizer 2000. This device allows measurements for particle size lower limit of 0.02 µm. An experimental method is proposed in this contribution for the use of this device for measuring the sedimentation rates of soil microparticles. It is based on measuring the time during which soil microparticles of a defined diameter pass certain distance. The size of soil microparticles in space and time is defined by probability. Probability is defined in the form of grain-size distribution functions. The proposed method was investigated in an experiment. The settling rates of soil microparticles sampled at three localities in the East Slovakian Lowland were monitored. The results proved the applicability of the presented method for the analysis of soil microparticles (especially clay microparticles) sedimentation. The advantage of the proposed method is its robustness, elimination of human factor errors and measurement speed.

Acknowledgments

The work was created with the financial support of VEGA 2/0044/20 projects.

References

Aydin, E., Igaz, D., Lackóová, L., Horák, J. (2012): Comparison of methods for the preparation of soil samples and measuring the distribution of grain size fractions of soils in the River Nitra basin In Acta horticulturae et regiotecturae. ISSN 1335-2563, 2012, roč. 15, 27–30.

Dulovičová, R., Velísková, Y., Schügerl, R. (2021): Assesment of selected empirical formulas for computation of saturated hydraulic conductivity. In Acta Hydrologica Slovaca, 2021, vol. 22, no. 1, 78-87. ISSN 2644-4690. DOI: 10.31577/ahs-2021-0022.01.0009

Gomboš, M. (2012): The Impact of Clay Minerals on Soil Hydrological Processes. In Clay Minerals in Nature – Their Characterization, Modification and Application. – InTech, 2012, 1–30. ISBN 978-953-51-0738-5. https://doi.org/10.5772/47748

Gomboš, M., Pavelková, D., Kandra, B., Tall, A. (2019): Impact of Soil Texture and Position of Groundwater Level on Evaporation from the Soil Root Zone. Dana Pavelková, Branislav Kandra, Andrej Tall. In Water Resources in Slovakia: Part I Assessment and Development: The Handbook of Environmental Chemistry. – Berlin; Heidelberg: Springer International Publishing, 2019, 167–184. ISBN 978-3-319-92853-1. ISSN 1867-979X.

Gomboš, M., Tall, A., Kandra, B., Balejčíková, L., Pavelková, D. (2018a): Geometric Factor as the Characteristics of the Three-Dimensional Process of Volume Changes of Heavy Soils. In Environments., 2018, vol. 5, no. 4, art. num. 45. DOI: 10.3390/environments5040045

Gomboš, M., Tall, A., Trpčevská, J., Kandra, B., Pavelková, D., Balejčíková, L. (2018b): Sedimentation Rate of Soil Microparticles. In Arabian Journal of Geosciences., 2018, vol. 11, no. 20, art. num. 635. DOI: 10.1007/s12517-018-4002-8

Hašková, L. (2007): Verification of the single stone design in bio-corridor riverbed by means of one- and two-dimensional model. In Pollack Periodica. Vol. 2, No. 3 (2007), s. 127-134. ISSN 1788-1994 (2007: 0.000 - SJR). V databáze: SCOPUS; DOI: 10.1556/Pollack.2.2007.3.11.

Igaz, D., Aydin, E., Šinkovičová, M., Šimanský, V., Tall, A., Horák, J. (2020): Laser diffraction as an innovative alternative to standard pipette method for determination of

soil texture classes in central Europe. In Water. ISSN 2073-4441 online, 2020, vol. 12, iss. 5, article number 1232 [16 s.]. https://doi.org/ 10.3390/w12051232.

Igaz, D., Štekauerová, V., Horák, J., Kalúz, K., Čimo, J. (2011): The analysis of soils hydrophysical characteristics in the Nitra river basin. In: Influence of anthropogenic activities of water regime of lowland territory. Physics of soil water: 8th International conference, 18th Slovak-Czech-Polish scientific seminar, Vinianske Lake, May, 17–19. 2011, Slovak Republic. Bratislava: Institute of Hydrology SAV, 2011. ISBN 978-80-89139-23-1, 141–150.

Mihalache, D., Ilie, L., Marin, D. I., Calciu, I. (2010): The new methods for measuring soil texture. In Seria Agricultusră-Montanologie-Cadastru; Analele Universităţii Craiova, Romania, 2010; Volume 40, 486–490.

Šinkovičová, M., Igaz, D., Aydin, E., Jarošová, M. (2017): Soil particle size analysis by laser diffractometry: result comparison with pipette method. In WMCAUS 2017 – World Multidisciplinary Civil Engineering-Architecture-Urban Planning Symposium. 1st ed. 1 CD-ROM (843 s.). ISBN 978-80-270-1974-8. WMCAUS. Praha: WMCAUS, 2017, [13] s., CD-ROM. Indexované v: SCOPUS, WoS

Skalová, J., Kotorová, D., Igaz, D., Gomboš, M., Nováková, K. (2015): Regionalizácia Pedotransferových Funkcií Vlhkostných Retenčných Kriviek Pôdy [Regionalization of Pedotransfer Functions of Soil Moisture Retention Curves]; STU: Bratislava, Slovakia, 2015. (In Slovak)

Šoltész, A., Baroková, D., Červeňanská, M., Čubanová, L. (2019): Determination of impact of groundwater pumping on water resources in adjacent area. In SGEM 2019. 19th International Multidisciplinary Scientific GeoConference. Volume 19. Science and Technologies in Geology, Exploration and Mining: conference proceedings. Albena, Bulgaria, 30 June – 6 July 2019. 1. vyd. Sofia: STEF 92 Technology, 2019, S. 153-160. ISSN 1314-2704. ISBN 978-619-7408-77-5. SCOPUS: 2-s2.0-85073692671; DOI: 10.5593/sgem2019/1.2/S02.020.

Šoltész, A., Zeleňáková, M., Čubanová, L., Šugareková, M., Abd-Elhamid, H. (2021): Environmental Impact Assessment and Hydraulic Modelling of Different Flood Protection Measures. Water 2021, 13, 786. https://doi.org/10.3390/w13060786

Števulová, N., Balintová, M., Zeleňáková, M., Eštoková, A., Vilčeková, S. (2017): Environmental Engineering in the Slovak Republic. IOP Conf. Ser. Earth Environ. Sci. 2017, 92, 012064

Tall, A., Kandra, B., Gomboš, M., Pavelková, D. (2019): The influence of soil texture on the course of volume changes of soil. In Soil and Water Research., 2019, vol. 14, no. 2, 57–66. DOI: 10.17221/217/2017-SWR

Taubner, H., Roth, B., Tippkötter, R. (2009): Determination of soil texture: Comparison of the sedimentation method and the laser-diffraction analysis. J. Plant Nutr. Soil Sci. 2009, 172, 161–171. [CrossRef]

Velísková, Y. (2010): Changes of water resources and soils as components of agro-ecosystem in Slovakia. Növénytermelés 2010, 59, 203–206.

Yang, X., Zhang, Q., Li, X., Jia, X., Wei, X., Shao, M. (2015): Determination of soil texture by laser diffraction method. Soil Phys. Hydrol. Soil Sci. Soc. Am. J. 2015, 79, 1556–1566. [CrossRef]

Zhu, L., Chen, J., Liu, D. (2016): Morphological quantity analysis of soil surface shrinkage crack and its numerical simulation. Nongye Gongcheng Xuebao/Trans. Chin. Soc. Agric. Eng. 2016, 32, 8–14.

Zvala, A., Šurda, P., Vitková, J. (2021): Moisture changes in the organic horizon of the forest soil under different tree species. In Acta Hydrologica Slovaca, 2021, vol. 22, no. 1, 106–112. ISSN 2644-4690. DOI: 10.31577/ahs-2021-0022.01.0012

Ing. Milan Gomboš, CSc. (*corresponding author, e-mail: gombos@uh.savba.sk)
RNDr. Andrej Tall, PhD.
Ing. Dana Pavelková, PhD.
Ing. Branislav Kandra, PhD.
Institute of Hydrology SAS
Dúbravská cesta 9
84104 Bratislava
Slovak Republic